

Coverpicture from González et al., (2007) *Prog Biophys Mol Biol.* 94(1-2):66-106.





FACULTY OF MEDICINE  
AND HEALTH SCIENCES

# ***Role and regulation of connexin hemichannels in cellular ATP release***

**Elke De Vuyst**

Thesis submitted in fulfillment of the requirements for the degree of  
"Doctor of Medical Science"

Academic Year 2007 - 2008

Promotor: Prof. Dr. Luc Leybaert

Faculty of Medicine and Health Sciences  
Department of Physiology and Pathophysiology

Thesis submitted to fulfil the requirements for the degree of Doctor of Medical Science  
June 2008

Promotor: Prof. Dr. Luc Leybaert  
Ghent University, Belgium

Chairman: Prof. Dr. Claude Cuvelier  
Ghent University, Belgium

Reading committee: Prof. Dr. Bert Vanheel  
Ghent University, Belgium

Prof. Dr. Romain Lefebvre  
Ghent University, Belgium

Prof. Dr. Jan Tavernier  
Ghent University, Belgium

Prof. Dr. Johan Vereecke  
Catholic University of Leuven, Belgium

Other members: Prof. Dr. Howard Evans  
Cardiff University, UK

Prof. Dr. Christian Giaume  
Collège de France, France

Prof. Dr. Laurent Combettes  
Université de Paris Sud, France

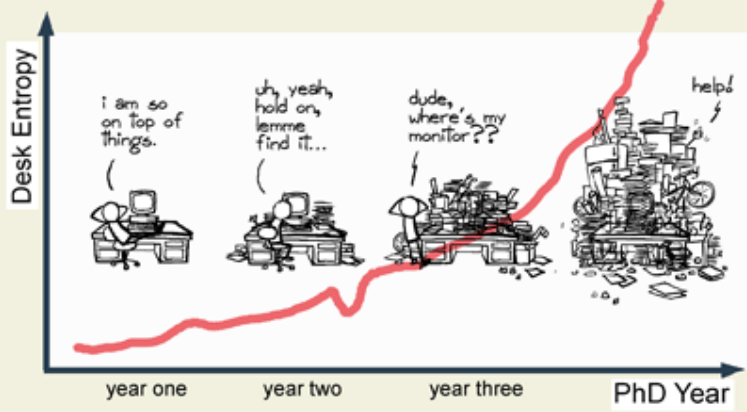
Prof. Dr. Marc Bracke  
Ghent University, Belgium



## DESK ENTROPY

### Definition

Desk entropy is a spatiodynamic quantity that measures a workspace's degree of disorder, and the inability to find anything when you really need it. Any spontaneous activity, whether productive or unproductive, disperses crap matter and increases overall desk entropy. Efforts to reverse desk entropy are temporary, and inevitably decrease over time.



Units: Junk-height/Area

## List of abbreviations

Å	Ångstrom
AA	Arachidonic acid
AACOCF3	Arachidonyl trifluoromethyl ketone
ABC transporter	ATP-binding cassette transporter
ADP	Adenosine diphosphate
AIP	Autocamtide-2-related inhibitory peptide
AMP	Adenosine monophosphate
ATP	Adenosine triphosphate
A.U.	Arbitrary units
BAPTA	1,2-bis( <i>o</i> -aminophenoxy)ethane- <i>N,N,N',N'</i> -tetraacetic acid
bFGF	Basic fibroblast growth factor
Bz-ATP	2'-3'- <i>O</i> -(4-benzoylbenzoyl)-ATP
cADPR	Cyclic ADP ribose
CALP1	Ca <sup>2+</sup> -like peptide
CaM	Calmodulin
CaMBP	CaM binding protein
CaMK	Ca <sup>2+</sup> /CaM dependent kinase
CF	Carboxyfluorescein
CFDA-AM	Carboxyfluorescein diacetate acetoxy methylester
CSF	Cerebrospinal fluid
CFTR	Cystic fibrosis transmembrane regulator
cGMP	Cyclic guanosine monophosphate
CK1	Casein kinase 1
COX	Cyclooxygenases
CYP	Cytochrome P450
cTMP	Cyclic thymidine monophosphate
Cx	Connexin
DAPI	4',6-diamidino-2-phenylindole
DMEM	Dulbecco's modified Eagle medium
DMSO	Dimethyl sulfoxide
DTT	Dithiothreitol
ECL	Enhanced chemiluminescence
EDTA	Ethylenediaminetetraacetic acid
EGF	Epithelial growth factor
EGFR	Epithelial growth factor receptor
EGTA	Ethylene glycol-bis(2-aminoethylether)- <i>N,N,N',N'</i> -tetraacetic acid
ELDT	Electroporation loading and dye transfer
E-NPP	Ectonucleotide pyrophosphatase-phosphodiesterase
E-NTPDase	Ectonucleotide triphosphate diphosphohydrolase
ER	Endoplasmic reticulum
ERAD	Endoplasmic reticulum associated degradation
Erk	Extracellular signal regulated kinase
ET-1	Endothelin-1
EtBr	Ethidium bromide
FACS	Fluorescence activated cell sorting
FBS	Foetal bovine serum
FGFR	Fibroblast growth factor receptor
FITC	Fluorescein isothiocyanate

FRAP	Fluorescence recovery after photobleaching
GA	Glycyrrhetic acid
GAP	GTPase activating protein (not to be confused with Gap)
GDP	Guanosine diphosphate
$\gamma$ -GT	$\gamma$ -glutamyl transpeptidase
GPCR	G protein coupled receptor
GSH	Reduced glutathione
GTP	Guanosine triphosphate
HBSS	Hanks' balanced salt solution
HEPES	4-(2-hydroxyethyl)piperazine-1-ethanesulfonic acid
ICCD	Intensified charge coupled device
IL-1 $\beta$	Interleukin-1 beta
InsP	Inositolmonophosphate
InsP <sub>2</sub>	Inositolbisphosphate
InsP <sub>3</sub>	Inositoltrisphosphate
InsP <sub>4</sub>	Inositoltetrakisphosphate
K <sub>d</sub>	Dissociation constant
kDa	Kilodalton
LPA	L- $\alpha$ -lysophosphatidic acid
LO	Lipoxygenases
LPS	Lipopolysaccharide
MAPK	Mitogen activated protein kinase
mRNA	Messenger RNA
mV	Millivolt
MW	Molecular weight
NAD <sup>+</sup>	Nicotinamide adenine dinucleotide
NO	Nitric oxide
NOS	Nitric oxide synthase
NP-EGTA-AM	<i>o</i> -nitrophenyl-ethyleneglycol-bis(2-aminoethylether)- <i>N,N,N',N'</i> -tetraacetic acid acetoxymethyl ester
Ox-ATP	Adenosine 5'-triphosphate periodate oxidized sodium salt
Panx	Pannexin
PBS	Phosphate buffered salt solution
PDGFR	Platelet derived growth factor receptor
PGE2	Prostaglandin E <sub>2</sub>
PI	Propidium iodide
PKA	Protein kinase A
PKC	Protein kinase C
PLA	Phospholipase A
PLC	Phospholipase C
PMA	Phorbol 12-myristate 13-acetate
pS	Picosiemens
PtdIns(4,5)P <sub>2</sub>	Phosphatidylinositol-4,5-bisphosphate
PP2	4-amino-5-(4-chlorophenyl)-7-( <i>t</i> -butyl)pyrazolo[3,4- <i>d</i> ]pyrimidine
RIPA	Radio immuno precipitation assay
ROS	Reactive oxygen species
RYR	Ryanodine receptor
SDS-PAGE	Sodium dodecyl sulphate-poly-acrylamide gel electrophoresis
SH2	Src Homology 2
SH3	Src Homology 3

SHP-2	Src homology 2 domain containing phosphotyrosine phosphatase
siRNA	Small interfering RNA
SLDT	Scrape loading and dye transfer
SNAP	Synaptosome-associated protein
SNARE	Soluble <i>N</i> -ethyl maleimide-sensitive fusion attachment protein receptor complex
SOC	Store operated Ca <sup>2+</sup> -channel
SR	Sarcoplasmic reticulum
TEA	Tetraethylammonium
TGN	Trans-Golgi network
TMA	Tetramethylammonium
TNF- $\alpha$	Tumor necrosis factor $\alpha$
TPA	12-O-tetradecanoylphorbol-13-acetate
TRITC	Tetramethyl rhodamine isothiocyanate
UTP	Uridine triphosphate
VAMP	Vesicle associated membrane protein
VDAC	Voltage dependent anion conductance channel
VEGFR	Vascular endothelial growth factor receptor
v-Fps	Viral-Fps
VRAC	Volume regulated anion channel
VSOR	Volume sensitive outward rectifying
v-Src	Viral-Src
ZO-1	Zonula occludens-1

<b>Samenvatting</b> .....	<b>1</b>
<b>Summary</b> .....	<b>5</b>
<b>Résumé</b> .....	<b>9</b>
<b>Chapter 1: Introduction</b> .....	<b>13</b>
<b>1.1 Cell-cell communication and homeostasis</b> .....	<b>14</b>
1.1.1 Connexins.....	15
1.1.2 Innexins .....	16
1.1.3 Pannexins .....	17
1.1.4 Connexin trafficking, oligomerization and degradation .....	17
<b>1.2 Channel gating</b> .....	<b>22</b>
1.2.1 Selective connexin permeability and conductance .....	22
1.2.2 Gating by transjunctional voltage and membrane potential .....	27
1.2.3 Effect of $pH_i$ on gap junctional communication .....	30
1.2.4 Phosphorylation and gating .....	32
1.2.4.1 General aspects of phosphorylation .....	32
1.2.4.2 Cell cycle related changes in Cx43 phosphorylation .....	34
1.2.4.3 Phosphorylation of Cx43 by PKC.....	36
1.2.4.4 Phosphorylation of Cx43 by tyrosine protein kinases.....	36
1.2.4.4.1 Non-receptor tyrosine protein kinases.....	37
1.2.4.4.2 Receptor tyrosine protein kinases .....	39
1.2.4.5 G protein coupled receptors (GPCR).....	41
1.2.4.6 Phosphorylation of Cx43 by casein kinase 1 (CK1) and other kinases.....	42
1.2.5 Regulation of connexin gap junctional channels by changes in $[Ca^{2+}]_i$ .....	44
<b>1.3 Hemichannels: unpaired gap junctional channels</b> .....	<b>47</b>
1.3.1 Channel inhibitors and Gap peptides.....	48
1.3.2 Substances released by open hemichannels .....	51
1.3.2.1 Release of ATP.....	51
1.3.2.2 Release of glutamate.....	52
1.3.2.3 Release of $NAD^+$ .....	52
1.3.2.4 Release of glutathione.....	53
1.3.2.5 Release of prostaglandin $E_2$ .....	53
1.3.3 Hemichannel responses to $[Ca^{2+}]_i$ .....	54
1.3.4 Hemichannel responses to $[Ca^{2+}]_e$ .....	55
1.3.5 Other release mechanisms .....	56
1.3.5.1 Pannexin hemichannels.....	56
1.3.5.2 $P_2X$ receptor pores .....	57
1.3.5.3 Cystic Fibrosis Transmembrane Regulator.....	57
1.3.5.4 Volume and voltage-dependent anion channel .....	58
1.3.5.5 Voltage-gated $Cl^-$ -channels.....	58
1.3.5.6 Volume-regulated anion channels.....	58
1.3.5.7 Maitotoxin activated pore .....	59
1.3.5.8 Exocytosis.....	59
<b>Chapter 2: Aim of the study</b> .....	<b>61</b>
<b>2.1 What is the mechanism and the molecular pathway of <math>Ca^{2+}</math>-triggered ATP release via hemichannels?</b> .....	<b>62</b>
<b>2.2 Are connexin hemichannels and gap junctional channels regulated in a similar way?</b> .....	<b>63</b>

2.3	Is there an alternative for the widely used SLDT technique? .....	63
<b>Chapter 3: Material and Methods.....</b>		<b>65</b>
3.1	Cell culture .....	66
3.2	Reagents .....	66
3.3	Hemichannel functioning .....	67
3.4	Gap junctional communication.....	69
3.5	Ca <sup>2+</sup> -imaging.....	70
3.6	Photoliberation of Ca <sup>2+</sup> .....	73
<b>Chapter 4: Intracellular calcium changes trigger Cx32 hemichannel opening..</b>		<b>75</b>
4.1	Introduction.....	77
4.2	Material and Methods .....	78
4.2.1	Cell cultures .....	78
4.2.2	Agents .....	78
4.2.3	Extracellular ATP measurements .....	79
4.2.4	Photoactivation of Ca <sup>2+</sup> .....	80
4.2.5	Ca <sup>2+</sup> -imaging .....	80
4.2.6	Dye uptake .....	81
4.2.7	Scrape loading and dye transfer (SLDT).....	81
4.2.8	Western blotting .....	82
4.2.9	Data analysis and statistics .....	82
4.3	Results .....	83
4.3.1	Divalent-free (DF) solutions trigger ATP release that is dependent on [Ca <sup>2+</sup> ] <sub>i</sub> in ECV304 .....	83
4.3.2	Directly increasing [Ca <sup>2+</sup> ] <sub>i</sub> triggers ATP release in ECV304 .....	85
4.3.3	DF- and Ca <sup>2+</sup> -triggered ATP release are inhibited by gap junction blockers and a Cx32 Gap peptide in ECV304.....	85
4.3.4	DF- and Ca <sup>2+</sup> -triggered ATP release and dye uptake are inhibited by Cx32 Gap peptides and a CaM antagonist in C6-Cx32.....	86
4.3.5	P <sub>2</sub> X <sub>7</sub> receptors are not involved in ATP release .....	89
4.3.6	Vesicular release slightly contributes to Ca <sup>2+</sup> -triggered ATP release in C6-Cx32.....	93
4.3.7	Relation between [Ca <sup>2+</sup> ] <sub>i</sub> and ATP release or dye uptake in C6-Cx32 .....	93
4.4	Discussion.....	96
<b>Chapter 5: Ca<sup>2+</sup>-activation and inactivation of ATP release via Cx43 hemichannels is controlled by a CaM-AA-ROS-NO signaling cascade .....</b>		<b>99</b>
5.1	Introduction.....	101
5.2	Material and Methods .....	102
5.2.1	Cell culture .....	102
5.2.2	Agents .....	102
5.2.3	Extracellular ATP measurements .....	103
5.2.4	Dye uptake studies .....	103

5.2.5	Ca <sup>2+</sup> -imaging .....	103
5.2.6	Western blotting .....	104
5.2.7	siRNA .....	104
5.2.8	Scrape loading and dye transfer (SLDT) .....	105
5.2.9	Data analysis and statistics .....	105
<b>5.3</b>	<b>Results .....</b>	<b>106</b>
5.3.1	The Ca <sup>2+</sup> -ionophore A23187 triggers ATP responses in Cx43 expressing cells .....	106
5.3.2	Ca <sup>2+</sup> -triggered ATP release is inhibited by siRNA treatment, blocked by <sup>43</sup> Gap 26 and 27 peptides and does not involve major contributions of vesicular release, Panx1 hemichannels or P <sub>2</sub> X <sub>7</sub> pores .....	108
5.3.3	CaM and Ca <sup>2+</sup> /CaMK contribute to A23187-triggered ATP release .....	112
5.3.4	Ca <sup>2+</sup> /CALP1-triggered ATP release also involves AA signaling .....	115
5.3.5	ROS and NO also contribute to the downstream signaling cascade .....	117
<b>5.4</b>	<b>Discussion .....</b>	<b>118</b>

## **Chapter 6: Connexin hemichannels and gap junction channels are differentially influenced by lipopolysaccharide and basic fibroblast growth factor.....123**

<b>6.1</b>	<b>Introduction .....</b>	<b>125</b>
<b>6.2</b>	<b>Materials and Methods .....</b>	<b>127</b>
6.2.1	Cells and reagents .....	127
6.2.2	Plasmid DNA purification and transfection .....	127
6.2.3	Gap junctional communication .....	128
6.2.4	Cellular ATP release .....	128
6.2.5	Western blotting .....	129
6.2.6	Data analysis and statistics .....	130
<b>6.3</b>	<b>Results .....</b>	<b>130</b>
6.3.1	ATP release triggered in Cx43-transfected cells by divalent-free extracellular conditions is related to hemichannel opening .....	130
6.3.2	Carboxyterminal truncation of Cx43 does not affect gap junctional communication but abolishes ATP responses in HeLa-Cx43 .....	132
6.3.3	Activation of PKC and c-Src reduces gap junctional communication and ATP responses in C6-Cx43 .....	134
6.3.4	LPA inhibits gap junctional coupling and ATP responses in C6-Cx43, whereas LPS inhibits coupling but stimulates ATP release .....	136
6.3.5	LPA and LPS inhibit ATP responses in HeLa-Cx43, but LPS potentiates these responses in carboxyterminal truncated HeLa-Cx43 .....	138
6.3.6	bFGF has similar effects as LPS .....	139
6.3.7	bFGF and LPS potentiate DF-triggered ATP release in HeLa-Cx26 .....	141
6.3.8	LPS potentiation of ATP responses involves AA signaling .....	142
<b>6.4</b>	<b>Discussion .....</b>	<b>144</b>

## **Chapter 7: In situ bipolar electroporation for localized cell loading with reporter dyes and investigating gap junctional coupling.....149**

<b>7.1</b>	<b>Introduction .....</b>	<b>151</b>
<b>7.2</b>	<b>Material and Methods .....</b>	<b>152</b>
7.2.1	Cell cultures .....	152
7.2.2	Electroporation procedure .....	153
7.2.3	Scrape loading and dye transfer .....	155

7.2.4	Fluorescence recovery after photobleaching .....	156
7.2.5	Western blotting .....	156
7.2.6	Immunocytochemistry .....	157
7.2.7	Data analysis and statistics .....	157
<b>7.3</b>	<b>Results .....</b>	<b>158</b>
7.3.1	Experiments with a low molecular weight dyes .....	158
7.3.2	Experiments with higher molecular weight dyes .....	160
7.3.3	Experiments on cells coupled by gap junctions.....	161
<b>7.4</b>	<b>Discussion.....</b>	<b>167</b>
<b>Chapter 8: Discussion and Perspectives.....</b>		<b>171</b>
<b>8.1</b>	<b>Discussion.....</b>	<b>172</b>
8.1.1	Intracellular Ca <sup>2+</sup> -changes trigger Cx32 hemichannel opening.....	172
8.1.2	Cx43 hemichannel regulation by intracellular Ca <sup>2+</sup> -changes: involvement of various signaling pathways.....	172
8.1.3	Connexin hemichannels and gap junction channels are differentially influenced by lipopolysaccharide and basic fibroblast growth factor .....	174
8.1.4	In situ bipolar electroporation for localized cell loading with reporter dyes and investigating gap junctional coupling.....	175
<b>8.2</b>	<b>General discussion.....</b>	<b>176</b>
8.2.1	Gap peptides.....	176
8.2.2	Intracellular Ca <sup>2+</sup> : gap junctions versus hemichannels.....	179
8.2.3	Distinct modulation of gap junctions and hemichannels: role of arachidonic acid .....	182
<b>8.3</b>	<b>Future perspectives .....</b>	<b>184</b>
<b>Chapter 9: References.....</b>		<b>187</b>



## Samenvatting

Multicellulaire organismen vereisen verschillende vormen van cel-cel communicatie. Er zijn twee mechanismen van communicatie belangrijk op dit niveau, nl. paracrine communicatie, via het vrijstellen van kleine moleculen, diffusie in de extracellulaire ruimte en vervolgens binding op de overeenkomstige receptor van een naburige cel en activatie van de stroomafwaarts gelegen signaaltransductie cascade. Het tweede mechanisme omvat de interactie tussen membraan-eiwitten van naburige cellen, een belangrijk voorbeeld hiervan zijn gap junctions die het cytoplasma van twee naburige cellen verbinden. Deze junctions laten de diffusie-gemedieerde passage toe van ionen en kleine moleculen ( $\leq 1.2$  kDa) en zijn opgebouwd uit connexine eiwitten in vertebraten. Talrijke studies hebben reeds eerder aangetoond dat halve gap junction kanalen, zogenaamde hemikanalen, openen onder bepaalde omstandigheden en op deze manier een loslatingsweg vormen voor kleine moleculen.

In hoofdstuk 4 onderzochten we de relatie tussen connexine hemikanalen opgebouwd uit Cx32 en intracellulaire  $\text{Ca}^{2+}$ -concentraties ( $[\text{Ca}^{2+}]_i$ ). In deze studie werd hemikanaal opening indirect bestudeerd door enerzijds de hoeveelheid ATP die vrijgesteld werd te bepalen, en anderzijds door de opname van een kleine reporter kleurstof (propidium iodide - PI) te registreren. Verhoging van  $[\text{Ca}^{2+}]_i$  door foto-activatie van  $\text{Ca}^{2+}$  vanuit inactieve precursors in het cytoplasma, of door stimulatie van  $\text{Ca}^{2+}$ -influx met behulp van een  $\text{Ca}^{2+}$ -ionofor A23187 induceerde de vrijstelling van ATP en de opname van PI vanuit het extracellulaire milieu. Dit wees op de activatie van een bidirectionele signaalweg. De betrokkenheid van hemikanalen was gebaseerd op de volgende criteria: (i) inhibitie door peptiden die identiek zijn met een korte sequentie van het connexine eiwit, (ii) inhibitie door hemikanaal/gap junction kanaal blokkeerders, (iii) vergelijking van de respons tussen Cx32 exprimerende cellen en de overeenkomstige controle cellen en (iv) de uitsluiting van andere loslatingswegen, zoals de  $\text{P}_2\text{X}_7$  receptor porie. Door gebruik te maken van verschillende A23187 concentraties konden we een dosis-antwoord curve opstellen voor  $\text{Ca}^{2+}$ -geïnduceerde ATP vrijstelling en kleurstofopname. Onze resultaten toonden aan dat de grootte van de  $\text{Ca}^{2+}$ -stimulus kritisch was en dat hemikanaal gemedieerde responsen enkel optraden wanneer  $[\text{Ca}^{2+}]_i$  tussen 200 nM en 1,000 nM was. De maximale respons werd gemeten bij een  $[\text{Ca}^{2+}]_i$  rond 500 nM. Inhibitie van CaM (calmoduline) onderdrukte de  $\text{Ca}^{2+}$ -geïnduceerde hemikanaal responsen. Dit toonde aan dat CaM kan optreden als een intermediaire component. CaM kan rechtstreeks inwerken op Cx32 via de  $\text{Ca}^{2+}$ /CaM-Cx32 interactie enerzijds, anderzijds kan  $\text{Ca}^{2+}$ /CaM ook  $\text{Ca}^{2+}$ /CaM afhankelijke kinasen activeren.

In hoofdstuk 5 werd er overschakeld naar Cx43 exprimerende cellen. Cx43 is het meest wijdverspreide connexine en evidentie voor een interactie met CaM was eveneens beschikbaar vanuit de literatuur. Dit deed ons vermoeden dat Cx43 hemikanalen ook

gereguleerd konden worden door verandering in  $[Ca^{2+}]_i$ . De betrokkenheid van hemikanalen werd gestaafd met criteria die analoog zijn als deze gebruikt in hoofdstuk 4, maar werden verder aangevuld door de inhiberende werking van siRNA die de expressie van Cx43 onderdrukte enerzijds, en anderzijds, door de verschillende  $[Ca^{2+}]_i$  gevoeligheid van connexin hemikanalen in vergelijking met Panx1 hemikanalen. Dit werd reeds eerder beschreven in de literatuur. De  $Ca^{2+}$ -geïnduceerde hemikanaal responsen vertoonden een klokvormige concentratie-antwoord curve, met een maximale ATP vrijstelling bij een  $[Ca^{2+}]_i$  van 500 nM. Deze resultaten waren vergelijkbaar met de resultaten behaald voor Cx32. De  $Ca^{2+}$ -geïnduceerde ATP vrijstelling werd geïnhibeerd door: (i) CaM en CaMK-II antagonisten, (ii) blokkeerders van de arachidonzuur (AA) signaaltransductieweg, (iii) anti-oxidanten en (iv) antagonisten van NO productie. CALP1, een CaM agonist, induceerde ATP vrijstelling die volledig onderdrukt werd door antagonisten van de AA signaaltransductieweg. Exogeen toegediend AA induceerde ook ATP loslating die gereduceerd werd door anti-oxidanten, antagonisten van NO synthese en door veranderingen in  $[Ca^{2+}]_i$  te bufferen. Deze studie toonde de volgende signaaltransductie cascade aan:  $Ca^{2+}$  - CaM - CaMK-II - cPLA<sub>2</sub> - AA - vrije zuurstof radicalen en NO, met een terugkoppeling vertrekkende van AA naar  $[Ca^{2+}]_i$  die de ATP loslating versterkt.

Uit deze twee studies besluiten wij dat hemikanalen geactiveerd worden door gematigde verhogingen in  $[Ca^{2+}]_i$  in de grootte-orde van 500 nM en dat sterke stijgingen in  $[Ca^{2+}]_i$  de hemikanalen opnieuw sluiten. De  $Ca^{2+}$ -geïnduceerde hemikanaal responsen worden bewerkstelligd door de activatie van een complexe signaaltransductie cascade die sommige gekende hemikanaal activatoren omvat.

In de vorige hoofdstukken werd aangetoond dat hemikanaal opening geïnduceerd werd door een stijging in  $[Ca^{2+}]_i$ . Dit is in tegenstelling tot de talrijke bevindingen die aantonen dat een stijging in  $[Ca^{2+}]_i$  gap juncties sluit. Dit toont aan dat hemikanalen en gap juncties niet noodzakelijk op dezelfde wijze gereguleerd worden. In hoofdstuk 6 bestudeerden we de regulatie van hemikanaal responsen en gap junctionele communicatie door activatie van verschillende kinasen. Talrijke connexine eiwitten worden gefosforyleerd ter hoogte van hun carboxyterminaal domein, voornamelijk op serine residuen, maar ook op threonine en tyrosine. Een basaal niveau van fosforylatie is vereist voor de opbouw en correcte functie van gap juncties die samengesteld zijn uit Cx43. Talrijke studies hebben reeds aangetoond dat de invloed van groeifactoren, oncogene eiwit kinasen, hormonen en ontstekingsfactoren op gap juncties gemedieerd wordt door fosforylatie van Cx43 (aminozuur 236 - 382). Hemikanaal opening werd in deze studie geïnduceerd door de cellen bloot te stellen aan een oplossing die geen extracellulaire tweewaardige kationen bevat (DF-inductie). Gap junctionele communicatie werd bestudeerd door de transfer van een fluorescente rapporterkleurstof naar

naburige cellen te registreren. Ons werk toonde aan dat bepaalde stimuli zoals PKC activatie, c-Src en LPA gap juncties en hemikanalen op een gelijkaardige manier beïnvloedde. In tegenstelling tot deze bevinding, hadden LPS en bFGF een verschillende invloed op hemikanalen in vergelijking met gap juncties. Dit effect was afhankelijk van het gebruikte celtype en de aan- of afwezigheid van het carboxyterminaal domein. In C6-Cx43 cellen stimuleerden LPS en bFGF de DF-geïnduceerde ATP vrijstelling, in Hela-Cx43 cellen daarentegen inhibeerden beide substanties de hemikanaal opening. Wanneer het carboxyterminaal domein verwijderd werd (Hela-Cx43 $\Delta$ C) verdween de DF-geïnduceerde ATP vrijstelling, maar zowel LPS als bFGF herstelden deze ATP loslating. Gelijklopend met deze resultaten was de observatie dat in Hela-Cx26 LPS en bFGF ook stimulerende eigenschappen hadden. Deze bevindingen suggereren de betrokkenheid van verschillende signaaltransductiewegen in verschillende celsoorten. Voorgaande studies hadden reeds aangetoond dat zowel LPS als bFGF een activatie van PLA<sub>2</sub> konden induceren via fosforylatie van deze laatste. Antagonisten van de AA metabole signaaltransductieweg onderdrukte het LPS stimulerend effect en AA bootste de stimulerende effecten van LPS en bFGF na en dit in de drie celtypes (C6-Cx43, Hela-Cx43 $\Delta$ C en Hela-Cx26). We concludeerden dat de celspecifieke effecten van LPS en bFGF afhankelijk waren van het evenwicht tussen de fosforylatie en de activatie van de AA metabole signaaltransductie weg.

Er zijn reeds verschillende methoden bekend voor de studie van cel-cel koppeling. Sommige technieken hebben belangrijke nadelen die gerelateerd zijn aan enerzijds veranderingen in  $[Ca^{2+}]_i$  veroorzaakt door insertie van de elektrode (elektrofysiologie) of door de lading van de kleurstof (micro-injectie en het laden van de kleurstof via het *scrapen* van een cel monolaag) en anderzijds door het meten van de cel-cel koppeling in één enkele cel. Het doel van dit luik van het onderzoek was de ontwikkeling van een nieuwe methode om gap junctionele communicatie te kwantifiëren. In hoofdstuk 7 werd een fluorescente kleurstof in een celmonolaag geladen door elektroporatie. In een eerste stap optimaliseerden we de elektroporatie instellingen opdat minimale celdood en maximale ladingsefficiëntie zou optreden. In een volgende stap werd de transfer van de kleurstof naar niet geladen naburige cellen bepaald. Dit werd gekwantificeerd door de standaard afwijking van het Gaussiaans diffusieprofiel te bepalen of door de spatiale constante van het exponentieel verval aan de flank van de Gauss curve te bepalen. Onze resultaten toonden aan dat de lading van een kleurstof via elektroporatie een betere methode is om gap junctionele koppeling te bestuderen, wanneer dit vergeleken werd met de lading van een kleurstof door gebruik te maken van zogenaamde *cell scraping*.

Een belangrijke observatie in deze thesis is dat connexine hemikanalen, gap junctie kanalen en pannexine hemikanalen op een verschillende manier gereguleerd worden door

intracellulair  $\text{Ca}^{2+}$ . Onder normale omstandigheden zijn hemikanalen gesloten en gap junctie kanalen open. Als reactie op AA vrijstelling gaan hemikanalen open, terwijl gap juncties nu gaan sluiten. Verhoging van  $[\text{Ca}^{2+}]_i$  in de grootte-orde van enkele honderden nanomolair activeert hemikanalen, terwijl een verdere stijging van  $[\text{Ca}^{2+}]_i$  de sluiting van hemikanalen induceert. Deze sluiting lijkt echter wel gemedieerd te worden door een ander mechanisme dan de sluiting van gap junctie kanalen onder invloed van verhoogde  $[\text{Ca}^{2+}]_i$ . Door het belang van ATP als energiemolecule in de cel en de sterke betrokkenheid in de paracriene signalisatie suggereren wij dat ATP vrijstelling strikt gereguleerd moet worden. Dit vereist de aanwezigheid van meerdere loslatingswegen die onder controle staan van verschillende signaaltransductie cascaden en een fijn-regulatie van de diverse loslatingswegen door de belangrijke signaal molecule, intracellulair  $\text{Ca}^{2+}$ . Op deze manier zal onder omstandigheden dat de gap junctionele communicatie belemmerd is, de cel-cel communicatie toch gered worden door de loslating van paracriene boodschapperstoffen.

## Summary

Multicellular organisms require different forms of cell-cell communication to coordinate the activity in a cell population. Two mechanisms have been identified supporting this communication. The first mechanism relies on paracrine signaling, involving the release of a messenger, diffusion in the extracellular space, binding to the corresponding receptor on neighboring cells and activation of downstream signaling pathways. The second mechanism is mediated by protein-protein interactions between adjacent cells, one important example is mediated by gap junctions, connecting the cytoplasm of two neighboring cells. Gap junctions are channels with a large diameter that allow the transfer of small molecules ( $\leq 1.2$  kDa) between two adjacent cells and are composed of connexin proteins in vertebrates. In addition, there have been numerous reports that half gap junction channels, called hemichannels, present in the plasma membrane may also open under certain conditions, forming a conduit for the release of small molecules into the environment.

In chapter 4, we aimed to investigate the regulation of connexin hemichannels composed of Cx32 by changes in intracellular  $\text{Ca}^{2+}$ -concentration ( $[\text{Ca}^{2+}]_i$ ). In this study, performed on immortalized cell lines that express Cx32, hemichannel opening was studied indirectly by measuring the release of cellular ATP and the uptake of a small, fluorescent, hemichannel permeable reporter dye (propidium iodide - PI) into the cell. Elevation of  $[\text{Ca}^{2+}]_i$  by either photo-activation of  $\text{Ca}^{2+}$  from an inactive precursor probe present in the cytoplasm, or by applying the  $\text{Ca}^{2+}$ -ionophore A23187 triggered the release of ATP and the uptake of PI, indicating the activation of a bidirectional pathway. The involvement of hemichannels was based on the following observations: (i) inhibition of the responses by peptides that were identical to a short sequence of the connexin protein, (ii) inhibition of the responses by hemichannel/gap junction channel blockers, (iii) comparing the responses in Cx32 expressing cells with the corresponding wild type cells, and (iv) exclusion of alternative pathways, like the  $\text{P}_2\text{X}_7$  receptor pore. By applying various A23187 concentrations, we constructed a bell-shaped concentration-response curve for  $\text{Ca}^{2+}$ -triggered ATP release. Our results indicated that the magnitude of the  $\text{Ca}^{2+}$ -stimulus was critical, and only  $[\text{Ca}^{2+}]_i$  above 200 nM and beneath 1,000 nM were able to trigger ATP release and dye uptake, with a maximal response around 500 nM of  $[\text{Ca}^{2+}]_i$ . Blocking CaM (calmodulin) activation suppressed  $\text{Ca}^{2+}$ -induced hemichannel responses to baseline level, suggesting that this protein acts as an intermediate component between increased  $[\text{Ca}^{2+}]_i$  and hemichannel responses. CaM may act either directly on Cx32 via  $\text{Ca}^{2+}$ /CaM-Cx32 interaction, or indirectly via  $\text{Ca}^{2+}$ /CaM dependent kinases (CaMK-II).

In chapter 5, we switched to a Cx43 expressing system: Cx43 is the most ubiquitously expressed connexin and evidence for an interaction between Cx43 and CaM was available

from the literature. As for Cx32, this interaction made us hypothesize that Cx43 hemichannel opening is also regulated by  $[Ca^{2+}]_i$ . The involvement of hemichannels in  $Ca^{2+}$ -triggered ATP release was confirmed here by the criteria formulated in the previous chapter, and the additional criteria: (i) inhibition of hemichannel related responses by silencing the *gjal* gene (Cx43), and (ii) the different regulation of pannexin and connexin hemichannels observed upon comparing the results of activation of these two channels by  $[Ca^{2+}]_i$ . The  $Ca^{2+}$ -induced Cx43 hemichannel responses showed a bell-shaped concentration-response curve, with maximal ATP release around 500 nM  $[Ca^{2+}]_i$ , comparable to our data obtained with Cx32.  $[Ca^{2+}]_i$ -triggered hemichannel responses were blocked by: (i) antagonists of CaM and  $Ca^{2+}$ /CaMK-II, (ii) inhibitors of the arachidonic acid (AA) metabolic pathway, (iii) scavengers of free radicals, and (iv) inhibitors of NO synthesis. CALP1, a CaM agonist, triggered ATP release that was completely suppressed by antagonists of the AA pathway. Exogenously applied AA also triggered hemichannel responses that were inhibited by free radical scavengers, inhibitors of NO synthesis, and buffering  $[Ca^{2+}]_i$ . These results indicate activation of a signaling pathway that involves the following components:  $Ca^{2+}$  - CaM - CaMK-II - cPLA<sub>2</sub> - AA - ROS (reactive oxygen species) - NO, with a feed-back loop from AA to  $[Ca^{2+}]_i$  that amplifies the ATP responses.

From these two studies we conclude that hemichannel responses were activated with intermediate  $[Ca^{2+}]_i$  increases in the range of 500 nM, and closed again at higher  $[Ca^{2+}]_i$ . The  $Ca^{2+}$ -induced hemichannel responses were mediated by a complex signaling cascade, including some known hemichannel activators, such as the production of ROS and NO synthesis.

In the previous two chapters, we showed activation of hemichannel responses by increased  $[Ca^{2+}]_i$ . This finding is in contrast to the observation that gap junctional coupling is reduced by elevating  $[Ca^{2+}]_i$ , indicating that hemichannels and gap junction channels, although composed of the same protein are not always regulated in the same way. In [chapter 6](#), our goal was to investigate regulation of hemichannels and gap junction channels by kinase activating stimuli. Most of the connexins are phosphorylated *in vivo*, primarily on serine residues and to a lesser extent on threonine and tyrosine residues located in the carboxyterminal domain. A basal degree of phosphorylation seems to be required for the assembly and functioning of gap junctions composed of Cx43. Numerous studies have demonstrated that the influence of growth factors, oncogene protein kinases, hormones, and inflammatory mediators on gap junctional communication is mediated by phosphorylations on the carboxyterminal domain of the protein (amino acids 236 - 382). Hemichannel responses were triggered in this study by exposing the cells to a solution with low extracellular divalent cations (DF-trigger), and gap junctional communication was determined by quantification of

the transfer of a fluorescent reporter dye between neighboring cells, using either fluorescence recovery after photobleaching (FRAP) or scrape loading and dye transfer (SLDT). Our work demonstrated that some stimuli like PKC activation, c-Src transfection or LPA influenced gap junction channels and hemichannels in a similar inhibitory manner. In contrast, LPS and bFGF differentially influenced both type of channels. The effect of both substances was dependent on the cell type and the presence or absence of the carboxyterminal domain. In C6-Cx43 cells, LPS and bFGF potentiated DF-triggered ATP release via hemichannels, whereas in HeLa-Cx43 cells both substances inhibited this response. Removal of the carboxyterminal domain in HeLa-Cx43 cells (HeLa-Cx43 $\Delta$ C) abolished the ATP release, but LPS and bFGF treatment restored the hemichannel responses. Likewise, HeLa cells expressing Cx26, which has a short carboxyterminus, displayed hemichannel potentiation by LPS and bFGF. These observations suggested the contribution of other signaling pathways activated in certain cell types. Previous studies had demonstrated that LPS and bFGF may activate and translocate cPLA<sub>2</sub> via phosphorylation, thereby releasing AA from the membrane. In line with this, antagonists of the AA metabolic pathway inhibited the LPS enhancing effect on hemichannel responses and AA itself mimicked the enhancing effect of LPS and bFGF in C6-Cx43 cells, HeLa-Cx43 $\Delta$ C cells and HeLa-Cx26 cells. Taken together, our results demonstrate that the cell type specific effect of hemichannel responses were dependent on the balance between phosphorylation (inhibition) and activation of the AA signaling pathway (stimulation).

Several methods are available to study gap junctional communication, but most of them have some disadvantages, either related to  $[Ca^{2+}]_i$  changes brought about by impalement with the electrode (electrophysiology) or loading with the reporter dye (micro-injection and scrape loading and dye transfer (SLDT)), or to the fact that they report single cell coupling and not the average degree of cell-cell coupling. In [chapter 7](#), we explored a new method to quantify gap junctional communication by loading a fluorescent reporter dye in a cell monolayer via electroporation. In a first step, we optimized the electroporation settings to minimize cell death and maximize loading efficiency. In a next step, we aimed to study the transfer of the dye, loaded by electroporation, to non-loaded neighboring cells (electroporation loading and dye transfer - ELDT). We quantified the spread of the dye by determining the standard deviation of the Gaussian diffusion profile or the spatial constant of the decaying exponential dye spread at the flanks of the Gauss curve. Our results show that the degree of coupling determined with ELDT is significantly larger than observed with SLDT.

An interesting common point that emerges from our studies is the observation that hemichannel regulation is different from gap junction channel regulation. Hemichannels are closed and gap junctions are open under normal circumstances. In response to AA, hemichannels appear to open and gap junctions close. An elevation of  $[Ca^{2+}]_i$  in the range of

---

some hundred nanomolars activates the hemichannel responses, and stronger  $[Ca^{2+}]_i$  stimuli again inhibit the hemichannels and also the gap junction channels. However, the inhibition of hemichannels by strong  $[Ca^{2+}]_i$  elevation appears to be mediated by a mechanism different from the one involved in inhibition of gap junctions.

Our results indicate that the regulation of connexin hemichannels, gap junction channels, and Panx1 hemichannels by intracellular  $Ca^{2+}$  differs significantly. Given the importance of ATP as an energy substrate in the cell as well as its widespread involvement in paracrine signaling, we hypothesize that ATP release must be under exquisite and tight control. This necessitates multiple release mechanisms, a large array of control signals and a fine-tuning of the release mechanism to the most important control signal, which is intracellular  $Ca^{2+}$ . In this way, when gap junction channels are closed, cell-cell communication may be rescued via paracrine signaling pathways through the release of messengers by the various release pathways present in the cells.



## Résumé

Au sein des organismes pluricellulaires, l'existence de mécanismes de communication intercellulaire est indispensable afin de coordonner l'activité des cellules d'une même population. Deux mécanismes capables d'assurer cette communication ont été décrits. Le premier repose sur la signalisation paracrine, impliquant la libération d'un messager, sa diffusion dans l'espace extracellulaire, sa liaison aux récepteurs correspondants sur les cellules voisines et l'activation d'une cascade de signaux dans les cellules. Le second mécanisme est lié à l'interaction des protéines membranaires, comme les jonctions communicantes. Ces jonctions communicantes sont également appelées jonctions lacunaires car elles forment un pore reliant entre le cytoplasme de deux cellules voisines et permettent ainsi l'échange de petites molécules ( $\leq 1.2$  kDa) entre les deux cellules adjacentes. Chez les vertébrés, ce pore est constitué par l'association de deux éléments transmembranaires, appelés héli-canaux et constitués de connexine. De nombreux travaux mettent en évidence que lorsqu'ils ne sont pas associés au sein des jonctions lacunaires, les héli-canaux présents dans la membrane plasmique des cellules, pourraient également ouvrir, dans certaines conditions, permettre la libération de petites molécules dans l'environnement extracellulaire.

Dans le chapitre 4, nous avons étudié l'incidence des variations de la concentration intracellulaire en calcium ( $[Ca^{2+}]_i$ ) sur la régulation des héli-canaux composés de Cx32. L'ouverture des héli-canaux a été évaluée indirectement en mesurant la libération d'ATP ainsi que l'incorporation d'iodure de propidium dans des cellules immortalisées exprimant la Cx32. L'augmentation de  $[Ca^{2+}]_i$  provoquée par photo-activation du calcium à partir d'un probe inactive ou par l'application de l'ionophore calcique A23187 induit le relargage d'ATP depuis le cytoplasme des cellules et l'incorporation d'iodure de propidium indiquant l'activation d'échanges bidirectionnels à travers la membrane plasmique des cellules. L'implication des héli-canaux dans ces échanges est basée sur les observations suivantes: (i) ces échanges sont inhibés par des peptides synthétiques analogues des connexines, (ii) ainsi que par les inhibiteurs des jonctions lacunaires et des héli-canaux, (iii) l'absence de réponse dans les cellules n'exprimant pas Cx32 et (iv) l'exclusion de la participation d'autre voies tel que les pores formés par les récepteurs  $P_2X_7$ . La courbe dose-réponse construite à partir de la réponse des cellules en réponse à l'application de différentes concentrations de A23187 présente une forme en cloche et indique l'existence de valeurs calciques critiques pour stimuler le relargage d'ATP et l'incorporation d'iodure de propidium pour des valeurs de  $[Ca^{2+}]_i$  comprises entre 200 nM et 1,000 nM, la réponse maximale étant obtenue pour une  $[Ca^{2+}]_i$  voisine de 500 nM. Le blocage de l'activation de la calmoduline (CaM) prévient l'ouverture des héli-canaux induite par le  $Ca^{2+}$ , ce qui suggère que cette protéine participe à la réponse des héli-canaux à l'augmentation de  $[Ca^{2+}]_i$  soit directement via une interaction

entre le complexe  $\text{Ca}^{2+}/\text{CaM}$  avec la Cx32 ou indirectement via l'activation de kinases dépendante du complexe  $\text{Ca}^{2+}/\text{CaM}$  (CaMK-II).

Dans le chapitre 5, nous nous sommes intéressés à la Cx43 à l'aide de cellules exprimant cette connexine. Cx43 est la plus ubiquitaire des connexines et de nombreuses données de la littérature mettent en évidence l'existence de son interaction avec la CaM. Nous avons donc étudié la possibilité que l'ouverture des héli-canaux composés de Cx43 soit également régulée par la  $[\text{Ca}^{2+}]_i$ . La participation de ces héli-canaux au relargage d'ATP induit par le  $\text{Ca}^{2+}$  a été confirmée de la même façon que dans le chapitre précédent. En complément, il a été montré que (i) l'extinction du gène *gjal* codant pour Cx43 inhibe la réponse des héli-canaux aux variations de la  $[\text{Ca}^{2+}]_i$  et (ii) des mécanismes de régulation des héli-canaux de connexine différents de ceux des héli-canaux de pannexine ont été mis en évidence. La courbe de la réponse des héli-canaux Cx43 aux variations de la  $[\text{Ca}^{2+}]_i$  présente une forme en cloche avec une libération d'ATP maximale pour une  $[\text{Ca}^{2+}]_i$  d'environ 500 nM, comparable à celle obtenue avec Cx32. Nous avons également montré que la réponse des héli-canaux Cx43 aux variations de la  $[\text{Ca}^{2+}]_i$  sont bloquées par: (i) les antagonistes de la CaM et de  $\text{Ca}^{2+}/\text{CaMK-II}$ , (ii) les inhibiteurs de la voie métabolique de l'acide arachidonique (AA), (iii) les piègeurs de radicaux libres, et (iv) les inhibiteurs de la synthèse du NO. De plus, CALP1, un agoniste de la CaM, provoque un relargage d'ATP qui est complètement supprimée par les antagonistes de la voie de l'AA. Enfin, l'application d'AA exogène déclenche également une ouverture des héli-canaux qui peut-être inhibé par les piègeurs de radicaux libres, les inhibiteurs de la synthèse de NO et les chélateurs du  $\text{Ca}^{2+}$ . Ces résultats indiquent l'activation d'une voie de signalisation qui comporte les éléments suivants:  $\text{Ca}^{2+}$  - CaM - CaMK-II - cPLA<sub>2</sub> - AA - ROS - NO, avec une boucle de rétro-action de l'AA sur la  $[\text{Ca}^{2+}]_i$  qui amplifie le relargage d'ATP.

En résumé, ces deux études démontrent que les héli-canaux s'ouvrent lors d'augmentation de la  $[\text{Ca}^{2+}]_i$  à une valeur voisine de 500 nM et se referment pour de plus fortes concentration. La réponse des héli-canaux aux variations de la concentration calcique sont dépendantes d'une cascade d'activation complexe, incluant plusieurs activateurs connus des héli-canaux tel que la production de radicaux libres ou la synthèse de NO.

Dans les deux chapitres précédents, nous avons montré l'activation des héli-canaux en réponse aux augmentations de  $[\text{Ca}^{2+}]_i$ . Ce résultat est en contradiction avec l'observation d'un couplage inter-cellulaire par les jonctions lacunaires réduit lors de l'élévation de la  $[\text{Ca}^{2+}]_i$  et indique que bien qu'ils soient composé de la même protéine, les hémicanaux et les jonctions lacunaires ne sont pas régulés de la même façon. Dans le chapitre 6, nous nous sommes attachés à étudier la régulation des hémicanaux et des jonctions lacunaires en réponse à

l'activation des protéines kinases. En effet, *in vivo* la plupart des connexines sont phosphorylées, principalement sur des résidus de sérine et dans une moindre mesure de tyrosine et de thréonine situés dans le domaine carboxyterminal des connexines. Un niveau basal de phosphorylation semble donc requis pour l'assemblage et le fonctionnement des jonctions lacunaires composé de Cx43. Plusieurs études ont démontré que l'effet de nombreux stimuli (facteurs de croissance, protéines kinases oncogène, hormones, médiateurs de l'inflammation) sur la communication par les jonctions lacunaires est médié par des phosphorylations de sites situés dans le domaine carboxyterminal de la protéine (acides aminés 236 - 382). Dans cette étude, nous avons étudié la réponse des héli-canaux déclenchée par l'exposition des cellules aux faibles concentrations extracellulaires en ions divalents, et la communication entre les cellules par les jonctions lacunaires a été déterminée en mesurant soit la redistribution de fluorescence après photoblanchiment (FRAP) soit le transfert d'une molécule fluorescente entre les cellules adjacentes (SLDT pour Scrape Loading and Dye Transfer; la technique de la charge et le transfert de marqueur par griffe). Ces travaux ont montré que certains stimuli comme l'activation de la PKC, la transfection par le c-Src ou la LPA inhibaient à la fois le fonctionnement des jonctions communicantes et celui des héli-canaux. En revanche, d'autres stimuli comme le LPS et le bFGF exercent des effets différents sur les deux types de canaux. De plus, l'effet de ces deux substances est dépendant du type de cellule et de la présence du domaine carboxyterminal. Dans les cellules C6-Cx43, le LPS et le bFGF potentialisent le relargage de l'ATP par les héli-canaux induits par les faibles concentrations en ions divalents extracellulaire, alors que dans les cellules HeLa-Cx43 ces deux substances inhibent cette réponse. La délétion du domaine carboxyterminal de Cx43 dans les cellules HeLa-Cx43 (HeLa-Cx43ΔC) abolit la libération d'ATP par les héli-canaux, mais celle-ci est restaurée par le traitement au LPS ou au bFGF. De même, dans les cellules HeLa exprimant Cx26, qui possède un domaine carboxyterminal très court, le traitement au LPS ou au bFGF potentialise la réponse des héli-canaux. L'ensemble de ces observations suggérait l'activation d'autres voies de signalisation dans certains types de cellules. Il a notamment été montré que le LPS et le bFGF peuvent activer et transloquer cPLA<sub>2</sub> par phosphorylation, libérant ainsi de l'AA de la membrane. Il apparaissait donc intéressant de tester l'hypothèse que l'AA soit un second messager de l'effet du LPS et du bFGF sur la réponse des héli-canaux. Nous avons ainsi montré que les antagonistes de la voie de l'AA bloquent la restauration de la réponse des héli-canaux par le LPS ou le bFGF. De plus, l'AA lui-même reproduit les effets potentialisateurs du LPS et du bFGF sur la réponse des héli-canaux dans les C6-Cx43, les HeLa-Cx43ΔC et les HeLa-Cx26. L'ensemble de ces résultats démontre que la spécificité de la réponse des héli-canaux selon le type cellulaire est tributaire de l'équilibre entre la phosphorylation (inhibition) et l'activation de la voie de signalisation de l'AA (stimulation).

De nombreuses méthodes permettent d'étudier la communication intercellulaire par les jonctions lacunaires, cependant la plupart présentent de nombreux inconvénients. Dans chapitre 7, nous avons donc évalué une nouvelle méthode permettant de quantifier ces intercommunications basée sur l'incorporation d'une sonde fluorescente par électroporation. Dans un premier temps, nous avons optimisé les paramètres d'électroporation afin de minimiser la mort cellulaire, et d'augmenter l'efficacité de chargement. Puis, nous avons étudié le transfert de la sonde fluorescente depuis les cellules chargées par électroporation, vers les cellules voisines non chargées par cette technique appelé ELDT pour la charge et le transfert de marqueur par électroporation. La quantification de la communication par le transfert de marqueur est faite par déterminer la déviation standard ou la constante spatiale de la propagation exponentielle diminuante. Nos résultats montrent que le degré de couplage déterminé avec ELDT est sensiblement plus grand quand on se compare avec la technique de la charge et le transfert de marqueur par griffe.

En conclusion, nos travaux indiquent que la régulation du fonctionnement des hémi-canaux est différente de celles des jonctions lacunaires. Dans les conditions normales les hémi-canaux sont fermés et les jonctions lacunaires ouvertes. A l'inverse, en réponse à l'AA, les hémi-canaux s'ouvrent tandis que les jonctions lacunaires se ferment. Une élévation de la  $[Ca^{2+}]_i$  de l'ordre de quelques centaines de nanomolaires active les hémi-canaux alors que des augmentations de  $[Ca^{2+}]_i$  plus importantes inhibent à la fois les hémi-canaux et les jonctions lacunaires. Toutefois, cette inhibition des hémi-canaux et des jonctions lacunaires par les fortes  $[Ca^{2+}]_i$  semble induites par des mécanismes différents. Enfin, nos résultats suggèrent que la régulation par  $[Ca^{2+}]_i$  est différente entre des jonctions lacunaires et des hémi-canaux, constitués soit de connexine soit de pannexin. Donnée l'importance d'ATP comme substrat d'énergie cellulaire, aussi bien que son participation répandue en la signalisation paracrine, nous suggérons que la libération d'ATP doit être régulée très serrée. Ceci demande plusieurs mécanismes de libération, une grande rangée des signaux de contrôle et une régulation très stricte du rélagage d'ATP par le calcium cytoplasmique. De cette manière, dans les conditions où les jonctions lacunaires sont fermées, la communication cellulaire est à nouveau assurée par les voies de signalisation paracrine grâce à la libération messagers par ces différentes voies de sécrétion présentes dans les cellules.

# Chapter

## ***1 Introduction***

In theory, there is no difference between theory and practice,  
but in practice there is a great deal of difference.

-Chernicoff's Law-

## 1.1 Cell-cell communication and homeostasis

The formation of multicellular organisms necessitated the development of different forms of cell-cell communication to coordinate the activity of different groups of cells. Specialized but distinct structures have evolved independently to provide direct cell-to-cell communication in plants (plasmodesmata - Meiners et al. (1988)), fungi (septal pores - Belozerskaya (1998)) and animals (gap junctions - Finbow et al. (1983)). Rustom et al. (2004) recently discovered tunneling nanotubes which represented a novel form of direct communication between mammalian cells. These nanotubes were correlated with the transfer of organelles and membrane vesicles from one cell to another (Rustom et al., 2004). In contrast to gap junctions, tunneling nanotubes can accomplish long range communication between dislodged cells and have a diameter of 5 - 20 Å (Ångstrom - Gerdes et al. (2007)).

Gap junctions are the only junctional structures conserved in all multicellular organisms from mesozoa (minuscule, worm-like parasites) to humans. Despite the maintenance of a morphological similar structure (heptalaminar appearance with an intercellular gap) and functional properties (permeable to ions and molecules  $\leq 1.2$  kDa; kilodalton), genomic analysis revealed an interesting case of convergent evolution across the animal kingdom, whereby unrelated protein families have evolved to perform similar functions. It has been demonstrated that gap junctions in protostomes (like nematodes and flies) are composed of innexins (Phelan and Starich, 2001; Bauer et al., 2005; Phelan, 2005), whereas in deuterostomes (including all vertebrates) gap junctions are composed of connexin proteins (Willecke et al., 2002). Innexins are currently regarded as the most ancient proteins that provide intercellular communication in primitive organisms (diploblasts) that precede the protostome/deuterostome bifurcation (Alexopoulos et al., 2004). Innexins were inherited by protostomes, while connexins arose *de novo* in deuterostomes. Recently, a novel family of gap junction genes, the pannexins, were discovered in the genomes of the vertebrates and tunicates (invertebrate chordates - Panchin et al. (2000)). It is suggested that innexins and pannexins belong to a single superfamily (Yen and Saier, 2007).

Gap junction channels composed of connexins, innexins or pannexins all span the plasma membrane of the two connected cells and are multimeric complexes resulting from the association of two hemichannels, each composed of six connexins/innexins/pannexins. These proteins all share the same membrane topology: amino- and carboxyterminal domains located in the cytosol, 4 transmembrane spanning  $\alpha$ -helices, two extracellular loops that form anti-parallel  $\beta$ -sheets stabilized by intramolecular disulfide bonds (Foote et al., 1998), and one cytoplasmic loop. These three proteins are characterized by regularly spaced cysteine residues in the two extracellular loops (Unger et al., 1999). Whereas connexins contain three such cysteine residues, innexins and pannexins only contain two, although the spacing of these

cysteine residues in the second extracellular loop of pannexins differs from that of innexins (Hua et al., 2003).

### 1.1.1 Connexins

Mammalian connexins are encoded by a gene family of close to 20 members (21 genes in the human and 20 in the mouse genome - Willecke et al. (2002)). Although nomenclature is under debate, encoded proteins are currently designated CxMW (where MW represents the molecular weight in kDa of the protein, ranging from 25 to 60 kDa). Gene nomenclature is indicated by *gjaN*, *gjbN* and *gjcN*, where a (group II; Cx33, 37, 40, 43, 46, 50, 59, 62, the non-mammalian Cx39.9 and the fish-specific Dr17927), b (group I; Cx25, 26, 30, 30.3, 31, 31.1, 32 and the fish-specific groups of DrCx28.6, 33.8 and 34.4) and c (group III; IIIa: Cx31.9, 36, 39.2, 40.1 and the fish-specific Dr17927; group IIIb: Cx31.3, 45, 47 and the non-mammalian Cx43.4) refer to the subfamilies based on sequence similarity and *N* refers to the order in which they were described (Kumar and Gilula, 1996; Sohl and Willecke, 2003; Cruciani and Mikalsen, 2007). Gap junction channels exhibit conductances that vary between 5 and 370 pS (picosiemens - Moreno and Lau (2007)) and cells may express more than one connexin isoform, which can result in the formation of heteromeric connexin hemichannels and heterotypic gap junction channels (Figure 1). Variation in connexin stoichiometry provides a basis for the selectivity of channels and a mechanism that allows cells to dynamically regulate their intercellular communication properties (Saez et al., 2003). Heteromeric compatibility corresponds loosely to a and b connexin subfamilies (Harris, 2001; Cottrell and Burt, 2005) and connexins not belonging to either of these subgroups have been found to form heteromers with either a connexins (Koval et al., 1995) or b connexins (Altevogt et al., 2002). To date, no connexin has been identified that forms normal heteromeric channels with a and b subfamily connexins. In contrast to innate heteromeric compatibility, innate heterotypic compatibility does not correlate with a or b subfamily membership (Elfgang et al., 1995; Harris, 2001), but is determined by the second extracellular loop (White et al., 1995; Harris, 2001).

Connexins are no longer viewed as passive pores for the free non-selective transfer of ions and small molecules, but are now believed to fulfill specific functions. Proof of this concept came from studies in which one connexin was replaced by another via genetic knock-in studies, thereby providing a direct test for the importance of connexin quality versus quantity in intercellular communication (Plum et al., 2000; White, 2002). Several studies have already shown that hemichannels before docking into gap junction channels open under several physiological and pathological conditions and in this way form a conduit for the release of small molecules (Goodenough and Paul, 2003).

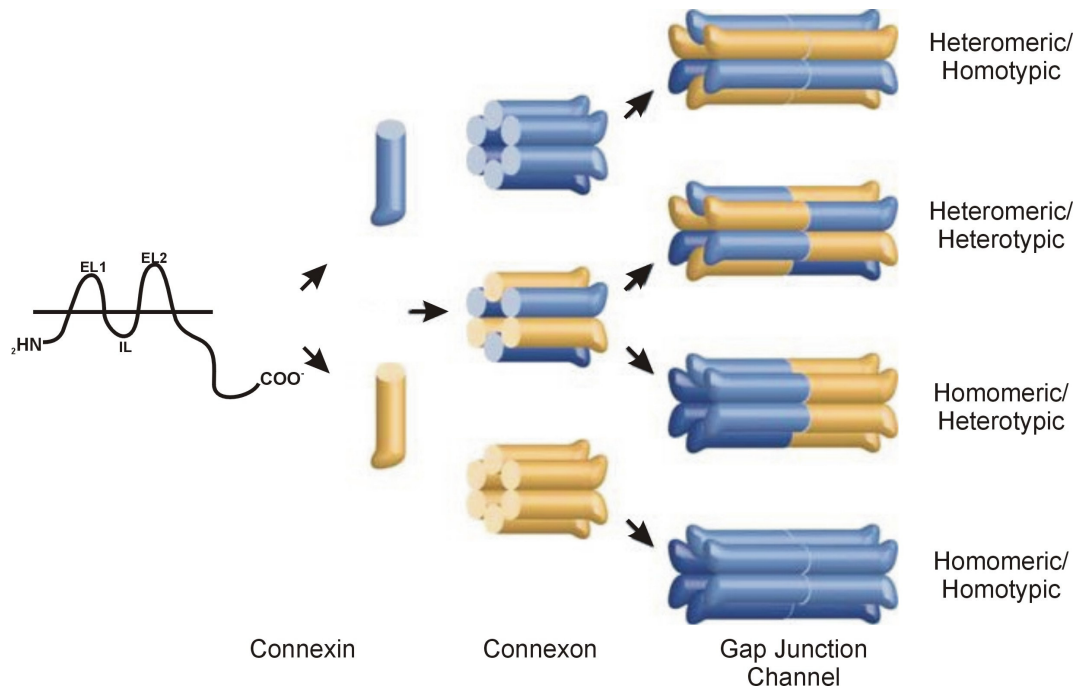


**Figure 1: Schematic representation of hemichannels and gap junction channels**

Six connexins oligomerize to form connexons or hemichannels. Hemichannels of two neighboring cells align to form functional gap junction channels. Different connexins can selectively interact with each other to form homomeric, heteromeric and heterotypic channels, differing in their content and spatial arrangement of connexin subunits. Figure adapted from Mese et al. (2007).

### 1.1.2 Innexins

In total, 25 *Caenorhabditis elegans* (*Ce-INX*) and 8 *Drosophila melanogaster* (*Dm-INX*) innexins have been identified. These proteins have a high sequence homology, but are not functionally interchangeable and are probably engaged in similar roles as connexins (Curtin et al., 2002; Stebbings et al., 2002; Li et al., 2003; Starich et al., 2003; Bauer et al., 2004; Dykes et al., 2004). In line with the basic properties of connexin channels, some innexins can form both heteromeric and heterotypic channels. It has recently been shown by Bao et al. (2007) that innexins from *Hirudo medicinalis* (*Hm-INX1*, *Hm-INX2*, *Hm-INX3*, and *Hm-INX6*) form functional hemichannels with a single channel conductance of 250 pS (*Hm-INX1*) and 500 pS (*Hm-INX2*, 3 and 6) when being overexpressed in *Xenopus laevis* oocytes (Bao et al., 2007). These channels are activated by increasing intracellular  $\text{Ca}^{2+}$ -concentrations ( $[\text{Ca}^{2+}]_i$ ) to the micromolar range, and by depolarization to -20 mV (millivolt - Bao et al. (2007)).



### 1.1.3 Pannexins

Currently, there are three known pannexins in human and rodent genomes and orthologous sequences have been identified in *Danio rerio* and *Ciona intestinalis* (Sasakura et al., 2003; Baranova et al., 2004; Bruzzone et al., 2005). Pannexins are referred to with the abbreviation Panx, followed by the progressive Arabic number that distinguish them. Northern blot analysis indicate that Panx1 and Panx2 transcripts are present in many rodent tissues, including brain and spinal cord, eye, thyroid, prostate and kidney (Bruzzone et al., 2003; Ray et al., 2005; Vogt et al., 2005; Weickert et al., 2005). The widespread distribution of Panx1 is confirmed in human tissues, with the highest levels being found in heart, gonads and skeletal muscle (Baranova et al., 2004). The presence of Panx1 transcripts in adult human skeletal muscle is odd given the syncytial nature of this tissue, which does not form gap junctions (Bruzzone et al., 2003; Ray et al., 2005). If the Panx1 protein is indeed expressed, it may function as a hemichannel or have intrinsic signaling properties. In addition, Panx2 distribution appears to be restricted to the brain in humans (Baranova et al., 2004), while being co-expressed with Panx1 in many organs in rodents (Bruzzone et al., 2003). Panx3 transcripts are only detected in the skin, which lacks Panx1 and Panx2 mRNA. Homomeric Panx1 hemichannels, homomeric Panx3 hemichannels and heteromeric Panx1-Panx2 hemichannels are functional, while homomeric Panx2 hemichannels are not (Bruzzone et al., 2003; Penuela et al., 2007).

### 1.1.4 Connexin trafficking, oligomerization and degradation

Connexins are co-translationally inserted into the endoplasmic reticulum (ER) membranes and transported via the Golgi apparatus and the *trans*-Golgi network to the plasma membrane in vesicles (Figure 2 - Segretain and Falk (2004)). Along with the trafficking from the ER to the plasma membrane, connexins oligomerize into hexameric structures called connexons or hemichannels, via dimeric and tetrameric intermediates (Segretain and Falk, 2004). *In vitro* approaches have shown that this oligomerization process is calmodulin (CaM) dependent (Ahmad et al., 2001). Removal of the CaM binding site in Cx32 inhibits the formation of hemichannels and results in the intracellular accumulation of connexins (Ahmad et al., 2001). During transport, hemichannels are kept in a closed configuration in the organelle membrane, by the CaM interaction, to maintain a steep ionic gradient between the cell's luminal and cytoplasmic environment (Peracchia et al., 2000a).

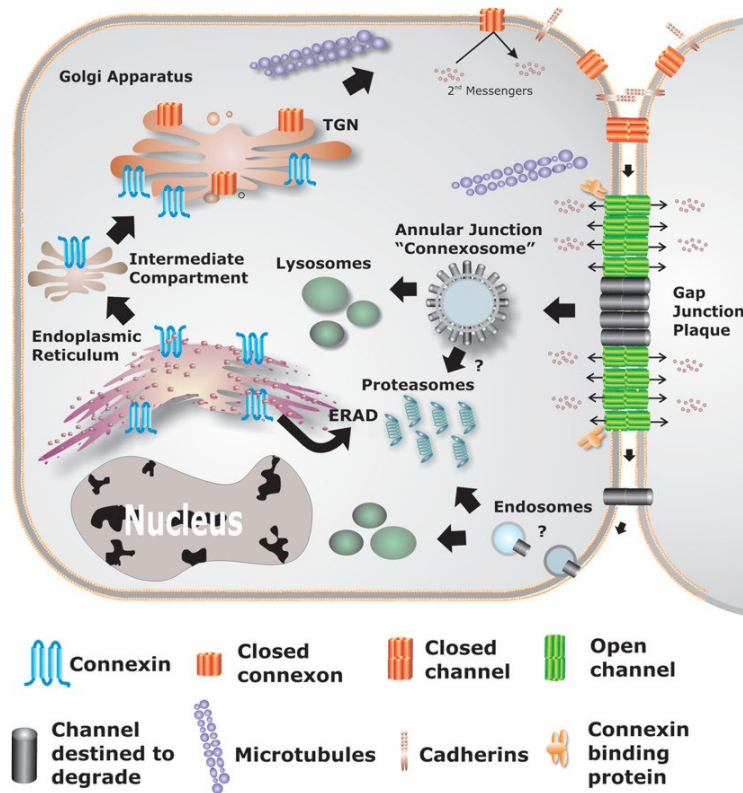


**Figure 2: The life cycle of connexons and gap junction channels**

Connexins are co-translationally inserted into the ER. Connexins with abnormal conformation undergo ER-associated degradation (ERAD). After passage through the intermediate component of the Golgi apparatus connexins are completely oligomerized. New hemichannels are recruited to the borders of the existing gap junctional plaque and older channels are found in the center of the plaque.

Gap junctional plaques are internalized into one of the two neighboring cells as a double-membrane structure commonly referred to as annular gap junctions or connexosomes. These structures are further degraded by lysosomes and proteasomes (Laird, 2006).

The transit from the ER to the plasma membrane is connexion specific: Cx26 transport depends on the presence of intact microtubuli, while Cx32 trafficking is mediated by a functional Golgi apparatus (George et al., 1999; Falk, 2000; Martin et al., 2001). The microtubule-dependent transport to the plasma membrane explains the rapid formation of Cx26 hemichannels relative to other subtypes in some tissues (Kojima et al., 1994; Nadarajah et al., 1997; Labarthe et al., 1998; Locke, 1998). Cx43 levels at the plasma membrane can also be modulated by fast-track assembly pathways that operate independently of the Golgi apparatus and require an intact microtubule network (Paulson et al., 2000; Lauf et al., 2002). The presence of a leucine at position 28 in Cx26 and Cx43 may partially explain the ability of these connexins to follow a rapid microtubule-dependent pathway under certain conditions, since Cx32 contains an isoleucine at this position and the mutation Cx32 I28L adopted the post-translational, microtubule-dependent trafficking associated with Cx26 and Cx43 (Martin et al., 2001). Hemichannels that reach the center of the plaque become internalized for

degradation as annular gap junctions or connexosomes (Jordan et al., 2001; Segretain and Falk, 2004; Laird, 2005; Laird, 2006).

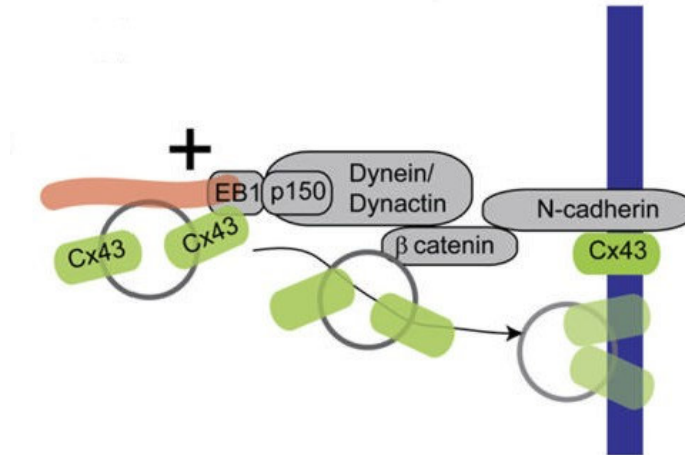


**Figure 3: Trafficking of Cx43 hemichannels to the plasma membrane at the site of cell-cell contacts**

Cx43 hemichannels are transported to the plasma membrane via a microtubule-mediated mechanism. Microtubuli are linked via EB1 to the dynein/dynactin complex, that interacts with cadherins via the linker protein,  $\beta$ -catenin. In this way, Cx43 hemichannels are preferentially inserted in the membrane in the proximity of the adherens junctions (Shaw et al., 2007).

In multiple tissues, gap junctions co-localize with adherens junctions, formed by cadherins. At the cardiac intercalated discs the adherens junctions are assembled prior to the formation of the Cx43 gap junction plaque (Angst et al., 1997). Several studies indicate that a correct establishment of adherens junctions is required for a correct formation of the gap junctional plaque (Jamora and Fuchs, 2002). Shaw et al. (2007) have shown that knocking-down p150(Glued) (a subunit of the dynein/dynactin complex), knocking-down EB1 (a microtubule plus-end-tracking protein; +TIPS) or knocking down  $\beta$ -catenin (a cytoplasmic binding partner of the cadherins) results in a disrupted gap junction formation (Shaw et al., 2007). These authors propose a mechanism, whereby hemichannels preferentially reach the plasma membrane at the site of the adherens junctions via a direct microtubule-mediated delivery. p150(Glued) localizes at the adherens junctions through direct binding of  $\beta$ -catenin (Ligon et al., 2001). EB1 associates with rapidly growing microtubule plus-ends (Schuyler and Pellman, 2001) and binds to p150(Glued), providing a link between microtubules and the adherens junctions (Askham et al., 2002; Hayashi et al., 2005). Furthermore, EB1 also interacts with Cx43 forming a bridge between the gap junction plaque and the adherens junctions, thereby facilitating hemichannel delivery at sites of cell-cell contact via direct microtubule-mediated transport (Figure 3 - Shaw et al. (2007)). This model suggests that disruption of adherens junctions contributes directly to the rearrangement of gap junctions, as observed in some cancer cells.

The majority of plasma membrane proteins have a relatively slow turn-over rate with half-lives exceeding 24 h (Hare and Taylor, 1991). Surprisingly though, gap junction channels are rather dynamic structures which are constantly renewed at the cell surface. Pulse-chase experiments have revealed that many connexins have a high turn-over rate with half-lives ranging from 1.5 (Cx43) to five hours (Cx26 - Musil et al. (1990a); Laird et al. (1991); Darrow et al. (1995); Herve et al. (2007)). Similar results have been reported in whole organs (Beardslee et al., 1998) and intact animals (Fallon and Goodenough, 1981). While it is apparent that not all connexins are short-lived (Cx46 in the lens has a half-life of more than one day - Jiang et al. (1993)), the exceptional metabolic lability of many members of the connexin family suggests that processes involving degradation may provide a mechanism to regulate gap junctional communication under normal and pathological conditions (Traub et al., 1983; Luke and Saffitz, 1991; Laird, 1996; Beardslee et al., 1998; Musil et al., 2000). Two major pathways for the degradation of cellular proteins have been described: the lysosome and the proteasome. Both processes are involved in the degradation of gap junctions (Figure 2). Lysosomes are membrane-bound organelles that contain an array of acidic hydrolases, including proteolytic enzymes (Bohley and Seglen, 1992), which commonly degrade membrane proteins, receptors and macromolecules that enter the cell via endocytosis (Hicke, 1999). In contrast, the proteasome is a large multi-protein complex, responsible for the regulated degradation of most cytosolic and nuclear proteins, as well as some membrane proteins (Coux et al., 1996).

The participation of lysosomes in the degradation of gap junctional plaques was proposed after the observation of clathrin-coated intracellular vesicle-like double-membrane structures, called annular gap junctions or connexosomes (Bjorkman, 1962; Larsen et al., 1979; Mazet et al., 1985; Gregory and Bennett, 1988; Severs et al., 1989; Vaughan and Lasater, 1990; Naus et al., 1993; Huang et al., 1996). Clathrin-mediated endocytosis is directed by a tyrosine-based sorting signal (Canfield et al., 1991; Bonifacino and Dell'Angelica, 1999). This sequence is present in the carboxyterminal domain of many connexins (Thomas et al., 2003) and corresponds to the consensus sequence Yxx $\phi$  (where Y is tyrosine, x is any amino acid and  $\phi$  is a hydrophobic amino acid, such as valine, phenylalanine or isoleucine). The alternative potent clathrin adaptor Dab2 (Disabled-2) is recruited to Cx43 gap junctions, through a direct interaction between the aminoterminal phosphotyrosine binding (PTB) domain of Dab2, with the tyrosine-based sorting signal present in the carboxyterminal domain of Cx43 (Figure 4 - step 1). The distal portion of Dab2 binds the globular aminoterminal domain of the clathrin heavy chain and triggers clathrin lattice assembly. The GTPase dynamin is also recruited to the gap junctions, resulting in a double-membrane protrusion/invagination, neck restriction, and double-membrane scission (Figure 4 - step 2). In a next step, Dab2 associates through its carboxyterminal serine- and proline-rich region with

the carboxyterminal globular tail of myosin-VI that binds to the aminoterminal motor domain of actin filaments, resulting in the inward translocation of the double-membrane gap junction vesicle (Figure 4 - step 3; Piehl et al. (2007)). Connexosomes undergo a maturation process from double-membrane vacuoles to multivesicular endosomes with a single limiting membrane (Figure 4 - step 4 and 5; Leithe et al. (2006)). This transformation is associated with trafficking of Cx43 to the early and late endosome, prior to degradation by the lysosome (Leithe et al., 2006). In light of the lack of annular gap junctions in some cell types, it is unlikely that this represents the sole mechanism for connexin degradation.

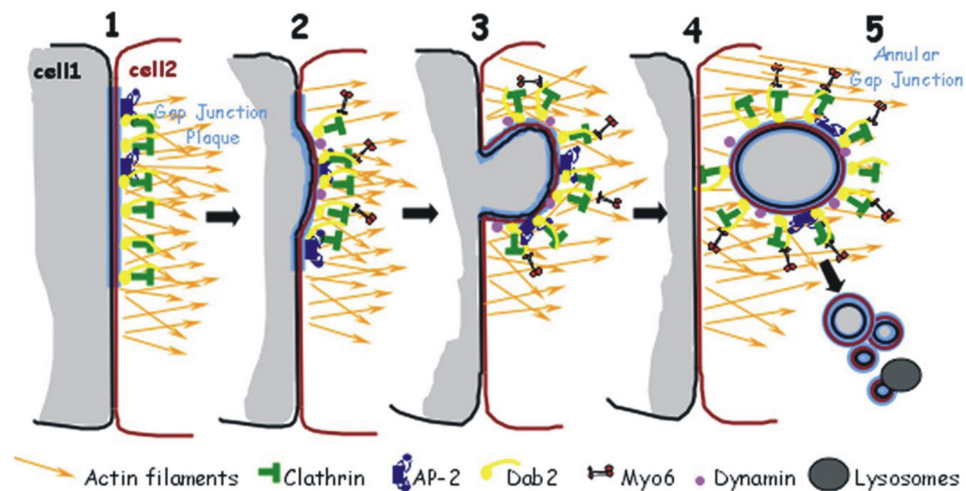


**Figure 4: Schematic overview of internalization of gap junctions**

(1) Clathrin is recruited to Cx43 containing gap junctions via the clathrin adaptor protein Dab2 and AP-2. (2-3) Dynamin is also recruited to the gap junctions to trigger double-membrane protrusions/invaginations, neck restriction and double-membrane scission. (4) The binding between Dab2 and Myosin-VI (Myo6) results in the inward translocation of the internalized double-membrane gap junction vesicle. (5) The formed annular gap junction fragments into smaller vesicles that are degraded by the lysosomal pathway (Piehl et al., 2007).

Proteasomal degradation is directed by ubiquitination, a process whereby ubiquitin moieties are covalently attached to target proteins. This forms a signal for proteasomes to selectively recognize their substrate. Ubiquitination is mediated by an enzymatic cascade, including E1 (ubiquitin-activating enzyme), E2 (ubiquitin-conjugating enzyme) and E3 (ubiquitin-protein ligase, providing substrate specificity - Weissman (1997); Hershko and Ciechanover (1998)). Proteins can be conjugated to a single ubiquitin (Hicke and Dunn, 2003), to multiple mono-ubiquitins, or to a poly-ubiquitin side chain, in which the ubiquitins are linked through lysine residues (Leithe and Rivedal, 2007). An interaction between the proline-rich PY motif of Cx43 and the WW domain (a short phosphoserine and phosphothreonine binding motif) of Nedd4, an E3 ubiquitin-protein ligase, was shown and this interaction is modulated by Cx43 phosphorylation (Leykauf et al., 2006). The PY motif consists of xxPPxY, where P is proline and x any amino acid and overlaps with the tyrosine-based sorting signal (SPPGYKLV in Cx43) required for clathrin-mediated endocytosis (Thomas et al., 2003).

Together, these studies indicate that the proteasome and the lysosome probably cooperate to degrade connexins. Hereby, the proteasome provides partial proteolysis of the gap junctional plaque at the cell surface. This is necessary for the endocytotic machinery to further degrade the gap junctions. Electron microscopy studies provide evidence for such a mechanism, as gap junctions are broken up into small aggregates in hepatocytes during removal from the plasma membrane (Fujimoto et al., 1997). Alternatively, proteasomal activity may affect the turn-over of other molecules, which are directly involved in gap junction endocytosis. Further work is certainly needed to understand the exact mechanism of connexin degradation in full detail.

## 1.2 Channel gating

The word gating is often used loosely to refer to molecular channel transitions in its way to opening and closing, broadly meaning that during gating, a conductive pathway becomes either physically available or unavailable (Hille, 1978). In this way, any sub-cellular level in which gap junction channels or hemichannels undergo a conformational change that reversibly alters their permeability can be considered as a gating event. The activity of gap junctions, expressed by the macroscopic conductance ( $G_j$ ), is determined by three factors: (i) the number of channels present at the plasma membrane ( $N$ ), (ii) the open probability ( $P_o$ ), and (iii) the unitary conductance of the channel ( $\gamma_j$  - Herve et al. (2007)). These three parameters are correlated to each other ( $G_j = N \times P_o \times \gamma_j$ ), but only two of them are related to real gating (unitary conductance and open probability).  $N$ , the number of channels, can be affected by inserting or removing hemichannels from the plasma membrane. Although this will certainly affect gap junctional communication or hemichannel responses, it cannot be considered as a gating phenomenon.

### 1.2.1 Selective connexin permeability and conductance

Small hydrophilic molecules  $\leq 1.2$  kDa are able to move through the gap junction pore, with a 20 Å diameter in Cx43 and mediate in this way the direct transfer of signals and small metabolites between the cytoplasm of two neighboring cells, which are said to be coupled. Gap junctional coupling is however not indiscriminant, it is a highly delimited process dependent on the connexin isoforms comprising the junctions. An obvious and conceptually simple approach for the study of channel permeability is to introduce a visible tracer, such as a fluorescent reporter dye, into the cell and measure its diffusion into neighboring cells. These tracer dyes must exhibit two characteristics: (i) they must be hydrophilic enough to prevent direct transfer through the lipid bilayer of the cell membrane, and (ii) they must be small enough to fit the aqueous pore of gap junction channel (Table 1 - Schwarzmann et al. (1981)).

Molecule	Molecular Weight (Dalton)	Charge
Hydroxycoumarin Carboxylic Acid	206	-6
DAPI (4',6-diamidino-2-phenylindole)	279	+2
Neurobiotin	287	+1
Ethidium Bromide	314	+1
Calcein Blue	321	0
Alexa 350	349	-1
6-Carboxyfluorescein	376	-2
Dichlorofluorescein	401	-1
Propidium Iodide	415	+2
Lucifer Yellow	443	-2
Alexa 488	570	-1
Calcein	623	-4
Alexa 594	759	-1

**Table 1: Synthetic reporter dyes used to evaluate gap junctional coupling**

Overview of synthetic dyes used to evaluate gap junctional communication. The net charge of the molecules is indicated at neutral pH. Neurobiotin is not fluorescent, but can be detected using fluorescent labeled avidin or streptavidin. Table adapted from Alexander and Goldberg (2003).

While fluorescent tracers can be used to detect large changes in gap junctional communication, other methods are needed to evaluate more subtle effects. Furthermore, synthetic reporter dyes may not accurately represent the ability of biological molecules to travel through gap junctions (Goldberg et al., 1999; Goldberg et al., 2000). Measuring the electrical conductance between two cells is exquisitely sensitive and can be quantified very precisely (Harris, 2001). This technique requires simultaneous voltage-clamping of two adjacent cells. In this mode of dual whole-cell-recording, voltage is controlled by currents that are introduced through electrodes placed into the cells. The intercellular flow of ions through gap junction channels can be calculated from the currents required to maintain the differences in membrane voltage, imposed between the paired cells in dual whole-cell clamp (Harris, 2001). The total conductance of the channel is calculated by dividing the transjunctional current, passing through the open channels by the voltage difference between the two coupled cells. Single channel transitions can be determined through the change of the clamp current, as the channel opens and closes (Veenstra and DeHaan, 1986; Harris, 2001). Dividing the total conductance by the unitary conductance will calculate the number of open channels at a given time point. A number of studies have illustrated the selective permeability of homotypic gap junctions for monovalent ions. While unitary conductances vary widely (25 pS for Cx45 and 350 pS for Cx37), the sequence of monovalent cation selectivity is the same for Cx43, Cx40, Cx37 and Cx45:  $K^+ > Na^+ > Li^+ > TMA > TEA$  (Veenstra et al., 1994a; Veenstra et al., 1995; Beblo and Veenstra, 1997; Wang and Veenstra, 1997).

Using a technique called transport specific fractionation, selective permeabilities of different connexin isoforms were determined (Bevans et al., 1998; Bevans and Harris, 1999; Ayad et al., 2006). This technique separates liposomes with channels from liposomes without channels

through an iso-osmotic density gradient formed by urea and sucrose solutions. Channels with an open probability higher than 0.001 % will mediate full exchange of osmolytes and will cause the liposome movement to the characteristic lower position. It was demonstrated that cGMP (cyclic guanosine monophosphate) and cAMP (cyclic adenosine monophosphate) pass equally well through homomeric Cx32 hemichannels. However, heteromeric Cx26-Cx32 hemichannels allow the passage of cGMP more efficiently, when compared to cAMP, indicating that the presence of Cx26 restricts the passage of the latter (Figure 5A - Bevans et al. (1998); Bevans and Harris (1999)). In subsequent work, these authors showed that nanomolar concentrations of cAMP and cGMP block the transfer of molecules through homomeric Cx32 and heteromeric Cx26-Cx32 hemichannels. Interestingly, this effect is specific in that other nucleotides, such as AMP (adenosine monophosphate), ADP (adenosine diphosphate), ATP (adenosine triphosphate), cTMP (cyclic thymidine monophosphate) and cCMP (cyclic cytidine monophosphate) are not effective. These data suggest high affinity interactions between Cx26/Cx32 and particular cyclic nucleotides, in this way controlling the intracellular flow of specific molecules (Bevans and Harris, 1999).

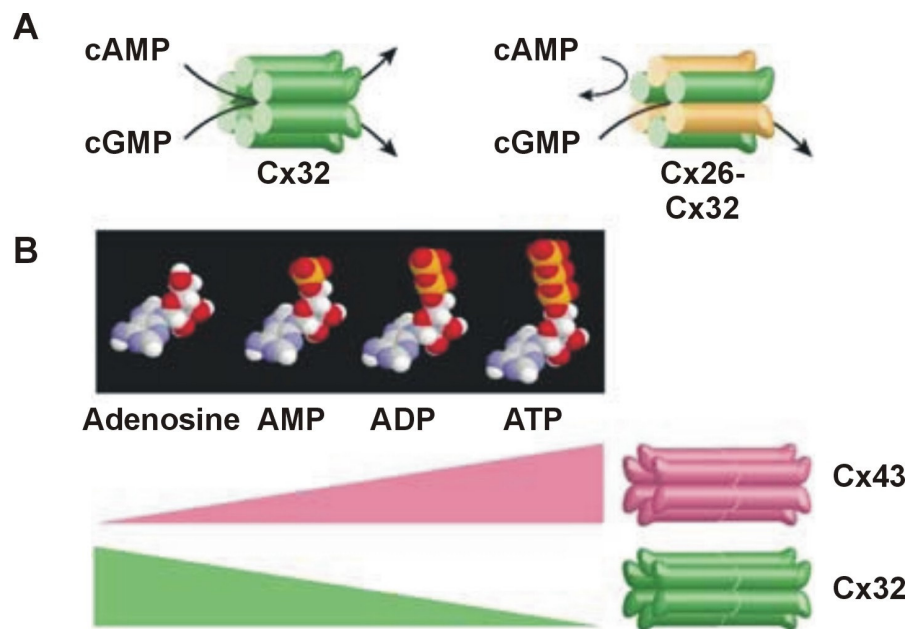


**Figure 5: Selective permeability of gap junctions to second messengers**

(A) cAMP and cGMP pass equally well through homomeric Cx32 hemichannels, whereas the transfer of cAMP is reduced by the presence of Cx26 in heteromeric Cx26-Cx32 hemichannels (Bevans et al., 1998; Bevans and Harris, 1999). (B) The addition of extra phosphate groups to adenosine changes its relative permeability through gap junctions. Cx32 gap junctions were more permeable to adenosine than channels formed by Cx43, whereas Cx43 gap junction channels were more permeable to ATP (Goldberg et al., 1999; Mese et al., 2004; Mese et al., 2007)

Ayad et al. (2006) has investigated the selective permeability of Cx26 and Cx32 channels for myoinositol and other inositol phosphates (1-InsP; 1,4-InsP<sub>2</sub>; 1,4,5-InsP<sub>3</sub>; 1,3,4-InsP<sub>3</sub>; 1,4,6-InsP<sub>3</sub>; 1,3,4,5-InsP<sub>4</sub>; and 3,4,5,6-InsP<sub>4</sub> - Figure 6) using transport specific fractionation (Ayad



et al., 2006). Homomeric Cx26, homomeric Cx32 and heteromeric Cx26-Cx32 hemichannels, irrespective of the Cx26-Cx32 composition ratio (Cx26-Cx32 ratio: 1:5; 2:4 and 5:1), were permeable to myoinositol, 1-InsP and 1,4-InsP<sub>2</sub>. Selectivity was only observed when more than two phosphate groups were present on the myoinositol ring and only for Cx26-Cx32 heteromeric channels. In each of the populations of heteromeric channels, the fraction of channels permeable to 1,4,6-InsP<sub>3</sub>, 1,3,4-InsP<sub>3</sub>, or 1,3,4,5-InsP<sub>4</sub> was far less than the fraction permeable to 1,4,5-InsP<sub>3</sub>. It may be concluded that connexin channels are fine-tuned to select among the cytoplasmic molecules to which they are exposed *in situ*. The ability of Cx26-Cx32 heteromeric channels to discriminate between different inositol trisphosphates (1,4,5-InsP<sub>3</sub>; 1,4,6-InsP<sub>3</sub> and 1,3,4-InsP<sub>3</sub>) was surprising, giving the fact that these isomers have the same molecular weight and net charge and that the only difference is the location of the phosphate groups on the myoinositol ring, affecting charge distribution and chemical reactivity of these groups. This finding emphasizes the importance of the spatial configuration of charged groups on the biological selectivity of permeation through connexin channels. The obtained data is most consistent with a mechanism in which, at least for Cx26-Cx32 heteromeric channels and this class of second messengers, a molecule must interact appropriately with a highly selective, but likely low affinity binding site in the pore in order to permeate and that molecules not interacting, cannot pass through the channel. The requirement of heteromericity for selectivity suggests that such a site involves structural contributions from more than one connexin isoform (Ayad et al., 2006). Examination of known inositol phosphate binding sites did however not reveal amino acid sequence similarity between Cx26/32 and conserved residues in the 1,4,5-InsP<sub>3</sub> receptor binding core or the 1,4,5-InsP<sub>3</sub> coordinating residues (Bosanac et al., 2002). The most unexpected finding in the study of Ayad et al. (2006) was that homomeric Cx26 channels were permeable to all inositol phosphates. This is inconsistent with the more restrictive permeability with increased Cx26 content reported in other studies (Bevans et al., 1998; Niessen et al., 2000; Locke et al., 2004). One possibility is that Cx26-Cx32 channels, because of their heteromeric nature, have an irregular or narrowed lumen relative to both types of homomeric channels (Ayad et al., 2006). Dynamic control of isoform composition of connexin channels in cells (Brisette et al., 1994; De Maio et al., 2000; De Maio et al., 2002) can dramatically change intercellular signaling, specifically for Cx26 and Cx32, often expressed in the same cell type, such as hepatocytes, and in the same channel (Stauffer, 1995; Bevans et al., 1998; Diez et al., 1999; Locke et al., 2004). These data suggest that cells could decrease selectivity among inositol phosphates by downregulating either Cx26 or 32 and enhance selectivity by making both proteins in equal amounts (Ayad et al., 2006). However, this scenario presents some questions in that about half of the connexins in the reconstituted channels were in the reverse orientation with respect to the connexin topology found in living cells. In addition, since no docking

occurs, this technique assays permeability of hemichannels and not gap junctional channels (Rhee et al., 1996; Bevans et al., 1998; Bevans and Harris, 1999).

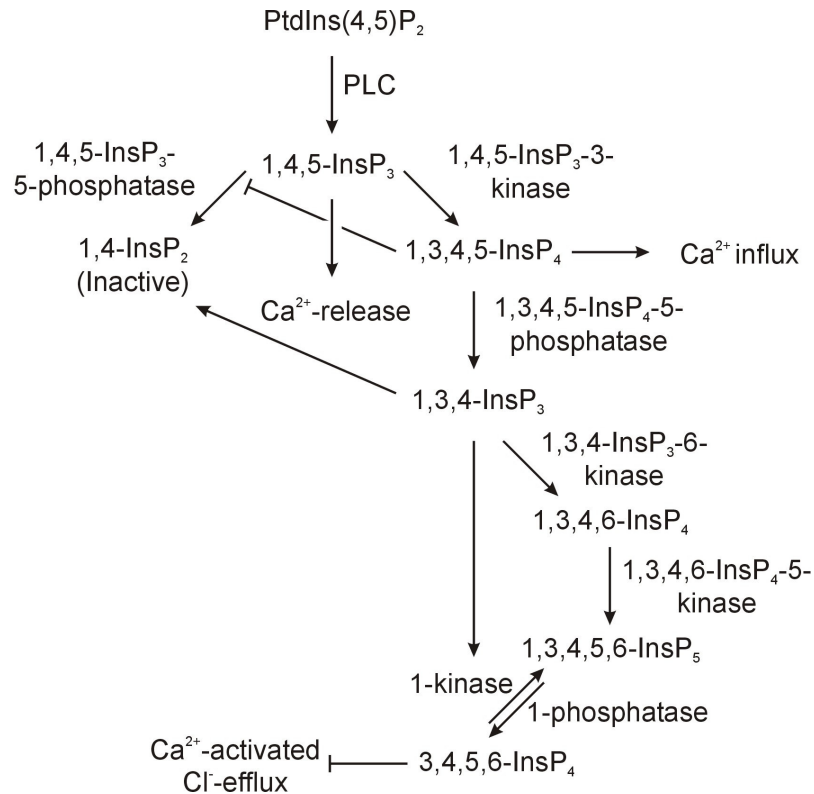


**Figure 6: 1,4,5-InsP<sub>3</sub> formation and degradation**

This scheme summarizes the formation and degradation of 1,4,5-InsP<sub>3</sub> from PtdIns(4,5)P<sub>2</sub> (phosphatidyl inositol-4,5-diphosphate). This scheme was composed from data presented in Shears (1998).

Goldberg et al. (1999, 2000) utilized fluorescence activated cell sorting (FACS) combined with a layered cell culture system to examine the transfer of endogenous metabolites (Table 2) between cells through gap junctions (Goldberg et al., 1999; Goldberg et al., 2000). Hereby ‘donor’ cells are metabolically labeled overnight and afterwards fluorescently stained with DiI, a non-gap junctional permeable dye. These cells are plated with unlabeled ‘receiver’ cells to yield confluent monolayers. After establishment of cell-cell contact and communication, the ‘donors’ were separated from the ‘receivers’ by FACS (Goldberg et al., 1999). These data revealed that Cx43 mediates the transfer of most molecules (glucose, glutamate, ATP, ADP and AMP) several fold more efficiently than Cx32. An exception of this rule was the transfer of adenosine, which was several fold better through channels formed by Cx32. This implies that phosphorylation of adenosine to ATP can shift its permselectivity from Cx32 to Cx43 about 2 - 3 orders of magnitude (Figure 5B - Goldberg et al. (2002)). In this way, the energy status of a cell is controlled via connexin expression and channel formation.

By combining data from several studies, one can conclude that size and charge alone do not exclusively dictate the relative abilities of unrelated molecules to pass through channels

composed of different connexin isoforms (Elfgang et al., 1995; Bevens et al., 1998; Goldberg et al., 1999). It is very important to realize that the selectivities reported in different studies cannot be deduced from the results of connexin channel permeability using the many fluorescent tracers available (Elfgang et al., 1995; Trexler et al., 1996; Veenstra, 1996; Cao et al., 1998; Goldberg et al., 1999; Weber et al., 2004; Ayad et al., 2006).

Second messengers	Molecular Weight (Dalton)	Charge
Glutamate	147	-1
Aspartate	171	-1
Myoinositol	180	0
1-InsP	258	-2
Adenosine	267	0
cAMP	329	-1
InsP <sub>2</sub>	336	-4
Sucrose	342	0
cGMP	345	-1
AMP	347	-2
Prostaglandin E <sub>2</sub>	352	δ-
InsP <sub>3</sub>	414	-6
ADP	427	-3
InsP <sub>4</sub>	492	-8
ATP	551	-4
Glutathione	612	-1
NAD <sup>+</sup> (Nicotinic adenosine dinucleotide)	741	+1

**Table 2: Molecular weight and charge of gap junction permeable second messengers**

Overview of the molecular weight and the net charge at neutral pH of different gap junction permeable second messengers. Table adapted from Alexander and Goldberg (2003).

### 1.2.2 Gating by transjunctional voltage and membrane potential

The transfer of ions and small molecules between adjacent cells is regulated by voltage differences. The conductance of all vertebrate junctions is sensitive to the voltage difference between the two cell interiors (transjunctional voltage,  $V_j$ ), while some connexin channels are also sensitive to absolute inside-outside voltage differences (membrane potential,  $V_m$ ). Connexin channels undergo transitions between multiple conductance states (a main open state, one or more subconductance states, and a closed state) driven by distinct voltage-gating mechanisms (Bukauskas et al., 1995; Moreno et al., 2002). Each hemichannel contains at least two  $V_j$ -gates, one fast and one slow. Several structures are involved in the voltage-induced regulation of the channels: (i) the presence of a voltage sensor (charged amino acids), and (ii) the transfer of electrical energy from the voltage sensor to mechanical energy producing conformational changes that result in opening/closing of the pore (Gonzalez et al., 2007).  $V_m$  can vary without any change in  $V_j$  when both  $V_m$ 's are changed simultaneously. The dual voltage sensitivity ( $V_m$  and  $V_j$ ) is probably mediated by the existence of two different gates

each of which specifically senses one type of potential difference. Each hemichannel in a gap junction channel has its own sets of  $V_j$ - and  $V_m$ -gates, which can interact internally within the hemichannel and also with those of the associated hemichannel from the adjacent cell.

The  $V_j$ -gating of homotypic channels varies in terms of polarity of closing, voltage sensitivity and kinetic properties. The conductance of most homotypic channels is maximal at  $V_j = 0$  mV, and it decreases symmetrically for positive and negative  $V_j$ -values to a non-zero conductance, termed the residual conductance ( $G_{jmin}$  - Harris et al. (1981); Spray et al. (1981)). Connexin channels diverge in the magnitude of the conductance component that is insensitive to  $V_j$ , calculated as the ratio of  $G_{jmin}$  to  $G_{jmax}$  and ranges from a  $G_{jmin}$  below 5 % (Cx45 channels) to values up to ~ 60 - 80 % (Cx36, hCx31.9 and mCx30.2 orthologs - Gonzalez et al. (2007)). The steepness of the  $G_j/V_j$ -curve and the voltage at which changes in  $G_j$  are half-maximal are characteristic for each connexin isoform. The reduction in channel conductance following moderate  $V_j$ -values is mainly associated with a fast (< 1 - 2 ms) transition from the main open state to a subconductance state (Veenstra et al., 1994b; Srinivas et al., 1999; Valiunas et al., 1999; Bukauskas et al., 2002; Xu et al., 2002). Transitions between the residual state and the closed state are less well-defined, are associated with large  $V_j$ -differences and often last tens of milliseconds (Bukauskas et al., 1995; Banach and Weingart, 2000). Accordingly, these two gating transitions are referred to as “fast  $V_j$ -gating” and “slow  $V_j$ -gating”. The latter is also known as “loop gating”, because it is associated with opening transitions, when gap junctions form and is presumably initiated by contact between the extracellular loops of two adjacent hemichannels (Bukauskas et al., 1995). The relative contribution of the fast and slow gating depends on the connexin composition of the channels. Both the aminoterminal domain and the first two residues at the putative first transmembrane/first extracellular border contribute to the slow  $V_j$ -gating (Rubin et al., 1992; Verselis et al., 1994; Oh et al., 1999; Oh et al., 2000; Oh et al., 2004). The valence of the sensor may be determined by the sum of the charges at these two domains.

The magnitude and polarity of fast  $V_j$ -gating in Cx26 and Cx32 is determined by charged amino acids at the aminoterminal domain (Gonzalez et al., 2007). In Cx26, the aminoterminal domain has the tendency to form an  $\alpha$ -helix and this helix may be placed deeper in the channel pore, due to the presence of a glycine hinge turn (Gonzalez et al., 2007). This inward movement initiates the  $V_j$ -gating process. In Cx43, the carboxyterminal domain is suggested to be an important component of fast  $V_j$ -gating. Carboxyterminal truncation of Cx43 (Cx43<sub>257stop</sub>) leads to the loss of the fast-kinetic component and induced novel gating properties. Hereby, junctional currents decayed exponentially with shorter time constants than those attributed to the slow component in the corresponding wild type junctions. Moreover, the steady state  $G_j/V_j$ -relationship was shifted towards smaller voltages and  $G_{jmin}$  decreased significantly (Revilla et al., 1999). It is suggested that the “ball-and-chain” model proposed to mediate gating of connexin channels by intracellular acidification (see further - Liu et al.

(1993); Morley et al. (1996)), is also applicable to the mechanism of fast  $V_j$ -gating (Anumonwo et al., 2001; Moreno et al., 2002).

Gap junctions with a  $V_m$ -dependent conductance can be classified into several groups: those that open upon depolarization (Cx45 - Barrio et al. (1997) and Cx57 - Manthey et al. (1999)), those that close upon depolarization (Cx26, Cx30, Cx32, and Cx43), and those that are insensitive to changes in  $V_m$  (Cx40, Cx42, Cx46, Cx56, and Cx38 - White et al. (1994)). The  $V_m$ -sensor for Cx43 is located near the fourth transmembrane region in the carboxyterminus (Revilla et al., 2000). Carboxyterminal truncation of Cx43 (Cx43<sub>242stop</sub>) abolishes  $V_m$ -sensitivity, while truncation at position 257, that greatly modified  $V_j$ -gating, had no effect on  $V_m$ -gating. These results indicate that the two charged residues between amino acid 242 and 257 (R243: positive charge and D245: negative charge) enhance the  $V_m$ -sensitivity. The closure of the gap junction channel, composed of Cx43, upon membrane depolarization is mediated by an outward movement of a positively charged voltage sensor, which includes amino acids R243 and D245 (Harris, 2001). The fact that  $V_j$ -gating of gap junction channels can be modified without influencing  $V_m$ -sensitivity indicates that  $V_m$ - and  $V_j$ -regulation of Cx43 junctional conductance is mediated by separate domains (Revilla et al., 2000).

Hemichannels show an altered  $V_m$ -sensitivity when compared to gap junctional channels. The  $V_m$ -sensitivity of a hemichannel might be unipolar or bipolar. The single channel conductance in bipolar hemichannels, such as Cx26, Cx30, Cx46, and Cx50, first increases with progressive depolarization and then, the current decreases upon depolarization to higher positive membrane potentials, due to inactivation of the hemichannel (Trexler et al., 1996; Valiunas and Weingart, 2000; Gonzalez et al., 2006). Opening at negative potentials (- 20 mV) is frequently mediated by transitions between the closed state and the main open state. As depolarization progresses, hemichannels remain stable in a high conductance open state, until the membrane potential reaches positive values. At this point, the hemichannels close to a subconductance state with rapid transitions (< 1 - 2 ms - Oh et al. (1999)). This model is consistent with a model of two gates in series operating at opposite polarity. In contrast, activation of other hemichannels, like Cx32 (Castro et al., 1999), Cx43 (Contreras et al., 2003b), and Cx45 (Valiunas, 2002) progresses monotonically with the degree of depolarization, without inactivation at high positive membrane potentials. The deactivation seen in hyperpolarization involves transitions from the main open state to the residual state where the hemichannel stays open for many seconds, before fully closing. The belief that there are two separate mechanisms of gating underlying the unipolar voltage behavior is based on the fact that in Cx32 hemichannels the transitions into and out of the residual state can be dissociated from transitions into and out of the main open state by varying the extracellular  $Ca^{2+}$ -concentrations ( $[Ca^{2+}]_e$ ). At normal physiological  $[Ca^{2+}]_e$  transitions into and out of the fully open state (~ 90 pS) are blocked, while transitions to the residual open

state ( $\sim 18$  pS) remain intact (Gomez-Hernandez et al., 2003). Consequently, a two-gate model with a unipolar voltage behavior is still valid, if the two gating processes operate at the same voltage polarity (opening at depolarization and closing at hyperpolarization).

To conclude, it may be suggested that slow gating always closes hemichannels upon hyperpolarization, whereas fast gating can close with either voltage polarity (Gonzalez et al., 2007). The conformational changes by which the sensor motion can induce gating transitions still remain to be elucidated.

### 1.2.3 Effect of $\text{pH}_i$ on gap junctional communication

Intracellular acidification acts as a general regulator of intercellular gap junctional communication (Francis et al., 1999; Stergiopoulos et al., 1999). In cardiac ventricular myocytes, an acute change in intracellular pH (physiological  $\text{pH}_i \sim 7.20$ ) is typically corrected for by the sarcolemmal movement of  $\text{H}^+$ -ions by the  $\text{Na}^+/\text{H}^+$ -exchanger (NHE), by the  $\text{Cl}^-/\text{HCO}_3^-$ -exchanger (Leem et al., 1999), and by a passive cell-to-cell  $\text{H}^+$ -flow through junctional channels (Zaniboni et al., 2003a). This movement of  $\text{H}^+$ -ions occurs via the permeation of mobile buffer molecules, such as histidyl dipeptides (homocarnosine: 100 Da and acetylcarnosine: 200 Da - Vaughan-Jones et al. (2002)). The high intracellular buffer concentrations ( $\sim 15$  mM - Zaniboni et al. (2003b); Swietach and Vaughan-Jones (2005)) indicate that significant quantities of  $\text{H}^+$ -ions might be shuttled in response to a modest transjunctional  $\text{pH}_i$  change (Zaniboni et al., 2003a). This is in contrast with the perception that intracellular acidosis closes gap junction channels (Turin and Warner, 1977; Ek-Vitorin et al., 1996; Duffy et al., 2002; Swietach et al., 2007b). Gating is believed to be mediated directly by  $\text{H}^+$ -titration of specific sites of the carboxyterminal domain of each Cx43 subunit (Duffy et al., 2002), and indirectly by a  $\text{H}^+$ -induced rise of  $[\text{Ca}^{2+}]_i$  (White et al., 1990). Swietach et al. (2007) showed that a modest, local increase in  $\text{H}^+$ -ions ( $\text{pH}_i \sim 6.90$ ) in one or more cells will increase gap junctional communication, permitting the passive dissipation of  $\text{H}^+$ -ions into neighboring cells and promoting in this way a myocardial pH syncytium (Swietach et al., 2007a). This spatial buffering of  $\text{H}^+$ -ions represents an energy-efficient form of  $\text{pH}_i$ -regulation. The dispersed  $\text{H}^+$ -ions will eventually be exported at a low rate across the sarcolemma. A stronger acidification ( $\text{pH}_i \sim 6.30$ ), caused by extreme metabolic stress, will inhibit gap junctional permeability, restricting the spatial spread of  $\text{H}^+$ -ions (Swietach et al., 2007a). The bell-shaped  $\text{pH}_i$  sensitivity of gap junctional communication is consistent with distinct overlapping  $\text{H}^+$ -activation ( $\text{pK} \sim 6.96$ ) and -inactivation ( $\text{pK} \sim 6.93$ ) processes of similar  $\text{pK}$ , producing a steady-state window of gap junctional permeability (Figure 7 - Swietach et al. (2007a)). In this model,  $\text{H}^+$ -titration of activation sites increase the junctional permeability, whereas simultaneous titration of activation and inactivation sites decrease the junctional communication (Swietach et al., 2007a). The relatively fast kinetics of  $\text{pH}_i$ -induced activation of gap junctional channels (up to 4-fold increase within 1 - 3 min) suggests a

regulation of open probability and channel conductance, rather than an increase in channel density.

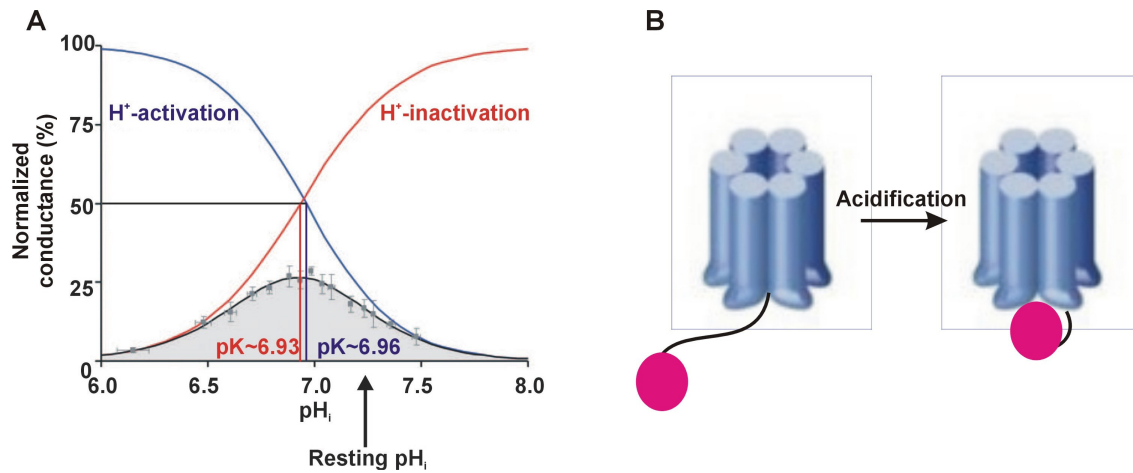


**Figure 7: Diagram of modulation of gap junctional communication by  $\text{pH}_i$**

(A) The cross-over of the sigmoidal activation and inactivation curve produces a steady-state biphasic relation between  $\text{pH}_i$  and gap junctional permeability.  $\text{pK}$  represents the  $\text{pH}_i$  at which the normalized conductance is reduced to 50 % of the maximum value. Resting  $\text{pH}_i$  indicates normal physiological  $\text{pH}_i$  (~ 7.20). Figure adapted from Swietach et al. (2007a). (B) Simplified scheme of the “ball-and-chain” model that closes gap junction channels upon intracellular acidification. The ball is formed by the carboxyterminal domain and binds to the intracellular loop “receptor” domain. For clarity, only one ball and chain are indicated on the figure, but in reality there are six of them per hemichannel (Delmar et al., 2004).

The “ball-and-chain” or “particle-receptor” model has been proposed as the mechanism underlying the intracellular acidification induced closure of gap junctions (Delmar et al., 2004). This model suggests that one region of the connexin forms the “ball” or “particle” which interacts directly with a second “receptor” region to close the gap junction channels. Hirst-Jensen et al. (2007) speculate that for Cx43 residues N312 - I382 (carboxyterminal domain) constitute the “ball”, whereas S255 - A311 represent the “chain” that modulates affinity between the intracellular loop and the carboxyterminal domain (Hirst-Jensen et al., 2007). Intracellular acidification induces: (i) the formation of an  $\alpha$ -helical structure in the second half of the intracellular loop (associated with protonated histidine residues - Duffy et al. (2002)), (ii) an interaction between the former domain and the carboxyterminus of Cx43 (Seki et al., 2004b), and (iii) homodimerization of the carboxyterminal domain (Sorgen et al., 2004). The latter increases the binding between the “receptor” (intracellular loop) and the “ball” (carboxyterminal domain), bringing the channel in a closed state (Seki et al., 2004b; Hirst-Jensen et al., 2007). The (weak) interaction between the carboxyterminal domain and the cytoplasmic loop at normal  $\text{pH}_i$  is most likely responsible for the residual state of the channel (Seki et al., 2004b; Sorgen et al., 2004; Hirst-Jensen et al., 2007).

## 1.2.4 Phosphorylation and gating

### 1.2.4.1 General aspects of phosphorylation

The degree of intercellular communication mediated by connexin gap junctions depends on the open probability of the channels, and this is a function of the phosphorylation degree. Moreover, phosphorylation controls cell-cell communication at several steps: (i) at the level of gene expression, (ii) assembly into gap junctions, (iii) channel gating, (iv) removal from the plasma membrane, and (v) protein degradation. Many connexins (Cx31, Cx32, Cx37, Cx40, Cx43, Cx45, Cx 46, Cx50, and Cx56) are known to contain consensus phosphorylation sites, and have been demonstrated to be phosphorylated by either a shift in their electrophoretic mobility on SDS-PAGE (Sodium Dodecyl Sulfate-poly-acrylamide gel electrophoresis) or direct incorporation of  $^{32}\text{P}$  (Saez et al., 1998; Lampe and Lau, 2000). It is presumably not a change in molecular weight that is detected via SDS-PAGE, since addition of a phosphate would only add 80 Da to the molecular weight, but rather a conformational change in the protein, triggered by these phosphorylations (caused by a reduction in SDS-binding to the protein, close to the phosphorylation sites). The carboxyterminal domain appears to be the primary region of phosphorylation, however Cx56 is also phosphorylated within the cytoplasmic loop, in addition to the carboxyterminal domain (Berthoud et al., 1997). No phosphorylations on the aminoterminal domain of connexins have been described until now.

Cx26 is the only connexin that is not phosphorylated (Traub et al., 1989), which is probably related to the short carboxyterminal domain with only a few amino acids. Since Cx26 can form functional gap junction channels, phosphorylation is not necessary for the formation of gap junction channels. Remarkably, PKC (protein kinase C) activation by TPA (12-*O*-tetradecanoylphorbol-13-acetate) treatment in Cx26 expressing cells resulted in a diminished Lucifer Yellow permeability and markedly decreased the channel conductance from 140 - 150 pS to smaller conductances (40 - 70 pS - Kwak et al. (1995a)). This might be a consequence of destabilization of Cx26 gap junctions, or modulation of Cx26 expression (Lee et al., 1992). Kojima et al. (1999) showed that TPA treatment induced a redistribution of Cx26 from the cytoplasm to the plasma membrane thereby increasing electrical coupling (Kojima et al., 1999).

Cx32 was the first connexin known to be phosphorylated (Saez et al., 1986). Activation of cAMP dependent kinase (PKA - protein kinase A) or PKC resulted in an elevated phosphorylation at S233 (Saez et al., 1986; Traub et al., 1987; Takeda et al., 1989; Saez et al., 1990) and this was correlated with a temporal increase in junctional conductance (Chanson et al., 1996). In liver cells, Cx32 is also phosphorylated by CaMK-II (Ca<sup>2+</sup>/CaM dependent protein kinase II), resulting in serine and threonine phosphorylation (Saez et al., 1990). The non-receptor tyrosine kinase v-Src (viral-Src) was however not able to phosphorylate Cx32 *in*



*vitro* (Swenson et al., 1990; Saez et al., 1998), but tyrosine phosphorylation of Cx32 was demonstrated after treatment with the epidermal growth factor (Diez et al., 1995). The functional consequence of this phosphorylation remains however unraveled.

PKA activation in Cx40 expressing SKHep1 cells increased both gap junctional permeability for Lucifer Yellow and conductance with 50 %. This was the consequence of a shift in the unitary conductance of 80 pS to 120 pS, resulting in an increase in total conductance of the gap junction channel (van Rijen et al., 2000).

Cx45 is phosphorylated mainly on serine residues, but also on threonine and tyrosine residues (Butterweck et al., 1994; Laing et al., 1994; Darrow et al., 1996; Hertlein et al., 1998). This results in a reduced gap junctional communication (Hertlein et al., 1998). In contrast, in HeLa-Cx45 cells, PMA (phorbol 12-myristate 13-acetate) treatment increased the electrical conductance with 50 % through a change in the open probability. A change in the phosphorylation status of this connexin, as judged by western blot analysis, was however not reported (van Veen et al., 2000).

Cx46 and Cx50, which are both expressed in the ocular lens fiber, are also phosphorylated, resulting in an altered gap junctional communication. Casein kinase 1 (CK1) has been shown to phosphorylate the sheep homologue of Cx50 (Cheng and Louis, 2001), while casein kinase 2 (CK2) was involved in the phosphorylation of the chicken homologue of Cx50 at S363, and this phosphorylation inhibited the cleavage of Cx50 by caspase-3 (Yin et al., 2001).

PKC ( $\alpha$ ,  $\beta$  and  $\gamma$  isotypes) was able to phosphorylate chicken lens Cx45.6 and Cx56 (Jiang and Goodenough, 1998), with Cx56 being phosphorylated in both the intracellular loop (S118) and the carboxyterminal domain (S493 - Berthoud et al. (1997)). S118 phosphorylation may act as a signal for increased degradation of the protein (Berthoud et al., 1997).

Cx43 contains multiple electrophoretic isoforms when analyzed by SDS-PAGE, including a faster migrating, non-phosphorylated form ( $P_0$  or NP), and at least two slower migrating forms ( $P_1$  and  $P_2$ ). The latter forms co-migrate with the  $P_0$  form following alkaline phosphatase treatment, suggesting that phosphorylation is the primary covalent modification detected by SDS-PAGE (Crow et al., 1990; Musil et al., 1990b). Phospho-amino acid analysis indicates that phosphorylation occurs primarily on serine residues (Musil et al., 1990b; Warn-Cramer et al., 1996; Lampe et al., 1998), although threonine and tyrosine phosphorylation has also been observed (Figure 8 - Crow et al. (1990); Swenson et al. (1990)). Phosphorylation at S364 and S365 leads to  $P_1$  formation and phosphorylation at S325, S328, and S330 is necessary for the  $P_2$  form (Solan and Lampe, 2007). Once the Cx43  $P_2$  form is incorporated into gap junctions, it becomes resistant to Triton X-100 extraction (Musil and Goodenough, 1991).

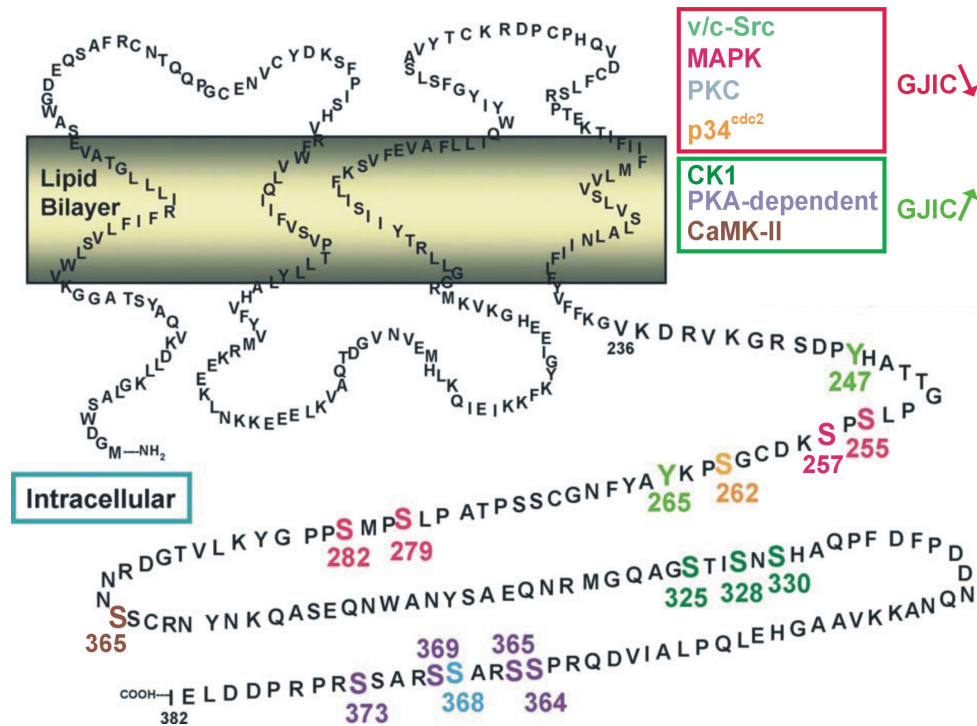


**Figure 8: Consensus phosphorylation sites in Cx43**

The carboxyterminal domain of Cx43 contains multiple consensus phosphorylation sites. Kinases that suppress gap junctional coupling are framed in red, while those that increase communication are framed in green. MAP kinase: mitogen activated protein kinase; PKC: protein kinase C; p34<sup>cdc2</sup>: cyclin B-dependent kinase; CK1: casein kinase 1; PKA: protein kinase A; CaMK-II: Ca<sup>2+</sup>/CaM dependent kinase II, GJIC: gap junctional intercellular communication. Figure adapted from Lampe and Lau (2004).

### 1.2.4.2 Cell cycle related changes in Cx43 phosphorylation

The degree of Cx43 phosphorylation increases 2.5 times during the S-phase and 4.5 times during the M-phase of the cell cycle, relative to the G<sub>0</sub>/G<sub>1</sub>-phase (Kanemitsu et al., 1998). This altered phosphorylation is reflected by a change in gap junctional communication during progression through the cell cycle. It is moderate during the G<sub>1</sub>/S-phase, increased in the S-phase, and decreased in G<sub>2</sub>/M (Stein et al., 1992; Xie et al., 1997; Bittman and LoTurco, 1999). Gap junctional communication is gradually restored as cells proceed through G<sub>1</sub>, with a complete recovery 1 - 4 hours after the telophase (Figure 9 - Stein et al. (1992); Xie et al. (1997)).

Immunofluorescence studies indicate that Cx43 is almost exclusively located at the plasma membrane during the G<sub>0</sub>-phase, and half of the protein resides in the Triton X-100-insoluble fraction and migrates as the P<sub>2</sub> isoform. During the S-phase, Cx43 is found both at the plasma membrane and in numerous cytosolic vesicles. The ratio of the Triton X-100-insoluble fraction to whole-cell Cx43 decreases and more Cx43 migrates at the P<sub>0</sub> and P<sub>1</sub> positions. During the M-phase, Cx43 is found almost entirely in the cytoplasm (large, clustered puncta - Xie et al. (1997); Lampe et al. (1998)) and phosphorylated to a distinct phospho-isoform,

called  $P_m$  or  $P_3$ , in a  $p34^{cdc2}$ -dependent way (Kanemitsu et al., 1998; Lampe et al., 1998). Despite the reduced plasma membrane staining, the amount of Triton X-100-insoluble material in mitotic cells is about the same as in the S-phase cells and contains the  $P_3$  form (Solan and Lampe, 2005). Gap junction assembly is also cell cycle-regulated, with  $G_0$ -phase cells being about 50 % more efficient at assembly than S-phase cells (Solan et al., 2003). This difference may account for the intracellular accumulation of Cx43 in S- and  $G_2$ /M-phase cells and corresponds to an increased phosphorylation of Cx43 at S368 (Solan et al., 2003). Presumably, decreasing gap junctional communication during mitosis is important in isolating mitotic cells and division-related signals from their non-dividing neighbors. Another possibility is that intracellular Cx43 plays an important functional role, as there is increasing evidence that Cx43 mediates growth control independently of gap junctional intercellular communication (Zhang et al., 2003; Doble et al., 2004).

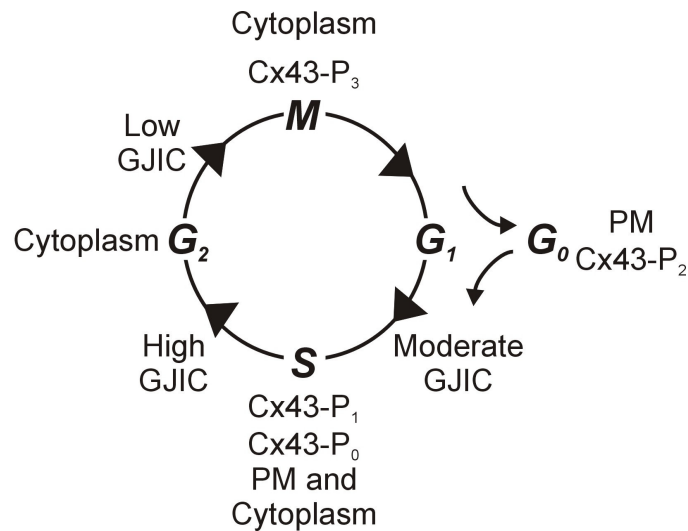


**Figure 9: Overview of Cx43 phosphorylation during the cell cycle progression**

The cell cycle consists of four phases: the M-phase (mitosis) includes nuclear and cytoplasmic division and is also known as cytokinesis; the  $G_1$ -phase is characterized by a high biosynthetic activity of the cell; during the S-phase the DNA replicates; in the  $G_2$ -phase there is increased synthesis of proteins involved in microtubule formation. Nonproliferative cells enter the  $G_0$ -phase, which is the common phase for fully differentiated cells. PM: plasma membrane, GJIC: gap junctional intercellular communication.

In general, Cx43 phosphorylation increases as cells progress through the S- and  $G_2$ -phase of the cell-cycle. Phosphopeptide/2-D gel electrophoresis of Cx43 isolated from metabolically labeled cells have shown that there are several distinct sites of phosphorylation during mitosis which are dependent on the activity of the cyclin B-dependent  $p34^{cdc2}$  kinase (Kanemitsu et al., 1998; Lampe et al., 1998), such as S255, S262 (Kanemitsu et al., 1998) and S368 (Solan et al., 2003).

### 1.2.4.3 Phosphorylation of Cx43 by PKC

Many PKC mediated effects on connexin phosphorylation and gap junctional communication are elucidated by the use of phorbol ester tumor promoters, such as TPA and PMA. In most cases, these PKC activators induce a strong, but transient decrease in gap junctional communication, as measured by dye transfer. However, dye permeability and conductance are differentially affected by TPA in neonatal rat cardiomyocytes (Kwak et al., 1995b). This might be explained by a smaller pore size restricting dye transfer, while the open probability and/or the number of channels is increased. Bao et al. (2007) showed that phosphorylation of all six subunits in Cx43 hemichannels abolished the permeability for large hydrophilic solutes, but not for small inorganic ions, and this was probably the consequence of a partial reduction of the effective cross-sectional area of the Cx43 pore opening (Bao et al., 2007). After phosphorylation of all Cx43 subunits, the pore remained permeable for the small probe ethyleneglycol (MW: 62 Da; 4.4 Å), indicating that a pore of significant size remained (Bao et al., 2007). PKC has been shown to phosphorylate Cx43 at S262, S368 (Saez et al., 1997; Lampe et al., 2000; Shah et al., 2002), and S372 (Saez et al., 1997; Lampe et al., 2000; Shah et al., 2002). However, phosphopeptide analysis showed that several other PKC mediated phosphorylation sites exist (Saez et al., 1997; Lampe et al., 2000). Some of these phosphorylations may be due to the activation of the MAP kinase/ERK (extracellular regulated kinase) pathway or p34<sup>cdc2</sup> kinase (Rivedal and Opsahl, 2001; Ruch et al., 2001; Cruciani and Mikalsen, 2002). Phosphorylation of S262 (Doble et al., 2004) is linked to increased cellular proliferation through an unknown mechanism (Doble et al., 2004), while S368 phosphorylation underlies the PMA induced reduction in intercellular communication and alteration of single channel behavior (Lampe et al., 2000).

The presence of several PKC isoforms ( $\alpha$ ,  $\beta$ , and  $\gamma$ ), the activation of different kinases by PMA/TPA, the complex kinetics of PMA/TPA action (affecting channel gating, gap junction assembly and connexin half-life), and the downregulation of PKC over time in the presence of PMA (reversing the effects) might explain the complexity and difference in separate studies in response to PKC activating stimuli.

### 1.2.4.4 Phosphorylation of Cx43 by tyrosine protein kinases

Tyrosine protein kinases can be subdivided into two classes: (i) the non-receptor protein tyrosine kinases, i.e. v-Src and v-Fps (viral-Fps), and (ii) the receptor protein tyrosine kinases, such as EGFR (Epidermal Growth Factor Receptor), PDGFR (Platelet Derived Growth Factor Receptor), VEGFR (Vascular Endothelial Growth Factor Receptor), and FGFR (Fibroblast Growth Factor Receptor).

#### 1.2.4.4.1 Non-receptor tyrosine protein kinases

Activation of v-Src and v-Fps led to a marked disruption in intercellular communication (Crow et al., 1990; Filson et al., 1990; Swenson et al., 1990; Kurata and Lau, 1994) and an increased degree of Cx43 phosphorylation on serine and tyrosine residues (Loo et al., 1995). Both kinases phosphorylate Cx43 on similar sites.

v-Src co-localizes and interacts with Cx43 at the plasma membrane (Kanemitsu et al., 1997; Loo et al., 1999). This interaction depends on an intact SH3 (Src Homology 3) and SH2 (Src Homology 2) domain of v-Src, the proline rich region of Cx43 (P274 - P284) and the phosphorylated Y247 and Y265 residues of Cx43 (Kanemitsu et al., 1997). Disruption of gap junctional communication by v-Src is a sequential event, whereby the SH3 domain of v-Src initially binds to the proline rich region of Cx43, bringing these two proteins in close proximity (Step 1 - Figure 10). This results in the phosphorylation of Y265 by the v-Src kinase domain (Step 2 - Figure 10), generating a second binding site in Cx43 that interacts with the SH2 domain of v-Src, stabilizing the v-Src/Cx43 interaction (Step 3 - Figure 10). The induced protein proximity leads to progressive phosphorylation of Cx43 at Y247, resulting in a disrupted gap junctional communication (Step 4 - Figure 10). This model suggests that phosphorylated Y265 may be important as a binding site, strengthening the interaction between Cx43 and v-Src, whereas phosphorylated Y247 may promote the closure of the channels (Lin et al., 2001).

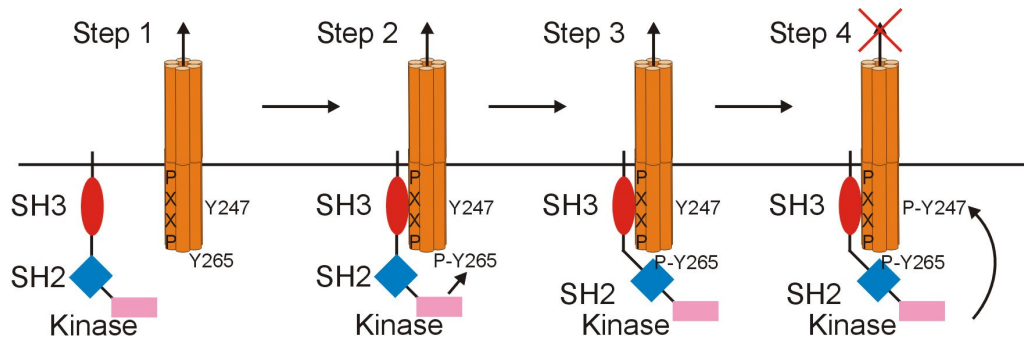


**Figure 10: Mechanism of v-Src mediated closure of Cx43 gap junctions**

Step 1: the SH3 domain of v-Src interacts with the proline-rich region of Cx43 (PXXP; P274 - P284). Step 2: this interaction brings the kinase domain of v-Src in close proximity to Y265, which is phosphorylated. Step 3: the phosphorylated Y265 residue provides a binding site for the SH2 domain of v-Src, with subsequent phosphorylation of Y247. Step 4: these phosphorylations result in the closure of the channel. Figure adapted from Warn-Cramer and Lau (2004).

In this model system, MAP kinase activation and serine phosphorylation of Cx43 were not required for v-Src's action. This conclusion was further supported by a study of Lin et al. (2006) where fibroblasts that expressed v-Src and a Cx43 mutant lacking the MAP kinase phosphorylation sites (S255A, S279A and S282A) were used. Hereby Cx43 was

phosphorylated on tyrosine residues and gap junctional communication was dramatically reduced (Lin et al., 2006).

Electrophysiological studies performed by Cottrell et al. (2003) suggested that the reduction of gap junctional communication induced by v-Src tyrosine phosphorylation of Cx43 was not due to a reduction in single channel conductance or a reduced number of gap junction channels present at the plasma membrane, but may be attributed to a reduction in the open probability of the channel (Cottrell et al., 2003). A critical regulatory role for the Cx43 carboxyterminal domain was supported by a study in which v-Src could not abolish gap junctional communication in *Xenopus laevis* oocytes expressing a truncated mutant of Cx43 (Cx43<sub>257stop</sub>), but the v-Src mediated inhibition in gap junctional communication could be completely restored by the co-expression of the carboxyterminal domain as a separate polypeptide (Homma et al., 1998; Zhou et al., 1999). Residue K241 - P280 appear to mediate the sensitivity of Cx43 for v-Src. These results suggest that the carboxyterminal domain does not need to be physically linked with the channel to exert its channel blocking effect, and may be mediated through a “ball-and-chain” or “particle-receptor” mechanism, as previously described for the pHi induced channel closure (Morley et al., 1996; Homma et al., 1998).

The role for tyrosine phosphorylation of Cx43 in v-Src mediated inhibition of gap junctional communication was questioned by (Zhou et al., 1999). They proposed another mechanism for the regulation of Cx43 channel closure by v-Src, mediated by the activation of the MAP kinase signaling cascade (Figure 11). These authors used a *Xenopus laevis* oocyte expression system showing that gap junctional communication established by the Cx43 Y265F and Cx43 Y247F single and the Cx43 Y265F/Y247F double mutant was disrupted by v-Src expressed from injected mRNA. These results indicated that the two tyrosine residues in Cx43 were not required for the disruption of gap junctional communication (Zhou et al., 1999). A quadruple serine mutant of Cx43 (S255A, S257A, S279A and S282A), lacking the MAP kinase phosphorylation sites (Figure 8), showed a reduced disruption of gap junctional communication when co-expressed with v-Src in oocytes. This indicated that v-Src phosphorylated Cx43 on serine residues by activated MAP kinase and not on tyrosine residues by activated v-Src (Zhou et al., 1999).

The reason for the discrepancies between different studies is not clear. In the presence of acutely expressed v-Src (Zhou et al., 1999) the effects on gap junctional communication may be different from those that occurred in cells with constitutive v-Src expression (Lin et al., 2001).

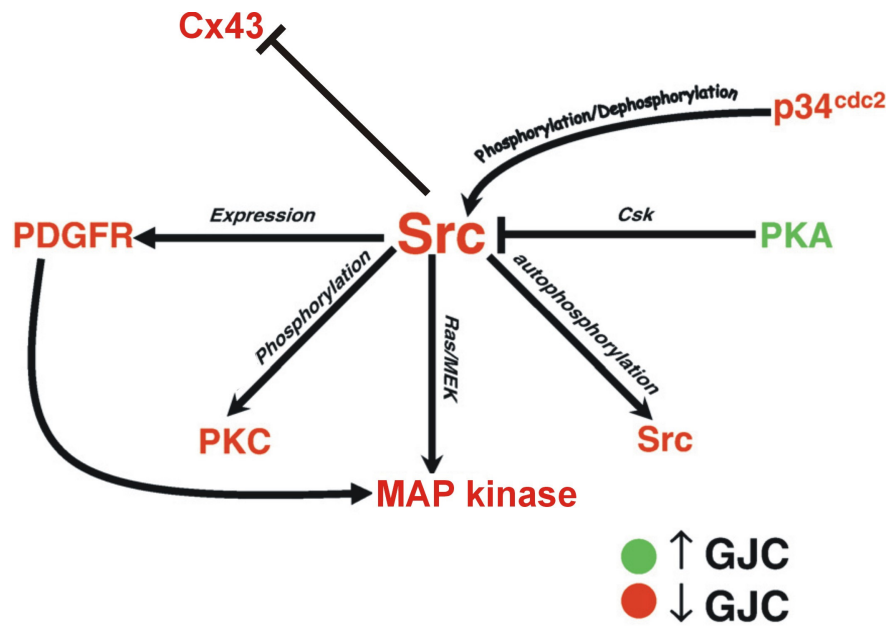


**Figure 11: Crosstalk between different pathways**

Src can be activated by  $p34^{cdc2}$  and inhibited by PKA. Src can directly phosphorylate Cx43, alternatively, Src can activate other kinases, such as the MAP kinase signaling cascade, and PKC, resulting in a diminished gap junctional communication. Moreover, Src can increase PDGFR expression. Upon activation, this receptor can augment MAP kinase and PKC activity to disrupt gap junctional communication, mediated by Cx43. Kinases that increase gap junctional communication are indicated in green, while those that decrease gap junctional communication are indicated in red. Figure is adapted from Pahuja et al. (2007).

#### 1.2.4.4.2 Receptor tyrosine protein kinases

The EGF receptor is a transmembrane tyrosine protein kinase receptor that forms homo- or heterodimers upon ligand binding, resulting in receptor autophosphorylation and the activation of its tyrosine kinase activity (Ullrich and Schlessinger, 1990). Tyrosine phosphorylation of residues in the carboxyterminal domain of the receptor provides docking sites for the assembly of signaling complexes through the binding of SH2 and PTB (phosphotyrosine binding) domains in adaptor proteins, such as Grb2/Sos (Schlessinger, 2000). This leads to the activation of the Ras/Raf/MEK/Erk (Schlessinger, 2000) and/or the c-Src/MEKK2/MEK5/Erk5 signaling pathways (Sun et al., 2003), inducing S255, S262, S279 and S282 phosphorylation of Cx43 (Figure 12 - Warn-Cramer et al. (1996); Warn-Cramer et al. (1998); Cameron et al. (2003); Solan and Lampe (2007)).

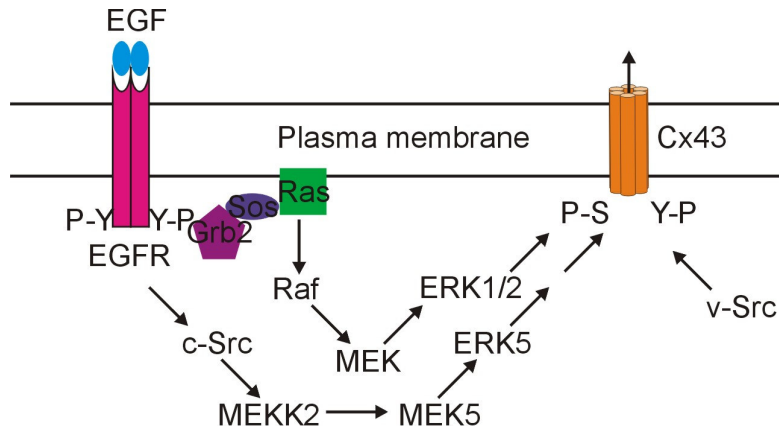


**Figure 12: Schematic overview of EGF mediated closure of Cx43 channels**

The ligand induced activation of EGFR (epidermal growth factor receptor) leads to autophosphorylation of the receptor and the formation of the phosphotyrosine binding sites for SH2 containing adaptor proteins such as Grb2/Sos. This results in the activation of the Ras/Raf/MEK/ERK and the c-Src/MEKK2/MEK5/ERK5 signaling pathways, inducing serine phosphorylation of Cx43. This process is associated with reduced gap junctional communication. Figure adapted from Warn-Cramer and Lau (2004).

In many cell types, activation of the EGF receptor results in a rapid and transient disruption of gap junctional communication and a marked increase in Cx43 phosphorylation on serine residues (Hossain et al., 1998; Rivedal and Opsahl, 2001). This disruption in gap junctional communication was not correlated with an altered Cx43 distribution (Lau et al., 1992), was independent of PKC activity, but was dependent on the activation of the downstream MAP kinase signaling pathway, which phosphorylated Cx43 on S255, S279 and S282 (Kanemitsu and Lau, 1993; Warn-Cramer et al., 1996). Cottrell et al. (2003) showed that the disruption of gap junctional communication after EGFR activation was correlated with a reduction in the open channel probability, rather than with a reduction in the unitary conductance (Cottrell et al., 2003). The regulation of gap junctional communication by EGFR activation was complicated by the observation that EGF treatment enhanced gap junctional communication in human kidney epithelial K7 cells (Vikhamar et al., 1998) as a consequence of p42 MAP kinase activation. The stimulated gap junctional communication upon EGF treatment was induced by an increased synthesis and transport of Cx43 to the plasma membrane (Vikhamar et al., 1998). This was in contrast with the results published by Leithe et al. (2004) and Yoshida et al. (2005), who showed that EGF induced the internalization and degradation of Cx43 gap junctional plaques after hyperphosphorylation by the activated MAP kinase cascade (Leithe and Rivedal, 2004; Yoshioka et al., 2005). A possibility is that EGF induced hyperphosphorylation of Cx43 is a signal for conjugation of ubiquitin moieties to Cx43, leading to degradation via the proteasomal pathway (Leithe and Rivedal, 2004).

Binding of PDGF to the PDGF receptor results in autophosphorylation and recruits diverse signal transduction molecules, such as GTPase activating proteins (GAP), phospholipase C $\gamma$ 1 (PLC $\gamma$ 1), SH2 domain containing phosphotyrosine phosphatase (SHP-2), c-Src and



phosphoinositol-3-kinase (PI-3K - Veracini et al. (2005)). PI-3K can activate the MAP kinase signaling pathway (Choudhury et al., 1997) and PKC (Jiang and Goodenough, 1998; Hossain et al., 1999a; Hossain et al., 1999b). PDGF treatment resulted in phosphorylation of S368 of Cx43 and rapidly reduced gap junctional communication in a transient way, as a consequence of reduced single channel conductance (Burt et al., 1991).

VEGFR is highly related to the PDGFR family and treatment with VEGF-A rapidly and reversibly disrupted gap junctional communication. This disruption was mediated by the activation of c-Src and the MAP kinase signaling cascade (Suarez and Ballmer-Hofer, 2001), resulting in phosphorylation of Cx43 on serine and threonine residues. Thuringer (2004) showed that VEGF resulted in Cx43 phosphorylation on tyrosine residues and this was correlated with a rapid internalization of Cx43 (Thuringer, 2004).

The FGF receptor is a large family of heparin-binding proteins with mitogenic activity for neural cells, endothelial cells, and cardiomyocytes (Pepper and Meda, 1992; Doble et al., 1996; Reuss et al., 1998). bFGF (basic fibroblast growth factor; FGF-2) plays a role in wound healing, angiogenesis and cell proliferation and participates in regulating gap junctional communication in the injured myocardium. The bFGF receptor co-localizes with Cx43 at the plasma membrane at the intercalated discs of cardiomyocytes and in the rat brain (Kardami et al., 1991; Yamamoto et al., 1991), suggesting a physical association between these two proteins. Long-term treatment (> 6 h) of cells with bFGF stimulated gap junctional communication in cardiac fibroblasts, as a consequence of increased Cx43 mRNA and protein levels (Doble and Kardami, 1995). In striking contrast, a short-term treatment of cardiomyocytes resulted in a rapid decrease in gap junctional communication, as a consequence of increased phosphorylation on serine residues through PKC activation (Doble et al., 1996).

Alltogether, these studies indicate that different growth factors lead to the activation of different signaling pathways, ultimately leading to phosphorylation of Cx43 at different residues, thereby uniquely influencing gap junctional communication.

#### **1.2.4.5 G protein coupled receptors (GPCR)**

Cx43 mediated gap junctional communication is transiently disrupted after stimulation of particular GPCR, such as those for endothelin, thrombin, nucleotides and bioactive lipids (Hill et al., 1994; Venance et al., 1995; Postma et al., 1998; Spinella et al., 2003; Blomstrand et al., 2004; Meme et al., 2004; Rouach et al., 2006), with a restoration of communication after ~ 20 - 60 min, depending on the GPCR involved (Postma et al., 1998). GPCR lack an intrinsic kinase activity, but are coupled to downstream signaling events, such as the activation of c-Src (Luttrell et al., 1999), the MAP kinase signaling pathway (Gudermann et al., 2000) and PLC $\beta$ 3 through an interaction with heteromeric G-proteins (guanine-nucleotide binding proteins), which undergo conformational changes, exchanging GDP (guanosine

diphosphate) for GTP (guanosine triphosphate), bound to the  $\alpha$ -subunit upon GPCR activation. The downstream signaling events of LPA, thrombin and neuropeptides were independent of  $\text{Ca}^{2+}$ -mobilization, PKC activation, activation of the MAP kinase signaling pathway, and Rho or Ras activation (Postma et al., 1998). Instead the LPA-activated GPCR appeared to require the kinase activity of c-Src to induce the changes in Cx43 gap junctional permeability (Postma et al., 1998). Hill et al. (1994) and Warn-Cramer et al. (1998) demonstrated a role for MAP kinase activity in LPA induced phosphorylation of Cx43 (Hill et al., 1994; Warn-Cramer et al., 1998). Whether c-Src kinase activity was required for MAP kinase activation and whether MAP kinase phosphorylation of Cx43 affected gap junctional communication in this system was not yet known. A study by van Zeijl et al. (2007) showed that transfection of active  $\text{G}\alpha_q$  played a key role in the regulation of Cx43 based gap junctional communication in normal fibroblasts (van Zeijl et al., 2007). Active  $\text{G}\alpha_q$  (but not  $\text{G}\alpha_i$ ,  $\text{G}\alpha_{12}$  or  $\text{G}\alpha_{13}$ ) activated  $\text{PLC}\beta_3$  leading to a depletion of  $\text{PtdIns}(4,5)\text{P}_2$  from the plasma membrane, resulting in a disruption of gap junctional communication.  $\text{PtdIns}(4,5)\text{P}_2$ -derived second messengers, such as  $1,4,5\text{-InsP}_3$ ,  $\text{Ca}^{2+}$  and PKC played no role in this disruption of gap junctional communication (van Zeijl et al., 2007). Zonula Occludens-1 (ZO-1) played an essential role in the  $\text{G}\alpha_q$  mediated disruption of gap junctional communication. It was shown that ZO-1 assembled Cx43 and  $\text{PLC}\beta_3$  in a single complex. In this way, localized changes in  $\text{PtdIns}(4,5)\text{P}_2$  may regulate gap junctional communication. The exact mechanism of this disruption still remains elusive (van Zeijl et al., 2007).

#### **1.2.4.6 Phosphorylation of Cx43 by casein kinase 1 (CK1) and other kinases**

The  $\delta$  isoform of CK1 interacts with Cx43 and phosphorylates it on S325, S328 and S330 (Cooper and Lampe, 2002; Solan and Lampe, 2007). Inhibition of CK1 resulted in an increased localization of Cx43 at the plasma membrane, and a reduced gap junctional communication (Figure 13 - Cooper and Lampe (2002)). CK1 is present in most tissues, in many cellular compartments, is constitutively active, has a number of substrates and prefers numerous negative charges aminoterminal to the target site. Because of CK1's requirement for a phosphate residue within its recognition sequence, it can phosphorylate substrates only in conjunction with other protein kinases (Gross and Anderson, 1998).

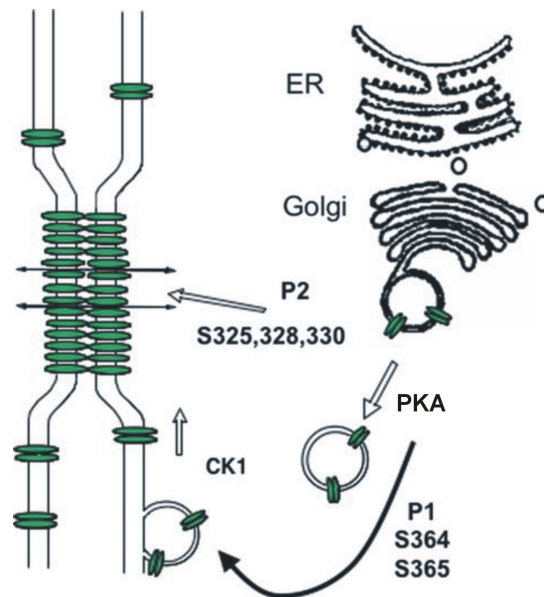


**Figure 13: PKA and CK1 phosphorylation of Cx43**

PKA mediates phosphorylation of Cx43 on S364 and S365. This results in the P<sub>1</sub> form and is required for trafficking of Cx43 to the plasma membrane. CK1 phosphorylates Cx43 hemichannels at S325, S328, and S330, leading to the formation of the P<sub>2</sub> form and incorporation into plaques (Solan and Lampe, 2007).

cAMP elevation induced PKA activation and this affected gap junctional communication. Three types of responses were found: (i) a slow increase in gap junctional communication, (ii) a rapid decrease in gap junctional communication, and (iii) a rapid increase in gap junctional communication (Stagg and Fletcher, 1990; Saez et al., 1993a). The first response was mainly dependent on an increased gene expression. The second mechanism was a consequence of increased cAMP levels and decreased gap junctional permeability (Cole and Garfield, 1986; Moore et al., 1991; Moreno et al., 1993), and the last mechanism was dependent on a cAMP induced increase in gap junctional communication and may occur by cell specific mechanisms resulting in an increased open probability, increased single channel conductance, enhanced incorporation of Cx43 hemichannels in gap junctional plaques or recruitment of Cx43 from the Golgi-located subpopulation. There is still some controversy on whether PKA phosphorylates Cx43 (Dasgupta et al., 2001) or not (Saez et al., 1993b; TenBroek et al., 2001). TenBroek et al. (2001) showed that PKA did not phosphorylate Cx43 directly, but that the enhanced assembly of Cx43 containing gap junctions was dependent on the basal phosphorylation of S364 and S365 by an unknown kinase (TenBroek et al., 2001). It is not known why different cell systems expressing the same connexin respond so differently to cAMP (Berthoud et al., 1992; Banrud et al., 1994; Granot and Dekel, 1994; Atkinson et al., 1995; Paulson et al., 2000; TenBroek et al., 2001). The most trivial possibility is that these rapid, but small, responses (Moore et al., 1991; Moreno et al., 1993) were overlooked in studies investigating the long-term effects of cAMP. In support of this possibility, the short-

term decrease in gap junctional communication was followed by a long-term increase in synthesis of Cx43 in *corpus cavernosum* smooth muscle cells (Moreno et al., 1993).

### 1.2.5 Regulation of connexin gap junctional channels by changes in $[Ca^{2+}]_i$

Free intracellular  $Ca^{2+}$ -concentrations ( $[Ca^{2+}]_i$ ) in the cytosol of resting cells is approximately 100 nM, 10,000-fold lower than those of external physiological media. Various extracellular stimuli promote an increase in  $[Ca^{2+}]_i$ , coming from the extracellular environment or from intracellular stores (ER) through the opening of a diverse array of  $Ca^{2+}$ -channels. This induces a rise in  $[Ca^{2+}]_i$  in the form of elemental  $Ca^{2+}$ -elevations called blips (1,4,5-InsP<sub>3</sub> receptor - 1,4,5-InsP<sub>3</sub>R - mediated) or quarks (ryanodine receptor - RYR - mediated) and puffs (1,4,5-InsP<sub>3</sub>R mediated) or sparks (RYR mediated), depending on the extent of the intracellular area covered (Figure 14 - Clapham (1995); Berridge et al. (2000)).

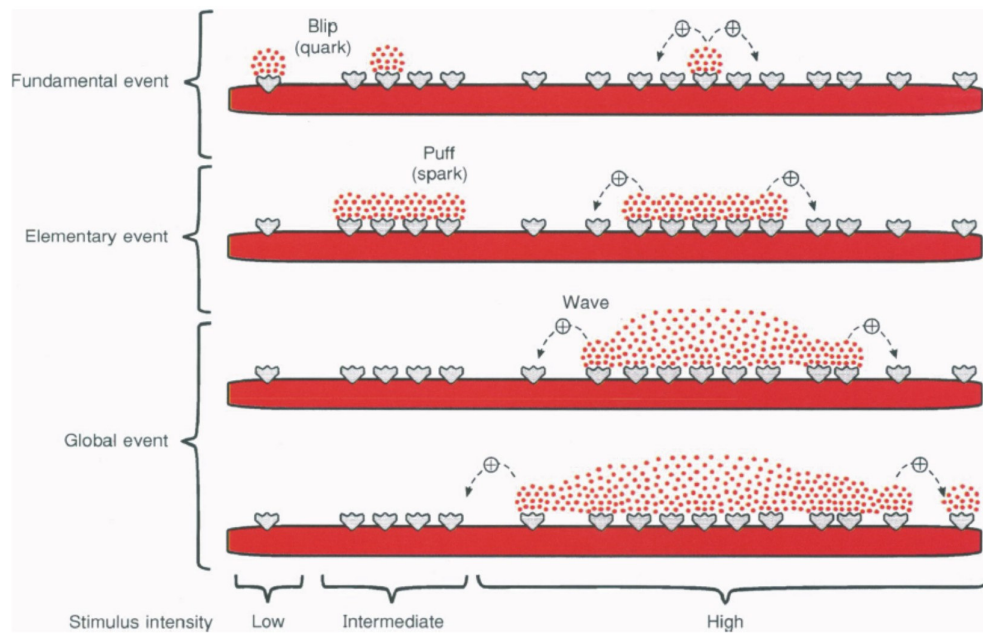


#### **Figure 14: Organization of intracellular $Ca^{2+}$ -signaling**

Fundamental events are characterized by the opening of single intracellular channels to give blips (1,4,5-InsP<sub>3</sub>R) or quarks (RYR). Elementary events, represented by puffs and sparks result from the coordinated opening of small groups of 1,4,5-InsP<sub>3</sub>R and RYR. These elementary events appear to be the basic building blocks of global events, which develop as an intracellular wave resulting from the progressive recruitment of neighboring receptors through a process of  $Ca^{2+}$ -induced  $Ca^{2+}$ -release (Berridge, 1997).

Elevating  $[Ca^{2+}]_i$  electrically uncouples insect gland cells (Rose and Loewenstein, 1975; Rose and Loewenstein, 1976), cardiac cells (Firek and Weingart, 1995), amphibian embryonic cells (Spray et al., 1982), rat lacrimal cells (Neyton and Trautmann, 1985), crayfish giant axons (Peracchia, 1990b; Peracchia, 1990a), Novikoff hepatoma cells (Lazrak and Peracchia, 1993),

astrocytes (Enkvist and McCarthy, 1994; Cotrina et al., 1998a), lens culture cells (Crow et al., 1994), pancreatic  $\beta$ -cells (Mears et al., 1995) and acinar cells (Yule et al., 1996; Chanson et al., 1999), osteoblasts (Schirrmacher et al., 1996) and cochlear supporting cells (Lagostena et al., 2001; Lagostena and Mammano, 2001), indicating that connexins are gated by  $[Ca^{2+}]_i$  either directly or indirectly. The exact range of  $[Ca^{2+}]_i$  that blocks gap junctional coupling is still unknown and may vary among connexins and cell types ( $[Ca^{2+}]_i \sim 380$  nM for Novikoff hepatoma cells - Lazrak and Peracchia (1993);  $[Ca^{2+}]_i \sim 600$  nM for astrocytes - Enkvist and McCarthy (1994) and  $[Ca^{2+}]_i \sim 400$   $\mu$ M in ruptured insect gland cells - Oliveira-Castro and Loewenstein (1971)). In A7r5 myocytes expressing Cx40 and Cx43, elevating  $[Ca^{2+}]_i$  in microdomains along the plasma membrane through the inhibition of the  $Na^+/K^+$ -pump or the  $Na^+/Ca^{2+}$ -exchanger, functionally uncoupled these cells, while global increases in  $[Ca^{2+}]_i$ , accompanied by more variable peripheral  $[Ca^{2+}]_i$  rises did not affect gap junctional communication (Matchkov et al., 2007). In this study, the authors were unable to show whether intracellular  $Ca^{2+}$  directly reduced the permeability of gap junctions or whether these  $Ca^{2+}$ -transients caused the activation of  $Ca^{2+}$ -sensitive messengers. Dakin and Li (2006) showed that capacitive  $Ca^{2+}$ -influx through store-operated  $Ca^{2+}$ -channels (SOCs - Parekh and Putney (2005)) induced cell-cell uncoupling in Cx43 expressing primary human fibroblast cells, in HeLa-Cx43 cells and in HeLa-Cx26 cells, while global  $[Ca^{2+}]_i$  changes up to micromolar levels were unable to reduce gap junctional communication (Dakin and Li, 2006). In contrast, Lurtz et al. (2003) showed that increasing  $[Ca^{2+}]_i$  by a  $Ca^{2+}$ -ionophore uncoupled lens epithelial cells (Lurtz and Louis, 2003). This effect was prevented by incubating the cells with an inhibitor of CaM. A possible explanation for the wide range of  $[Ca^{2+}]_i$  reported to block gap junctional communication is the presence of efficient internal buffering mechanisms, creating large  $Ca^{2+}$ -gradients inside the cell. This is supported by very slow  $Ca^{2+}$ -diffusion in the cytosol, with a diffusion coefficient ranging from 13 to 65  $\mu$ m<sup>2</sup>/s in *Xenopus laevis* oocytes (Allbritton et al., 1992). It is not likely that intracellular  $Ca^{2+}$  directly acts on connexin channels, because this would suggest the presence of negative charges on the cytoplasmic side of the pore. There is however only one acidic residue (glutamate) marking the transition between the fourth transmembrane domain and the carboxyterminal domain, resulting in six glutamate residues in one hemichannel. This is incapable of binding  $Ca^{2+}$  with sufficient high affinity to account for gating effective  $[Ca^{2+}]_i$  in the nanomolar range (Peracchia, 2004). Furthermore, this residue cannot discriminate between  $Ca^{2+}$  and  $Mg^{2+}$  and is not located near the pore opening. It is reasonable to believe that the effect of intracellular  $Ca^{2+}$  on gating is mediated by an intermediate component, such as CaM. CaM is the most abundant and well-known  $Ca^{2+}$ -sensor (Means and Dedman, 1980; Chin and Means, 2000). It is expressed in all eukaryotic cells and modulates basic cellular processes such as cell growth, differentiation, proliferation, cell survival and cell motility. The crystal structure of the  $Ca^{2+}$ -bound form of CaM shows an elongated molecule with two globular domains,

arranged in a *trans*-configuration. These domains are connected by a long extended central  $\alpha$ -helix, which acts as a flexible tether. Each domain consists of two helix-loop-helix motifs (EF hands) and is able to bind one  $\text{Ca}^{2+}$ -molecule, resulting in a changed orientation of the two EF hands of each domain, inducing the exposure of hydrophobic patches that bind CaM binding protein (CaMBP - Agell et al. (2002)). The carboxyterminal lobe binds  $\text{Ca}^{2+}$  with a higher affinity (dissociation constant;  $K_d \sim 10^{-7}$  M) than the aminoterminal lobe ( $K_d \sim 10^{-6}$  M). These  $K_d$ -values fall within the range of normal  $[\text{Ca}^{2+}]_i$  changes exhibited for most cells. Activated CaM can activate  $\text{Ca}^{2+}$ /CaM dependent kinases (CaMKI-V - Soderling (1999); Means (2000)) and  $\text{Ca}^{2+}$ /CaM dependent phosphatases (calcineurin - Klee et al. (1998)) regulating the phosphorylation status of many proteins. It was shown that CaM can pass through invertebrate and vertebrate gap junction channels (Curran and Woodruff, 2007), but the exact connexin composition of these gap junctions is however not mentioned. CaM interacts with Cx26 (Blodow et al., 2003), Cx30 (Blodow et al., 2003), Cx32 (Torok et al., 1997), Cx35 (Burr et al., 2005), Cx36 (Burr et al., 2005), Cx37 (Sotkis et al., 2001), Cx38 (Peracchia, 2004), Cx43 (Torok et al., 1997; Zhou et al., 2007), Cx50 (Zhang and Qi, 2005), perch Cx35 (Burr et al., 2005), mouse Cx36 (Burr et al., 2005), and perch Cx34.7 (Burr et al., 2005). Three potential CaM binding sites, characterized by the presence of basic and bulky hydrophobic residues (Rhoads and Friedberg, 1997), have been identified in Cx32, two of them are located at the aminoterminal domain (site N1: residues  $\sim 1 - 22$ , and site N2: residues  $\sim 18 - 22$ ) and one is located in the carboxyterminal domain (site C1: residues  $\sim 208 - 226$ ; Peracchia (1988); Peracchia (2004)). Site N1 and C1 bind CaM in a  $\text{Ca}^{2+}$ -dependent way, with a  $K_d$ -value of 27 nM and 1.2  $\mu\text{M}$  respectively (Torok et al., 1997). In site N1, CaM binding is determined by residues W3, V14 and I20. In the C1 region A216 and A218 mediate CaM binding (Torok et al., 1997). The CaM binding site in Cx35 and Cx36 has a  $K_d$ -value of 11 nM and 72 nM respectively (Burr et al., 2005). Mapping the binding site of CaM in Cx43 has led to conflicting results. Torok et al. (1997) identified a CaM binding site with a  $K_d$ -value of 1.2  $\mu\text{M}$  in the aminoterminal domain (residue 1 - 16; Torok et al. (1997)). Zhou et al. (2007) identified a CaM binding domain located in the second half of the intracellular loop of Cx43 with a  $K_d \sim 0.7 - 1 \mu\text{M}$  (Zhou et al., 2007). The stoichiometry of the interaction is close to 1:1, and remarkably, upon binding of Cx43, the  $K_d$  for the  $\text{Ca}^{2+}$ /CaM interaction decreased from 2.9  $\mu\text{M}$  to 1.6  $\mu\text{M}$  and the Hill coefficient increased from 2.1 to 3.3 (Zhou et al., 2007). Peracchia et al. (2000) proposed a “cork-type” gating model in which the cytoplasmic mouth of the pore is physically obstructed by a CaM lobe (Peracchia et al., 2000b). Hereby the negative charges of the CaM lobe bind to the Cx32 pore (basic, positively charged residues) by electrostatic and hydrofobic interactions. In this “cork” model the aminoterminal CaM lobe acts as the gating element, activated by an increase in  $[\text{Ca}^{2+}]_i$  above baseline levels, while the carboxyterminal lobe is anchored to the N1 site of Cx32 at basal  $\text{Ca}^{2+}$ -levels (Peracchia, 2004). Although evidence is accumulating for a direct role of CaM in

gating, an indirect way involving CaMK and  $\text{Ca}^{2+}$ /CaM dependent phosphatases is still possible.

Although most studies showed an inhibition of gap junctional communication by elevated  $[\text{Ca}^{2+}]_i$ , reports indicating that gap junction channels may open by increased  $\text{Ca}^{2+}$ /CaM signaling exist (Delage and Deleze, 1998; Blodow et al., 2003; de Pina-Benabou et al., 2005). Increasing  $[\text{Ca}^{2+}]_i$  up to 2.6  $\mu\text{M}$  induced an elevated channel conductance in heart myocytes (Delage and Deleze, 1998). However, inhibiting CaM activation could not prevent the intracellular  $\text{Ca}^{2+}$ -induced increase in gap junctional coupling. This is in contrast with the study from Blodow et al. (2003), who showed that channel conductance mediated by Cx26 was suppressed by blocking CaM in Hensen cells (derived from the cochlea). De Pina-Benabou et al. (2005) showed that elevating  $[\text{Ca}^{2+}]_i$ , up to 500 nM, by the activation of voltage-gated  $\text{Ca}^{2+}$ -channels induced an increase in gap junctional coupling in astrocytes. The altered gap junctional communication was not mediated by a direct interaction of intracellular  $\text{Ca}^{2+}$  with the connexin subunit, but was related to the activation of a downstream signaling pathway, such as CaMK (de Pina-Benabou et al., 2005). The increased coupling was however not associated with a changed expression level of Cx43 or an altered distribution pattern. It was likely that the elevated gap junctional communication was mediated by increased open probability of the gap junction channels, due to Cx43 phosphorylation by CaMK-II on S296, S365, and S369 (Blom et al., 1999). The contradictory results may be due to the different  $[\text{Ca}^{2+}]_i$  under which gap junctional coupling was studied.

### 1.3 Hemichannels: unpaired gap junctional channels

It was previously accepted that connexin hemichannels (Figure 1) were closed before incorporation into gap junction channels. This was based on the fact that hemichannel opening was lethal for the cells. Since the past 5 - 10 years, many studies demonstrated functional hemichannels in many cell types, such as osteoblasts, osteocytes (Plotkin and Bellido, 2001), astrocytes, (Stout et al., 2002), cardiomyocytes (Shintani-Ishida et al., 2007), horizontal cells (Kamermans et al., 2001), retinal pigment epithelial cells (Pearson et al., 2005), and corneal endothelial cells (Gomes et al., 2005) by different independent techniques, such as immunocytochemistry, freeze fracture electron microscopy, dye uptake measurements, electrophysiological recordings, ion channel reconstitution in lipid bilayers or liposomes, release measurements of small molecules and biotinylation of cell surface proteins (Harris, 2001; Saez et al., 2005). The evidence presented in each of these studies should however be interpreted with caution, because many other release pathways are present in the cell (as further discussed in section 1.3.5). Uncontrolled opening of hemichannels may be dangerous for cells, because it can result in the loss of metabolites, the collapse of ionic

gradients and the entry of  $\text{Ca}^{2+}$ -ions. It is therefore clear that the open probability must be very low under conditions compatible with cell survival.

Connexin hemichannels may be opened by several stimuli, such as a reduction in  $[\text{Ca}^{2+}]_e$  (Ebihara et al., 2003), membrane depolarization (Contreras et al., 2003a), mechanical stress (Stout et al., 2002; Jiang and Cherian, 2003), metabolic inhibition and ischemia (John et al., 1999; Kondo et al., 2000; Contreras et al., 2002), elevation of 1,4,5- $\text{InsP}_3$  (Braet et al., 2003a; Braet et al., 2003b), increasing  $[\text{Ca}^{2+}]_i$  (Pearson et al., 2005), reducing the redox potential of the cell (Retamal et al., 2007b), ATP depletion (Vergara et al., 2003a; Vergara et al., 2003b) and the formation of reactive oxygen species (ROS - Ramachandran et al. (2007)). Opening of hemichannels is associated with the release of small signaling molecules, such as ATP (Stout et al., 2002), glutamate (Ye et al., 2003),  $\text{NAD}^+$  (Zocchi et al., 1999), glutathione (Rana and Dringen, 2007) and prostaglandin  $\text{E}_2$  (Cherian et al., 2005). The release of these messengers plays a very important role in signal transduction in many organs.

### 1.3.1 Channel inhibitors and Gap peptides

Carbenoxolone (glycyrrhetic acid-3 $\beta$ -O-hemisuccinate) and the  $\alpha$  and  $\beta$  stereoisomers of 18-glycyrrhetic acid ( $\alpha/\beta$ -GA) are lipophilic aglycones from liquorice root characterized by a steroidal structure. They exert an indirect and reversible effect on gap junctional channels at low concentrations (10 - 75  $\mu\text{M}$ ) without apparent toxicity. It was demonstrated that, within 30 min from application,  $\beta$ -GA (40  $\mu\text{M}$ ) completely blocked the intercellular dye transfer in a rat liver epithelial cell line, although the morphology of the gap junctional plaque was unaffected (Guan et al., 1996). With longer exposure times (4 h), evidence for disassembly of the gap junctional plaque became apparent (Guan et al., 1996). The uncoupling is associated with a disruption of the physical packing of the channels as seen by electron microscopy and freeze fracture. These triterpenoid saponins also affected connexin phosphorylation patterns by the activation of protein kinases and G-proteins (Takens-Kwak et al., 1992; Tordjmann et al., 1997; Taylor et al., 1998; Chaytor et al., 1999; Mambetisaeva et al., 1999; Boitano and Evans, 2000). The effects of carbenoxolone are not specific for connexin channels ( $\text{EC}_{50} \sim 50$  - 100  $\mu\text{M}$  for gap junctions and  $\text{EC}_{50} \sim 5$   $\mu\text{M}$  for hemichannels - Ye et al. (2003)), in that they also block other channels, such as  $\text{Ca}^{2+}$ -channels ( $\text{EC}_{50} \sim 48$   $\mu\text{M}$  - Vessey et al. (2004)), Panx1 hemichannels ( $\text{EC}_{50} \sim 5$   $\mu\text{M}$  - Bruzzone et al. (2005)), and the  $\text{P}_2\text{X}_7$  receptor pore ( $\text{EC}_{50} \sim 0.175$   $\mu\text{M}$  - Suadicani et al. (2006)). 18-glycyrrhetic acid ( $\text{EC}_{50} \sim 10$   $\mu\text{M}$  for gap junctions and  $\text{EC}_{50} \sim 2$  - 10  $\mu\text{M}$  for hemichannels - Eskandari et al. (2002)) also inhibits Panx1 hemichannels, although only at higher concentrations ( $\sim 50$   $\mu\text{M}$  - Bruzzone et al. (2005)). A direct interaction between carbenoxolone/18-glycyrrhetic acid and connexin and pannexin proteins was suggested as the mechanism to block channels composed of connexins/pannexins, but the exact interaction site is not yet known (Bruzzone et al., 2005).



Despite the widespread distribution of connexin gap junctions and hemichannels, there are relatively few agents known to block gap junction channels/hemichannels in a specific manner. Connexin mimetic peptides, further called Gap peptides, i.e. peptides that are identical to a short amino acid sequence on the connexin subunit (Table 3), were initially designed to produce connexin selective blockage of gap junctions (Dahl et al., 1994; Warner et al., 1995). These peptides were selected from a range of short peptides based on their ability to delay synchronized contraction by aggregating myocytes dissociated from chicken hearts (Warner et al., 1995). <sup>43</sup>Gap 26 and <sup>43</sup>Gap 27 mimic a sequence on the first and second extracellular loop respectively, inhibited gap junctional communication (EC<sub>50</sub> ~ 20 - 30 μM - Chaytor et al. (1997); Berman et al. (2002); Leybaert et al. (2003)), rhythmic contractions in rabbit arteries (Chaytor et al., 1997), the propagation of Ca<sup>2+</sup>-waves across groups of confluent cells (Boitano and Evans, 2000; Isakson et al., 2001), and electrical communication (Dora et al., 1999; Kwak and Jongsma, 1999). These Gap peptides comprise conserved domains (VCYD and SHVR in <sup>43</sup>Gap 26 and SRPTEK in <sup>43</sup>Gap 27), which are not consistently found in other cell surface proteins (Warner et al., 1995). Other peptides have been developed that incorporate small changes in the non-conserved peptide moieties, resulting in a variety of peptides directed at the 'Gap 26 region' or the 'Gap 27 region' (Chaytor et al., 1999; Evans and Boitano, 2001; Isakson et al., 2003; Evans et al., 2006). Two different protocols have been used to investigate the effect of the Gap peptides on gap junctional communication. In some cases, the peptides were applied before the cells had time to interact and form gap junctions (Dahl et al., 1994; Warner et al., 1995; Eugenin et al., 1998; Kwak and Jongsma, 1999; Gaietta et al., 2002). In this case, the peptides may prevent the docking of hemichannels. This mechanism is however less likely to occur, because Gap peptides had little or no effect on the size of the gap junctional plaque in HeLa cells stably transfected with Cx43-GFP (Berman et al., 2002). In other studies, inhibitory peptides were applied to tissues or cultured cells with established gap junctions (Chaytor et al., 1997; Boitano and Evans, 2000). This leads to a second, possible mechanism whereby the Gap peptides diffuse in the extracellular space surrounding the gap junctional plaque, and facilitate the breaking apart of previously formed gap junction channels. Disrupting the docking of channels beginning at the periphery of a gap junctional plaque may lead to an "unzipping" of gap junctions (Berthoud et al., 2000). A third possible mechanism has been proposed by Chaytor et al. (1997). Here, it was assumed that the extracellular loop peptides may bind to the connexin molecules in intact gap junction channels, inducing a conformational change that leads to channel closure. Recently, an interaction between <sup>43</sup>Gap 26 and the extracellular loops of Cx43 was found, while a scrambled form of the peptide (PSFDSRHCIKYYV) did not interact. These results point to a specific interaction between <sup>43</sup>Gap 26 and possibly the corresponding sequence on Cx43 (Liu et al., 2006), making the third mechanism the most

likely. The reversibility of the effects suggested that the Gap peptides did not target the connexin proteins for degradation.

Recently, the effect of Gap peptides has been investigated on presumed hemichannel responses. Both  $^{43}\text{Gap 26}$  and  $^{43}\text{Gap 27}$  blocked uptake of small hemichannel permeable dyes (Braet et al., 2003a; Braet et al., 2003b; Retamal et al., 2006; Retamal et al., 2007a), cellular ATP release (Braet et al., 2003a; Braet et al., 2003b; Vandamme et al., 2004; Pearson et al., 2005; Dobrowolski et al., 2007), currents through hemichannels in taste buds (Romanov et al., 2007), and the propagation of  $\text{Ca}^{2+}$ -waves (Braet et al., 2003a; Braet et al., 2003b; Vandamme et al., 2004; D'Hondt et al., 2007). Similar to Gap 26 and Gap 27 that mimics a sequence on the first and the second extracellular loop of the connexin protein, a pannexin mimetic peptide,  $^{10}\text{Panx 1}$ , has been developed. This peptide mimics a sequence on the first extracellular loop, and inhibits ATP mediated dye uptake in Panx1 expressing cells (Pelegrin and Surprenant, 2006; Pelegrin and Surprenant, 2007).

Substantial evidence is accumulating that Gap peptides block hemichannels and gap junction channels composed of connexin proteins. Despite this, it was recently reported that connexin and pannexin mimetic peptides did not exhibit specificity for either of the channels (Wang et al., 2007), although the inhibitory effects of the Gap peptides on Panx1 channel currents were rather limited. It was suggested that these peptides inhibit conductance through the channel by steric block of the pore. These findings were based on similar effects of inhibition that were obtained with PEG1500. Although the latter was used in millimolar concentrations, compared to micromolar concentrations for the peptides. Furthermore, in this study a chimeric Cx32EL1Cx43 protein was used, which makes it difficult to compare the results.

Name	Protein	Protein domain	Sequence	Reference
$^{43}\text{Gap 26}$	Cx43	EL1	VCYDKSFPISHVR	Dahl et al. (1994) Warner et al. (1995)
$^{43}\text{Gap 27}$	Cx43	EL2	SRPTEKTIFII	Dahl et al. (1994) Warner et al. (1995)
$^{40}\text{Gap 27}$	Cx40	EL2	SRPTEKNVFIV	Evans and Boitano (2001) Chaytor et al. (1999)
$^{10}\text{Panx 1}$	Panx1	EL1	WRQAAFVDSY	Pelegrin and Surprenant (2006)

**Table 3: Sequence of pannexin and connexin mimetic peptides**

This table demonstrates the sequence of some of the frequently used extracellular loop peptides.

## 1.3.2 Substances released by open hemichannels

### 1.3.2.1 Release of ATP

The naturally occurring nucleotide ATP is present in every living cell and is well-known for its role in intracellular energy metabolism. In addition to this, extracellular ATP is thought to contribute to the regulation of a variety of other biological processes, including cardiac function, neurotransmission, muscle contraction, vasodilation, bone metabolism, liver glycogen metabolism and inflammation (Agteresch et al., 1999; Hoebertz et al., 2003). The intracellular ATP concentration is usually very high (2 - 5 mM), but the physiological ATP concentration in the plasma is much lower (400 - 700 nM - Ryan et al. (1996)). The molecular weight of ATP is 551 Da (Table 2), which is much lower than the cut-off limit for hemichannels ( $\leq 1.2$  kDa), indicating that this molecule can be released via open hemichannels.

Ecto-enzymes, which are involved in the degradation of extracellular ATP, include four families that partially share tissue distribution and substrate specificity: (i) the ectonucleotide triphosphate diphosphohydrolase (E-NTPDase) family, (ii) the ectonucleotide pyrophosphatase-phosphodiesterase (E-NPP) family, (iii) alkaline phosphatases, and (iv) ecto-5'-nucleotidase (CD73). The first family catalyzes the sequential degradation of ATP and ADP to AMP. The second family catalyzes the conversion of cAMP to AMP and ATP and ADP to AMP. The third family induces the degradation of ATP, ADP, and AMP to adenosine. Finally, the fourth family is represented by CD73 which catalyzes the hydrolysis of AMP to adenosine (Bours et al., 2006; Yegutkin, 2008). Membrane-bound receptors mediate cell signaling by ATP and its degradation products. Two families of purinergic receptors have been defined to date, namely  $P_1$  and  $P_2$  receptors (Bours et al., 2006; Burnstock, 2007).  $P_1$  receptors belong to the family of GPCR and are activated by adenosine. The  $P_2$  receptors are activated by ATP and subdivided into two subfamilies, i.e.  $P_2X$  and  $P_2Y$ .  $P_2X$  receptors are ligand-gated ion channels of which seven subtypes were identified  $P_2X_{1-7}$  (Khakh, 2001), while  $P_2Y$  receptors are GPCR of which eight subtypes were characterized ( $P_2Y_{1,2,4,6,11-14}$ ).

ATP release from various cell types (Dubyak and el-Moatassim, 1993) contributes to  $Ca^{2+}$ -wave propagation in astrocytes (Guthrie et al., 1999; Cotrina et al., 2000), osteocytes (Jorgensen et al., 2002) and retinal pigment epithelial cells (Pearson et al., 2005). Subsequent binding of ATP on  $P_2$  purinergic receptors on adjacent cells induced an increase in  $[Ca^{2+}]_i$  (Guthrie et al., 1999).  $P_2Y$  receptor activation is linked to the activation of PLC, with subsequent production of 1,4,5-InsP<sub>3</sub> and an elevation of  $[Ca^{2+}]_i$  (Burnstock, 2006). Activation of  $P_2X$  receptors result in the activation of an ion channel and influx of extracellular  $Ca^{2+}$  (Romanov et al., 2007).

### 1.3.2.2 Release of glutamate

Glutamate is widely recognized to be the main excitatory neurotransmitter in the brain and it mediates excitatory synaptic transmission through the activation of ionotropic glutamate receptors that are sensitive to NMDA (N-methyl-D-aspartate), AMPA ( $\alpha$ -amino-3-hydroxy-5-methyl-4-isoxazolepropionic acid), or kainate (Won et al., 2002). It is however important to realize that glutamate has also many other important roles in the brain, including oxidation for energy, incorporation into proteins, and formation of glutamine,  $\gamma$ -aminobutyric acid, and glutathione (McKenna, 2007). Under normal resting conditions, extracellular glutamate concentrations are in the range of 1 - 10  $\mu$ M. During high neural activity the concentration of this molecule increases 100-fold (100  $\mu$ M - 1 mM; McKenna (2003)) and the extracellular glutamate is cleared from the synaptic cleft through astrocytes (Danbolt, 2001). As a consequence, astrocytes have a high intracellular glutamate content (0.2 mM). Under ischemic conditions, hemichannels are opened (Contreras et al., 2002) and glutamate (MW 147 Da - Table 2) can be released through open hemichannels (Ye et al., 2003). In this way, astrocytes may contribute to high extracellular glutamate levels, which is excitotoxic for different cell types.

### 1.3.2.3 Release of NAD<sup>+</sup>

The steep electrochemical gradient between the millimolar intracellular NAD<sup>+</sup>-levels and the 40 - 100 nM values measured in the extracellular environment provides the driving force for the release of this molecules under physiological conditions (Bruzzone et al., 2001b). It was shown by Bruzzone et al. (2001) that NAD<sup>+</sup> may leave the cell via open hemichannels composed of Cx43 (Bruzzone et al., 2001a; Bruzzone et al., 2001b), and in this way becomes available as a substrate for the active site of the CD38 ecto-enzyme by which it is converted to cADPR (cyclic adenosine diphosphate ribose - De Flora et al. (2004)). This cADPR is then transported back to the cytoplasm by CD38, where it may act on its target, the RYR, according to an autocrine signaling mechanism (Figure 15). Alternatively, cADPR can also work in a paracrine manner, diffusing to CD38 on neighboring cells, causing the release of [Ca<sup>2+</sup>]<sub>i</sub> from the intracellular stores. A RYR mediated increase in [Ca<sup>2+</sup>]<sub>i</sub> activates PKC, resulting in the phosphorylation of Cx43, and reducing the permeability of the hemichannels (Bao et al., 2007). This prevents: (i) the excessive loss of NAD<sup>+</sup>, (ii) the rise of cADPR, and (iii) the emptying of intracellular Ca<sup>2+</sup>-stores with a possible cytotoxic effect.

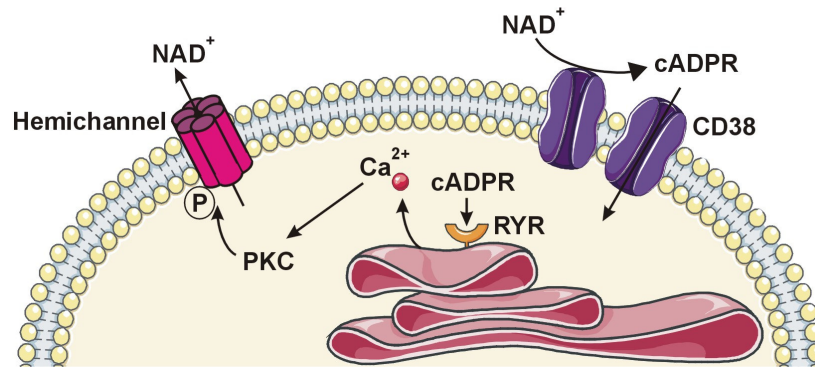


**Figure 15: Autocrine NAD<sup>+</sup> mediated Ca<sup>2+</sup>-signaling**

Hemichannel opening induced the release of NAD<sup>+</sup> (nicotinamide adenine dinucleotide). In the extracellular environment NAD<sup>+</sup> is converted to cADPR (cyclic ADP ribose) by the ecto-enzyme CD38, which also mediates the uptake of cADPR. cADPR binds on the RYR (ryanodine receptor) and induced the release of [Ca<sup>2+</sup>]<sub>i</sub> from the intracellular stores. Increased [Ca<sup>2+</sup>]<sub>i</sub> activates PKC (protein kinase C), leading to a phosphorylation of Cx43 hemichannels, and in this way reducing the permeability, providing negative feed-back. This scheme is based on the data presented in De Flora et al. (2004).

### 1.3.2.4 Release of glutathione

The tripeptide glutathione (GSH), composed of the amino acids  $\gamma$ -L-glutamyl-L-cysteinyl-glycine, plays an important role in the anti-oxidative defense of the brain. GSH is present in tissues in the low millimolar range (Slivka et al., 1987) and in the low micromolar range in the CSF (cerebrospinal fluid). This peptide is found to be elevated during ischemia (Anderson et al., 1989; Orwar et al., 1994). Intracellularly, GSH reacts with radicals and the thiol group of the cysteine residue functions as an electron donor for the reduction of peroxides (Dringen, 2000; Dringen and Hirrlinger, 2003). It was demonstrated that GSH was released through open hemichannels (Rana and Dringen, 2007) and in this way formed a key player for the metabolic interaction between astrocytes and neurons. The availability of cysteine determines the level of neuronal GSH (Dringen et al., 1999), but uptake of intact GSH into cultured neurons has not been observed (Sagara et al., 1993). The mechanism of GSH supply from astrocytes to neurons has recently been resolved: the first step is the export of GSH from astrocytes. Extracellular GSH is then converted to the dipeptide CysGly by the astroglial ecto-enzyme  $\gamma$ GT ( $\gamma$ -glutamyl transpeptidase - Dringen (2000)). CysGly is subsequently hydrolyzed by the aminopeptidase N, resulting in the formation of cysteine and glycine (Dringen, 2000). These amino acids are taken up by neurons and are used as a precursor for neuronal GSH (Dringen et al., 1999). Extracellular GSH may function as a first line defense against ROS generated in the extracellular space.

### 1.3.2.5 Release of prostaglandin E<sub>2</sub>

Osteocytes are star-shaped cells that are dispersed throughout the mineralized matrix and emit signals that stimulate osteoblast differentiation into osteocytes (Palumbo et al., 1990; Nefussi

et al., 1991; Aarden et al., 1994). Cx43 gap junctions and hemichannels in osteocytes have essential, but distinct roles in transmitting the signals elicited by mechanical stimulation to other bone cells and the extracellular matrix to promote bone formation and remodeling. Mechanical stress triggers the hemichannel mediated release of prostaglandin E<sub>2</sub> (PGE<sub>2</sub>) from MLO-Y4 cells through the recruitment of Cx43 hemichannels to the plasma membrane (Cherian et al., 2005). PGE<sub>2</sub> is a skeletal anabolic agent that increases the bone mass in animals (Jee et al., 1985) and long-term release is significantly reduced in osteoporotic bone cells (Sterck et al., 1998). The released PGE<sub>2</sub> functions in an autocrine manner, activating EP<sub>2</sub> receptor signaling, increasing cAMP and activating PKA, which in turn stimulates gap junctional communication and Cx43 expression (Cheng et al., 2001b; Cherian et al., 2003; Cherian et al., 2005).

### 1.3.3 Hemichannel responses to [Ca<sup>2+</sup>]<sub>i</sub>

Recent work in our research group, showed that elevation of 1,4,5-InsP<sub>3</sub> by photoliberation of caged-InsP<sub>3</sub> in rat endothelial cells (GP8 and RBE4) and human epithelial bladder cancer cells (ECV304) triggered the release of ATP (Braet et al., 2003a; Braet et al., 2003b). This triggered ATP release was completely inhibited by  $\alpha$ -GA, the trivalent ions Gd<sup>3+</sup> and La<sup>3+</sup> and the Gap peptides <sup>43</sup>Gap 26 and <sup>43</sup>Gap 27. These results correspond to the connexin expression in these cell lines (Cx43). These results were consistent with the opening of hemichannels, resulting in the release of ATP and subsequent paracrine signaling (Braet et al., 2003a; Braet et al., 2003b). Photoreleasing Ca<sup>2+</sup> from NP-EGTA in a single cell did however not trigger any significant ATP release, which was consistent with the absence of propagating Ca<sup>2+</sup>-changes to neighboring cells (Braet et al., 2003b). This finding was in contrast with the observation that 1,4,5-InsP<sub>3</sub>-triggered ATP release was dependent on changes in [Ca<sup>2+</sup>]<sub>i</sub>, because BAPTA (Ca<sup>2+</sup>-chelating agent) largely suppressed the triggered ATP release (Braet et al., 2003b). A possible explanation is that 1,4,5-InsP<sub>3</sub> released Ca<sup>2+</sup> from the intracellular stores focally, and this in close association to the Ca<sup>2+</sup>-sensitive ATP release pathway, such as hemichannels (Petersen et al., 1999; Montero et al., 2001).

Similar results were obtained by Pearson et al. (2005). In this study, spontaneous intracellular Ca<sup>2+</sup>-transients in specific trigger cells in the retinal pigment epithelium (RPE) induced the release of ATP and the uptake of a small fluorescent reporter dye. An effect that was completely blocked by the gap junction/hemichannel inhibitors  $\alpha$ -GA, carbenoxolone, retinoic acid and <sup>43</sup>Gap 26, while the scrambled peptide (PSFDSRHCIYKYV) was without an effect (Pearson et al., 2005). This indicated that intracellular Ca<sup>2+</sup>-triggered ATP release was mediated by hemichannels composed of Cx43, located at the retinal face of the RPE cells. The released ATP subsequently diffused into the ventricular zone of the adjacent neural retina, where it acted on P<sub>2</sub>Y receptors of the neural progenitor cells, stimulating mitosis and proliferation (Pearson et al., 2005). Extracellular ATP also binds on P<sub>2</sub>Y receptors present on

neighboring RPE cells, evoking an increase in  $[Ca^{2+}]_i$  and the propagation of a  $Ca^{2+}$ -wave. These results provide strong evidence for the activation and opening of connexin hemichannels under physiological conditions.

### 1.3.4 Hemichannel responses to $[Ca^{2+}]_e$

The total  $[Ca^{2+}]_e$  is under physiological conditions in the order of 2.2 - 2.6 mM (free  $[Ca^{2+}]_e \sim 1.1 - 1.4$  mM; Parfitt and Kleerekofer (1980); Stewart and Broadus (1987)). During ischemia and anoxia in the central nervous system,  $[Ca^{2+}]_e$  drops to values less than 10 % of control, i.e.  $\sim 0.1$  mM (Xiong and MacDonald, 1999). Furthermore, the extracellular fluid space decreases to approximately 50 % of control, meaning that almost all extracellular  $Ca^{2+}$  is translocated into the cell (Kristian and Siesjo, 1998). Extracellular free  $Ca^{2+}$  is known to influence the gating of homomeric hemichannels composed of different connexin subunits (Cx26 - Muller et al. (2002); Stong et al. (2006); Cx32 - Gomez-Hernandez et al. (2003); Cx43 - Thimm et al. (2005); Liu et al. (2006); Cx46 - Pfahnl and Dahl (1999); and Cx45 - Valiunas (2002)) and induces a reversible conformational change of the hemichannel structure. This change is specific for  $[Ca^{2+}]_e$ , because similar changes in  $[Mg^{2+}]_e$  and  $[Ni^{2+}]_e$  are unable to influence the gating of hemichannels (Muller et al., 2002).

Removal of extracellular  $Ca^{2+}$  increased the Cx26 hemichannel pore diameter from 6 to 15 Å. This was the consequence of a rotation of the cytoplasmic, but not the extracellular connexin domains, thereby opening the hemichannel. It was remarkably that an intracellular conformational change affected the extracellular hemichannel surface (Muller et al., 2002). Furthermore, it was shown that lowering  $[Ca^{2+}]_e$  from 1.8 mM to  $\leq 1.6$  mM in an otherwise iso-osmotic environment, resulted in the opening of Cx43 hemichannels (Quist et al., 2000; Thimm et al., 2005). This was the consequence of unfolding the extracellular loops of Cx43 and exposing the hydrophobic domains, suggesting a gating mechanism based on hydrophobic interactions (Thimm et al., 2005). When  $[Ca^{2+}]_e$  was lowered to 1.4 mM, two thirds of all Cx43 hemichannels present in BICR-M1Rk cells were opened (Thimm et al., 2005). For hemichannels composed of Cx32, a direct interaction between divalent cations and a site in the external vestibule of the pore regulates opening of hemichannels. A ring of 12 aspartate residues, formed by D169 of one Cx32 subunit and D178 of an adjacent subunit, was responsible for the binding of six  $Ca^{2+}$ -ions per hemichannel, and in this way closing the channel (Gomez-Hernandez et al., 2003). Lowering  $[Ca^{2+}]_e$  below 0.5 mM resulted in a 5-fold increase in unitary conductance in Cx32 expressing cells. These large decreases in  $[Ca^{2+}]_e$  are associated with brain anoxia and ischemia. These results indicate that connexin hemichannels might function as an exquisite sensor of extracellular  $Ca^{2+}$  and in this way regulate cell function and growth (Hofer and Brown, 2003).

### 1.3.5 Other release mechanisms

#### 1.3.5.1 Pannexin hemichannels

Panx1, 2 and 3 are the vertebrate orthologues of the invertebrate innexins (Panchin, 2005), with Panx1 and 3 being more homologous to each other than to Panx2 (Baranova et al., 2004; Penuela et al., 2007). These proteins form channels with properties that are similar to connexin hemichannels, and distinction between both channel types is difficult. Pannexin hemichannel opening is induced by membrane depolarization, mechanical stimulation, elevation of  $[Ca^{2+}]_i$ , hypotonic stress and hypoxia (Bruzzone et al., 2003; Bruzzone et al., 2005; Locovei et al., 2006a; Locovei et al., 2006b). In contrast to hemichannels formed by connexins, pannexin hemichannels are insensitive to changes in  $[Ca^{2+}]_e$ , despite the presence of two aspartate residues that could provide  $Ca^{2+}$ -binding (Bruzzone et al., 2005). Panx1 opening induced by mechanical stimulation resulted in the formation of a pore with a unitary conductance of 475 pS and at least four substates (with 5 %, 25 %, 30 %, and 90 % of the maximal conductance) were identified (Bao et al., 2004a). Biochemical and electrophysiological evidence indicated that Panx1 interacted with Panx2 and Panx3 (Penuela et al., 2007), forming heteromeric Panx1-Panx2 or Panx1-Panx3 hemichannels characterized by an altered current amplitude and modified voltage-gating kinetics compared to homomeric Panx1 and Panx3 hemichannels (Bruzzone et al., 2003). Extracellular ATP might indirectly induce Panx1 hemichannel responses by binding on metabotropic  $P_2Y$  ( $P_2Y_1$  or  $P_2Y_2$ ) (Locovei et al., 2006b) or ionotropic  $P_2X_7$  receptors (Pelegriin and Surprenant, 2006; Locovei et al., 2007) resulting in an increase in  $[Ca^{2+}]_i$ , which activated Panx1 hemichannels (Locovei et al., 2006b; Pelegriin and Surprenant, 2006; Locovei et al., 2007). In this way, extracellular ATP application can induce the further release of ATP (ATP-induced ATP release - Anderson et al. (2004)). It was speculated that the gating of pannexin hemichannels is regulated by post-translational modifications, such as phosphorylation and glycosylation. Both the cytoplasmic loop and the carboxyterminal domain contain several consensus sites for distinct protein kinases (Barbe et al., 2006). In contrast to connexins, Panx1 and Panx3 are N-glycosylated on the second extracellular loop at position N254 (Panx1) and the first extracellular loop at position N71 (Panx3) respectively and this appears to be important for membrane targeting (Boassa et al., 2007; Penuela et al., 2007). The glycosylation interferes with the close apposition necessary to make a tight seal between two hemichannels in order to form pannexin gap junction channels. It is quite remarkable that the degree of Panx1 glycosylation is highly variable among different tissues, suggesting that the functional role of Panx1 in each of these tissues is differentially regulated by the degree of glycosylation (Penuela et al., 2007).



### 1.3.5.2 P<sub>2</sub>X receptor pores

The purinergic P<sub>2</sub>X receptors are ionotropic channels and respond to the application of ATP and other nucleotides with the formation of a cation conductance channel (North, 2002). Sustained activation with high ATP concentrations of P<sub>2</sub>X<sub>2</sub>, P<sub>2</sub>X<sub>4</sub>, P<sub>2</sub>X<sub>5</sub> and P<sub>2</sub>X<sub>7</sub> receptors resulted in the formation of a pore ( $\leq 900$  Da) and induced irreversible permeabilization, cell lysis and apoptosis (Ferrari et al., 2006). P<sub>2</sub>X<sub>7</sub> receptors can be distinguished from other P<sub>2</sub>X receptors by their low affinity for ATP and their potentiation by decreased extracellular divalent cations (Ca<sup>2+</sup> and Mg<sup>2+</sup> - Virginio et al. (1997)). This could indicate that ATP<sup>4-</sup> might actually be the ligand or that divalent cations bind on the receptor and exert allosteric inhibition (North, 2002). The P<sub>2</sub>X<sub>7</sub> receptor pore functions as a homomultimeric complex composed of three to six subunits (North, 2002). The cytoplasmic carboxyterminal domain is essential for pore formation (Cheewatrakoolpong et al., 2005) and the E496A polymorphism abolishes the latter (Gu et al., 2001). These ionotropic purinergic receptor pores form an alternative pathway for the release of ATP, glutamate and aspartate (Duan et al., 2003). Recent studies however indicate that the pore linked to P<sub>2</sub>X<sub>7</sub> receptor activation actually corresponds to Panx1 hemichannels (Pelegriin and Surprenant, 2006; Locovei et al., 2007), offering an explanation for the similar pharmacological sensitivity.

### 1.3.5.3 Cystic Fibrosis Transmembrane Regulator

The CFTR (cystic fibrosis transmembrane regulator) is a transporter protein that forms a voltage-independent anion channel with a single channel conductance between 6 and 10 pS. The activation of the channel is dependent on phosphorylation by PKA and on the presence of MgATP (Anderson et al., 1991; Jentsch et al., 2002). The anion selectivity of the channel follows the sequence Br<sup>-</sup>  $\geq$  Cl<sup>-</sup> > I<sup>-</sup> > F<sup>-</sup>. The protein consists of six transmembrane  $\alpha$ -helices and two nucleotide binding folds (NBF) linked by a regulatory domain containing numerous phosphorylation sites (Riordan et al., 1989). NBF1 is required for channel opening and determines the closed time of the channel, while NBF2 regulates the open time of the channel. Recently, it was suggested that the CFTR channel might form a pore with a diameter of 5.3 Å, but it is not clear whether a single CFTR molecule is sufficient to form a pore, or whether the pore is multimeric. The literature concerning the release of ATP (6 - 7 Å) mediated via the CFTR channel is controversial: Sprague et al. (1998) showed that erythrocytes from healthy individuals released ATP in response to mechanical deformation, while erythrocytes from patients with cystic fibrosis did not (Sprague et al., 1998; Cantiello, 2001). These results could however not be confirmed by Grygorczyk et al. (1996, 1997) indicating that CFTR may only have a regulatory role in ATP release (Grygorczyk et al., 1996; Grygorczyk and Hanrahan, 1997). A possibility is that the release of ATP is mediated by the interaction between the CFTR channel and a separate ATP permeable channel (Braunstein et al., 2001).

#### 1.3.5.4 Volume and voltage-dependent anion channel

The volume- and voltage-dependent anion conductance channel (VDAC) is a major conduit for the release of newly synthesized ATP in the outer mitochondrial membrane (Benz, 1994). Later studies showed that this channel was also present in the plasma membrane of several cell types (Dermietzel et al., 1994). VDACS are voltage-dependent, with a rather symmetric voltage-gating response to voltages around zero mV, closing in response to either depolarization and hyperpolarization (Benz, 1994; Shoshan-Barmatz and Gincel, 2003; Colombini, 2004; Rostovtseva et al., 2004). These channels form a maxi anion pore with a molecular weight cut-off in the range of 5 kDa, a conductance of more than 500 pS, and a pore diameter of 25 Å. Permeability studies showed that a variety of nucleotides enter the pore equally well, but they interact with an intra-pore binding site with affinities that range over a factor 40, in the order  $\beta$ -NADPH >  $\beta$ -NADH >  $\alpha$ -NADH > ATP/GTP > ADP >  $\beta$ -NAD > AMP >> UTP (Rostovtseva et al., 2002a). The ability to distinguish ATP from UTP suggested a specificity for purine bases (Rostovtseva et al., 2002b; Rostovtseva et al., 2002a). It was suggested that the ATP-flux through the channel was determined by specific sites within the channel and not by the overall charge density of the pore (Komarov et al., 2005).

#### 1.3.5.5 Voltage-gated Cl<sup>-</sup> channels

All voltage-gated channels (ClC 1-7, ClC-K 1,2 and ClC 0) close at strong negative voltages and open upon membrane depolarization (Pusch et al., 2002). These channels form dimers with two identical pores that are regulated by two independent gating processes, one of which acts on each individual pore (fast gating) and one which acts on both pores as a common gate (slow gating - Jentsch et al. (2002)). The voltage-dependent gating of those channels is modulated by extracellular anions and pH (Furukawa et al., 1998). ClC channels control the resting potential in muscle cells (ClC-1) and in some neurons (ClC-2), while others are involved in the transport of NaCl in the kidney (ClC-K1 and ClC-K2). These channels are subdivided in three classes, determined by their conductance *in situ*: small (< 10 pS), middle (10 - 100 pS) and large (> 100 pS). ClC channels may also be candidates for ATP release channels (Schwiebert and Zsembery, 2003).

#### 1.3.5.6 Volume-regulated anion channels

Volume-regulated anion channels (VRAC or VSOR - volume-sensitive outward rectifying) are activated by cell swelling in response to hypotonic medium (Eggermont et al., 2001). The molecular identity and the pathway transducing volume changes to channel activation remains elusive (Jentsch et al., 2002). Mongin et al. (1999) found evidence for two forms of VRACs in cultured astrocytes with identical biophysical properties (Mongin et al., 1999). One form was impermeable to aspartate and glutamate, but permeable to Cl<sup>-</sup> and taurine, and required

tyrosine kinase activity and this was involved in volume control. The second form was permeable to aspartate, glutamate, taurine, and  $\text{Cl}^-$  and was independent of tyrosine kinase activity. Application of ATP, together with a hypo-osmotic environment induced a 10-fold increase in aspartate and taurine release (Mongin and Kimelberg, 2002), and chelation of intracellular  $\text{Ca}^{2+}$  inhibited both channels (Mongin and Kimelberg, 2002). The pore radius of these channels is estimated to be 7 Å (Ternovsky et al., 2004), and corresponds very closely to the radius of  $\text{ATP}^{4-}$  and  $\text{MgATP}^{2-}$  (Sabirov and Okada, 2004). This correlates with the voltage-dependent block of the VRACs by extracellular ATP (Tsumura et al., 1996; Hisadome et al., 2002). VRACs contribute to the release of excitatory amino acids and ATP (Perez-Pinzon et al., 1995).

### 1.3.5.7 Maitotoxin activated pore

Maitotoxin, isolated from the dinoflagellate *Gambierdiscus toxicus*, is a water-soluble polyether with a molecular weight of 3,422 Da (Gusovsky and Daly, 1990). Several studies indicate that maitotoxin acts via a plasma membrane protein, which is modified by extracellular and intracellular trypsin digestion (Leech and Habener, 1998). Until now the receptor remains unidentified (Escobar et al., 1998). At low concentrations, maitotoxin activates a non-selective cation channel ( $\text{EC}_{50} = 450 \text{ fM}$ ), while at higher concentrations a cytolytic/oncotic pore is formed (Schilling et al., 1999), allowing small organic molecules with a molecular mass < 800 Da to enter or exit the cell (Schilling et al., 1999). The size of the pore increased with the time that the cells were exposed to maitotoxin and the ion flux followed the sequence:  $\text{Ca}^{2+}$ , ethidium bromide (314 Da), YO-PRO (655 Da), fura-2 (830 Da) and POPO-3 (1,222 Da). The pore formed by maitotoxin is strongly attenuated by decreasing temperature and was dependent on the presence of extracellular  $\text{Ca}^{2+}$  (Schilling et al., 1999), which cannot be replaced by  $\text{Mg}^{2+}$  or  $\text{Mn}^{2+}$ , and only partially by  $\text{Ba}^{2+}$  (Martinez-Francois et al., 2002).

### 1.3.5.8 Exocytosis

The molecular machinery involved in exocytosis includes the soluble *N*-ethyl maleimide-sensitive fusion attachment protein receptor complex (SNARE). This complex consists of syntaxin, synaptobrevin 2 (VAMP 2) and the synaptosome-associated protein (SNAP 25). Exocytosis requires the accumulation of a substance inside synaptic vesicles. Two essential protein complexes are necessary for this process, the v-ATPase and the vesicular transmitter transporters. The former pumps protons inside the vesicular lumen, leading to acidification. This pH-gradient between the vesicular lumen and the cytoplasm allows the uptake of the transmitter in the vesicle via vesicular transmitter transporters, while protons are transported to the cytoplasm (Montana et al., 2006). Exocytosis is certainly a hallmark of neuronal

functioning, but it has recently been investigated in other cells, for example in the electrically non-excitabile astrocytes in the brain. Two types of vesicles were detected: dense core vesicles and clear electron-lucent vesicles (Calegari et al., 1999; Maienschein et al., 1999). This implicates a dual secretory pathway, one for the release of low molecular weight substances such as ATP and glutamate and one for the release of high molecular weight proteins, such as secretogranin II (Calegari et al., 1999). Furthermore, astrocytes release glutamate from large vesicles via two secretion modes (Chen et al., 2005): “kiss-and-run” enables rapid and economical vesicle recycling and limits the rate of transmitter release, while permanent vesicle fusion is associated with the full collapse of the vesicle membrane into the plasma membrane, leading to the release of most of the vesicle content. Those different exocytotic modes are correlated with different forms of synaptotagmin. It is considered that “kiss-and-run” exists at synapses; however, the question remains open as to whether this is a major mode of fusion that can rapidly recycle vesicles and control quantal response at many synapses (He and Wu, 2007). Vesicular mediated release is dependent on an increase of  $[Ca^{2+}]_i$  (Parpura et al., 1994) and vesicles expressing synaptobrevin 2 fuse more readily, but not exclusively, at astrocytic processes compared to the astrocytic body (Crippa et al., 2006).

# Chapter

## 2

### *Aim of the study*

I give them experiments, and they respond with speeches

-Louis Pasteur-

Previous investigations in our group have shown that elevating 1,4,5-InsP<sub>3</sub> (inositol trisphosphate) in a single cell triggered a transient increase of [Ca<sup>2+</sup>]<sub>i</sub> that propagated to neighboring cells as an intercellular Ca<sup>2+</sup>-wave (Braet et al., 2003b). The 1,4,5-InsP<sub>3</sub>-triggered Ca<sup>2+</sup>-wave was inhibited by α-GA (glycyrrhetic acid - gap junction/hemichannel blocker) and the Gap peptide <sup>43</sup>Gap 26 indicating that connexin channels were involved (Braet et al., 2003b). Several lines of evidence indicated that the mechanism of the Ca<sup>2+</sup>-wave propagation also contained an extracellular paracrine component (Hassinger et al., 1996; Cotrina et al., 1998b; Guthrie et al., 1999). Furthermore, 1,4,5-InsP<sub>3</sub> triggered the release of ATP (adenosine triphosphate), and this response was dependent on downstream [Ca<sup>2+</sup>]<sub>i</sub> increases and was largely suppressed by the gap junction blocker α-GA and <sup>43</sup>Gap 26. In subsequent work, it was however impossible to trigger ATP release in connexin expressing cells by directly increasing [Ca<sup>2+</sup>]<sub>i</sub>. This finding is in conflict with the observation that 1,4,5-InsP<sub>3</sub>-triggered ATP release was inhibited by buffering [Ca<sup>2+</sup>]<sub>i</sub> changes with the intracellular Ca<sup>2+</sup>-chelator, BAPTA-AM. The research work presented in this thesis started with the question whether changes in [Ca<sup>2+</sup>]<sub>i</sub> were the trigger for ATP release in connexin expressing cells. We aimed to determine whether increasing [Ca<sup>2+</sup>]<sub>i</sub> was sufficient to induce ATP release in connexin expressing cells, and to substantiate the evidence that this release occurred via hemichannels.

## 2.1 What is the mechanism and the molecular pathway of Ca<sup>2+</sup>-triggered ATP release via hemichannels?

In a cell, several pathways exist that mediate the release of paracrine messengers including pannexin hemichannels (Bruzzone et al., 2003), the P<sub>2</sub>X<sub>7</sub> receptor pore (North, 2002), anion channels (Strange et al., 1996; Eggermont et al., 2001), the maitotoxin pore (Lundy et al., 2004), and vesicular mediated release (Parpura et al., 1994). Some of these mechanisms can be activated by [Ca<sup>2+</sup>]<sub>i</sub> changes. In [chapter 4](#), we addressed the question whether increasing [Ca<sup>2+</sup>]<sub>i</sub> can trigger ATP release mediated by hemichannel opening. This study was performed on immortalized cell lines that expressed Cx32 (connexin 32), either endogenously, or after stable transfection of the cells. Cx32 contains several CaM (calmodulin) binding sites and in this way is a good candidate for regulation by [Ca<sup>2+</sup>]<sub>i</sub>. In this study, we aimed to investigate the intracellular Ca<sup>2+</sup>-sensitivity of connexin hemichannel responses making use of Gap peptides and blockers of alternative ATP release pathways.

In a next step, we wanted to determine whether intracellular Ca<sup>2+</sup> directly influenced connexin hemichannel opening or whether an intermediate component was required. In [chapter 5](#), we investigated the responses of Cx43 hemichannels to changes in [Ca<sup>2+</sup>]<sub>i</sub> and explored the pathway leading from an elevation in [Ca<sup>2+</sup>]<sub>i</sub> to the opening of hemichannels. Cx43 also contains CaM binding site(s). We started from Ca<sup>2+</sup>/CaM and progressively incorporated subsequent signaling steps into the cascade leading to hemichannel mediated ATP release.

## **2.2 Are connexin hemichannels and gap junctional channels regulated in a similar way?**

Most of the connexins are phosphorylated *in vivo*, primarily on serine residues and to a lesser extent on threonine and tyrosine residues located in the carboxyterminal domain (Crow et al., 1990; Musil et al., 1990b; Swenson et al., 1990; Warn-Cramer et al., 1996; Lampe et al., 1998). The degree of phosphorylation affects gating of hemichannels and gap junctional channels. In this part of the study, we wanted to determine the effect of Cx43 phosphorylation on hemichannel functioning (measured by the release of ATP) and compare this to gap junctional coupling (quantified by dye transfer). Under normal resting conditions, hemichannels and gap junctional channels behave differently in that gap junction channels are open most of the time (allowing direct cell-cell communication), while hemichannels have a low open probability. We hypothesize that other stimuli, such as kinases, might also regulate hemichannels and gap junctional communication in a different way.

Cx43 is an ubiquitously expressed connexin with multiple phosphorylation sites: a non-phosphorylated P<sub>0</sub> form and at least two phosphorylated forms, commonly referred to as P<sub>1</sub> and P<sub>2</sub>. In [chapter 6](#), we studied the effect of several kinase activating stimuli, such as PMA (PKC activator), LPA, LPS and bFGF (three broad spectrum kinase activators) on hemichannel and gap junctional functioning. In this study, ATP release was triggered with a widely accepted trigger of hemichannel opening, consisting of exposure of the cells to a solution with low extracellular divalent cations. The involvement of hemichannels was investigated by using Gap peptides and excluding other release mechanisms.

## **2.3 Is there an alternative for the widely used SLDT technique?**

Several techniques are available for the study of gap junctional communication, but they all have advantages and disadvantages. Electrophysiology is the most sensitive and precise method to determine channel currents and conductance of gap junction channels. This technique is however difficult to perform, requires specialized equipment, and this technique cannot be performed on confluent cultures. Microinjection requires the injection of a gap junction permeable fluorescent dye in one cell, and the spread to neighboring cells is quantified. In this technique the plasma membrane of the cell is disrupted, and this can influence the coupling between the cells. Fluorescence recovery after photobleaching (FRAP - Wade et al. (1986); Deleze et al. (2001)), and local activation of a fluorescent molecular probe (LAMP - Dakin et al. (2005)), quantify the transfer of the dye under physiological circumstances, but only in one cell or a small group of cells. The main disadvantage of these

techniques is that they do not allow the quantification of dye transfer in a large population of cells at the same time. For this purpose scrape loading and dye transfer (SLDT - el-Fouly et al. (1987)) can be used. Hereby, a confluent monolayer of cells is scraped or scratched with a very sharp syringe needle and this opens the plasma membrane inducing the uptake of the fluorescent reporter dye in the cytoplasm. As normal membrane permeability is re-established, the tracer becomes trapped in the cytosol and, with time, diffuses from the loaded cells to the non-loaded, adjacent cells that are connected via gap junctions. This technique has the disadvantage that the cells are damaged, which may affect gap junctional coupling.

Because of these disadvantages, our aim was to explore a new technique that allowed the quantification of gap junctional coupling in many cells at once and with minimal cell damage. In [chapter 7](#), we optimized a new method to introduce a gap junction permeable dye into the cell with minimal disturbance of cell viability. Electroporation is a widely used technique to bring plasma impermeable compounds into cells (Golzio et al., 2004) and was used previously in our lab to introduce caged-InsP<sub>3</sub> in a monolayer of adherent cells (Braet et al., 2004). Our first aim was to optimize the settings for efficient cell loading with fluorescent reporter dyes associated with minimal cell death. In the next step, we evaluated dye transfer between connexin expressing cells and quantified this in different, independent ways and compared this dye transfer with the well-known scrape loading and dye transfer technique.



# Chapter

## 3

### *Material and Methods*

Science is a wonderful thing if one does not have to earn one's living at it  
-Albert Einstein-

### 3.1 Cell culture

HeLa cell lines are derived from a human cervical adenocarcinoma and were stably transfected with Cx43 (connexin 43 - HeLa-Cx43), the truncated mutant of Cx43 (Cx43<sub>239stop</sub> - HeLa-Cx43 $\Delta$ C - Omori and Yamasaki (1999)) or Cx26 (HeLa-Cx26 - Mesnil et al. (1996)). These cells were kindly provided by Prof. Dr. H. Yamasaki and grown in DMEM supplemented with 10 % fetal bovine serum and 2 mM glutamine.

C6 is a rat glioma cell line, induced by injection of N-nitrosomethylurea in the brain. All C6 cells were kindly provided by Prof. Dr. C. C. G. Naus and grown in DMEM-Ham's F12 (1:1) supplemented with 10 % fetal bovine serum and 2 mM glutamine. These cells were stably transfected with Cx43 (C6-Cx43 - Zhu et al. (1991)), Cx32 (C6-Cx32 - Bond et al. (1994)) or with the Panx1 protein coupled to a myc-tag (C6-Panx1-Myc - Lai et al. (2007)).

ECV304 cells were originally described as a spontaneously transformed human umbilical cord cell line (Takahashi et al. (1990) - European Collection of Animal Cell Cultures (ECACC), Salisbury, UK), but have later been identified as a human bladder carcinoma epithelial cell line, identical to T24 (MacLeod et al., 1999). These cells were grown in Medium-199 supplemented with 10 % fetal bovine serum and 2 mM glutamine. Several subclones of ECV304 cells were used in this study, i.e. a subclone with major Cx32 expression and a subclone that showed no expression of the major connexins (Cx32 and Cx43).

HEK293 cells are originally derived from human embryonic kidneys and these cells have many properties of immature neurons (Shaw et al., 2002). The P<sub>2</sub>X<sub>7</sub> receptor was stably transfected in these cells by Humphreys et al. (1998) and kindly provided by Prof. Dr. G. Dubyak (Humphreys et al., 1998). The cells were grown in DMEM supplemented with 10 % fetal bovine serum and 2 mM glutamine.

### 3.2 Reagents

Fluo-3 acetoxymethyl ester (fluo-3-AM), fura-2 acetoxymethyl ester (fura-2-AM), calcein-acetoxymethyl ester (calcein-AM) and 5-carboxyfluorescein diacetate-acetoxymethyl ester (5-CFDA-AM), *o*-nitrophenyl-ethyleneglycol-bis(2-aminoethylether)-*N,N,N',N'*-tetraacetic acid acetoxymethyl ester (NP-EGTA-AM), ethylenedioxybis(*o*-phenylenitrilo)tetraacetic acid acetoxymethyl ester (BAPTA-AM), 4-bromo-A23187 (A23187), 6-carboxyfluorescein (6-CF), dextran fluorescein conjugate (MW 3 kDa, 10 kDa and 40 kDa), Sypro Ruby Orange Protein Blot Stain, 4',6-diamidino-2-phenylindole (DAPI) and propidium iodide (PI) were obtained from Molecular Probes (Invitrogen). Thapsigargin, W7, KN62, Adenosine 5'-triphosphate periodate oxidized sodium salt (ox-ATP), 2'-3'-*O*-(4-benzoylbenzoyl)-ATP (bz-

ATP), bafilomycin A1, botulinum toxin B, tetanus toxin, carbenoxolone, indomethacin, arachidonic acid (AA), N-acetyl-L-cysteine,  $\alpha$ -tocopherol succinate, superoxide dismutase (SOD), N $\omega$ -nitro-L-arginine, Phorbol 12-myristate 13-acetate (PMA), L- $\alpha$ -lysophosphatidic acid (LPA), lipopolysaccharide (LPS; *Escherichia coli* O111:B4), PD098.059, U0126, chelerythrine, genistein, and 18-glycyrrhetic acid ( $\alpha$ -GA) were from Sigma (Bornem, Belgium), dantrolene sodium salt and xestospongine-C from Calbiochem (Darmstadt, Germany) and ryanodine and caffeine from Alomone Labs (Jerusalem, Israel). Arachidonyl trifluoromethyl ketone (AACOCF<sub>3</sub>), baicalein, autocamtide-2-related inhibitory peptide (AIP - KKALRRNDAVEAL), and Ca<sup>2+</sup>-like peptide (CALP1 - VAITVLVL) were from Tocris Cookson (Avonmouth, United Kingdom). 4-Amino-5-(4-chlorophenyl)-7-(*t*-butyl)pyrazolo[3,4-*d*]pyrimidine (PP2) was from BIOMOL Research Laboratories (Plymouth Meeting, MA), basic fibroblast growth factor (bFGF) was from Roche Diagnostics (Vilvoorde, Belgium), and ampicillin was from Invitrogen. The Gap peptides <sup>32</sup>Gap 24 (GHGDPLHLEEVKC, intracellular loop, position 110 - 122 from Cx32), <sup>32</sup>Gap 27 (SRPTEKTVFT, extracellular loop 2, position 182 - 191 from Cx32), <sup>43</sup>Gap 27 (SRPTEKTIFII, extracellular loop 2, position 201 - 210 from Cx43), <sup>43</sup>Gap 26 (VCYDKSFPISHVR, extracellular loop 1, position 64 - 76 from Cx43) were synthesized by solid-phase chemistry and purified by HPLC to 95 % purity.

### 3.3 Hemichannel functioning

The extracellular ATP concentration is approximately 10 nM under basal conditions, while the intracellular concentration is 2 - 5 mM, 10<sup>6</sup>-fold more. If a pathway for ATP is activated or opened, this molecule exits the cell down an electrochemical gradient. Release of 1 % of the intracellular ATP pool is sufficient to maximally activate all receptors. Thus, signaling via extracellular ATP can occur without compromising the cellular metabolism. Cellular ATP release was measured using a bioluminescent luciferin/luciferase assay kit (Sigma) and was determined directly in the medium above the cells. The degree of light emitted corresponded to the amount of ATP released by the cell culture.

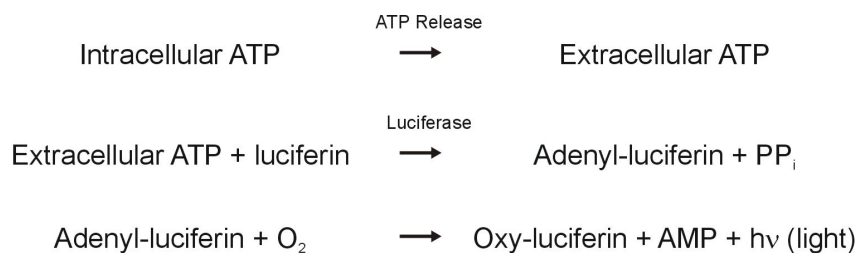


**Figure 16: Luciferin/luciferase reaction**

ATP is converted to light and this reaction is mediated by luciferin and luciferase from the firefly.

When ATP is the limiting factor, the light emitted is proportional to the ATP present (Figure 16). The amount of ATP released is used as a measure for the opening of hemichannels. In this protocol, 75  $\mu$ l ATP assay mix, prepared in HBSS-HEPES (Hanks' balanced salt solution; 25 mM HEPES, pH 7.4) at five-fold dilution was added to 150  $\mu$ l HBSS-HEPES above the cells and photon flux was counted during 10 s (Victor3; type 1420 multilabel counter, Perkin-Elmer, Brussels, Belgium). ATP release was triggered with DF-HBSS-HEPES (divalent free -  $\text{Ca}^{2+}$  and  $\text{Mg}^{2+}$  replaced with 4.4 mM EGTA) or by elevating intracellular  $\text{Ca}^{2+}$ -concentrations ( $[\text{Ca}^{2+}]_i$ ) through photoliberation of  $\text{Ca}^{2+}$  from NP-EGTA-AM, by applying the  $\text{Ca}^{2+}$ -ionophore A23187 or other agonists such as CALP1 and AA to the cells. Cells were seeded at a density of 25,000 cells/cm<sup>2</sup> and ATP release was accumulated over a period of 2.5 min for the photoliberation and DF protocol, and 5 min for all other stimuli. Photon counting of the luminescence signal was done (over 10 s) at the end of the stimulation/accumulation time. Baseline measurements were performed on separate cultures according to the same procedure, but with the standard HBSS-HEPES vehicle instead. The ATP assay was calibrated under baseline conditions (HBSS-HEPES) in the range of 1 - 30 pmoles, with the baseline ATP release corresponding to  $23.8 \pm 1.88$  pmoles ( $n = 152$ ) in ECV304,  $10.1 \pm 1.63$  pmoles ( $n = 255$ ) in C6-Cx32,  $14.53 \pm 4.02$  pmoles ( $n = 250$ ) in C6-Cx43, and  $17.87 \pm 4.96$  pmoles ( $n = 77$ ) in HeLa-Cx43. Taking into account that  $\sim 70,000$  cells/cm<sup>2</sup> were present and that the ATP content per cell is approximately  $100 \times 10^{-15}$  moles, we conclude that about 2 % of the cellular ATP content is released. Mechanical stimulation of cell cultures during manipulation was minimized, because small shocks to the cells produced by themselves measurable ATP release (Abraham et al., 1997). To exclude effects of the pharmacological agents on the bioluminescent luciferin/luciferase assay, all the agents were applied during a pre-incubation period and omitted during the assay.

Hemichannel opening can also be detected by assays that determine the uptake of a small reporter dye ( $\leq 1.2$  kDa - 1 mM PI or 0.4 mM 6-CF in HBSS-HEPES). We used PI instead of ethidium bromide (EtBr), because it was shown that Cx32 channels were more permeable for PI in comparison to EtBr (Charpantier et al., 2007). In our study, the cells were exposed for 5 min to the trigger solution, either DF solution or A23187 containing solution, and then washed 4 times with normal HBSS-HEPES. Nine images for each culture were acquired on a Nikon TE300 inverted microscope in epifluorescence mode with a x 10 objective and a Nikon DS-5M camera (Analis, Ghent, Belgium). The number of cells that took up the dye was counted in each image using ImageJ Software after application of a threshold corresponding to the upper level of the background signal. Cell counts were expressed as the percentage relative to the total number of cells in view of a x 10 objective counted after DAPI-staining. The selectivity of the dye uptake was verified with the reporters 6-CF (MW 376 Da) and dextran fluorescein (MW 10 kDa). Triggered dye uptake was significant for the hemichannel

permeable dye 6-CF, and nonsignificant for the hemichannel impermeable dye 10 kDa dextran fluorescein.

### 3.4 Gap junctional communication

Gap junctional communication is usually studied via the use of small, gap junction permeable fluorescent tracers. Two methods were used in this study to measure gap junctional coupling between cells: scrape loading and dye transfer (SLDT - el-Fouly et al. (1987)), and fluorescence recovery after photobleaching (FRAP - Wade et al. (1986); Deleze et al. (2001)). SLDT was developed by el-Fouly et al. (1987). In this approach a monolayer of adherent cells is scraped with a syringe needle in the presence of a gap junction permeant tracer, which enters the cells that are disrupted by the scrape (el-Fouly et al., 1987). A nominally  $\text{Ca}^{2+}$ -free solution is used to avoid  $\text{Ca}^{2+}$ -dependent closure of gap junctions in the ruptured cells taking up the dye. EGTA is not added to the buffer, because this tends to detach the cells after scraping. As normal membrane permeability is re-established, the tracer becomes trapped within the cytoplasm, and, with time, may move from the loaded cells into adjacent ones, that are connected by functional gap junctions. SLDT allows the rapid and simultaneous assessment of junctional communication in a large number of cells. A fluorescence diffusion profile is derived from the images, fitted to an exponential decaying function and the spatial constant ( $\lambda$ ) that corresponds to the level of intercellular dye spread is determined by non-linear regression curve fitting.

Wade et al. (1986) introduced FRAP. In this technique a monolayer of cells is ester-loaded with a fluorescent reporter dye, such as CFDA-AM or calcein-AM (Wade et al., 1986; Deleze et al., 2001). The nonpolar and hydrophobic esters are membrane permeant and diffuse into the cells, where they are hydrolyzed by cytoplasmic esterases, releasing their fluorescent, unesterified polar moieties. The latter compounds are hydrophilic and are trapped inside the cells due to their very low membrane permeability. In a next step, the cells are exposed to light of a very high intensity by spot exposure to the 488 nm line of an Argon laser, resulting in the photobleaching of the dye, rendering the dye unable to fluoresce. In a next step the return of the dye from the surrounding cells (referred to as recovery) was quantified at 488 nm excitation with a custom-made video-rate confocal scanning laser microscope with a x 40 oil immersion objective (Leybaert et al., 2005). Recovery was measured over a 5 min time period after photobleaching. From the return of fluorescence to the photobleached area, two parameters can be determined (Figure 17): (i) the percentage of recovery, i.e. the degree of fluorescence recovery relative to the situation before photobleaching; and (ii) the time constant of recovery, i.e. the time needed for the fluorescent molecules to migrate back to the photobleached area.

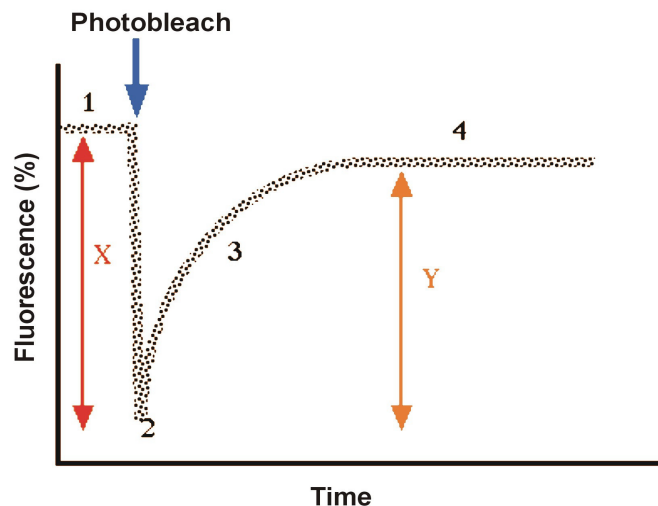


**Figure 17: Graphical presentation of data collected during a FRAP experiment**

The baseline of fluorescence is recorded (1) before the photobleaching occurs (blue arrow) so that the fluorescence intensity is reduced significantly (2). The fluorescence in the photobleached area increases as unbleached molecules diffuse back into this area (3). Finally, there is a stabilization of the amount of fluorescence recovery and a flat line is obtained (4). The percent recovery uses the formula:  $(Y/X) \times 100 = \% \text{ recovery}$ . In the diagram, the percentage of fluorescence lost due to photobleaching is X and the amount of fluorescence that returned to the bleached area is Y.

### 3.5 $\text{Ca}^{2+}$ -imaging

Imaging of free  $[\text{Ca}^{2+}]_i$  is monitored with an inverted epifluorescence microscope (Nikon Eclipse TE 300, Analis, Ghent, Belgium), using the  $\text{Ca}^{2+}$ -sensitive probes fluo-3-AM or fura-2-AM. The emission spectrum of fluo-3 displays an increase in fluorescence with increasing  $[\text{Ca}^{2+}]_i$  for excitation at 488 nm (Figure 18A). The excitation spectrum of fura-2 is such that at 340 nm excitation the fluorescence intensity is low in a  $\text{Ca}^{2+}$ -free solution and at 380 nm excitation, the fluorescence intensity is high (Figure 18B). Cultures were ester-loaded with 10  $\mu\text{M}$  fluo-3-AM or 5  $\mu\text{M}$  fura-2-AM for 1 h at room temperature in HBSS-HEPES, followed by a 30 min de-esterification period.

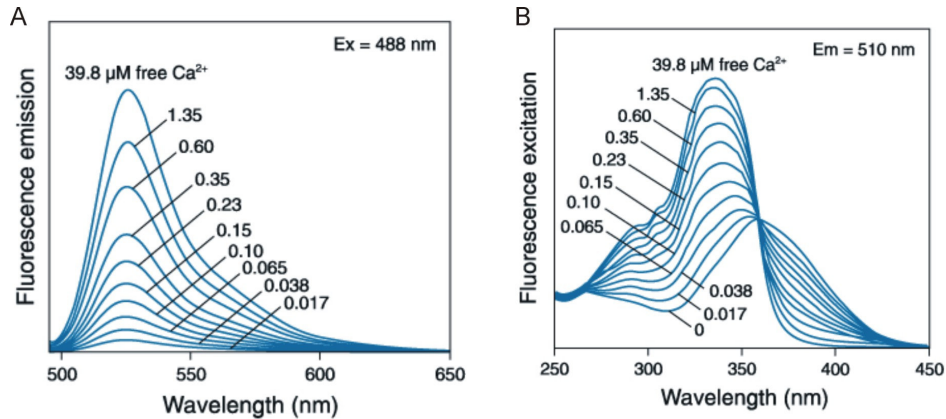


**Figure 18: Fluorescence emission spectrum of fluo-3 and excitation spectrum of fura-2**

(A) Fluo-3 is essentially nonfluorescent unless bound to  $\text{Ca}^{2+}$ . This  $\text{Ca}^{2+}$ -sensitive probe exhibits a  $K_d$  of 390 nM for  $\text{Ca}^{2+}$ , and has an emission wavelength of 525 nm. Fluo-3 exhibits a strong  $\text{Ca}^{2+}$ -dependent fluorescence enhancement. (B) Fura-2 is an UV (ultraviolet) light excitable, ratiometric  $\text{Ca}^{2+}$ -indicator, and it is the dye of choice for ratio-imaging microscopy, in which it is more practical to change excitation wavelengths than emission wavelengths. Upon binding  $\text{Ca}^{2+}$ , fura-2 exhibits an absorption shift that can be observed by scanning the excitation spectrum between 300 and 400 nm, while monitoring the emission at  $\sim 510$  nm. This dye exhibits a high selectivity for  $\text{Ca}^{2+}$  when compared to  $\text{Mg}^{2+}$ . Nevertheless,  $\text{Ca}^{2+}$ -binding is discernibly perturbed by physiological levels of  $\text{Mg}^{2+}$ : the  $K_d$  for  $\text{Ca}^{2+}$  of fura-2 is  $\sim 135$  nM in  $\text{Mg}^{2+}$ -free- $\text{Ca}^{2+}$ -buffers and  $\sim 224$  nM in the presence of 1 mM  $\text{Mg}^{2+}$  (Invitrogen-Molecular Probes: a guide to fluorescent probes and labeling technologies).

Cells were viewed with a x 40 oil immersion objective (CFI Plan Fluor, Nikon). Fluo-3 fluorescence images were obtained by excitation at 485 nm, reflection off a dichroic mirror with cut-off at 505 nm, and emission band-pass filtering at 535 nm (485DF22, 505DRLPXR, and 535DF35 filters respectively from Omega Optical, Brattleboro, VT). For fura-2 images a filterswitch (Cairn, Kent, UK) that provides alternating excitation between 340 and 380 nm was used. Excitation light was separated from emission light using a 430 nm dichroic mirror, the emitted light was collected through an emission filter with a center wavelength of 510 nm (40 nm bandwidth). Images were acquired with an intensified CCD (Extended Isis camera, Photonic Science, East Sussex, UK) and stored in a PC equipped with a frame grabber (Data Translation, DT 3152, Marlboro, MA - Figure 19). Ratio images were generated with software written in Microsoft Visual C++ 6.0, after standard background and shade correction procedures. Fura-2 *in vitro* calibrations were performed with  $\text{Ca}^{2+}$ -free (10 mM EGTA, 130 mM KCl, 5  $\mu\text{M}$  penta- $\text{K}^+$  Fura-2 salt and 10 mM HEPES pH 7.2) and  $\text{Ca}^{2+}$ -saturating (10 mM  $\text{CaCl}_2$ , 130 mM KCl, 5  $\mu\text{M}$  penta- $\text{K}^+$  Fura-2 salt and 10 mM HEPES pH 7.2) solutions that were sandwiched between two coverslips; a  $K_d$  of 224 nM was used to convert ratios to  $[\text{Ca}^{2+}]_i$  with the following formula (Grynkiewicz et al., 1985):

$$[\text{Ca}^{2+}]_i = K_d \times F_0/F_S \times (R - R_{\min})/(R_{\max} - R)$$

Where  $K_d$  is the dissociation constant (depends on the indicator, but also on pH, ionic strength, cell line, etc.),  $R$  is the fluorescence ratio at both wavelengths,  $R_{\min}$  is the minimum ratio value,  $R_{\max}$  is the maximum ratio value,  $F_S$  is the fluorescence at 480 nm at saturating  $[Ca^{2+}]$  and  $F_0$  is fluorescence at zero  $[Ca^{2+}]$ .

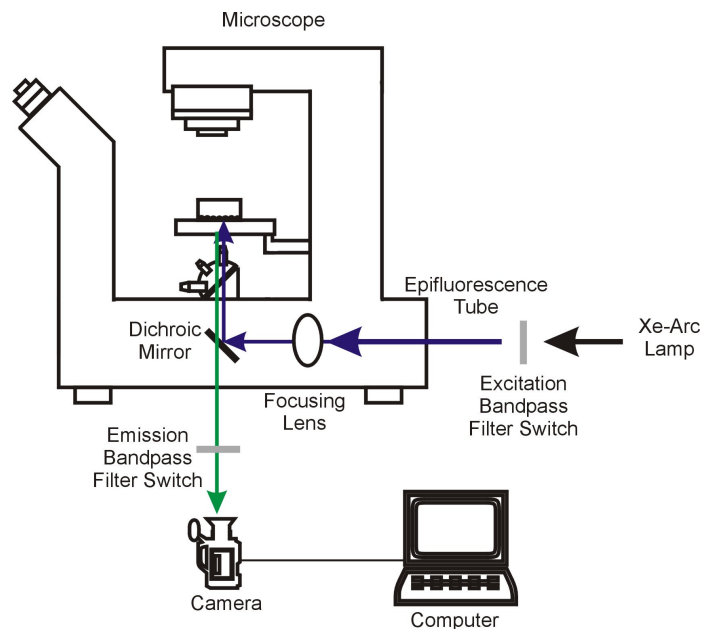


**Figure 19: Microscope system used for  $Ca^{2+}$ -imaging**

A Xe-Arc lamp supplies the excitation light, and an excitation bandpass filter switch provides light from the correct wavelength (485 nm for fluo-3 and 340/380 nm for fura-2). The light enters the microscope epifluorescence tube to produce a uniform illumination field. The dichroic mirror (transmission cut-off at 505 nm for fluo-3 and 430 nm for fura-2) reflects the short-wave length excitation light to the specimen. The long-wavelength fluorescence signal emitted by fluo-3 or fura-2 in the cells (525 nm for fluo-3 and 510 nm for fura-2) passes through the dichroic mirror, is collected through an emission filter and is captured by an intensified CCD camera.

Simultaneous  $Ca^{2+}$  and PI imaging was performed with triple excitation wavelength switching (340, 380 and 560 nm, each applied over 1 s, resulting in a  $Ca^{2+}$ /PI image pair every 3 s) in combination with a triple band dichroic mirror and emission bandpass filter (XF2050 and XF3063, respectively, Omega Optical). Separation of the three emission light channels was very good and there was no influence of PI fluorescence on the fura-2 images when 10  $\mu$ M PI was used. Cells on glass bottom microwells were superfused on the stage of the microscope at a rate of 1 ml/min. Each experiment in which PI positive cells appeared in response to the  $Ca^{2+}$ -trigger was concluded with an inspection of the PI channel at different Z objective positions to verify that the PI positivity was not located in a cell occasionally overlaying the cell originally in focus.



### 3.6 Photoliberation of $\text{Ca}^{2+}$

Flash photolysis of a photo activatable  $\text{Ca}^{2+}$ -probe provides a means of controlling the release of  $\text{Ca}^{2+}$  - both spatially and temporally. UV field illumination was used to photorelease  $\text{Ca}^{2+}$  from the NP-EGTA-AM probe. The AM ester does not bind  $\text{Ca}^{2+}$  until its ester group is removed by intracellular esterases. After UV illumination the affinity for  $\text{Ca}^{2+}$  is decreased  $\sim 12,500$ -fold, with a corresponding increase in  $K_d$  from 80 nM to 1 mM. Furthermore, the low affinity for  $\text{Mg}^{2+}$  ( $K_d \sim 9$  mM) makes NP-EGTA essentially insensitive to physiological  $[\text{Mg}^{2+}]_i$ .

Light from a 100 W Hg-arc lamp with a quartz collector lens (LH-M100C-1, Nikon) was bandpass-filtered at 330 nm (330WB80, Omega Optical, Brattleboro, VT), reflected by a mirror (10D510AL.2, Newport, Leuven, Belgium) and focussed on the cell culture (Figure 20). The cells were exposed for 2 s to the UV light and a 2.5 min collection period was included after the photostimulus to allow the accumulation of ATP. The energy density at a 5 s exposure time was calculated from power experiments with a UV power meter (model 1830-C with 818-UV detector, Newport) to be in the order of  $500 \text{ mJ/cm}^2$ . The efficiency of photoliberating caged compounds by UV illumination was determined by exposing a thin layer of caged-ATP ( $1 \mu\text{M}$ ) to the UV light and measuring the amount of photoliberated ATP with a bioluminescent luciferin/luciferase assay kit (see section 3.4). The attenuation of the photolytic UV light by its passage through the cell monolayer (reduction to 72 %) was determined by UV power measurements under conditions with and without cells. Baseline (control) experiments were performed on cultures loaded with the vehicle alone. Varying the loading time of the ester resulted in different  $[\text{Ca}^{2+}]_i$  after UV-illumination.

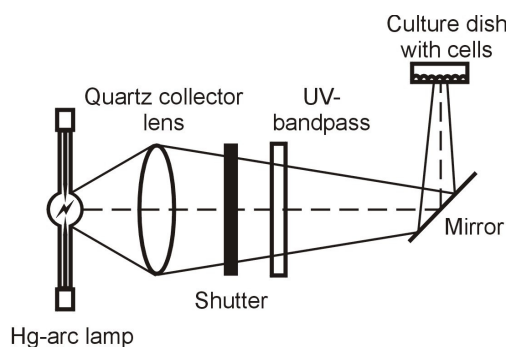


**Figure 20: Optical set-up used for photoliberation of caged-compounds**

A focussed image of the Hg-arc lamp is formed at the level of the cells on a culture dish by the use of a quartz collector lens. The light passes through a manually controlled shutter and a UV bandpass filter.



# Chapter

## 4

### ***Intracellular calcium changes trigger connexin 32 hemichannel opening***

Elke De Vuyst<sup>1</sup>, Elke Decrock<sup>1</sup>, Liesbet Cabooter<sup>1</sup>, George R Dubyak<sup>2</sup>, Christian C Naus<sup>3</sup>, W Howard Evans<sup>4</sup> and Luc Leybaert<sup>1</sup>

<sup>1</sup> Department of Physiology and Pathophysiology, Faculty of Medicine and Health Sciences, Ghent University, Ghent, Belgium

<sup>2</sup> Department of Physiology and Biophysics, School of Medicine, Case Western Reserve University, Cleveland, OH, USA

<sup>3</sup> Department of Cellular and Physiological Sciences, Faculty of Medicine, University of British Columbia, Vancouver, BC, Canada

<sup>4</sup> Department of Medical Biochemistry and Immunology, Cardiff University School of Medicine, Cardiff, UK

Published in EMBO J. **25**:34-44 (2006)

Text and illustrations are modified from the published version

Science never solves a problem without creating ten more.  
-George Bernard Shaw-

### Abstract

Connexin hemichannels have been proposed to act as a diffusion pathway for the release of extracellular messengers like ATP (adenosine triphosphate) and many others, based on connexin expression models and inhibition by gap junction blockers. Hemichannels are opened by various experimental stimuli, but the physiological intracellular triggers are currently not known. We investigated the hypothesis that an increase in cytoplasmic  $\text{Ca}^{2+}$ -concentration ( $[\text{Ca}^{2+}]_i$ ) triggers hemichannel opening. The involvement of hemichannels was confirmed by the use of peptides that are identical to a short amino acid sequence of the connexin subunit to specifically block hemichannels, but not gap junction channels. Our work performed on connexin 32 (Cx32) expressing cells showed that an increase in  $[\text{Ca}^{2+}]_i$  triggers ATP release and dye uptake that is dependent on Cx32 expression, blocked by Cx32 (but not Cx43) Gap peptides and a calmodulin (CaM) antagonist, and critically depend on  $[\text{Ca}^{2+}]_i$  elevation within a window situated around 500 nM. Our results indicate that  $[\text{Ca}^{2+}]_i$  elevation triggers hemichannel opening, suggesting that these channels are under physiological control.

## 4.1 Introduction

The basic fuel molecule of the cell, ATP, has gained a lot of interest over the last decade as a paracrine messenger in various cell and tissue types (Novak, 2003). Besides being a remarkably versatile molecule, nonexcitable cells can be invoked to release ATP by widely differing stimuli, including mechanical cell stimulation (Stout et al., 2002), shear stress (Cherian et al., 2005), hypotonic cell swelling (Boudreault and Grygorczyk, 2004), elevation of intracellular inositol trisphosphate (1,4,5-InsP<sub>3</sub> - Braet et al. (2003a)) or exposure to low or zero [Ca<sup>2+</sup>]<sub>e</sub> conditions (Arcuino et al., 2002). The ATP releasing mechanisms involved appear to be equally diverse (reviewed in Lazarowski et al. (2003)), including vesicular release, active transport via ABC transporters and diffusion via stretch-activated channels, voltage-dependent anion channels, pores opened by P<sub>2</sub>X<sub>7</sub> receptors or connexin hemichannels. Connexin hemichannels are hexameric high-conductance plasma membrane channels (single channel conductance ~ 90 and 220 pS for Cx32 and 43, respectively - Contreras et al. (2003a); Gomez-Hernandez et al. (2003)) that are normally closed and can act as a conduit for ATP, NAD<sup>+</sup> (nicotinamide adenine dinucleotide), glutamate, glutathione and prostaglandin E<sub>2</sub> when opened (Bruzzone et al., 2001a; Bennett et al., 2003; Ebihara, 2003; Goodenough and Paul, 2003; Ye et al., 2003; Cherian et al., 2005; Rana and Dringen, 2007). Hemichannels are closed at normal millimolar [Ca<sup>2+</sup>]<sub>e</sub>, but open when [Ca<sup>2+</sup>]<sub>e</sub> is lowered (Li et al., 1996; Pfahnl and Dahl, 1999; Quist et al., 2000; Muller et al., 2002; Ye et al., 2003; Thimm et al., 2005). A Ca<sup>2+</sup>-binding site composed of aspartate residues facing the external side has been reported for Cx32 hemichannels and is thought to translate changes of [Ca<sup>2+</sup>]<sub>e</sub> to changes in channel gating (Gomez-Hernandez et al., 2003). Hemichannels also open in response to membrane depolarization and mechanical stimulation in a *Xenopus laevis* oocyte expression system (Trexler et al., 1996; Bao et al., 2004b), under conditions of metabolic inhibition in astrocytes, myocardial cells or renal epithelial cells (John et al., 1999; Kondo et al., 2000; Contreras et al., 2002; Vergara et al., 2003a; Vergara et al., 2003b), after *Shigella* invasion of epithelial cells (Tran Van Nhieu et al., 2003) and in response to extracellular UTP (uridine triphosphate) in C6 glioma cells expressing Cx32 or Cx43 (Cotrina et al., 1998b). The physiological intracellular signals controlling hemichannel opening are currently not known, but UTP-triggered ATP release via hemichannels was dependent on intracellular Ca<sup>2+</sup>-mobilization (Cotrina et al., 1998b). We demonstrated that photoactivation of 1,4,5-InsP<sub>3</sub> in Cx43 expressing cells triggers Ca<sup>2+</sup>-dependent ATP release that is blocked by gap junction blockers and peptides that mimic a short sequence on the Cx43 subunit (Braet et al., 2003a; Braet et al., 2003b), indicating that 1,4,5-InsP<sub>3</sub> and downstream signals activate hemichannel opening (Leybaert et al., 2003). Recent work from the group of Mobbs and co-workers (Pearson et al., 2005) also points to [Ca<sup>2+</sup>]<sub>i</sub> changes triggering Cx43 hemichannel opening in native retinal pigment epithelium. The aim of the present work was to determine whether increases in

$[Ca^{2+}]_i$  are sufficient to trigger hemichannel opening as investigated with gap peptides and connexin expression systems. Our results obtained in Cx32 expressing cells demonstrate that direct elevation of  $[Ca^{2+}]_i$  by photoactivation of  $Ca^{2+}$  in the cytoplasm or stimulation of  $Ca^{2+}$ -entry with the  $Ca^{2+}$ -ionophore A23187 triggers ATP release and hemichannel permeable dye uptake that was dependent on Cx32 expression and completely blocked by Cx32 Gap peptides and CaM inhibition. Pores linked to  $P_2X_7$  receptor activation were excluded and vesicular ATP release contributed to a limited extent, but hemichannel mediated release was by far the predominant component. Our work shows that hemichannels can be activated by physiological  $[Ca^{2+}]_i$ , opening up a wide range of future investigations on hemichannel involvement under both physiological and pathological circumstances.

## 4.2 Material and Methods

### 4.2.1 Cell cultures

We used ECV304 (bladder cancer epithelial cells - ECACC, Salisbury, UK), C6 glioma wild type (C6-WT), C6 stably transfected with Cx32 (C6-Cx32 - Bond et al. (1994)) or Cx43 (C6-Cx43 - Zhu et al. (1991)) and HEK293 cells stably transfected with  $P_2X_7$  receptors (HEK293- $P_2X_7$  - Humphreys et al. (1998)). ECV304 was maintained in Medium-199 (Invitrogen, Merelbeke, Belgium), C6 in DMEM-Ham's F12 (1:1) and HEK293- $P_2X_7$  in DMEM, all supplemented with 10 % fetal bovine serum and 2 mM glutamine. Cells were seeded at a density of 25,000 or 50,000 cells/cm<sup>2</sup> (specified further) on either glass bottom microwells (MatTek Corporation, Ashwood, MA), Nunclon four-well plates (NUNC Brand Products, Denmark) or 24-well plates (Falcon3047, Becton Dickinson, Erembodegem, Belgium) and used for experiments the next day (subconfluent cultures). The experiments were carried out in Hanks' balanced salt solution buffered with 25 mM HEPES (HBSS-HEPES, pH 7.4).

### 4.2.2 Agents

Fluo-3 acetoxymethyl ester (fluo-3-AM; 10  $\mu$ M), fura-2-AM (5  $\mu$ M), *o*-nitrophenyl-ethyleneglycol-bis(2-aminoethylether)-*N,N,N',N'*-tetraacetic acid acetoxymethyl ester (NP-EGTA-AM; 5  $\mu$ M), 1,2-bis(*o*-aminophenoxy)ethane-*N,N,N',N'*-tetraacetic acid acetoxymethyl ester (BAPTA-AM; 5  $\mu$ M), 4-bromo-A23187 (A23187), 6-carboxyfluorescein (6-CF), dextran fluorescein conjugate (MW 10 kDa) and propidium iodide (PI) were obtained from Molecular Probes (Invitrogen). Thapsigargin (1  $\mu$ M), W7 (20  $\mu$ M), KN62 (1  $\mu$ M), adenosine triphosphate periodate oxidized sodium salt (ox-ATP; 100  $\mu$ M), 2'-3'-*O*-(4-benzoylbenzoyl)-ATP (Bz-ATP; 2  $\mu$ M), bafilomycin A1 (100  $\mu$ M), botulinum toxin B (1.5 nM), carbenoxolone (100  $\mu$ M) and  $\alpha$ -glycyrrhetic acid ( $\alpha$ -GA; 50  $\mu$ M)) were from Sigma (Bornem, Belgium), dantrolene sodium salt (25  $\mu$ M) and xestospongine-C from Calbiochem

(Darmstadt, Germany) and ryanodine (10  $\mu$ M) and caffeine (10 mM) from Alomone Labs (Jerusalem, Israel). The Gap peptides  $^{32}$ Gap 24 (GHGDPLHLEEVKC, intracellular loop, position 110 - 122; 0.25 mg/ml),  $^{32}$ Gap 27 (SRPTEKTVFT, extracellular loop 2, position 182 - 191; 0.25 mg/ml) and  $^{43}$ Gap 27 (SRPTEKTIFII, extracellular loop 2, position 201 - 210; 0.25 mg/ml) were synthesized by solid-phase chemistry and purified by HPLC to 95 % purity (Sigma-Genosys). Monoclonal mouse anti-rat Cx43 antibody was obtained from Transduction Laboratories (Becton Dickinson; 1/500), polyclonal rabbit anti-rat Cx32 antibody from Sigma (1/1,000) and polyclonal rabbit anti-rat P<sub>2</sub>X<sub>7</sub> antibody plus the corresponding antigenic peptide (residue 576 - 595 from rat P<sub>2</sub>X<sub>7</sub>) from Alomone Labs (Jerusalem, Israel; 1/1,000).

### 4.2.3 Extracellular ATP measurements

Cellular ATP release was determined with a luciferin/luciferase assay kit (Sigma) and was measured either in a sample collected from the medium bathing the cells (sample procedure) or directly in the medium above the cells (plate reader procedure). In the sample procedure, 100  $\mu$ l of 200  $\mu$ l bathing medium was transferred to 100  $\mu$ l ATP assay mix solution used at five-fold dilution, and the photon flux was counted with a photomultiplier luminometer (type 9924B, Thorn-Emi Electron Tubes, Middlesex, UK; 10 s counting time). In the plate reader procedure, 75  $\mu$ l ATP assay mix prepared in HBSS-HEPES (at five-fold dilution) was added to 150  $\mu$ l medium above the cells and photon flux was counted (Victor3, type 1420 multilabel counter, Perkin-Elmer, Brussels, Belgium). ATP release was triggered with a DF-HBSS-HEPES (divalent cation free - Ca<sup>2+</sup> and Mg<sup>2+</sup> replaced with 4.4 mM EGTA), by photoactivation of Ca<sup>2+</sup> inside the cells (described below) or by applying A23187 or other agonists mentioned in the text. Standard cell seeding density was 25,000 cells/cm<sup>2</sup>, but 50,000 cells/cm<sup>2</sup> for DF stimulation and simultaneous Ca<sup>2+</sup>/PI imaging. Cellular ATP release was accumulated over a period of trigger exposure: 2.5 min for DF-conditions and 5 min for A23187; for Ca<sup>2+</sup>-photoactivation, a 2.5 min collection period was included after the short photostimulus. Baseline measurements were carried out on separate cultures with the same procedure, but with standard HBSS-HEPES vehicle instead. The ATP assay was calibrated in the range of 1 - 30 pmoles, with the baseline corresponding to  $23.8 \pm 1.88$  pmoles (n = 152) in ECV304 and  $10.1 \pm 1.63$  pmoles (n = 155) in C6-Cx32. The DF stimulus increased ATP release to  $351 \pm 17.9$  % (n = 122), while 2  $\mu$ M A23187 increased it to  $230 \pm 12.4$  % (n = 186) in C6-Cx32. Taking into account the number of cells that display dye uptake (see further) and  $100 \times 10^{-15}$  moles (5 mM) intracellular ATP contents per cell (Allue et al., 1996), both stimuli were calculated to trigger the release of approximately 2 % of the cellular ATP contents (in line with previous estimates - Braet et al. (2004)). All pharmacological or inhibitory agents were pre-incubated for the times indicated in HBSS-HEPES at room temperature or in culture medium at 37 °C for incubations lasting 30 min or longer, and were not present during stimulation. The same protocol applies for dye uptake experiments described further.

#### 4.2.4 Photoactivation of $\text{Ca}^{2+}$

Ester-loading with NP-EGTA was carried out with 5  $\mu\text{M}$  NP-EGTA-AM in 1 ml HBSS-HEPES for the times indicated, followed by 30 min de-esterification, all performed at room temperature. UV field illumination during 2 s was used to photoliberate  $\text{Ca}^{2+}$  in a large zone of NP-EGTA-loaded cells on glass bottom microwells, as described in detail in Braet et al. (2004). Baseline measurements were carried out in cultures that were exposed to the UV light, but were not loaded with NP-EGTA.

#### 4.2.5 $\text{Ca}^{2+}$ -imaging

Cell cultures were loaded with fluo-3-AM or fura-2-AM by ester-loading for 1 h as described for NP-EGTA-AM. Imaging was performed on an inverted epifluorescence microscope (Nikon Eclipse TE 300, Analis, Ghent, Belgium) with an x 40 oil immersion objective and a filterswitch (Cairn, Kent, UK) providing 485 nm excitation for fluo-3 and excitation alternating between 340 and 380 nm for fura-2 (each applied over 1 s, resulting in one  $\text{Ca}^{2+}$ -image every 2 s). Fluo-3 measurements were carried out with a standard FITC dichroic mirror and emission filter; for fura-2 the dichroic mirror had a 430 nm reflection cut-off and was bandpass emission filtered at 510 nm (40 nm bandwidth). Images were acquired with an intensified CCD (Extended Isis camera, Photonic Science, East Sussex, UK) and stored in a PC equipped with a frame grabber (Data Translation, DT 3152, Marlboro, MA). Ratio images were generated with software written in Microsoft Visual C++ 6.0, after standard background and shade correction procedures. Fura-2 *in vitro* calibrations were carried out with  $\text{Ca}^{2+}$ -free (10 mM EGTA, 130 mM KCl, 5  $\mu\text{M}$  pentaK<sup>+</sup> fura-2 salt and 10 mM HEPES, pH 7.2) en  $\text{Ca}^{2+}$ -saturating solutions (10 mM  $\text{CaCl}_2$ , 130 mM KCl, 5  $\mu\text{M}$  pentaK<sup>+</sup> fura-2 salt and 10 mM HEPES pH 7.2); a  $K_d$  of 224 nM was used to convert ratios to  $[\text{Ca}^{2+}]_i$ .

Simultaneous  $\text{Ca}^{2+}$  and PI imaging was performed with triple excitation wavelength switching (340, 380 and 560 nm, each applied over 1 s, resulting in a  $\text{Ca}^{2+}$ /PI image pair every 3 s) in combination with a triple band dichroic mirror and emission bandpass filter (XF2050 and XF3063, respectively, Omega Optical, Brattleboro, VT). Separation of the three emission light channels was excellent and the PI fluorescence had no discernable influence on the fura-2 images (Figure 39A and D). Cells on glass bottom microwells were superfused on the stage of the microscope at a rate of 1 ml/min. Each experiment where PI positive cells appeared in response to the  $\text{Ca}^{2+}$ -trigger was concluded with an inspection of the PI channel at different Z objective positions to verify that the PI positivity was not located in a cell occasionally overlaying the cell originally in focus. The  $[\text{Ca}^{2+}]_i$  time courses presented are measurements at the center of the PI positive spot and are representative for the time course at other locations within the same cell.



#### 4.2.6 Dye uptake

Dye uptake was determined with the hemichannel permeable reporter dye PI (1 mM). In the combined  $\text{Ca}^{2+}$ /PI imaging experiments, the PI concentration was lowered to 10  $\mu\text{M}$  to minimize fluorescence from the PI containing superfusate during recording and to avoid saturation of the ICCD camera at PI positivities. In all dye uptake experiments, except the combined  $\text{Ca}^{2+}$ /PI imaging experiments described before, the protocol was such that the cells were exposed for 5 min to the trigger solution and were then washed four times with HBSS-HEPES. Images, nine for each culture, were acquired on a Nikon TE300 inverted microscope in epifluorescence mode (TRITC excitation/emission) with a x 10 objective and a Nikon DS-5M camera (Analis, Namur, Belgium). The number of PI positive cells was counted in each image using ImageJ software after application of a threshold corresponding to the upper level of the background signal. Cell counts were expressed in the graphs as a percentage relative to the total number of cells in view counted after DAPI staining ( $65 \pm 4.5$  cells per x 10 objective camera field for 25,000 cells/cm<sup>2</sup> seeding density and  $127 \pm 7.8$  for 50,000 cells/cm<sup>2</sup>; n = 36). Overall, the number of PI positive cells was  $1.2 \pm 0.1$  (747 images from 83 experiments) in baseline,  $16.6 \pm 0.7$  (333 images from 37 experiments) with DF and  $7.6 \pm 0.4$  (414 images from 46 experiments) with 2  $\mu\text{M}$  A23187, corresponding to a percentual increase of 1383 % for DF and 633 % for A23187. In the combined  $\text{Ca}^{2+}$ /PI experiments where imaging was carried out with an x 40 objective (Figure 39), the chance of finding a cell responding to A23187 was in the order of one every two x 40 camera fields. A very large number of experiments on different cultures (n = 120) was therefore necessary to obtain meaningful data. The selectivity of dye uptake was verified with the fluorescent reporters 6-CF (MW 376 Da) and dextran fluorescein (MW 10 kDa - x 40 objective, FITC excitation/emission). DF-triggered dye uptake was significant for the hemichannel permeable dye 6-CF (baseline  $1.04 \pm 0.496$  % of the cells, trigger  $10.6 \pm 1.99$  %, n = 9, p<0.0003) and nonsignificant for the hemichannel impermeable 10 kDa dextran (baseline  $0.80 \pm 0.56$  %, trigger  $2.39 \pm 1.02$  %, n = 9). Experiments with the A23187-trigger (2  $\mu\text{M}$ ) gave similar results (6-CF: baseline  $3.75 \pm 1.75$  % of the cells, trigger  $20.9 \pm 6.07$  %, n = 9, p<0.008; 10 kDa dextran: baseline  $1.03 \pm 1.03$  %, trigger  $3.75 \pm 2.01$  %, n = 9).

#### 4.2.7 Scrape loading and dye transfer (SLDT)

Confluent monolayer cultures were washed two times with nominally  $\text{Ca}^{2+}$ -free HBSS-HEPES (CF-HBSS-HEPES). Cells were incubated during 1 min in CF-HBSS-HEPES containing 0.4 mM 6-CF; a linear scratch (one per culture) was made across the cell layer using a syringe needle and the cells were left for another minute in the same solution. Cultures were then washed four times with HBSS-HEPES, left for 15 min at room temperature and images were taken with a Nikon TE300 inverted microscope in epifluorescence mode (FITC

excitation/emission) with a x 10 objective and a Nikon DS-5M camera (Analis, Namur, Belgium). A fluorescence diffusion profile was derived from the images, fitted to an exponential decaying function, and the spatial constant of intercellular dye spread was determined.

#### **4.2.8 Western blotting**

Cell protein lysates were extracted with radio immuno precipitation assay buffer (RIPA - 25 mM Tris, 50 mM NaCl, 0.5 % NP40, 0.5 % deoxycholate, 0.1 % SDS, 5.5 %  $\beta$ -glycerophosphate, 1 mM DTT, 2 % phosphatase inhibitor cocktail, 2 % mini EDTA-free protease inhibitor cocktail) and sonicated by three 10 s pulses. Total protein was determined with a Biorad DC protein assay kit (Nazareth, Belgium) and a plate reader. Proteins were separated on a 10 % Bis-Tris gel (Invitrogen) and transferred to a nitrocellulose membrane (GE Healthcare, Buckinghamshire, UK). Blots were probed with antibodies, followed by horseradish peroxidase conjugated goat anti-rabbit IgG or goat anti-mouse (Cell Signalling, Beverly) and detection was carried out with the ECL chemiluminescent reagent (GE Healthcare).

#### **4.2.9 Data analysis and statistics**

The data are expressed as mean  $\pm$  s.e.m., with 'n' denoting the number of independent experiments on different cultures. In dye uptake experiments, 'n' reflects the number of images. The variations in baseline and triggered signals observed in some figures represent normal variability between different experimental groups; in some cases it may be related to different experimental conditions (e.g. the presence of DMSO). Comparison of two groups was carried out using a one-tailed unpaired t-test, with a p-value below 0.05 indicating significance. Comparison of more than two groups was carried out with one-way ANOVA and a Bonferroni post test. Statistical significance is indicated in the graphs with a single symbol (\* or #) for  $p < 0.05$ , two symbols for  $p < 0.01$  and three symbols in case  $p < 0.001$ . Some substances or treatments also influenced the baseline signal, but these effects most often did not reach significance with ANOVA. Selected comparisons for baseline effects were redone with a t-test, and significant differences, if relevant, are given in the figure legend.

## 4.3 Results

### 4.3.1 Divalent-free (DF) solutions trigger ATP release that is dependent on $[Ca^{2+}]_i$ in ECV304

Exposure of cells to solutions with lowered or zero extracellular  $Ca^{2+}$  and  $Mg^{2+}$  triggers ATP and glutamate release and this has been applied in various cell types to investigate connexin hemichannel opening (Arcuino et al., 2002; Stout et al., 2002; Ye et al., 2003). We used ECV304 cells from which a subclone with prominent Cx32 expression (Figure 21) was selected to study the role of  $[Ca^{2+}]_i$  changes in triggering ATP release via hemichannels.

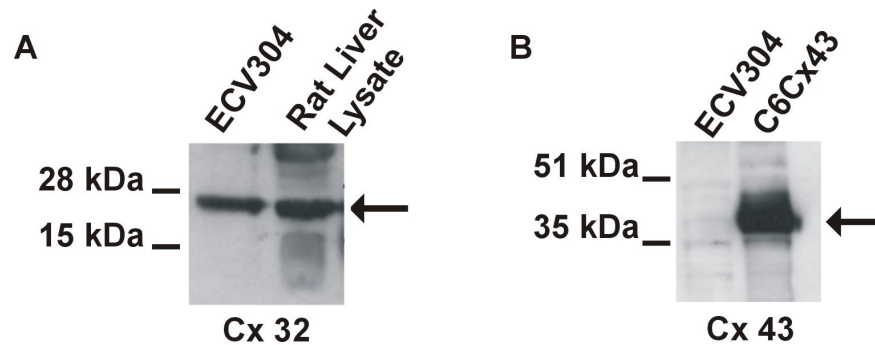


**Figure 21: Connexin expression in the ECV304 cell line**

(A) The ECV304 cell line showed a clear Cx32 expression. (B) There was no discernable Cx43 expression in this cell line. Rat liver lysate was used as a positive control for Cx32 expression and the C6 cell line stably transfected with Cx43 (C6-Cx43) was used as a positive control for Cx43 expression.

Incubating ECV304 cells in zero  $[Ca^{2+}]_e$  and  $[Mg^{2+}]_e$  solutions (DF solutions, applied 2.5 min) triggered ATP release that was significantly above baseline. This was associated with transient and oscillatory changes in  $[Ca^{2+}]_i$  as observed in fluo-3 imaging experiments. The ATP release in response to DF conditions varied between experiments and ranged from approximately 175 to 500 % of baseline. Buffering  $[Ca^{2+}]_i$  with BAPTA (5  $\mu$ M BAPTA-AM, 45 min loading time) or blocking the intracellular  $Ca^{2+}$ -store SERCA pumps with thapsigargin (1  $\mu$ M, 10 min incubation before exposure to DF conditions results in emptying the  $Ca^{2+}$ -stores) significantly reduced the ATP response (Figure 22).

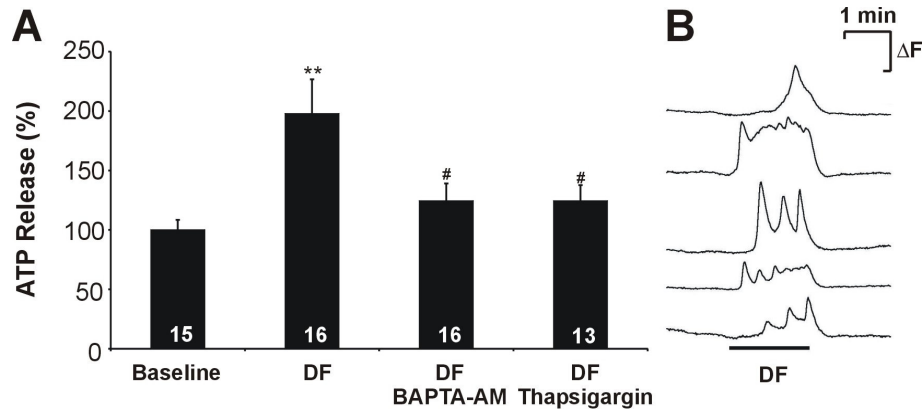


**Figure 22: Role of [Ca<sup>2+</sup>]<sub>i</sub>-changes in DF-triggered ATP release in ECV304 cells**

(A) DF exposure of ECV304 cells triggered ATP accumulation in the medium that was assayed after a 2.5 min stimulation interval. Baseline and triggered ATP release were measured in different experimental groups. Buffering [Ca<sup>2+</sup>]<sub>i</sub> with BAPTA or emptying the Ca<sup>2+</sup>-stores with thapsigargin reduced DF-triggered ATP release. Inhibitors were absent during the stimulation protocol. (B) [Ca<sup>2+</sup>]<sub>i</sub> dynamics in response to DF exposure, demonstrating transient, steady and oscillatory changes. [Ca<sup>2+</sup>]<sub>i</sub>-changes are given as an increase in fluo-3 fluorescence (ΔF, arbitrary units). Star signs indicate significance compared to baseline, while number signs represent significance compared to DF-trigger.

Blocking 1,4,5-InsP<sub>3</sub> receptors (1,4,5-InsP<sub>3</sub>R) with xestospongine-C (2 - 10 μM, 10 min), ryanodine receptors (RyR) with dantrolene (25 μM, 10 min) or pre-emptying RyR-sensitive Ca<sup>2+</sup>-stores with caffeine (10 mM, 30 min) all significantly inhibited DF-triggered ATP release (Figure 23). 1,4,5-InsP<sub>3</sub>- and RyR-sensitive Ca<sup>2+</sup>-stores are thus involved in the ATP response, and, in line with this, photoactivation of 1,4,5-InsP<sub>3</sub> in the cytoplasm (Braet et al., 2003b) and exposure to the alkaloid Ry (10 μM, 15 min) or caffeine (10 mM, 15 min) as a stimulus triggered significant ATP release (175 ± 38 % for Ry and 400 ± 81 % for caffeine, compared to 100 ± 12 % baseline level, n = 15, p < 0.05 and < 0.0005, respectively).

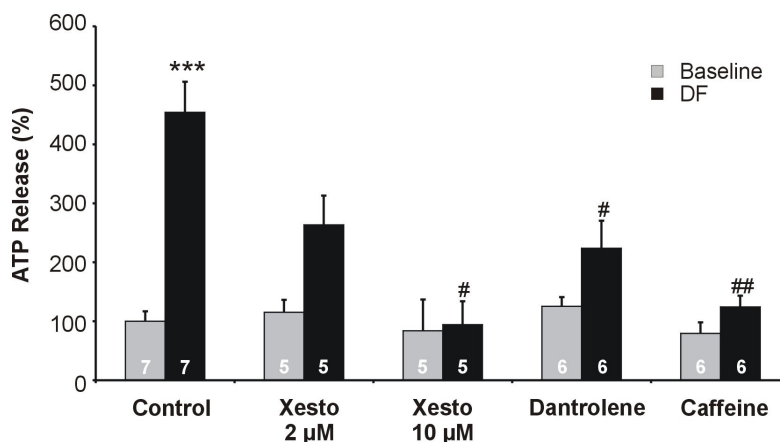


**Figure 23: Influence of 1,4,5-InsP<sub>3</sub>R and RyR pharmacology on DF-triggered ATP release in ECV304 cells**

Xestospongine-C reduced DF-triggered ATP release at 2 μM and completely blocked it at 10 μM. Blocking RyR with dantrolene or pre-emptying Ca<sup>2+</sup>-stores with caffeine also reduced the response. Star signs indicate significance compared to baseline, while number signs represent significance compared to DF-trigger in control conditions.

### 4.3.2 Directly increasing $[Ca^{2+}]_i$ triggers ATP release in ECV304

Photoactivation of  $Ca^{2+}$  from the ester-loaded NP-EGTA (5  $\mu$ M NP-EGTA-AM, 10 min - Ellis-Davies and Kaplan (1994)) triggered significant ATP release. However, prolonged ester-loading (1 h), applied to increase the amount of photoliberated  $Ca^{2+}$ , did not trigger significant ATP release. Stimulating  $Ca^{2+}$ -entry with the  $Ca^{2+}$ -ionophore A23187 (1  $\mu$ M, 4 min) triggered significant ATP release, but its application at higher concentrations (10  $\mu$ M) or longer incubations (10 min) failed to do so (Figure 24).  $[Ca^{2+}]_i$ -changes thus trigger ATP release, but the response disappears with stronger stimulation.

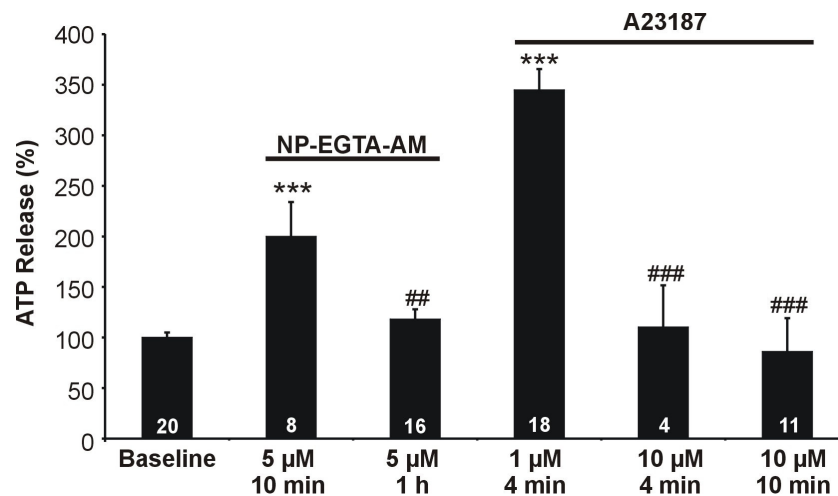


**Figure 24: Increasing  $[Ca^{2+}]_i$  triggers ATP release in ECV304 cells**

Photoactivation of  $Ca^{2+}$  from NP-EGTA or stimulation of  $Ca^{2+}$ -entry with A23187 triggered ATP release. Prolonging NP-EGTA ester-loading to 1 h or increasing the A23187 concentration or exposure time did not trigger ATP responses. Star signs indicate significance compared to baseline, while number signs represent significance compared to trigger.

### 4.3.3 DF- and $Ca^{2+}$ -triggered ATP release are inhibited by gap junction blockers and a Cx32 Gap peptide in ECV304

DF-triggered ATP release was significantly inhibited by the gap junction blockers  $\alpha$ -GA (50  $\mu$ M, 30 min) and carbenoxolone (100  $\mu$ M, 30 min - Figure 25A). In line with the connexin expression pattern of ECV304 (Figure 21),  $^{32}$ Gap 24 (0.25 mg/ml - 174  $\mu$ M, 30 min), a 13 amino acid peptide identical to the sequence on the intracellular loop of Cx32, completely blocked the ATP response, while  $^{43}$ Gap 27 (0.25 mg/ml - 191  $\mu$ M, 30 min), an 11 amino acid peptide that corresponds to a sequence on the second extracellular loop of Cx43, only showed a small, although significant, inhibition (Figure 25B). This last effect is probably related to a low Cx43 background expression, that could not be detected via Western blot analysis, because  $^{43}$ Gap 27 was previously found to have no effect on Cx32 hemichannels (Figure 30 and Braet et al. (2003a)).

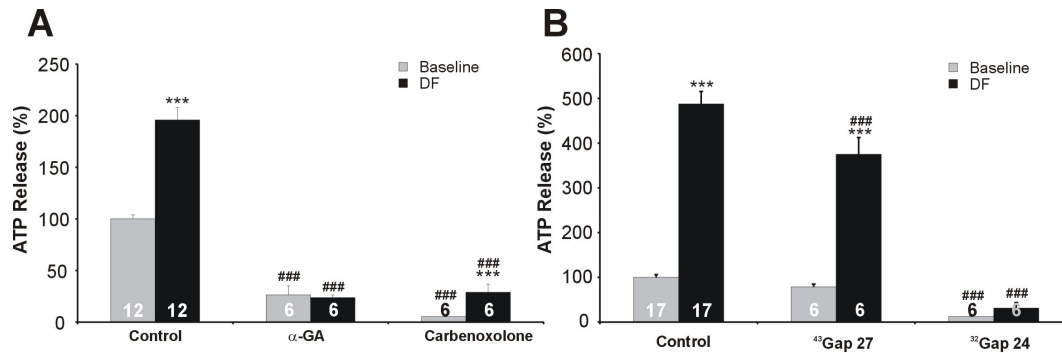


**Figure 25: Effect of connexin channel inhibitors on DF-triggered ATP release in ECV304 cells**  
 (A)  $\alpha$ -GA and carbenoxolone completely blocked DF-triggered ATP release in ECV304 cells. (B) <sup>32</sup>Gap 24 completely abolished DF-triggered ATP release, while <sup>45</sup>Gap 27 only weakly inhibited it. These results correspond to the connexin expression pattern in these cells (presence of Cx32). Star signs indicate significance compared to baseline, while number signs represent significance compared to control conditions.

Carbenoxolone and <sup>32</sup>Gap 24 also significantly inhibited ATP release triggered by Ca<sup>2+</sup>-photoactivation (Figure 26A) and A23187 (Figure 26B). In some of the experiments, inhibitor substances caused significant inhibition of the baseline signal, indicating involvement of hemichannels under basal conditions. In all these cases, the net ATP release (trigger minus baseline) and relative response (trigger over baseline ratio) were significantly below control ( $p < 0.05$ ) except for the carbenoxolone experiment of Figure 25A, where the relative response appeared to be increased (an atypical response not observed in other experiments).

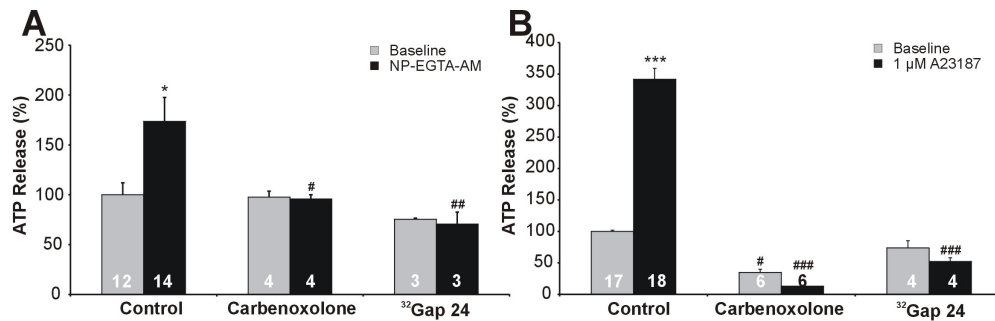


**Figure 26: Effect of carbenoxolone and <sup>32</sup>Gap 24 on Ca<sup>2+</sup>-triggered ATP release in ECV304 cells**  
 Carbenoxolone and <sup>32</sup>Gap 24 blocked ATP release triggered by an increase in [Ca<sup>2+</sup>]<sub>i</sub> elicited by photoactivation of NP-EGTA (A), or by exposing the cells to 1 μM A23187 (B). Star signs indicate significance compared to baseline, while number signs represent significance compared to control conditions.

#### 4.3.4 DF- and Ca<sup>2+</sup>-triggered ATP release and dye uptake are inhibited by Cx32 Gap peptides and a CaM antagonist in C6-Cx32

The experiments on ECV304 cells strongly indicate a role for [Ca<sup>2+</sup>]<sub>i</sub> in triggering ATP release via Cx32 hemichannels. We switched to another model system making use of C6 glioma cells to further establish hemichannel involvement based on both comparisons between wild type (WT) and Cx32 expressing C6 cells (Bond et al., 1994) and Gap peptides

as specific hemichannel blockers. DF conditions and A23187 (2  $\mu$ M, 5 min) triggered significant ATP release in C6-Cx32 that was blocked with carbenoxolone (Figure 27) and  $^{32}$ Gap 24 (Figure 28).

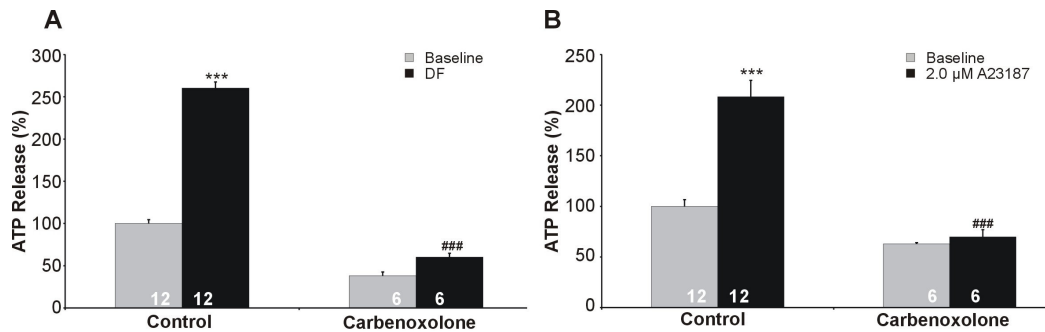


**Figure 27: Influence of carbenoxolone on DF- and A23187-triggered ATP release in C6-Cx32 cells**

Carbenoxolone completely blocked ATP release triggered by DF-conditions (A) and 2.0  $\mu$ M A23187 in C6-Cx32 cells (B). In (A) baseline of carbenoxolone treated cells was significantly different from the baseline in control conditions ( $p < 0.001$ ). Star signs indicate significance compared to baseline, while number signs represent significance compared to control conditions.

$^{32}$ Gap 27 (0.25 mg/ml - 214  $\mu$ M, 30 min), a peptide that is identical to a sequence on the second extracellular loop of Cx32, blocked DF- and A23187-triggered ATP release to a similar extent as  $^{32}$ Gap 24 (Figure 28). Both DF- and A23187-triggered ATP release were not significantly above baseline in C6-WT and were significantly lower as compared to C6-Cx32 (insets in Figure 28). In Figure 28A, DF exposure appears to trigger some ATP release in C6-WT (nonsignificant with ANOVA, but significantly above baseline with a t-test -  $p < 0.05$ ), which may be related to a low connexin background expression or the operation of other DF-responsive ATP release mechanisms.

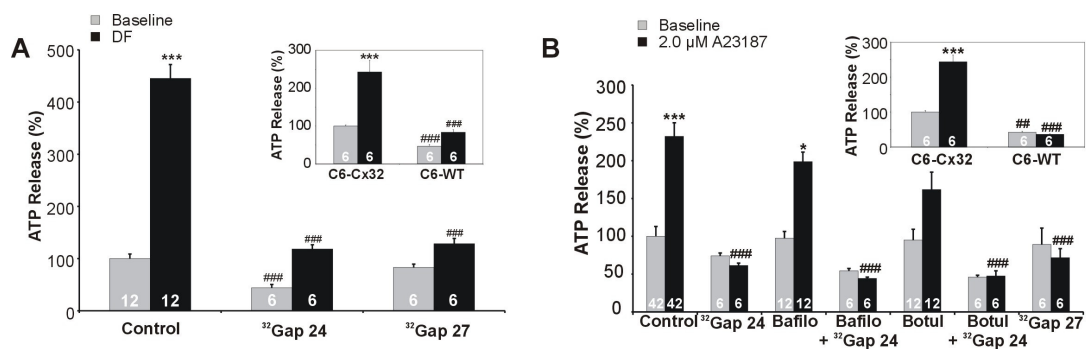


**Figure 28: Inhibitory effect of Cx32 Gap peptides and blockers of exocytosis on DF- and A23187-triggered ATP release in C6-Cx32 cells**

(A) The Gap peptides  $^{32}$ Gap 24 and  $^{32}$ Gap 27, drastically inhibited DF-triggered ATP release in C6-Cx32. DF-triggered ATP release was significantly lower in C6-WT as compared to C6-Cx32 (inset in A). (B)  $^{32}$ Gap 24 and  $^{32}$ Gap 27 blocked the ATP response triggered by exposure to A23187. Bafilomycin A1 (Bafilo) had no effect, while botulinum toxin B (Botul) showed slight but nonsignificant inhibition (triggered ATP release was however not significantly above baseline). The ATP response was completely blocked by adding  $^{32}$ Gap 24 together with either of the toxins, and was absent in C6-WT (inset in B). Star signs indicate significance compared to baseline, while number signs represent significance compared to control conditions.

The two Cx32 Gap peptides had no effect on gap junctional coupling as investigated with SLDT after 0.5 h incubation (Figure 29), similar to our observations with  $^{43}\text{Gap 27}$  in Cx43 expressing cells (Braet et al., 2003a). Longer exposures to  $^{43}\text{Gap 27}$  (Braet et al., 2003a; Braet et al., 2003b) and  $^{32}\text{Gap 27}$  do however inhibit coupling (Figure 29A), presumably by preventing the formation of new gap junction channels or by the longer time needed to reach target interaction sites, which are less accessible in the gap junction channel configuration. Remarkably,  $^{32}\text{Gap 24}$  did not inhibit dye spreading in C6-Cx32 cells, not even after long (24 h) incubation periods, indicating that this peptide can be used as a specific inhibitor of hemichannels composed of Cx32 (Figure 29B).

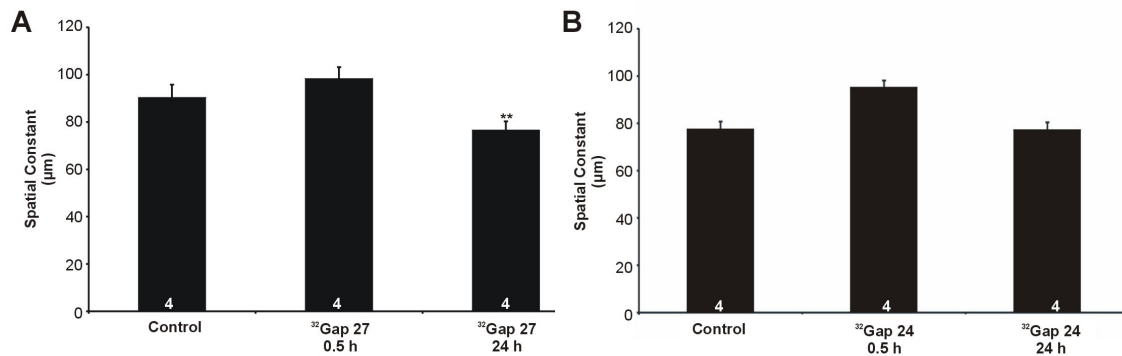


**Figure 29: Effect of Gap peptides on gap junctional coupling in C6-Cx32 cells**

(A)  $^{32}\text{Gap 27}$  that is identical to a sequence on the second extracellular loop of Cx32 inhibited gap junctional coupling, as measured via SLDT, after a 24 h incubation period. Shorter exposure times did not affect dye spread. (B)  $^{32}\text{Gap 24}$  that corresponds to a sequence on the intracellular loop of Cx32 had no effect on gap junctional coupling, not even after 24 h. Star signs indicate significance compared to control conditions.

The effect of the Gap peptides is specific for the corresponding connexin isoform. The Cx43 Gap peptide  $^{43}\text{Gap 27}$  did not influence DF-triggered ATP release in C6-Cx32 (Figure 30A), but A23187-triggered ATP release was slightly, but significantly suppressed (Figure 30B).  $^{32}\text{Gap 24}$  was without effect on DF-triggered ATP release in C6-Cx43 cells (Figure 30C).



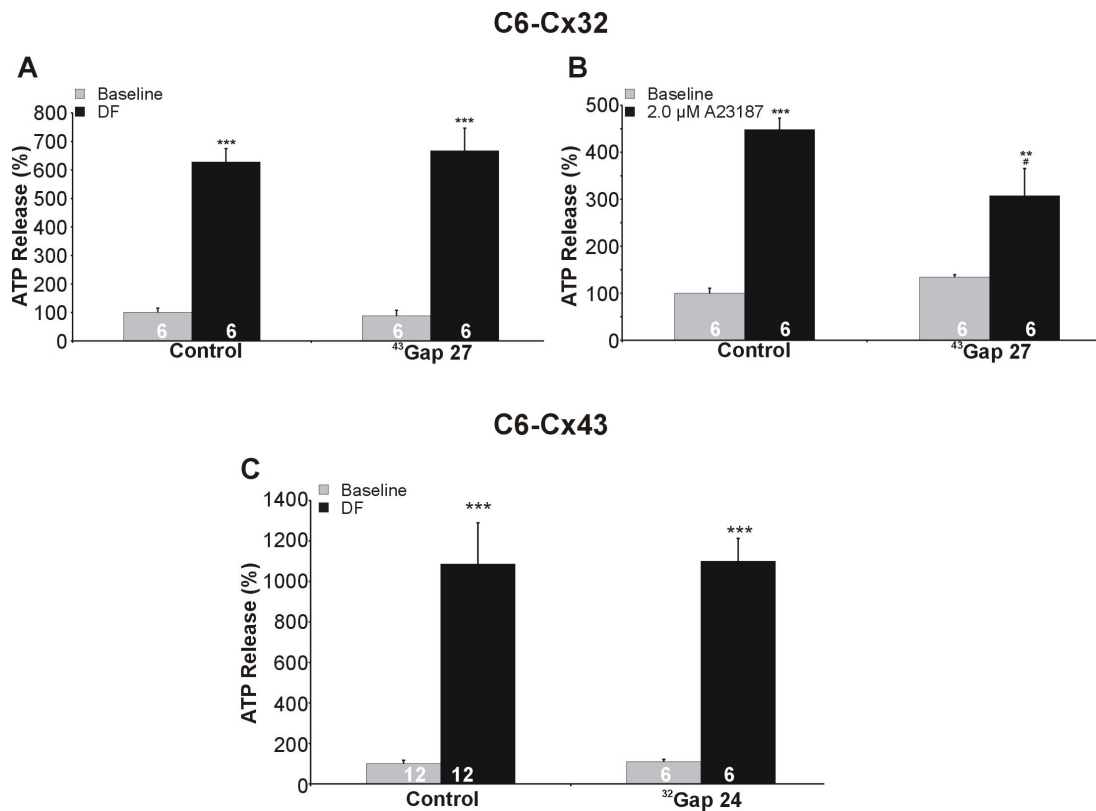
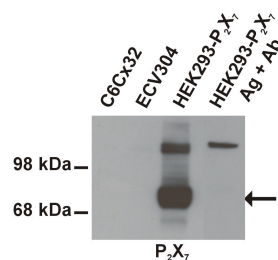


**Figure 30: Effect of Gap peptides on DF- and A23187-triggered ATP release in C6 cells**

(A) The Gap peptide <sup>43</sup>Gap 27 had no effect on DF-triggered ATP release in C6-Cx32. (B) <sup>43</sup>Gap 27 had a small, significant effect on A23187-triggered ATP release in C6-Cx32 cells. (C) Incubating C6-Cx43 cells with <sup>32</sup>Gap 24 showed that this Gap peptide had no influence on DF-triggered ATP release. Star signs indicate significance compared to baseline, while number signs represent significance compared to control conditions.

#### 4.3.5 P<sub>2</sub>X<sub>7</sub> receptors are not involved in ATP release

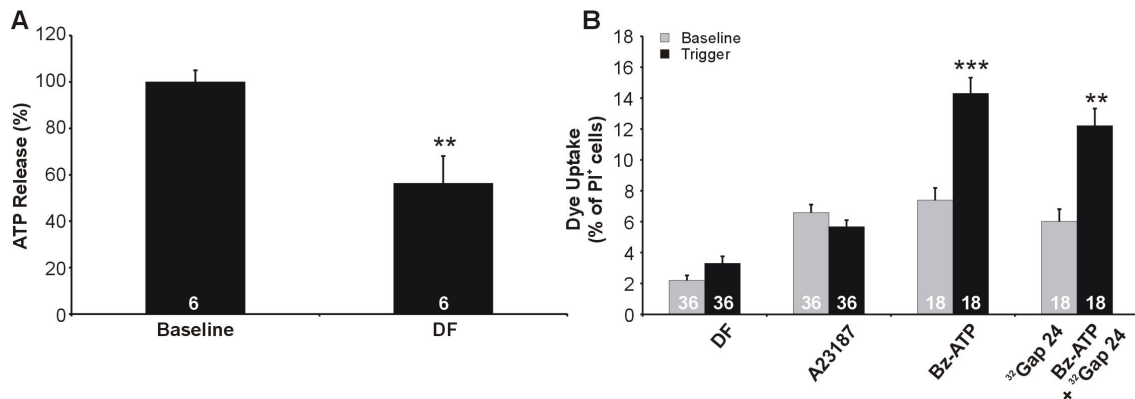
Activation of P<sub>2</sub>X<sub>7</sub> receptors triggers pore formation, and activates an ATP release pathway (Duan et al., 2003) that should be distinguished from hemichannels (Parpura et al., 2004; Spray et al., 2006). ECV304 and C6-Cx32 cells did however not express the P<sub>2</sub>X<sub>7</sub> protein (Figure 31).



**Figure 31: P<sub>2</sub>X<sub>7</sub> receptor expression in the used cell lines**

Western blot analysis showed no expression of the P<sub>2</sub>X<sub>7</sub> protein in C6-Cx32 or ECV304. HEK293 cells stably transfected with the P<sub>2</sub>X<sub>7</sub> receptor protein (Humphreys et al., 1998) were used as positive control. The specificity of the antibody was verified by pre-incubating the antibody with the corresponding antigenic peptide (amino acids 576 - 595 of the rat P<sub>2</sub>X<sub>7</sub> receptor) for 1 h at room temperature, resulting in the disappearance of the signal.

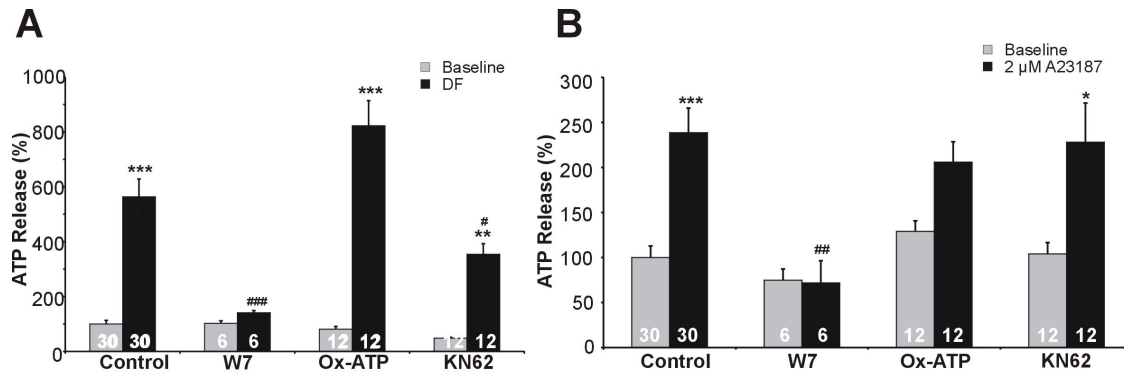
HEK293- $P_2X_7$  cells did not show ATP release in response to DF conditions, moreover the ATP response was diminished by 50 % (Figure 32A). This finding was in contrast with previous observations that report potentiation of pore formation in conditions of low extracellular divalent cations (North, 2002). Furthermore, exposure to DF solutions or to A23187 did not trigger PI uptake in HEK293- $P_2X_7$  cells; Bz-ATP triggered significant PI uptake in these cells, but this response was not significantly affected by  $^{32}$ Gap 24 (Figure 32B).



**Figure 32: Pore opening in HEK293- $P_2X_7$  cells**

(A) Exposing HEK293- $P_2X_7$  cells to DF conditions did not trigger significant ATP release. (B) DF and A23187 (2  $\mu$ M) did not stimulate significant dye uptake, while Bz-ATP (2  $\mu$ M, 30 min) was an effective stimulus.  $^{32}$ Gap 24 did not significantly inhibit the Bz-ATP-triggered response. Star signs indicate significance compared to control conditions.

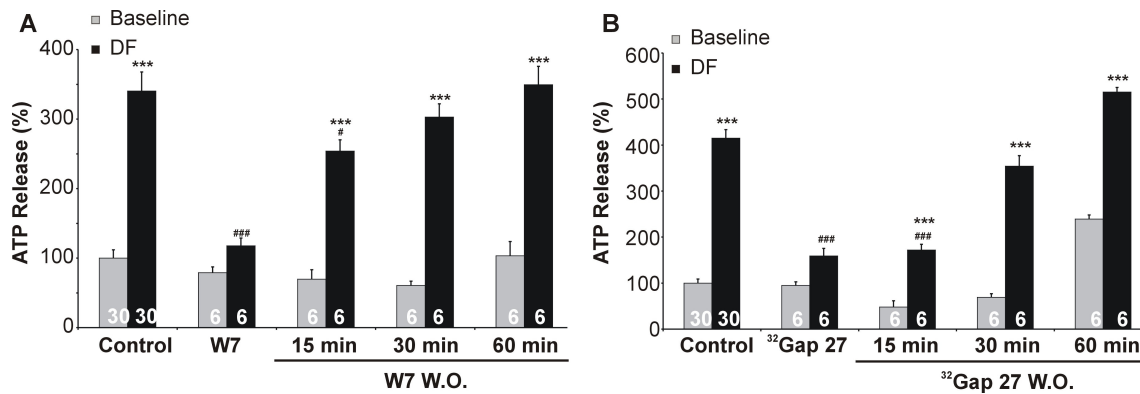
Ox-ATP (100  $\mu$ M, 1 h), an irreversible  $P_2X_7$  receptor antagonist that blocks pore formation by covalently modifying the receptor (Surprenant et al., 1996; North, 2002), did not inhibit DF- and A23187-triggered ATP release in C6-Cx32 (Figure 33). KN62, another  $P_2X_7$  antagonist (North, 2002), significantly inhibited DF-triggered ATP release (Figure 33A), but was without effect on ATP release triggered by A23187 (Figure 33B). This is probably not related to  $P_2X_7$  receptor antagonism, but might be the result of inhibition of  $Ca^{2+}$ /CaM dependent kinases acting on the connexins (Hidaka and Yokokura, 1996). Cx32 contains two cytoplasmic CaM binding domains (Torok et al., 1997) that may be involved in the  $Ca^{2+}$ -triggered ATP responses. The CaM antagonist W7 (20  $\mu$ M, 1 h) was as potent as the Cx32 Gap peptides in blocking DF- and A23187-triggered ATP release (Figure 33).



**Figure 33:** CaM is involved in ATP release in C6-Cx32 cells, but the  $P_2X_7$  receptor pore does not contribute

(A) CaM inhibition with W7 drastically blocked DF-triggered ATP release in C6-Cx32 cells. The  $P_2X_7$  receptor antagonist ox-ATP had no effect, but KN62 displayed significant inhibition. (B) A23187-triggered ATP release was completely blocked by the CaM antagonist, W7, but ox-ATP and KN62 had no significant effects on  $Ca^{2+}$ -triggered ATP release. Star signs indicate significancy compared to baseline, while number signs represent significancy compared to control conditions.

The inhibitory effect of W7 and the Gap peptides on DF-triggered ATP release was reversible when these substances were replaced by control solution (Figure 34): inhibition by W7 completely disappeared after 30 min washout (Figure 34A), inhibition by  $^{32}Gap$  27 (Figure 34B) took also almost 30 min to disappear and  $^{32}Gap$  24 (Figure 34C) took almost 60 min to reverse after replacement. The effect of various washout periods on DF-triggered ATP release was assessed by experiments on different cultures.



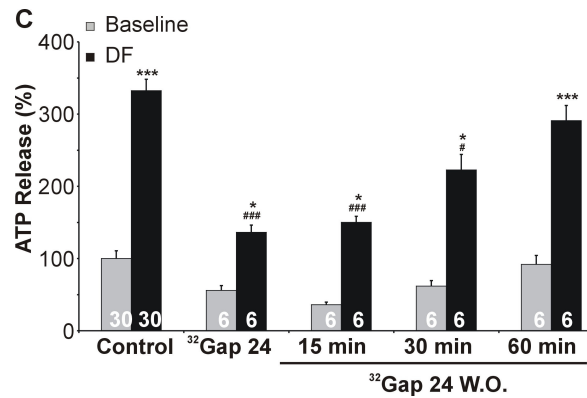


**Figure 34: Recovery of DF-triggered ATP release following wash out of W7, <sup>32</sup>Gap 27, and <sup>32</sup>Gap 24**  
DF-triggered ATP release completely recovered to control conditions after W7 (A), <sup>32</sup>Gap 27 (B), and <sup>32</sup>Gap 24 (C) were replaced by control solutions. Star signs indicate significance compared to baseline, while number signs represent significance compared to control conditions.

DF conditions and A23187 triggered significant uptake of the hemichannel permeable reporter dye PI (Figure 35), but not of hemichannel impermeable dyes (see section 4.2.6) in C6-Cx32 cells. Dye uptake was significantly lower in C6-WT as compared to C6-Cx32 with both DF- and A23187-triggers (inset in Figure 35B and D). DF- and A23187-triggered dye uptake in C6-Cx32 was blocked by carbenoxolone, <sup>32</sup>Gap 24 and W7 (Figure 35B and D).

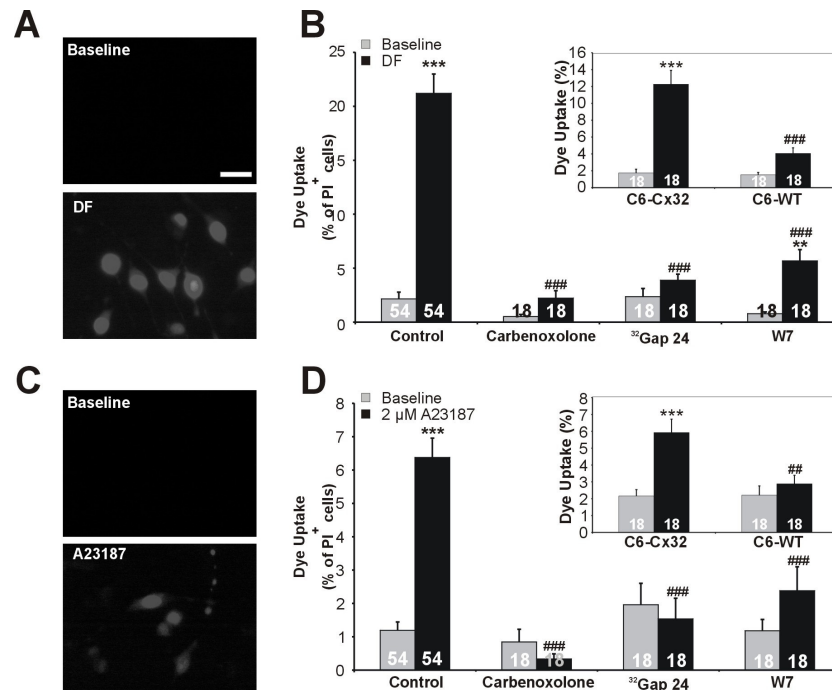


**Figure 35: DF conditions and A23187 trigger PI uptake in C6-CX32 cells**

(A and C) Example images illustrating baseline and triggered dye uptake in C6-Cx32 cells (scalebar: 20  $\mu$ m). (B) DF-triggered PI uptake was blocked by carbenoxolone, <sup>32</sup>Gap 24 and W7, and was significantly lower in C6-WT (inset in B). (D) A23187-triggered PI uptake in C6-Cx32 was inhibited by carbenoxolone, <sup>32</sup>Gap 24 and W7, and absent in C6-WT (inset in D). Star signs indicate significance compared to baseline, while number signs represent significance compared to control conditions.

### 4.3.6 Vesicular release slightly contributes to $\text{Ca}^{2+}$ -triggered ATP release in C6-Cx32

Elevation of  $[\text{Ca}^{2+}]_i$  is a known stimulus for exocytosis (Montana et al., 2006). To exclude the involvement of this ATP release mechanism, we incubated the cells with inhibitors of vesicular mediated release. Botulinum toxin B (1.5 nM, 24 h), a protease that cleaves the v-SNARE protein synaptobrevin (Schiavo et al., 1992), significantly reduced DF-triggered ATP release in C6-Cx32, but bafilomycin A1 (100  $\mu\text{M}$ , 1 h), a v-ATPase inhibitor known to inhibit ATP storage (Coco et al., 2003), had no effect (Figure 36). With both toxins a reduction of the average value of A23187-triggered ATP release was seen in C6-Cx32, but this effect was not significant (Figure 28B). Addition of  $^{32}\text{Gap}$  24 together with botulinum toxin B or bafilomycin A1 (the last 30 min) depressed the ATP response to below baseline levels, indicating predominance of the release component inhibited by the Cx32 Gap peptide (Figure 28B).

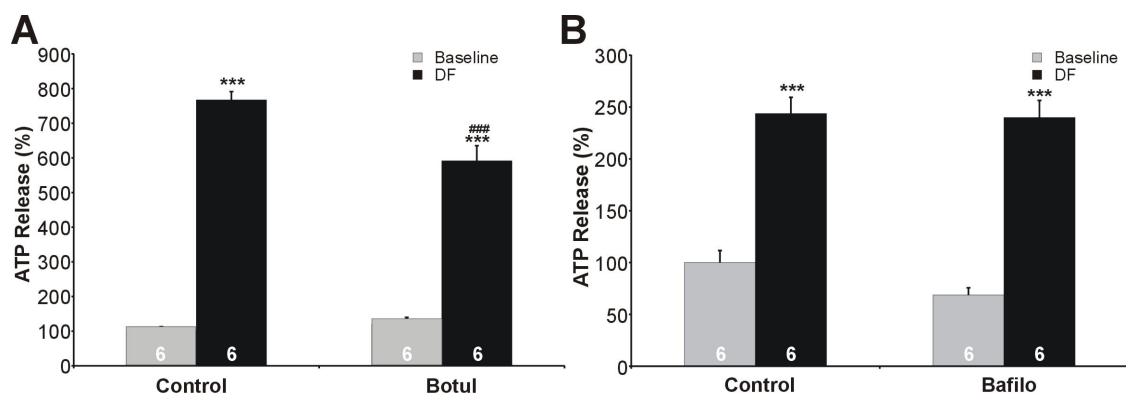


**Figure 36: Involvement of exocytosis in DF-triggered ATP release in C6-Cx32**

Botulinum toxin B (Botul) slightly but significantly inhibited DF-triggered ATP release, while bafilomycin A1 (Bafilo) had no effect. The difference in the magnitude of the trigger is probably related to the different experimental conditions. Star signs indicate significance compared to baseline, while number signs represent significance compared to control conditions.

### 4.3.7 Relation between $[\text{Ca}^{2+}]_i$ and ATP release or dye uptake in C6-Cx32

We tested various A23187 concentrations to construct a dose-response curve for  $\text{Ca}^{2+}$ -triggered ATP release. These experiments confirmed the observations in ECV304 cells (Figure 24) and demonstrated a response curve with activation of ATP release within a very narrow range of A23187 concentrations (only 1.5 and 2  $\mu\text{M}$  were effective - Figure 37A); a similar sharp response pattern was found for A23187-triggered dye uptake (Figure 37B). Expression of ATP release (Figure 38C) or dye uptake (Figure 38D) as a function of the  $[\text{Ca}^{2+}]_i$  (measured with fura-2) obtained with various A23187 concentrations (Figure 38B) demonstrated a bell-shaped response curve with a maximal response at  $\sim 500$  nM.

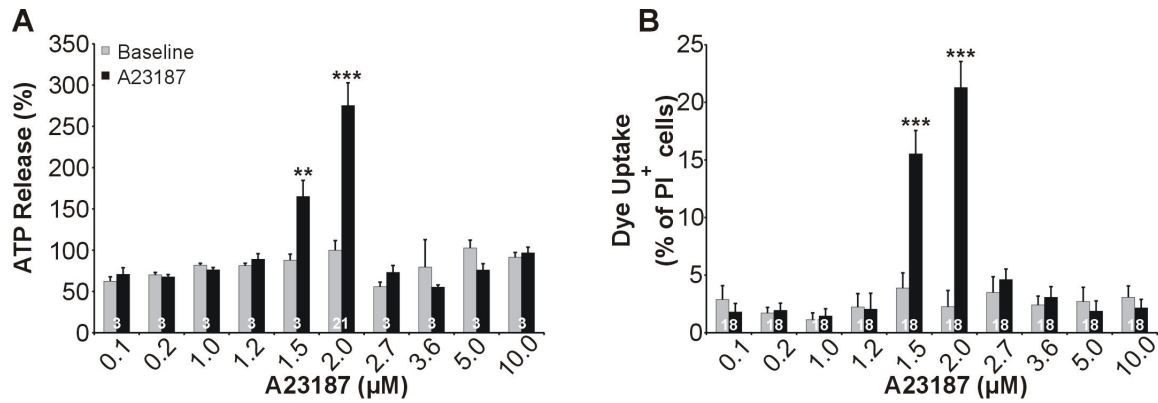


**Figure 37: Dose-response curve for A23187-triggered ATP release and dye uptake in C6-Cx32**

(A) A23187 only triggered significant ATP responses at 1.5 and 2 μM, while responses were absent at lower or higher concentrations. (B) Dose-response curve for Ca<sup>2+</sup>-triggered dye uptake, illustrating the same narrow concentration dependence as observed for ATP release. Star signs indicate significance compared to the corresponding baseline.

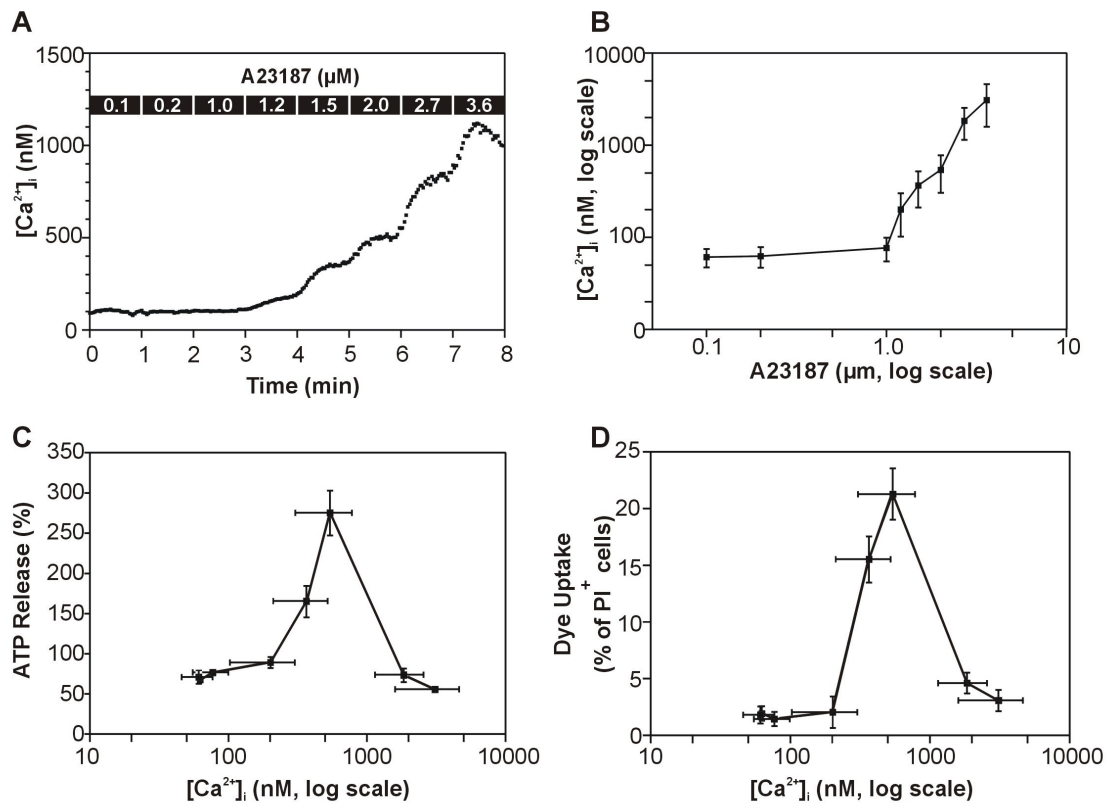


**Figure 38: ATP release and dye uptake expressed in function of [Ca<sup>2+</sup>]<sub>i</sub> in C6-Cx32**

(A) Time course of [Ca<sup>2+</sup>]<sub>i</sub> responses to increasing A23187 concentrations as determined in Ca<sup>2+</sup>-imaging experiments. (B) Average peak value of [Ca<sup>2+</sup>]<sub>i</sub> response to various A23187 concentrations (n = 4). ATP release (C) and dye uptake (D) expressed as a function of [Ca<sup>2+</sup>]<sub>i</sub> (graph constructed from data presented in Figure 37A/B and Figure 38B).

We further investigated the relation between [Ca<sup>2+</sup>]<sub>i</sub> changes and dye uptake by simultaneous imaging of [Ca<sup>2+</sup>]<sub>i</sub> and the PI fluorescence in individual cells. Under baseline conditions,

sparse PI positive cells could be distinguished ( $\times 40$  objective). Closer inspection of these cells demonstrated that the dye was located at small discrete spots most often at the periphery of the cell (Figure 39A and F). This staining pattern is different from the nuclear and cytoplasmic staining shown in Figure 35A and C, probably because the PI concentration was 100-times lower and the exposure time was shorter in these experiments. Resting  $[Ca^{2+}]_i$  in baseline PI positive cells was  $96.5 \pm 12.4$  nM ( $n = 20$ ), which is slightly but significantly ( $p < 0.02$ ) higher than resting  $[Ca^{2+}]_i$  in PI negative cells in the same cultures, i.e.  $62.5 \pm 8.7$  nM ( $n = 20$ ) or  $61.0 \pm 13.7$  nM from the experiments used in Figure 38B. Upon exposure of the cultures to  $2 \mu\text{M}$  A23187, additional PI positive cells appeared in Figure 39I and J. The intensity of these PI spots increased with time and  $[Ca^{2+}]_i$  (Figure 40A), and attained half-maximal intensity at  $463 \pm 102$  nM  $[Ca^{2+}]_i$  ( $n = 12$ ), which is in the range of the  $\sim 340$  nM half-maximum concentration for activation of the ATP and dye uptake responses derived from the graphs in Figure 38C and D. The peak  $[Ca^{2+}]_i$  increase triggered by  $2 \mu\text{M}$  A23187 was slightly but not significantly higher in cells that subsequently became PI positive as compared to cells that remained PI negative ( $622 \pm 107$  nM versus  $515 \pm 100$  nM, respectively;  $n = 12$ ).

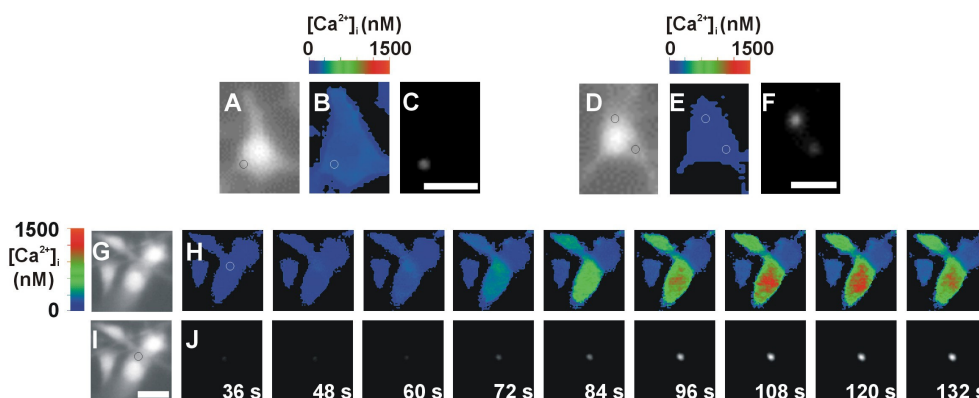


**Figure 39: Simultaneous imaging of  $[Ca^{2+}]_i$  and dye uptake in C6-Cx32**

(A-F) Examples illustrating resting  $[Ca^{2+}]_i$  in baseline PI positive cells. (A and D) Fura-2 loaded cells at 380 nm excitation. (B, E) Corresponding  $[Ca^{2+}]_i$  maps indicating 153 nM  $[Ca^{2+}]_i$  in B and 54 nM in E. The PI spots are indicated with small circles on the fura-2 and  $[Ca^{2+}]_i$  images. (C and F) PI imaging. (G) Fura-2 image at 380 nm excitation. (H) Time series of  $[Ca^{2+}]_i$  maps (times as indicated in J). The first image is before and subsequent images after exposure to  $2 \mu\text{M}$  A23187. (I) 380 nm image with indication of the PI spot (circle) observed in the next sequence. (J) Time series of PI images acquired simultaneously with the  $[Ca^{2+}]_i$  maps. A small spot at the periphery of a cell became PI positive when switching to  $2 \mu\text{M}$  A23187. The position of the PI spot is also indicated in (H). The intensity of the PI spot increased with time and  $[Ca^{2+}]_i$ . The white calibration bar measures  $20 \mu\text{m}$ .

In another series of experiments,  $[Ca^{2+}]_i$  changes were triggered with  $4 \mu\text{M}$  A23187 (increasing  $[Ca^{2+}]_i$  to  $3,300 \pm 530$  nM;  $n = 21$ ) and PI was introduced just after the peak (Figure 40B). A limited number of experiments ( $n = 3$ ) showed the appearance of PI during  $[Ca^{2+}]_i$  recovery in previously PI negative cells, indicative of hemichannel opening when  $[Ca^{2+}]_i$  decreases and falls into the concentration range of the right flank of the dose-response curves of Figure 38C and D.



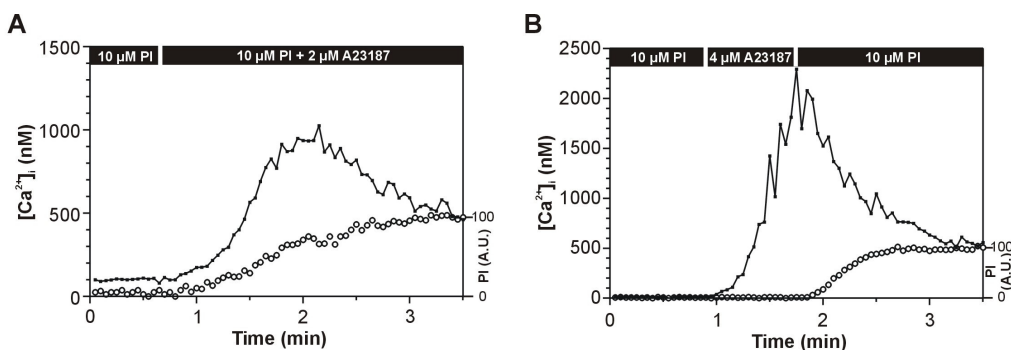


**Figure 40: Time course of  $[Ca^{2+}]_i$  and PI intensity**

Time course of  $[Ca^{2+}]_i$  and PI intensity (open circles) in the spot indicated in Figure 39H and I. The  $[Ca^{2+}]_i$  increase was associated with an increasing intensity of the PI spot (expressed in arbitrary units - A.U.). Half-maximal intensity was reached at ~ 800 nM in this experiment. (B) Experiment where PI was introduced after induction of a large  $[Ca^{2+}]_i$  increase with 4  $\mu$ M A23187. In this case, a PI spot appeared during the  $[Ca^{2+}]_i$  recovery phase.

## 4.4 Discussion

Exposure of cells to lowered extracellular divalent cation conditions is a well-known procedure to potentiate or trigger the opening of hemichannels (Stout et al., 2002; Ye et al., 2003). In Cx32 expressing ECV304 cells, DF-triggered ATP release was reduced by buffering  $[Ca^{2+}]_i$  and through the inhibition of the SERCA pump, 1,4,5-InsP<sub>3</sub>R or RYR. Directly increasing  $[Ca^{2+}]_i$  by stimulating  $Ca^{2+}$ -entry with A23187 or photoliberating  $Ca^{2+}$  in the cytoplasm also triggered ATP release. A23187 gave the largest responses and was therefore used in the remainder of the study. A23187 also triggered PI reporter dye uptake (but not of larger reporter molecules), indicating activation of a bidirectionally permeable pathway. ATP release triggered by A23187 or  $Ca^{2+}$ -photoactivation and dye uptake triggered with A23187 were all blocked (inhibited to the baseline or below) by gap junction blockers and <sup>32</sup>Gap 24 and <sup>32</sup>Gap 27, as was DF-triggered ATP release and dye uptake. Similar drastic blocking effects were previously reported for Cx43 Gaps (<sup>43</sup>Gap 26 and <sup>43</sup>Gap 27) on DF-, 1,4,5-InsP<sub>3</sub>- and mechanical stimulation-triggered ATP release in Cx43 expressing cells (Braet et al., 2003a; Braet et al., 2003b). <sup>32</sup>Gap 24 is a tridecapeptide composed of residue numbers 110 - 122 of Cx32. Unlike <sup>32</sup>Gap 27 that corresponds to a sequence on the second extracellular Cx32 loop, the <sup>32</sup>Gap 24 sequence is located on the intracellular Cx32 loop. Peptides identical to a sequence on the intracellular loop of Cx43 have previously been demonstrated to influence the gating of gap junction channels (residue numbers 119 - 144; Seki et al. (2004a)), but <sup>32</sup>Gap 24 was not found to have any effect on dye coupling between the cells in the present work. The details of peptide-connexin interactions leading to hemichannel block are currently unknown, but the effects of <sup>32</sup>Gap 24 are connexin-specific as this peptide did not influence DF-triggered ATP release in C6-Cx43 cells (see section 4.3.4) and <sup>43</sup>Gap 27 had no effect in C6-Cx32 and other Cx32 expressing cells (Braet et al., 2003a). If <sup>32</sup>Gap 24 interacts



with the intracellular loop, then either this loop must be accessible from the outside via the pore or the peptide must get access to the cytoplasm ( $^{32}\text{Gap 24}$  does not, however, contain any currently known cell-penetrating peptide sequence - sequences reviewed in Zorko and Langel (2005)).

The v-ATPase inhibitor bafilomycin A1, reported to inhibit vesicular ATP storage and  $\text{Ca}^{2+}$ -dependent ATP release in astrocytes (Coco et al., 2003), had no significant effect on DF- and A23187-triggered ATP release in C6-Cx32. Botulinum toxin B selectively cleaves the v-SNARE synaptobrevin (Schiavo et al., 1992) and similar toxins acting at the same target have been demonstrated to inhibit osmotic swelling-induced ATP release in epithelial cells (van der Wijk et al., 2003). The toxin inhibited DF-triggered ATP release and also slightly (but nonsignificantly) affected A23187-triggered ATP release. ATP release in C6-Cx32 thus appears to involve a small vesicular component. Exposing the cells to either of the toxins combined with a Cx32 Gap peptide completely suppressed A23187-triggered ATP release. The inhibition by the peptide, added alone or in combination with bafilomycin A1 or botulinum toxin B, was so nearly complete that the pathway blocked must be the predominant ATP release pathway or the one located most upstream in a cascade of ATP releasing signals or events.

An alternative ATP release pathway involves the activation of the  $\text{P}_2\text{X}_7$  receptor pore (Duan et al., 2003) that, upon exposure to ATP in the 100  $\mu\text{M}$  concentration range applied over several minutes, opens a pore that is permeable to molecules with a MW below 900 Da (North, 2002). ATP released by the cell, by whatever pathway, may thus activate these receptors and amplify the ATP responses. DF conditions potentiate  $\text{P}_2\text{X}_7$  pore opening (North, 2002), but these conditions are by themselves not sufficient to initiate pore opening, as illustrated in the experiments here shown with HEK293- $\text{P}_2\text{X}_7$  cells. The absence of  $\text{P}_2\text{X}_7$  receptor expression in ECV304 and C6-Cx32, together with the evidence obtained with  $\text{P}_2\text{X}_7$  receptor antagonists, the ineffectiveness of DF conditions to trigger ATP release as well as the inability of DF conditions and A23187 to trigger dye uptake in HEK293- $\text{P}_2\text{X}_7$  and the absence of any effect of  $^{32}\text{Gap 24}$  on dye uptake triggered in these cells by bz-ATP, excludes involvement of  $\text{P}_2\text{X}_7$  receptors. Faria et al. (2005) recently reported that A23187 triggers opening of a  $\text{P}_2\text{X}_7$ -related pore, presumably a pore activated by maitotoxin, that was furthermore inhibited by W7 (Faria et al., 2005). The identity of the maitotoxin receptor is currently not known, but the pore activated by this toxin are blocked by DF conditions rather than opened (Lundy et al., 2004) and are virtually inactive at room temperature (Schilling et al., 1999).

The present study shows that increasing  $[Ca^{2+}]_i$  triggers hemichannel permeable dye uptake and ATP release that are inhibited by gap junction blockers and Cx32 Gaps. This response is absent in C6-WT cells not expressing connexins. Vesicular ATP release contributes to a limited extent to the DF-triggered and A23187-triggered response, but the release pathway blocked by the peptides is the most prominent or upstream one. The magnitude of the  $Ca^{2+}$ -stimulus is critical in order to trigger hemichannel opening: both small and large stimuli were ineffective and only  $[Ca^{2+}]_i$  changes in the range between 200 nM and 1000 nM were successful.  $[Ca^{2+}]_i$  changes passing through the optimum concentration range towards a higher peak level are ineffective, presumably because the time spent within the trigger window is too short. The narrow bell-shaped response curve probably explains some controversy in the literature whether hemichannel mediated ATP release is or is not dependent on  $[Ca^{2+}]_i$ . Our work also indicates that baseline hemichannel activity allows PI to enter the cell, while having only small (although significant) effects on the resting  $[Ca^{2+}]_i$ . In line with this, A23187-triggered  $[Ca^{2+}]_i$  changes were slightly (but not significantly) larger in cells that experienced PI uptake and hemichannel opening as compared to those that remained PI negative. Presumably, PI influx through hemichannels is quite limited in the conditions used for these experiments and only stains RNA in close proximity to the channel.  $Ca^{2+}$ -influx through hemichannels is probably equally limited and/or effectively removed by  $Ca^{2+}$ -pumps or buffers.

The finding that increasing  $[Ca^{2+}]_i$  triggers hemichannel opening is not in contradiction with the widespread notion that  $[Ca^{2+}]_i$  elevation closes gap junction channels. Recent work from the group of Li and co-workers has elegantly demonstrated that only capacitative  $Ca^{2+}$ -entry via store-operated channels is effective in blocking gap junctional communication in primary human fibroblast cells (Dakin et al., 2005) and HeLa-Cx26 cells (Dakin et al., 2006), while  $Ca^{2+}$ -ionophores are without effect. How  $[Ca^{2+}]_i$  changes are linked to hemichannel opening is currently unknown. The CaM inhibitor W7 blocked  $Ca^{2+}$ -triggered ATP release and dye uptake as efficiently as the Cx32 Gap peptide, and the  $[Ca^{2+}]_i$  successfully activating ATP release (500 nM) were in the  $K_d$  range for  $Ca^{2+}$ /CaM interactions (500 nM - 5  $\mu$ M; Chin and Means (2000)), strongly pointing to the involvement of CaM in the signaling cascade. CaM may act either directly on CaM interaction sites on the connexin subunit, or indirectly via CaM dependent kinases. Further work is under way to characterize the  $Ca^{2+}$ -dependency of Cx43 hemichannels, which contain a single CaM interaction site (Zhou et al., 2007).

## Chapter

### 5

# ***Ca<sup>2+</sup>-activation of ATP release via Cx43 hemichannels is controlled by a CaM-AA-ROS-NO signaling cascade***

Elke De Vuyst<sup>1</sup>, Elke Decrock<sup>1</sup>, Marijke De Bock<sup>1</sup>, Marijke Van Moorhem<sup>1</sup>, Hiroshi Yamasaki<sup>2</sup>, Christian C Naus<sup>3</sup>, W Howard Evans<sup>4</sup>, and Luc Leybaert<sup>1</sup>

<sup>1</sup> Department of Physiology and Pathophysiology, Faculty of Medicine and Health Sciences, Ghent University, Ghent, Belgium

<sup>2</sup> Department of Bioscience, School of Science and Technology, Kwansai Gakuin University, Gakuin, Sanda 669-13, Japan

<sup>3</sup> Department of Cellular and Physiological Sciences, Faculty of Medicine, University of British Columbia, Vancouver, BC, Canada

<sup>4</sup> Department of Medical Biochemistry and Immunology, Cardiff University School of Medicine, Cardiff, UK

Manuscript submitted in Mol. Biol. Cell

If your experiment needs statistics, then you ought to have done a better experiment.  
-Lord Rutherford-

---

### Abstract

Connexin hemichannels are activated by various stimuli including depolarization and oxidative stress. We investigated in connexin 43 (Cx43) expressing cells the signaling events leading from an increase of cytoplasmic  $\text{Ca}^{2+}$ -concentration ( $[\text{Ca}^{2+}]_i$ ) to hemichannel mediated ATP release. Involvement of Cx43 hemichannels was concluded on the basis of gene silencing and the exclusion of other release mechanisms. Elevating  $[\text{Ca}^{2+}]_i$  with the  $\text{Ca}^{2+}$  ionophore A23187 triggered ATP release that peaked around 500 nM  $[\text{Ca}^{2+}]_i$  and was absent at low or high (above 1,000 nM) concentrations. A23187-triggered ATP responses were blocked by antagonists of calmodulin (CaM), CaM dependent kinase II, arachidonic acid (AA) metabolism and ROS/NO signaling. CaM activation with CALP1 triggered ATP release by itself that was again blocked by interfering with AA metabolism or ROS/NO signaling. CALP1-triggered ATP responses had an S-shaped concentration dependence, in contrast to the bell-shaped response curve obtained with the A23187 trigger. AA applied exogenously also triggered ATP release that was blocked by ROS/NO inhibition. The results indicate  $\text{Ca}^{2+}$ /CaM mediated activation of hemichannels via AA-ROS/NO signaling and suggest that hemichannel inactivation at high  $[\text{Ca}^{2+}]_i$  does not involve  $\text{Ca}^{2+}$ /CaM interactions.

## 5.1 Introduction

Gap junctions are specialized membrane structures that directly connect the cytoplasm of two neighboring cells, allowing the passage of small molecules such as amino acids, ions and second messengers (Sohl and Willecke, 2004). Vertebrate gap junctions are composed of proteins encoded by the connexin gene family and consist of two hemichannels each contributed by the cells that share this junctional channel. Hemichannels are hexameric high-conductance plasma membrane channels that are normally closed. The opening of hemichannels, in response to physiological conditions such as a modest  $[Ca^{2+}]_i$  increase (Pearson et al., 2005; De Vuyst et al., 2006) or pathological conditions such as lowered  $[Ca^{2+}]_e$  (Paul et al., 1991; Li et al., 1996; Quist et al., 2000; Thimm et al., 2005) and ischemia (John et al., 1999; Contreras et al., 2002; Thompson et al., 2006), forms a conduit for the release of paracrine signaling molecules, such as ATP (adenosine triphosphate),  $NAD^+$  (nicotinamide adenine dinucleotide), glutathione, glutamate and prostaglandins (Bruzzone et al., 2001a; Bruzzone et al., 2001b; Bennett et al., 2003; Ebihara, 2003; Goodenough and Paul, 2003; Ye et al., 2003; Cherian et al., 2005; Rana and Dringen, 2007). Uncontrolled opening of hemichannels can lead to the loss of ionic homeostasis and destabilization of the membrane potential, which can further influence hemichannel activity (Contreras et al., 2003a). Previous work has indicated that hemichannel mediated ATP release and dye uptake was triggered by  $[Ca^{2+}]_i$  changes induced by photoactivation of 1,4,5-InsP<sub>3</sub> (inositol trisphosphate - Braet et al. (2003a); Braet et al. (2003b)), photoliberation of  $Ca^{2+}$  or ionophore-triggered  $Ca^{2+}$ -entry into the cells (De Vuyst et al., 2006). In this study we investigated the signaling pathway leading from an elevation of  $[Ca^{2+}]_i$  to the opening of hemichannels composed of Cx43. We show here that elevating  $[Ca^{2+}]_i$  with the  $Ca^{2+}$ -ionophore A23187 triggered ATP release that was mediated via Cx43 hemichannels with a limited (but variable) contribution of a downstream vesicular release component, based on Cx43 gene (*gjal*) silencing, exclusion of pannexin (Panx1) hemichannels (Locovei et al., 2006a) and P<sub>2</sub>X<sub>7</sub> receptor pores (Suadicani et al., 2006), and experiments with Gap peptides (Evans et al., 2006), tetanus toxin, botulinum toxin and bafilomycin (Montana et al., 2006). Work with both agonists and antagonists of CaM, CaMK-II, AA and ROS/NO indicated involvement of these distinct signaling steps and in all cases Cx43 gene silencing completely blunted the induced responses. These results bring together hemichannel modulation by AA (Contreras et al., 2002; De Vuyst et al., 2007), ROS (Ramachandran et al., 2007) and NO (Retamal et al., 2006) into a hemichannel activation scheme that starts with  $Ca^{2+}$ /CaM interaction and culminates in ATP release. Interestingly, the  $Ca^{2+}$ /CaM interaction step was not involved in the disappearance of the hemichannel responses at high  $[Ca^{2+}]_i$ . Our results connect major signaling pathways of physiological and pathological cell function to control ATP release via Cx43 hemichannels. Given the wide range of cells expressing Cx43 (Laird, 2006) and the numerous targets of ATP as a paracrine

messenger (Novak, 2003; Di Virgilio, 2006), these findings put-up Cx43 hemichannels as forefront regulators of cellular ATP release.

## 5.2 Material and Methods

### 5.2.1 Cell culture

We used C6 glioma wild type (C6-WT), C6 stably transfected with Cx43 (C6-Cx43 - Zhu et al. (1991)), C6 stably transfected with Panx1-Myc (C6-Panx1-Myc - Lai et al. (2007)), HEK293 cells stably transfected with the P<sub>2</sub>X<sub>7</sub> receptor (HEK293-P<sub>2</sub>X<sub>7</sub> - Humphreys et al. (1998)) and HeLa cells stably transfected with Cx43 (HeLa-Cx43 - Omori and Yamasaki (1999)). C6 cells were maintained in DMEM:Ham's F12 (1:1 - Invitrogen, Merelbeke, Belgium) and HeLa and HEK293 cells were grown in DMEM all supplemented with 10 % foetal bovine serum and 2 mM glutamine. Cells were seeded at a density of 25,000 cells/cm<sup>2</sup> on either glass bottom microwells (MatTek Cooperation, Ashwood, MA) or 24 well plates (Falcon 3047, Becton Dickinson, Erembodegem, Belgium) and used for experiments the next day (subconfluent cultures). The experiments were performed in Hanks' balanced salt solution buffered with 25 mM HEPES (HBSS-HEPES; pH 7.4).

### 5.2.2 Agents

Fura-2-AM (5 µM), 4-Br-A23187 (A23187), Sypro Ruby Orange Protein Blot Stain, propidium iodide (PI; 1 mM) and BAPTA-AM (1,2-bis(*o*-aminophenoxy)ethane-*N,N,N',N'*-tetraacetic acid; 5 µM) were obtained from Molecular Probes (Invitrogen). Botulinum toxin B (1.5 nM), tetanus toxin (100 nM), bafilomycin A1 (100 nM), indomethacin (50 µM), AA, N-acetyl-L-cysteine (1 mM), α-tocopherol succinate (150 µg/ml), superoxide dismutase (200 µg/ml), Nω-nitro-L-arginine (100 µM), W7 (20 µM), and KN62 (1 µM) were from Sigma (Bornem, Belgium). AACOCF3 (arachidonyl trifluoromethyl ketone; 5 µg/ml), baicalein (30 µM), AIP (autocamtide-2-related inhibitory peptide; KKALRRNDAVEAL; 1 µM), and CALP1 (VAITVLVL) were from Tocris Cookson (Avonsmouth, United Kingdom). The Gap peptide <sup>43</sup>Gap26 (VCYDKSFPISHVR; 0.25 mg/ml) was synthesized by Genescript (Genescript Co., NJ, USA) and <sup>43</sup>Gap27 (SRPTEKTIFII; 0.25 mg/ml) was synthesized by Sigma-Genosys (Cambridge, United Kingdom; > 95 % purity). A23187 was prepared from a stock solution of 10 mM in DMSO (dimethylsulfoxide), AA from a stock of 10 mM in ethanol, and CALP1 from a 10 mM stock in distilled water.

### 5.2.3 Extracellular ATP measurements

ATP release was measured with an ATP bioluminescent luciferin/luciferase assay kit (Sigma) in combination with a luminometer plate reader (Victor3 1420 multi label counter; Perkin-Elmer, Zaventem, Belgium) on subconfluent cultures grown on 24-well plates (BD Bioscience, Erembodegem, Belgium). Seventy five microliter of ATP assay mix prepared in HBSS-HEPES (at 5-fold dilution) was added to 150  $\mu$ l solution bathing the cells. ATP release triggered by A23187, CALP1 and AA (concentrations as specified in text) was accumulated over a 5 min stimulation period and the photon flux was counted during 10 s at the end of this period. Baseline measurements were carried out on separate cultures, according to the same procedure but with HBSS-HEPES vehicle only. All pharmacological agents or inhibitors were pre-incubated with the cells in the CO<sub>2</sub> incubator at 37 °C for the time indicated, and were not present during stimulation to avoid interference with luminescence. ATP measurements were performed at room temperature. Average baseline ATP release was  $14.53 \pm 4.02$  pmoles (n = 250) for C6-Cx43 cells, and  $17.87 \pm 4.96$  pmoles (n = 77) for HeLa-Cx43 cells.

### 5.2.4 Dye uptake studies

Dye uptake was determined with the hemichannel permeable reporter dye PI according to a protocol described previously in De Vuyst et al. (2006) - for appropriate control experiments with hemichannel impermeable dyes we also refer to this study. Cells were exposed for 5 min to the trigger solution (A23187) containing 1 mM PI (room temperature) and were then washed 4 times with HBSS-HEPES. Images, 9 for each culture, were acquired on a Nikon TE300 inverted microscope in epifluorescence mode (TRITC excitation/emission) with a x 10 objective and a Nikon DS-5M camera (Analis, Namur, Belgium). The number of PI positive cells was counted in each image using ImageJ (<http://rsb.info.nih.gov/ij/>) software after application of a threshold corresponding to the upper level of the background signal. Cell counts were expressed in the graphs as a percentage relative to the total number of cells in view counted after DAPI staining. Average baseline PI positive cell counts in C6-Cx43 were  $4 \pm 0.7$  on a total of  $30 \pm 2.5$  cells per x 10 objective camera field for a 25,000 cells/cm<sup>2</sup> seeding density (n = 6).

### 5.2.5 Ca<sup>2+</sup>-imaging

Cell cultures were loaded with 5  $\mu$ M fura-2-AM in 1 ml HBSS-HEPES for 1 h, followed by a 30 min de-esterification period, all at room temperature. Imaging was performed on an inverted epifluorescence microscope (Nikon Eclipse TE 300, Analis, Ghent, Belgium) with a x 40 oil immersion objective and a filterswitch (Cairn, Kent, UK) providing excitation alternating between 340 and 380 nm (each applied over 1 s, resulting in one Ca<sup>2+</sup>-image every 2 s). The dichroic mirror had a 430 nm reflection cut-off and emission was bandpass filtered

at 510 nm (40 nm bandwidth). Images were acquired with an intensified CCD (Extended Isis camera, Photonic Science, East Sussex, UK) and stored in a PC equipped with a frame grabber (Data Translation, DT3152, Marlboro, MA). Ratio images were generated with software written in Microsoft Visual C++ 6.0, after standard background and shade correction procedures. Fura-2 *in vitro* calibrations were carried out with Ca<sup>2+</sup>-free solutions (10 mM EGTA, 130 mM KCl, 5 μM pentaK<sup>+</sup> fura-2 salt and 10 mM HEPES pH 7.2) and Ca<sup>2+</sup>-saturating solutions (10 mM CaCl<sub>2</sub>, 130 mM KCl, 5 μM pentaK<sup>+</sup> fura-2 salt and 10 mM HEPES pH 7.2); a K<sub>d</sub> of 224 nM was used to convert ratios to Ca<sup>2+</sup>-concentrations.

### 5.2.6 Western blotting

Cell protein lysates were extracted by treatment of confluent cultures with radioimmunoprecipitation assay buffer (RIPA - 25 mM Tris, 50 mM NaCl, 0.5% NP-40, 0.5% deoxycholate, 0.1% SDS, 5.5 % β-glycerophosphate, 1 mM dithiothreitol, 2 % phosphatase inhibitor cocktail, and 2 % mini EDTA-free protease inhibitor cocktail) and sonicated by three 10 s pulses. Separation of Triton X-100-soluble and -insoluble material was done essentially according to the method of Cooper and Lampe (2002) and performed as previously described in De Vuyst et al. (2007). Protein concentration was determined with a biorad DC protein assay kit, and absorbance was measured on a plate reader with a 590 nm long-pass filter. Proteins were separated by electrophoresis on a 10 % SDS-poly-acrylamide gel and transferred to a nitrocellulose membrane (GE Healthcare, Little Chalfont, Buckinghamshire, United Kingdom). Blots were probed with a rabbit polyclonal anti-rat Cx43 antibody (1/10,000; Sigma), a rabbit polyclonal anti-rat β-tubulin antibody (1/5,000; Abcam, Cambridge, United Kingdom), a rabbit polyclonal anti-rat P<sub>2</sub>X<sub>7</sub> antibody (1/1,000; Alomone Labs, Jerusalem, Israel), or a rabbit polyclonal anti-rat Panx1 antibody (1/1,000; Penuela et al. (2007)) followed by alkaline phosphatase conjugated goat anti-rabbit IgG or goat anti-chicken IgG (1/8,000 - 1/16,000; Sigma), and detection was done with nitro blue tetrazolium/5-bromo-4-chloro-3-indolyl phosphate reagent (Zymed, Invitrogen). ImageJ was used to quantify Western blot signals. A rectangular measurement window was drawn around the Cx43 band and β-tubulin band, and their respective intensities were determined. Loading control was performed by staining of the nitrocellulose membrane with Sypro<sup>®</sup> Ruby Protein Blot stain (Molecular Probes, Invitrogen) for 15 min or β-tubulin detection.

### 5.2.7 siRNA

Cx43 expression was suppressed by siRNA treatment with ON-TARGETplus SMARTpool siRNA from Dharmacon (Thermo Fisher Scientific, Erembodegem, Belgium) containing a mixture of four siRNA duplexes (5'-CAACAACCUCCUGGUCGCGAAAUU-3'; 5'-UGAUUGAAAUGUCGAGUUAUU-3'; 5'-CGUGAAGGGAAGAAGCGAUUU-3'; and 5'-



UUACUGAGAUUCUGCGAUAAU-3') all directed against different domains of *gjal*. A negative control siRNA was obtained from the same company (ON-TARGETplus siCONTROL, Dharmacon). siRNA is resuspended to a 50  $\mu$ M stock concentration and negative control siRNA is resuspended to a 20  $\mu$ M stock concentration in siRNA buffer (20 mM KCl, 6 mM HEPES, 0.2 mM MgCl<sub>2</sub>, pH 7.5). Transfection was performed with Dharmafect 1 transfection reagent and efficiency was in the order of ~ 85 %. Briefly, the cells were seeded at a density of 37,500 cells/cm<sup>2</sup> and transfected 24 h later with 62.5 nM/cm<sup>2</sup> siRNA, or the negative control siRNA, using 1.5  $\mu$ l of transfection reagent per cm<sup>2</sup>. Twenty four hours after transfection, the medium was replaced and the cells were incubated with C6 culture medium for another 24 h before the experiments were started.

### 5.2.8 Scrape loading and dye transfer (SLDT)

Confluent monolayer cultures were washed two times with nominally Ca<sup>2+</sup>-free HBSS-HEPES (CF-HBSS-HEPES). Cells were incubated during 1 min in CF-HBSS-HEPES containing 0.4 mM 6-CF; a linear scratch (one per culture) was made across the cell layer using a syringe needle and the cells were left for another minute in the same solution. Cultures were then washed four times with HBSS-HEPES, left for 15 min at room temperature and images were taken with a Nikon TE300 inverted microscope in epifluorescence mode (FITC excitation/emission) with a x 10 objective and a Nikon DS-5M camera (Analis, Namur, Belgium). A fluorescence diffusion profile was derived from the images, fitted to an exponential decaying function, and the spatial constant of intercellular dye spread was determined.

### 5.2.9 Data analysis and statistics

The data are expressed as mean  $\pm$  s.e.m., with 'n' denoting the number of independent experiments on different cultures. The variations in baseline and triggered signals observed in some figures represent normal variability between different experimental groups; in some cases it may be related to different experimental conditions (e.g. the presence of DMSO, ethanol or distilled water). Comparison of two groups was carried out using a one-tailed unpaired t-test, with a p-value below 0.05 indicating significance. Comparison of more than two groups was carried out with one-way ANOVA and a Bonferroni post test. Statistical significance is indicated in the graphs with a single symbol (\* or #) for p<0.05, two symbols for p<0.01 and three symbols in case p<0.001.

## 5.3 Results

### 5.3.1 The $\text{Ca}^{2+}$ -ionophore A23187 triggers ATP responses in Cx43 expressing cells

Exposing C6 or HeLa cells stably transfected with Cx43 to various concentrations of the  $\text{Ca}^{2+}$ -ionophore A23187 triggered ATP release that was significantly above baseline in the range of 1.2 - 2.7  $\mu\text{M}$  for C6-Cx43 and 2 - 2.2  $\mu\text{M}$  for HeLa-Cx43. Lower or higher A23187 concentrations did not result in significant ATP release (Figure 42A and B). Dye uptake studies in C6-Cx43 with PI gave a similar concentration-dependent response curve as for ATP release (compare Figure 42A and C). Significantly, C6 wild type cells (C6-WT) or C6 cells stably transfected with Panx1 containing a Myc-tag at the carboxyterminal end of the protein (C6-Panx1-Myc) displayed no detectable ATP release above baseline over the whole 0.1 to 5  $\mu\text{M}$  A23187 concentration range applied (Figure 42D), indicating that the responses in C6-/HeLa-Cx43 were related to the presence of Cx43. Western blot analysis of Cx43 expression in the cell lines used is illustrated in Figure 41.

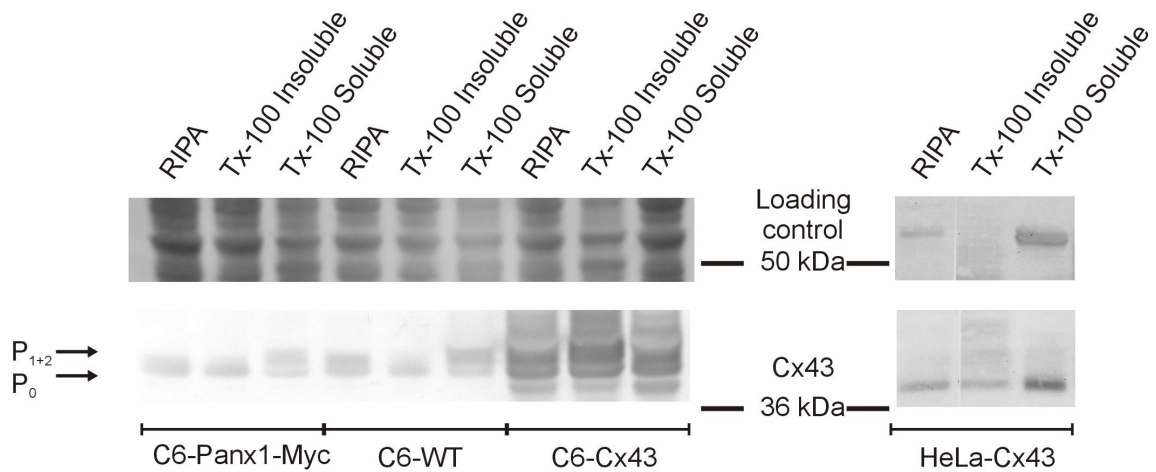


**Figure 41: Expression of Cx43 in the cell lines used in this study**

Cx43 expression was investigated in the different cell lines used: C6-Panx1-Myc, C6-WT, C6-Cx43, and HeLa-Cx43. Control of sample loading in the various lanes was performed by either a total protein stain with Sypro staining or with  $\beta$ -tubulin detection

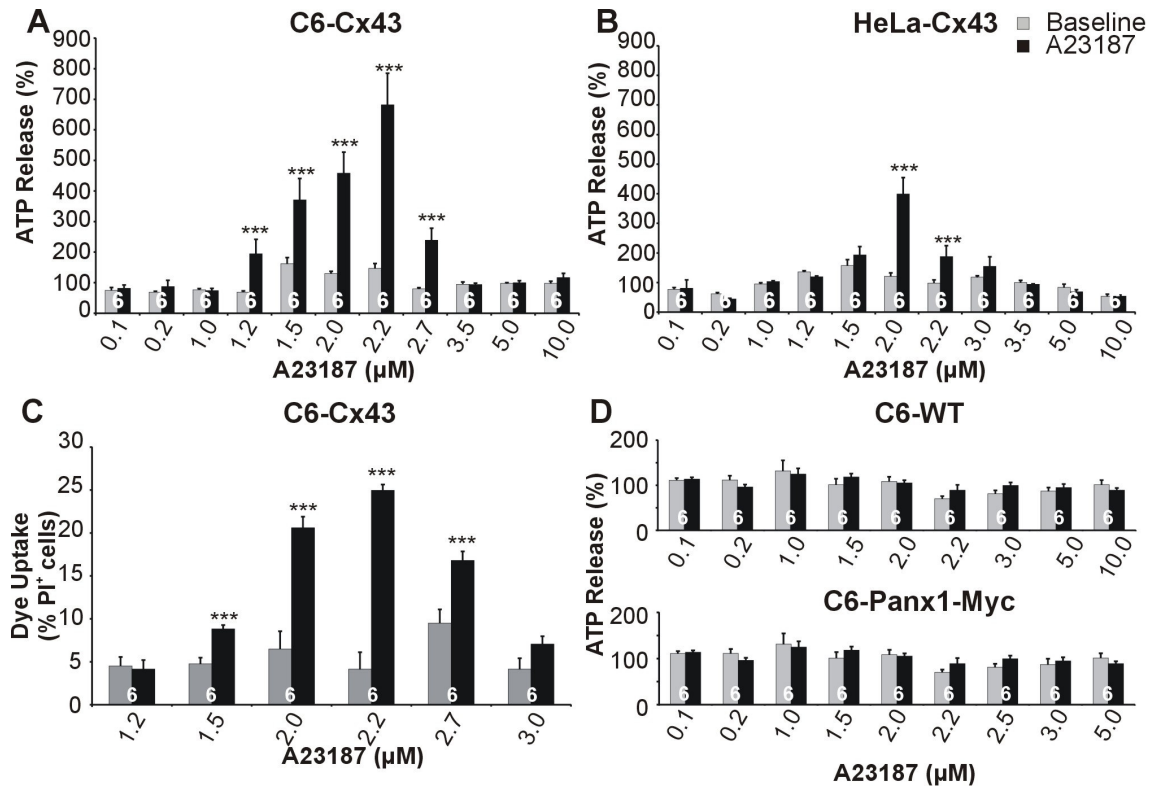


**Figure 42: Dose-response curve for A23187-triggered ATP release.**

(A) A23187 triggered significant ATP responses in C6-Cx43 cells at 1.2 μM, 1.5 μM, 2.0 μM, 2.2 μM, and 2.7 μM, with maximal response at 2.2 μM A23187. (B) In HeLa-Cx43 cells, A23187 triggered significant ATP release at 2.0 μM and 2.2 μM, while responses were absent at lower and higher concentrations. (C) A23187 triggered significant PI dye uptake in C6-Cx43 cells at 1.5 μM, 2.0 μM, 2.2 μM, and 2.7 μM with maximum response at 2.2 μM A23187. (D) A23187 triggered no significant ATP release in C6-WT cells (upper panel) or in C6-Panx1-Myc cells (lower panel). Star signs indicate significance compared to the corresponding baseline.

We recorded the changes of  $[Ca^{2+}]_i$  in response to various A23187 concentrations in both C6-Cx43 and HeLa-Cx43 cells. C6-Cx43 cells responded to ionophore application with a peak  $[Ca^{2+}]_i$  increase followed by a fast recovery to normal baseline levels (Figure 43A); in HeLa-Cx43, the recovery was somewhat slower (Figure 43B). Figure 43C illustrates the relation between the applied A23187 concentration and the peak  $[Ca^{2+}]_i$  value obtained in C6-Cx43 (grey) and HeLa-Cx43 (black). These data were used to construct a graph of ATP release as a function of the peak  $[Ca^{2+}]_i$  during ionophore stimulation (Figure 43D). These results indicate that the maximal ATP response occurred around 500 nM  $[Ca^{2+}]_i$  for C6-Cx43 and HeLa-Cx43 (Figure 43D), comparable to our previous findings in Cx32 expressing cells (De Vuyst et al. (2006) - see section 4.3.7).

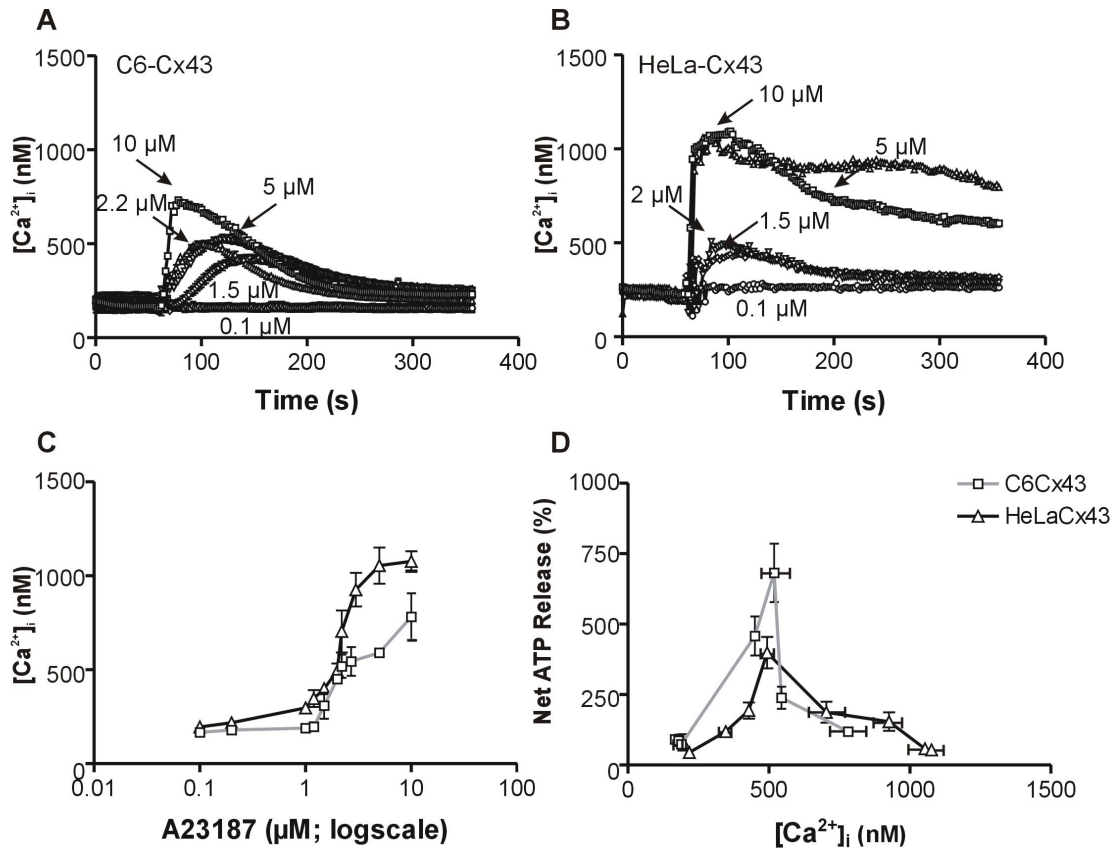


**Figure 43: ATP release as a function of  $[Ca^{2+}]_i$  in C6-Cx43 and HeLa-Cx43 cells.**

(A-B) Time course of  $[Ca^{2+}]_i$  changes after application of different ionophore concentrations in C6-Cx43 cells (A) and HeLa-Cx43 cells (B). (C)  $[Ca^{2+}]_i$  expressed as a function of A23187 concentrations in C6-Cx43 cells (grey) and HeLa-Cx43 cells (black). (D) ATP release expressed as a function of  $[Ca^{2+}]_i$  in C6-Cx43 cells (grey) and HeLa-Cx43 cells (black). These results are the averages of three independent experiments.

### 5.3.2 $Ca^{2+}$ -triggered ATP release is inhibited by siRNA treatment, blocked by $^{43}Gap$ 26 and 27 peptides and does not involve major contributions of vesicular release, Panx1 hemichannels or $P_2X_7$ pores

The involvement of Cx43 hemichannels was investigated by transfecting C6-Cx43 cells with siRNA directed against the *gal* gene (Cx43). Downregulation of Cx43 by the active siRNA mixture for Cx43 resulted in a strong inhibition of A23187-triggered ATP release, with the triggered responses being reduced to baseline level (Figure 44A). MOCK treated cells showed normal ATP responses and treatment with the negative control siRNA resulted in a modest (nonsignificant) potentiation of the ATP responses. Gap junctional coupling (SLDT) was also inhibited after siRNA transfection to a level comparable with C6-WT (~ 30  $\mu$ m) cells (compare Figure 44B to Figure 81C), indicating a strong downregulation of functional Cx43 channels. Western blot analysis showed that the expression of Cx43 was decreased by

approximately 40 % after siRNA transfection when compared to MOCK treated (transfection reagent only) or control cells (Figure 44C). Transfection of the negative control siRNA decreased the Cx43 expression by approximately 20 % (Figure 44C).

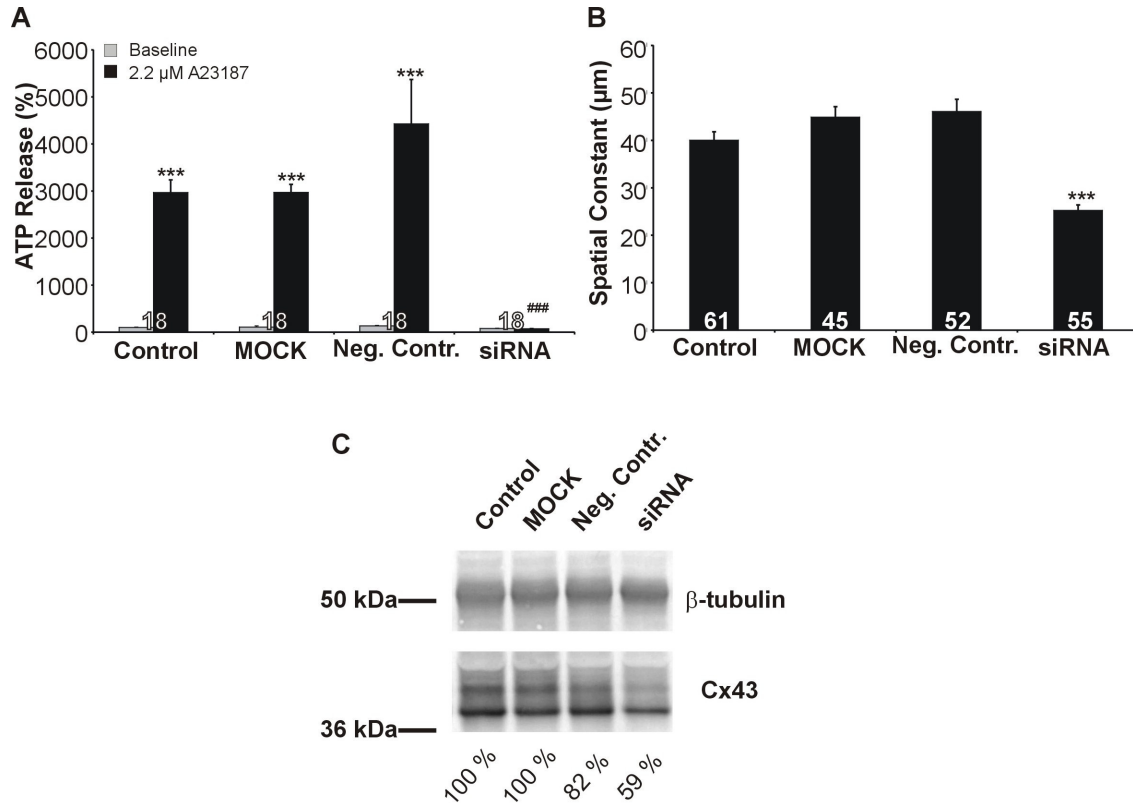


**Figure 44: Effect of siRNA transfection on C6-Cx43 cells**

(A) Transfection with the active siRNA mixture against the Cx43 gene *gjal* (marked siRNA on the graph) reduced A23187-triggered ATP release to baseline level. MOCK treatment (transfection reagent only) had no effect and transfection with the negative control siRNA gave a slight but nonsignificant stimulation. (B) Gap junctional coupling (SLDT) was also strongly reduced after siRNA transfection. (C) Cx43 expression in C6-Cx43 cells was suppressed after transfection with the active mixture of duplex siRNAs against *gjal* (siRNA). The scrambled siRNA duplex (Neg. Contr.) reduced Cx43 expression to a smaller extent; transfection reagent alone (MOCK) had no effect on Cx43 expression.  $\beta$ -tubulin detection was used to quantify Cx43 expression. Star signs indicate signficancy compared to the corresponding baseline in (A) and compared to control in (B). Number signs indicate signficancy compared to the trigger value in control conditions.

<sup>43</sup>Gap 26 and 27 are two peptides that are identical to a short sequence on the first and second extracellular loop of the connexin subunit respectively (Evans et al., 2006). <sup>43</sup>Gap 26 has been reported to inhibit ATP release and dye uptake triggered by low divalent cation solutions (Braet et al., 2003a), mechanical stimulation (Gomes et al., 2005) or metabolic inhibition with DTT (Retamal et al., 2006; Retamal et al., 2007a). Furthermore, <sup>43</sup>Gap 26 interacts with the extracellular loops of Cx43 (Liu et al., 2006) and inhibits hemichannel currents in Cx43 expressing taste cells (Romanov et al., 2007). A23187-triggered ATP release was completely blocked by pre-incubating the cells for 30 min with 0.25 mg/ml <sup>43</sup>Gap 26 (161  $\mu$ M) or <sup>43</sup>Gap

27 (191  $\mu\text{M}$ ) in C6-Cx43 (Figure 45) and HeLa-Cx43 (Figure 46). These results are in line with previous observations of potent block of ATP release triggered by  $[\text{Ca}^{2+}]_i$  changes (Braet et al., 2003a; Braet et al., 2003b; De Vuyst et al., 2006). The action of the Cx43 Gap peptides was concentration-dependent and characterized by half-maximal inhibition at 54  $\mu\text{M}$  for  $^{43}\text{Gap}$  26 and 95  $\mu\text{M}$  for  $^{43}\text{Gap}$  27 in C6-Cx43, and a large Hill coefficient (Figure 45C and D).

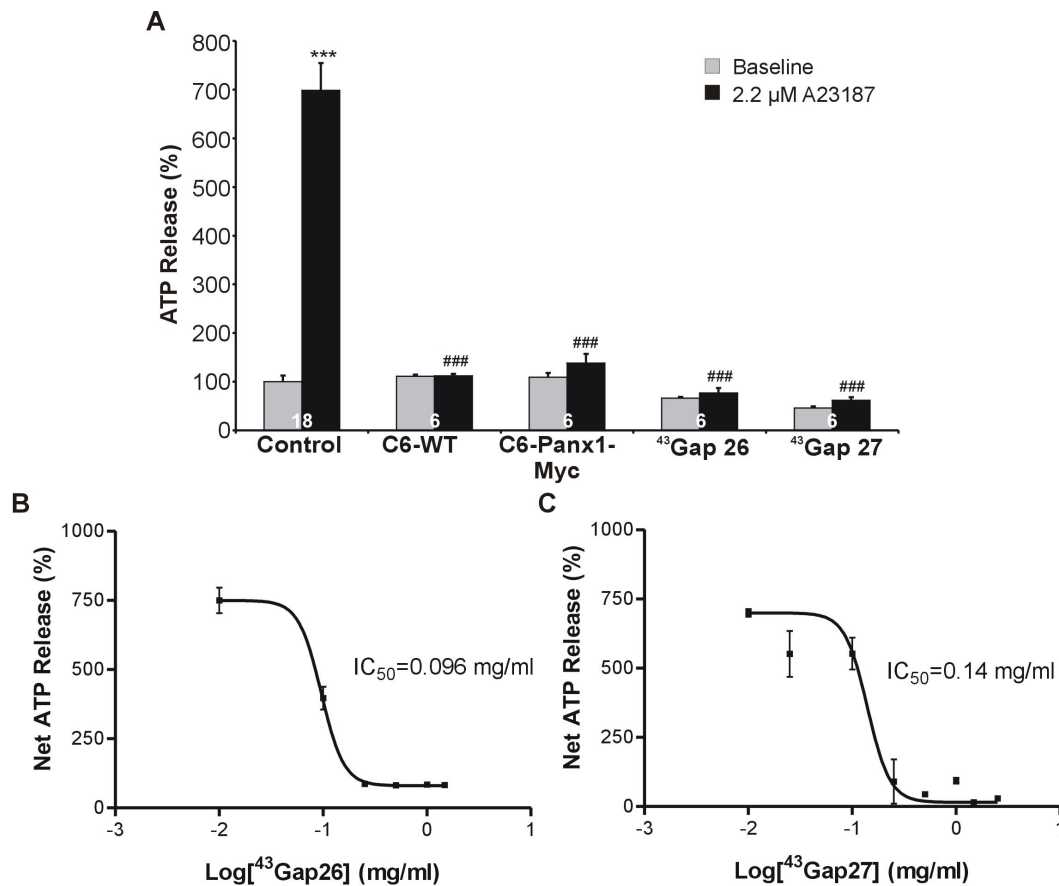


**Figure 45: A23187-triggered ATP release is blocked by  $^{43}\text{Gap}$  26 and  $^{43}\text{Gap}$  27 in C6-Cx43 cells**

(A) A23187-triggered ATP release was absent in C6-WT and C6-Panx1-Myc cells, and was suppressed by the Gap peptides  $^{43}\text{Gap}$  26 and  $^{43}\text{Gap}$  27. (B-C)  $^{43}\text{Gap}$  26 and  $^{43}\text{Gap}$  27 inhibited ATP release in a concentration-dependent way, with an  $\text{IC}_{50}$  value of 54  $\mu\text{M}$  for  $^{43}\text{Gap}$  26 and 95  $\mu\text{M}$  for  $^{43}\text{Gap}$  27. Both sigmoidal curves had a large Hill coefficient of three ( $n = 3$ ). Star symbols indicate significance compared to baseline and number signs indicate significance compared to the corresponding control bar.

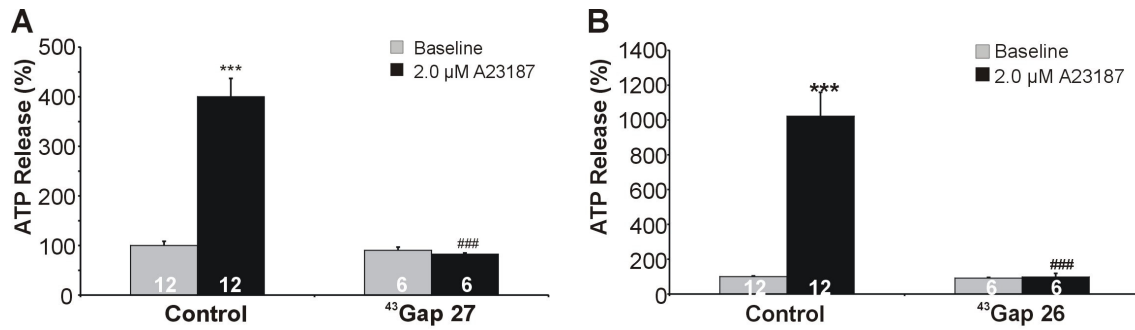


**Figure 46: Effect of Gap peptides on A23187-triggered ATP release in HeLa-Cx43 cells**

A23187-triggered ATP release was completely blocked by the Gap peptides <sup>43</sup>Gap 27 (A) and <sup>43</sup>Gap 26 (B) in HeLa-Cx43 cells. Star signs indicate significance compared to the corresponding baseline, while number signs represent significance compared to the control.

Involvement of Panx1 hemichannels and the P<sub>2</sub>X<sub>7</sub> receptor pore were also considered: the P<sub>2</sub>X<sub>7</sub> protein was absent in C6- and HeLa-Cx43 cells (Figure 47A), but prominent expression of the Panx1 protein was found in C6-cells, and to a lesser extent in HeLa-Cx43 cells (Figure 47B).

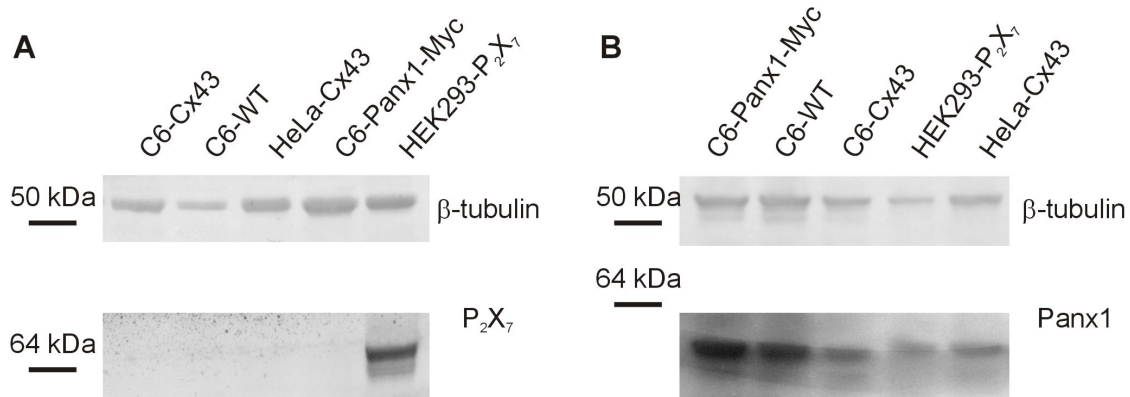


**Figure 47: Expression of P<sub>2</sub>X<sub>7</sub> and Panx1 in the used model system**

(A) Western blot analysis showed no expression of the P<sub>2</sub>X<sub>7</sub> receptor protein in different C6 cells or in HeLa-Cx43 cells, but a strong signal was present in HEK293-P<sub>2</sub>X<sub>7</sub>. (B) The Panx1 protein was present in C6-WT cells and HEK293-P<sub>2</sub>X<sub>7</sub>, and to a lesser extent in C6-Cx43 and HeLa-Cx43 cells. C6-Panx1-Myc cells were used as a positive control.

Botulinum toxin B (1.5 nM, 24 h) and tetanus toxin (100 nM, 24 h), two proteases that cleave the v-SNARE proteins synaptobrevin-2 and cellubrevin (Schiavo et al., 1992), did not affect A23187-triggered ATP release in C6-Cx43 and HeLa-Cx43 cells (Figure 48A-D). Bafilomycin A1 (100 μM, 1 h), an inhibitor of the v-ATPase that blocks ATP loading into vesicles (Coco et al., 2003), did neither inhibit A23187-triggered ATP release; in C6-Cx43 it unexpectedly potentiated the responses (Figure 48E). These results are in line with previous

results obtained with vesicular release blockers in C6-Cx43 and HeLa-Cx43 exposed to divalent free extracellular conditions (De Vuyst et al., 2007).

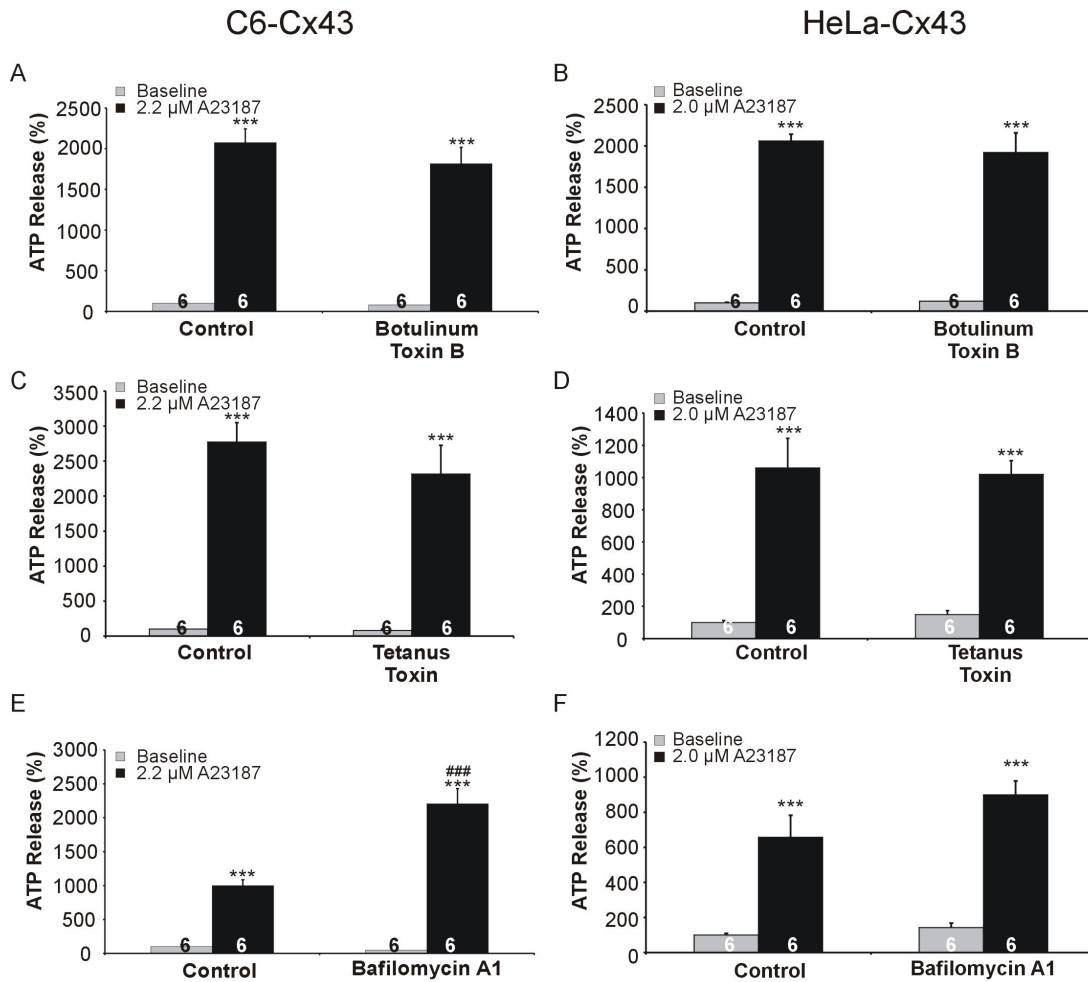


**Figure 48: Effect of vesicular release inhibitors on  $\text{Ca}^{2+}$ -triggered ATP responses**

(A-D) Botulinum toxin B and tetanus toxin did not inhibit A23187-triggered ATP release in C6-Cx43 or HeLa-Cx43 cells. (E-F) Bafilomycin A1 potentiated the response in C6-Cx43 but had no effect in HeLa-Cx43. Star signs indicate significance compared to the corresponding baseline, while number signs represent significance compared to the control.

All evidence taken together: (i) the inhibition of the responses by siRNA, (ii) the absence of responses in WT and Panx1 expressing cells, (iii) the inhibition of the responses by Gap peptides, (iv) the lack of significant inhibition by vesicular release blockers, and (v) the absence of  $\text{P}_2\text{X}_7$  expression, indicate that the  $\text{Ca}^{2+}$ -triggered ATP release in C6-/HeLa-Cx43 proceeds to a large extent via Cx43 hemichannels.

### 5.3.3 CaM and $\text{Ca}^{2+}$ /CaMK contribute to A23187-triggered ATP release

We further investigated the mechanisms of  $\text{Ca}^{2+}$ -triggered ATP release and first considered CaM. Cx43 is a CaM binding protein (Torok et al., 1997; Zhou et al., 2007) and incubating



the cells with W7 (20  $\mu$ M, 1 h), a CaM antagonist, completely abolished A23187-triggered ATP release in C6-Cx43 and HeLa-Cx43 cells (Figure 49), comparable with previous results obtained in C6-Cx32 cells (De Vuyst et al., 2006). CALP1 is a  $Ca^{2+}$ -like peptide that binds to the EF-hand  $Ca^{2+}$ -binding site of CaM and thereby acts as a CaM agonist (Villain et al., 2000). This peptide (100  $\mu$ M, 1 h) significantly potentiated A23187-triggered ATP release in C6-Cx43 and HeLa-Cx43 cells (Figure 49 - ATP responses above baseline were more than tripled in C6-Cx43). Activated CaM may activate  $Ca^{2+}$ /CaMK of which several subtypes exist (Soderling, 1999; Means, 2000). KN62 (1  $\mu$ M, 1 h) and AIP (1  $\mu$ M, 1 h - Ishida et al. (1995)), two CaMK-II inhibitors, significantly blocked A23187-triggered ATP release in C6-Cx43 and HeLa-Cx43 cells (Figure 49).

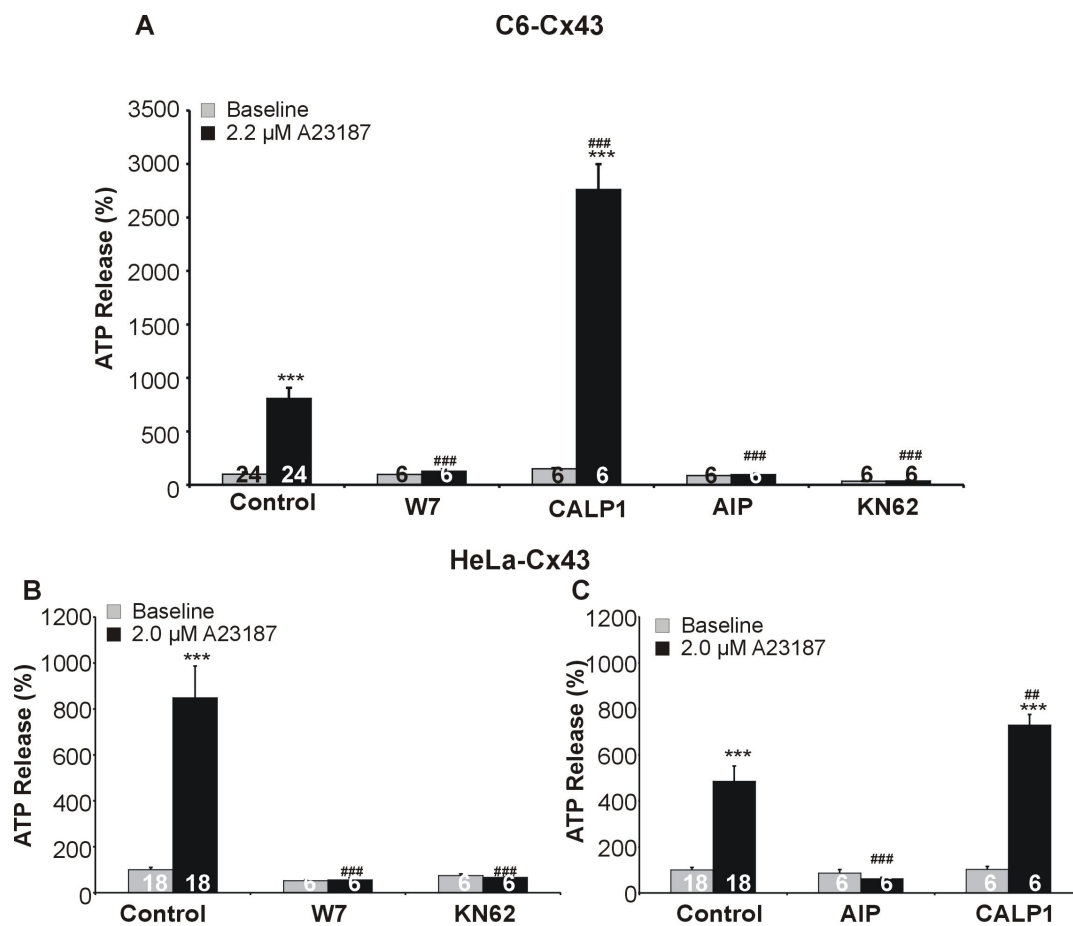


**Figure 49: A23187-triggered ATP release is mediated by activated CaM and CaMK-II in C6-Cx43 and HeLa-Cx43 cells**

The CaM inhibitor W7 completely inhibited A23187-triggered ATP release, while the CaM agonist CALP1 potentiated the A23187-triggered ATP release in C6-Cx43 cells (A) and HeLa-Cx43 cells (C). AIP and KN62 are two known CaMK-II antagonists and both inhibited A23187-triggered ATP release in C6-Cx43 cells (A) and HeLa-Cx43 cells (B and C). Star signs indicate significance compared to the corresponding baseline, while number signs represent significance compared to the control.

If CaM is involved in A23187-triggered ATP release, then CaM activation by CALP1 is expected to trigger ATP release without elevating  $[Ca^{2+}]_i$ . CALP1 (100  $\mu$ M, 5 min) indeed triggered significant ATP release in a concentration-dependent manner characterized by half-maximal stimulation at 87  $\mu$ M (Figure 50A). CALP1-triggered ATP release was completely inhibited after siRNA transfection (Figure 50B). The negative control siRNA duplex and the MOCK transfection slightly, but nonsignificantly, inhibited CALP1-triggered ATP release. Furthermore, CALP1-triggered ATP release was absent in C6-WT and C6-Panx1-Myc cells and completely suppressed by  $^{43}$ Gap 27 (Figure 50C).  $^{43}$ Gap 26 treatment did not completely inhibit CALP1-triggered ATP release, but the triggered component was completely abolished after co-incubating the cells with tetanus toxin ( $^{43}$ Gap 26 added during the last 30 min of the 24 h tetanus toxin incubation - Figure 50D), pointing to the contribution of a vesicular release component with the CALP1 stimulus. Botulinum toxin B, another inhibitor of vesicular mediated ATP release, had however no effect on CALP1-triggered ATP release.

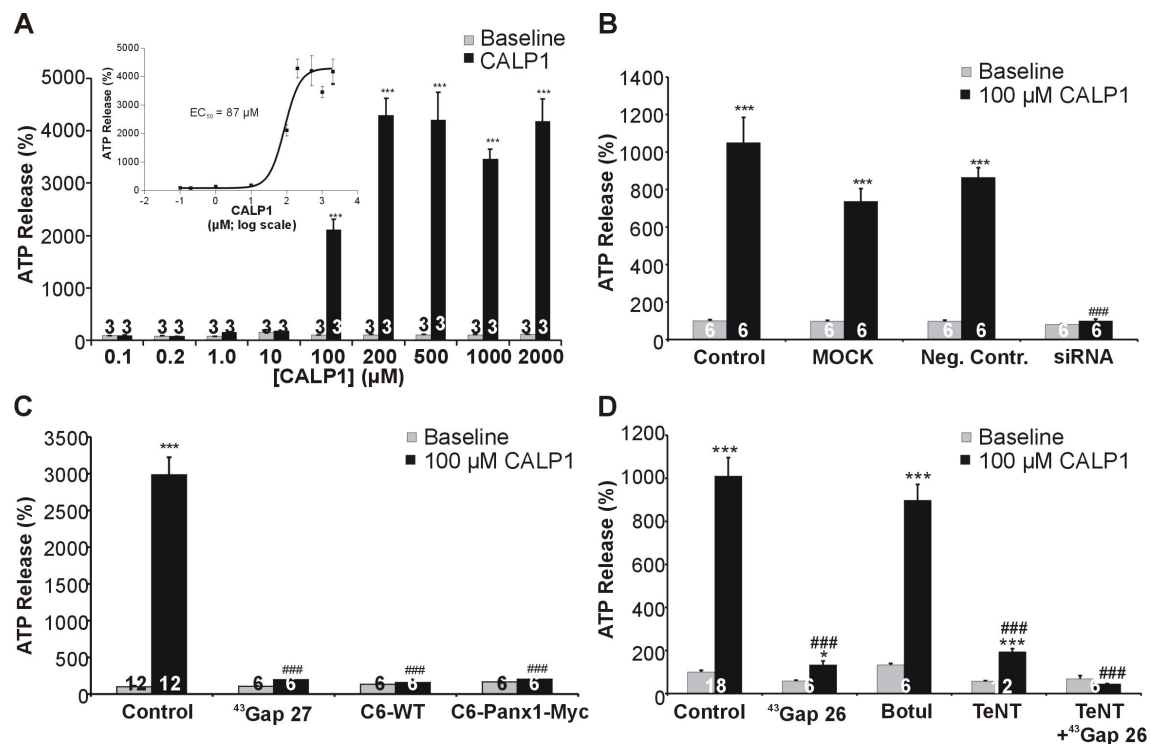


**Figure 50: CALP1 triggered significant ATP release in C6-Cx43 cells**

(A) CALP1 triggered ATP release in a dose-dependent way, with a half-maximal activation concentration of 87  $\mu$ M in C6-Cx43 cells. (B) CALP1-triggered ATP release was completely inhibited after downregulation of the *gjal* gene with siRNA, while the negative siRNA and the transfection reagent alone (MOCK) had only a slight, but nonsignificant effect when compared to control conditions. (C) CALP1-triggered ATP release was completely blocked by  $^{43}$ Gap 27 in C6-Cx43 cells and CALP1 did not trigger ATP release in C6-WT cells or C6-Panx1-Myc cells. (D)  $^{43}$ Gap 26 blocked CALP1-triggered ATP release to a large extent. The triggered component was completely blocked by co-incubating the cells with tetanus toxin. Tetanus toxin alone did also inhibit CALP1-triggered ATP release, while botulinum toxin B had no effect in C6-Cx43 cells. Star signs indicate significance compared to the corresponding baseline, while number signs represent significance compared to the control.

### 5.3.4 Ca<sup>2+</sup>/CALP1-triggered ATP release also involves AA signaling

Both elevated [Ca<sup>2+</sup>]<sub>i</sub> and CaMK-II may activate and translocate cPLA<sub>2</sub>, thereby activating the AA signaling cascade (Evans et al., 2001; Muthalif et al., 2001; Chakraborti, 2003). We investigated the involvement of the AA metabolic pathway with AACOCF<sub>3</sub>, an inhibitor of the Ca<sup>2+</sup>-dependent cPLA<sub>2</sub> and the Ca<sup>2+</sup>-independent iPLA<sub>2</sub> (5 μg/ml, 1 h - Riendeau et al., 1994), the lipoxygenase inhibitor baicalein (30 μM, 1 h - Vivancos and Moreno (2002)) and the cyclooxygenases inhibitor indomethacin (50 μM, 1 h - Fujiwara et al. (2006)). All three substances significantly reduced A23187-triggered ATP release in C6-Cx43 and HeLa-Cx43 cells (Figure 51A and B) and CALP1-triggered ATP release in C6-Cx43 cells (Figure 51C).

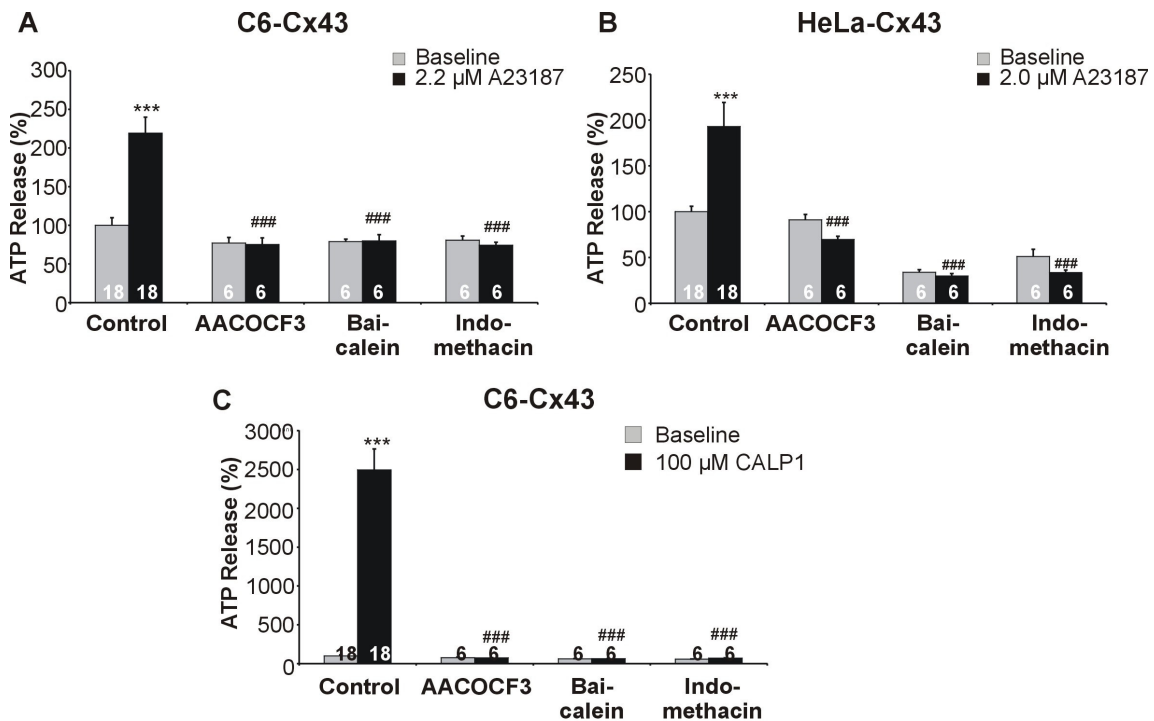


**Figure 51: Involvement of the AA metabolic pathway in A23187-triggered ATP release**

Inhibition of PLA<sub>2</sub> activation with AACOCF<sub>3</sub>, of lipoxygenase activation with baicalein or cyclooxygenase activation with indomethacin all drastically suppressed A23187-triggered ATP release in C6-Cx43 cells (A) and HeLa-Cx43 cells (B). (C) CALP1-triggered ATP release was also inhibited by inhibitors of the AA metabolic pathway. Star signs indicate significance compared to the corresponding baseline, while number signs represent significance compared to the control.

In addition, exogenously applied AA (5 - 10 μM, 2 h) significantly enhanced A23187-triggered ATP release, with the above baseline ATP release component being increased up to 5-fold for C6-Cx43 and about 8-fold for HeLa-Cx43 (Figure 52).

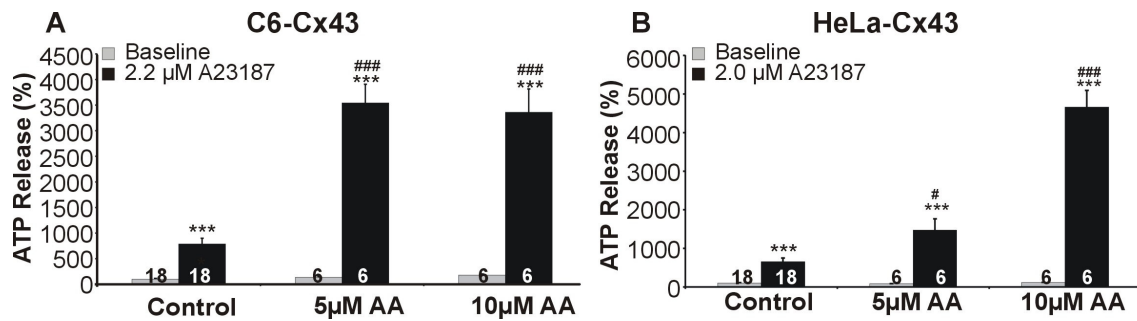


**Figure 52: AA potentiates A23187-triggered ATP release**

Exogenously applied AA enhanced A23187-triggered ATP release in C6-Cx43 cells (A) and HeLa-Cx43 cells (B). Star signs indicate significance compared to the corresponding baseline, while number signs represent significance compared to the control.

Incubating the cells with 50  $\mu$ M AA (5 min) triggered ATP release that was significantly above baseline in C6-Cx43 cells. AA-triggered ATP release was absent in C6-WT and C6-Panx1-Myc cells (Figure 53A). Furthermore AA-triggered ATP release was completely blocked after siRNA transfection (Figure 53B) and by  $^{43}$ Gap 26 and 27 (Figure 53C and D).

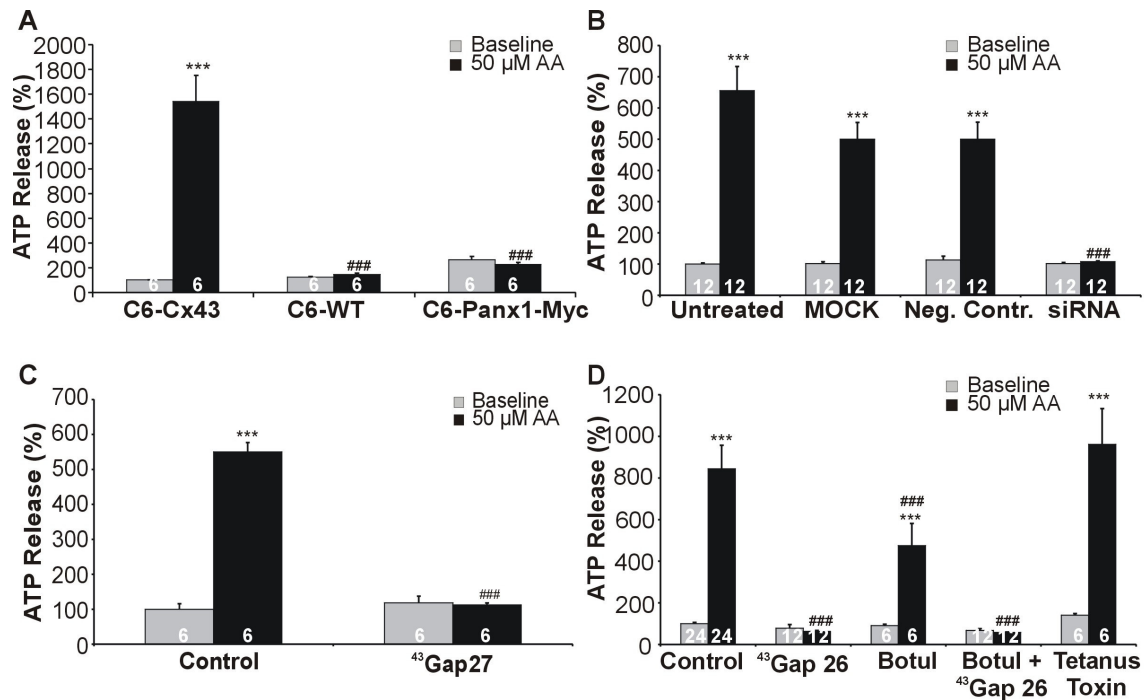


**Figure 53: AA triggered ATP release in C6-Cx43 cells**

(A) Exposing the cells to 50  $\mu$ M AA for 5 min triggered ATP release that was significantly above baseline in C6-Cx43 cells. AA-triggered ATP release was absent in C6-WT cells and C6-Panx1-Myc cells. (B) AA-triggered ATP release was completely suppressed after siRNA transfection that downregulates the *gjal* gene. (C)  $^{43}$ Gap 27 completely abolished AA-triggered ATP release in C6-Cx43 cells. (D) AA-triggered ATP release was suppressed below baseline by  $^{43}$ Gap26. Botulinum toxin B (botul) significantly inhibited the responses (triggered ATP release was however not significantly above baseline when compared with ANOVA, but was significantly higher with a t-test -  $p = 0.0008$ ) and the responses disappeared when combining toxin treatment with  $^{43}$ Gap 26. Tetanus toxin (TeNT) was without effect on AA-triggered ATP release. Star signs indicate significance compared to the corresponding baseline, while number signs represent significance compared to the control.

Botulinum toxin B significantly inhibited AA-triggered ATP release and co-incubating the cells with  $^{43}\text{Gap}$  26 together with this toxin depressed ATP response to baseline levels, indicating some contribution of vesicular ATP release (Figure 53D). Tetanus toxin was without effect on AA-triggered ATP release.

AA is a known trigger of  $[\text{Ca}^{2+}]_i$  changes (Damron and Bond, 1993; Mochizuki-Oda et al., 1993; Barrett et al., 2001; Erriquez et al., 2005) and we therefore tested whether  $[\text{Ca}^{2+}]_i$  buffering with BAPTA could influence the triggered ATP response. Ester-loading of the cells with BAPTA-AM (5  $\mu\text{M}$ , 1 h) strongly reduced AA-triggered ATP release to baseline levels in C6-Cx43 and HeLa-Cx43 (Figure 54).

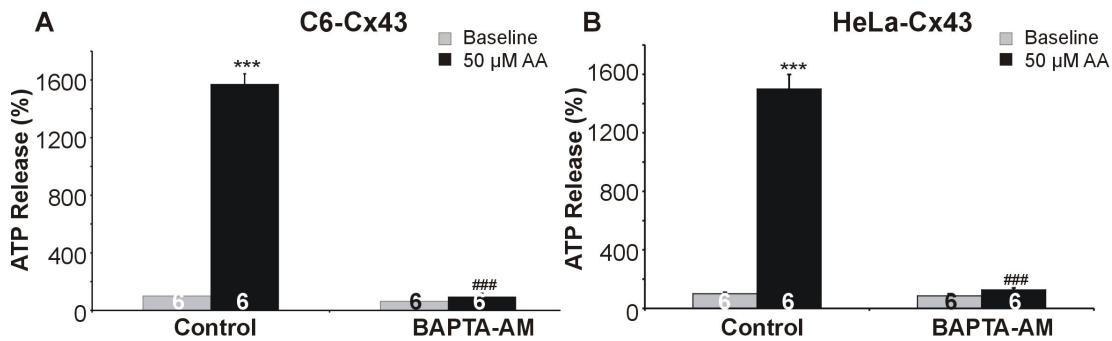


**Figure 54: AA-triggered ATP release: effect of intracellular  $\text{Ca}^{2+}$ -buffering**

Buffering  $[\text{Ca}^{2+}]_i$  with BAPTA-AM reduced the AA-induced ATP response to baseline level in C6-Cx43 and HeLa-Cx43. Star signs indicate significance compared to the corresponding baseline, while number signs represent significance compared to the control.

### 5.3.5 ROS and NO also contribute to the downstream signaling cascade

The metabolism of AA by cyclo- and lipoxygenases is associated with the production of ROS, such as  $\text{H}_2\text{O}_2$  and  $\text{O}_2^-$  (Katsuki and Okuda, 1995). Moreover, ROS can stimulate the synthesis of NO via NO synthase, by a yet unknown mechanism (Shimizu et al., 1997). To test the involvement of ROS and NO, we incubated the cells with the anti-oxidant and free radical scavenger N-acetyl-L-cysteine (1 mM, 1 h), the free radical scavenger  $\alpha$ -tocopherol succinate (150  $\mu\text{g}/\text{ml}$ , 1 h), superoxide dismutase (SOD; 200  $\mu\text{g}/\text{ml}$ , 1 h) that converts  $\text{O}_2^-$  to  $\text{H}_2\text{O}_2$  and N $\omega$ -nitro-L-arginine (100  $\mu\text{M}$ , 1 h), an inhibitor of NO synthesis. All these substances significantly inhibited ATP release triggered by A23187, CALP1 and AA (Figure 55).

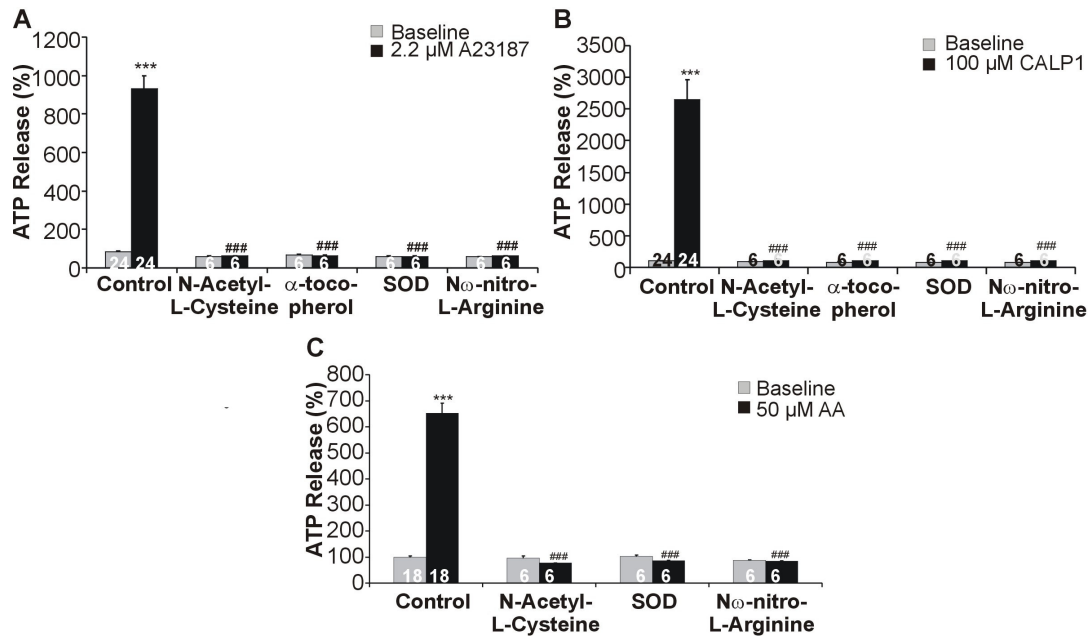


**Figure 55:** ROS and NO are involved in A23187-, CALP1-, and AA-triggered ATP release

Inhibiting the formation of ROS with N-acetyl-L-cysteine,  $\alpha$ -tocopherol succinate ( $\alpha$ -tocopherol), or superoxide dismutase (SOD) abolished A23187- (A), CALP1- (B) and AA-triggered ATP release (C). Inhibiting the formation of NO by N $\omega$ -nitro-L-Arginine also completely blocked triggered ATP release in C6-Cx43. Star signs indicate significance compared to the corresponding baseline, while number signs represent significance compared to the control.

## 5.4 Discussion

The aim of this work was to investigate the signaling cascade involved in hemichannel responses triggered by an increase in  $[Ca^{2+}]_i$ . Cell lines stably transfected with Cx43 demonstrated a bell-shaped ATP release and dye uptake with optimal response situated in the the 500 nM  $[Ca^{2+}]_i$  range. Further investigation of the mechanisms underlying  $Ca^{2+}$ -triggered ATP release with antagonists pointed to the involvement of CaM, CaMK-II, AA, ROS and NO. The ATP release triggered in response to the CaM agonist CALP1 and the exogenous application of AA further confirmed the basic steps of this cascade. Work with the various inhibitor substances on A23187-, CALP1-, and AA-triggered ATP release suggested a sequence order starting with CaM activation and ending with ROS/NO production. In addition, ATP release triggered by CALP1 and AA were inhibited by siRNA treatment and Gap peptides to the same extent as the A23187-triggered responses. There was however some evidence for the contribution of vesicular release with the CALP1 and AA stimuli. Finally, the signaling cascade also involved feed-back actions mediated by secondary  $[Ca^{2+}]_i$  changes. We will elaborate on each of these topics in more detail.

The contribution of hemichannels to the responses recorded in this study is based on the following elements: (i) the strong inhibitory effect of siRNA, considered as strong evidence

for hemichannel involvement (Spray et al., 2006), (ii) the absence of ATP release in WT and Panx1 expressing cells, (iii) lack of P<sub>2</sub>X<sub>7</sub> receptor expression, (iv) activation of a bidirectional pathway (uptake of reporter dyes and release of ATP), and (v) inhibition of the responses by <sup>43</sup>Gap 26 and <sup>43</sup>Gap 27. The former peptide interacts with the extracellular loops of Cx43 (Liu et al., 2006), strongly inhibits Cx43 hemichannel currents (Romanov et al., 2007), blocks hemichannel related responses in various model systems (Braet et al., 2003a; Gomes et al., 2005; Pearson et al., 2005; Retamal et al., 2007b) and does not work in a scrambled version (Pearson et al., 2005). A recent study from Wang et al. (2007) has suggested that <sup>43</sup>Gap 26 has little acute effects on Cx43 hemichannel currents in *Xenopus laevis* oocytes, and that the folding of the peptide is an important determinant for hemichannel inhibition due to a steric block of the pore (Wang et al., 2007). This study is difficult to reconcile with the available evidence quoted above, with differences possibly residing in the oocyte expression system used, the use of chimeric connexin constructs rather than native Cx43 and the argument for steric block being based on millimolar polyethylene glycol concentrations. Our work shows that inhibition of ATP release by <sup>43</sup>Gap 26 (and <sup>43</sup>Gap 27) is concentration-dependent with half-maximal inhibition at ~ 54 μM (~ 95 μM for <sup>43</sup>Gap 27) and a large Hill coefficient of 3, indicating cooperative interactions with a receptor site rather than steric block.

It is since long known that the effect of [Ca<sup>2+</sup>]<sub>i</sub> on gap junctions may involve CaM interactions with the connexin protein (Peracchia et al., 1983) and we therefore pursued our investigations in this direction. The evidence for CaM involvement in the present work is based on the inhibition of Ca<sup>2+</sup>-triggered ATP release by W7, the potentiation of the A23187-triggered ATP responses by the CaM activating peptide CALP1 and the triggering of ATP release by applying CALP1. Furthermore, the [Ca<sup>2+</sup>]<sub>i</sub> activating ATP release (500 nM) was in the K<sub>d</sub>-range reported for Ca<sup>2+</sup>/CaM interactions (0.5 - 5 μM - Chin and Means (2000)). CaMK-II is an important downstream target of CaM and experiments with the CaMK-II antagonists AIP and KN62 further support involvement of CaM signaling. An interesting observation was that ATP release increased with the concentration of the CALP1 agonist and there was no inhibition of the response at high concentrations like observed for Ca<sup>2+</sup> (compare Figure 42A and Figure 50A). This indicates that the bell-shaped dose-response curve of Ca<sup>2+</sup>-triggered ATP release can be functionally separated in an activation and an inactivation half, comparable with the pH<sub>i</sub> sensitivity of gap junctional communication (Swietach et al., 2007a). Elevation of [Ca<sup>2+</sup>]<sub>i</sub> and activated CaMK-II may work synergistically to induce a translocation of cPLA<sub>2</sub> from the cytosol to the membranes (Channon and Leslie, 1990; Qiu et al., 1998; Evans et al., 2001). Two Ca<sup>2+</sup>-ions bind to the aminoterminal CBL (Ca<sup>2+</sup>-binding ligand) domain of cPLA<sub>2</sub>, promoting the insertion of hydrophobic residues into the lipid bilayer (Perisic et al., 1998; Rizo and Sudhof, 1998) and CaMK-II phosphorylates cPLA<sub>2</sub> on S515, increasing its intrinsic activity by 2 - 3-fold (Muthalif et al., 2001), finally resulting in the

release of AA from the membranes. Released AA is further metabolized by cyclooxygenases, lipoxygenases, and cytochrome P450 (CYP) epoxygenases (Muralikrishna Adibhatla and Hatcher, 2006; Fleming, 2007). Cyclooxygenases and lipoxygenases result in the production of bioactive eicosanoids such as prostaglandins, thromboxanes and leukotrienes (Muralikrishna Adibhatla and Hatcher, 2006), CYP epoxygenases result in the formation of epoxyeicosatrienoic acids. Previous work has shown that AA signaling (especially cyclooxygenases and lipoxygenases) may modulate hemichannel related responses (Contreras et al., 2002; De Vuyst et al., 2007). Involvement of cyclooxygenases and lipoxygenases in the present work is based on inhibition of both  $\text{Ca}^{2+}$ - and CALP1-triggered ATP release by AACOCF3, baicalein and indomethacin, on the potentiation of ATP release triggered by both  $\text{Ca}^{2+}$  and CALP1 with AA, and on the fact that AA was able to trigger ATP release by itself. Activation of the AA signaling cascade also involves the formation of ROS (Katsuki and Okuda, 1995) that have recently been reported to result in hemichannel opening by depolarizing the cell (Ramachandran et al., 2007). In addition, ROS may activate NO synthase resulting in NO production (Shimizu et al., 1997) that may activate hemichannels by S-nitrosylation of Cx43 proteins (Retamal et al., 2006). The involvement of ROS and NO signaling was investigated here by applying various free radical scavengers and by inhibition of NO production with N $\omega$ -nitro-L-arginine. All these antagonists inhibited the ATP responses triggered by intracellular  $\text{Ca}^{2+}$ , CALP1 and AA, pointing to the involvement of ROS/NO in a common final part of the signaling sequence.

The experimental manipulations used in this study aiming at investigating the involvement of connexin hemichannels (siRNA, Gap peptides and others) and the various signaling steps (CaM, AA and ROS/NO) demonstrated a clear and strong inhibition of ATP release, often with the responses being reduced to baseline level. By contrast, the experiments with blockers of vesicular release were more variable. Tetanus toxin and botulinum toxin did not inhibit  $\text{Ca}^{2+}$ -triggered ATP release, but tetanus toxin significantly reduced ATP release triggered by CALP1 (Figure 50D) and botulinum toxin significantly inhibited AA-triggered ATP release (Figure 53D). In addition, bafilomycin A1 potentiated  $\text{Ca}^{2+}$ -triggered ATP release (Figure 48E). It is not clear why the responses to these agents differ so much between different triggers of ATP release - in earlier work we observed that botulinum toxin potentiated ATP release triggered by low extracellular  $\text{Ca}^{2+}$ -conditions (De Vuyst et al., 2007). Nevertheless, the inhibition of CALP1- and AA-triggered responses by tetanus and botulinum toxin respectively, suggests the involvement of a vesicular release component. This is not unexpected as work on  $\text{Ca}^{2+}$ -triggered ATP release in Cx32 expressing cells led us to a similar conclusion (De Vuyst et al., 2006). The vesicular release inhibitors however never blocked the responses to the degree observed with *gjal* gene silencing or the  $^{43}\text{Gap}$  26/27 peptides, suggesting that hemichannels give the spark for ATP release and the vesicular component is



activated further downstream, probably as a consequence of ATP-triggered ATP release (Anderson et al., 2004) mediated by  $[Ca^{2+}]_i$  or other signals. This brings us to another important point, which is the contribution of feed-back loops in the sequence leading to ATP release. Buffering  $[Ca^{2+}]_i$  changes by incubating the cells with BAPTA-AM strongly inhibited ATP release triggered by AA (Figure 54). The ability of AA to modulate voltage-dependent calcium currents has previously been described in detail (Mochizuki-Oda et al., 1993; Barrett et al., 2001; Erriquez et al., 2005). Furthermore, AA induces  $Ca^{2+}$ -entry from the intracellular stores (Damron and Bond, 1993). The inhibition of AA-triggered ATP release after buffering  $[Ca^{2+}]_i$  with BAPTA indicates a positive feed-back loop from AA to  $[Ca^{2+}]_i$  that is situated at the beginning of the sequence illustrated in Figure 56. A second positive feed-back loop may consist of  $Ca^{2+}$ -entry via open hemichannels leading to a further  $[Ca^{2+}]_i$  increase. Third, ATP released by other mechanisms may join the picture, as already suggested. The strong depression of ATP release, for example by each of the AA antagonists (Figure 51) or ROS/NO inhibition (Figure 55), and by Cx43 gene silencing (only partially reducing Cx43 protein expression) is probably related to the fact that if one of the intermediate signaling steps of the cascade becomes too small, amplification in the positive feed-back loop is lost and the response disappears.

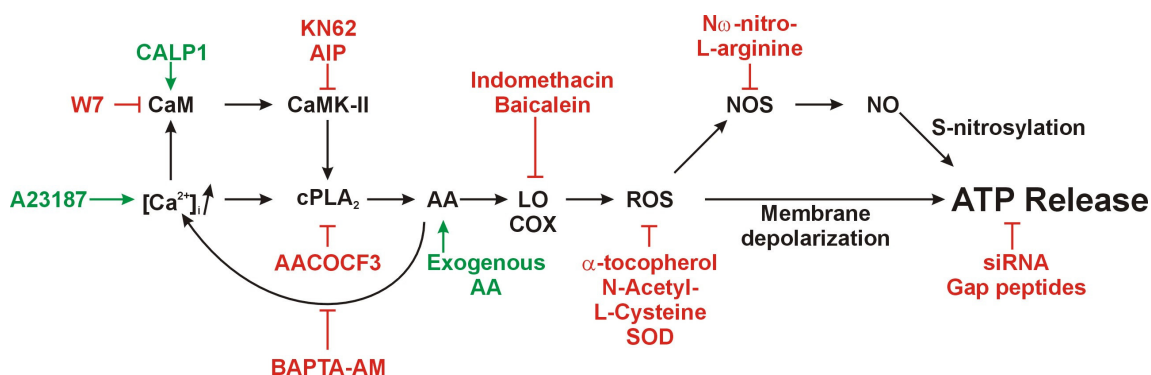


**Figure 56: Scheme summarizing the major findings of this study**

The applied inhibitors are indicated in red, while the agonists are marked green. An elevation of  $[Ca^{2+}]_i$  activates CaM, resulting in the activation of CaMK-II. These two stimuli lead to the activation of cPLA<sub>2</sub>, releasing AA from the membrane. AA is further metabolized by lipo- (LO) and cyclooxygenases (COX), resulting in the production of ROS. These free radicals can activate NO synthase (NOS), inducing the production of NO (Shimizu et al., 1997). The produced NO can S-nitrosylate Cx43 (Retamal et al., 2006), together with changes of the membrane potential by liberated ROS (Ramachandran et al., 2007), this may lead to the opening of connexin hemichannels (Contreras et al., 2003a). Several feed-back loops complicate the picture: AA triggers  $[Ca^{2+}]_i$ ; changes that feed-back to restart the sequence. Opening of hemichannels may feed-back by allowing  $Ca^{2+}$ -entry into the cells and released ATP may (auto)stimulate purinergic receptors again triggering  $[Ca^{2+}]_i$  changes and re-initiating the signaling cascade.

A modulating effect of AA products and ROS on hemichannel opening has previously been suggested, based on work with lipoxygenase inhibitors and free radical scavengers in an *in vitro* model of chemical ischemia (Contreras et al., 2002). Subsequent work has further substantiated the evidence for the redox status and ROS/NO controlling hemichannel

responses (Retamal et al., 2006; Ramachandran et al., 2007; Retamal et al., 2007b). Our work incorporates these signaling elements in a larger picture of  $\text{Ca}^{2+}$ -triggered hemichannel responses and further adds Cx43 to the list of hemichannels that respond to  $[\text{Ca}^{2+}]_i$  changes with a bell-shaped response curve as previously described for Cx32 (De Vuyst et al., 2006). Moreover, different mechanisms appear to be involved in activation of hemichannels with  $[\text{Ca}^{2+}]_i$  transients up to 500 nM and inactivation at higher  $[\text{Ca}^{2+}]_i$  values where  $\text{Ca}^{2+}/\text{CaM}$  is not involved. Apparently, this is different from the inhibition of gap junctions by elevated  $[\text{Ca}^{2+}]_i$  that is mediated by  $\text{Ca}^{2+}/\text{CaM}$  interactions (Peracchia, 2004). Cx43 is an ubiquitous protein expressed in a large array of cells (Laird, 2006), and the present work shows that the signaling steps involved in pathology (AA in inflammation, ROS in cell injury) and pathologic opening of hemichannels, are also involved in hemichannel control by  $[\text{Ca}^{2+}]_i$  changes in the physiological range.

The most remarkable observation of this work was the differential effect of intracellular  $\text{Ca}^{2+}$  and AA on hemichannel functioning and gap junctional communication, i.e. activation of Cx43 hemichannels and inhibition of gap junctional communication (as reported previously by Peracchia (2004) for intracellular  $\text{Ca}^{2+}$  and Giaume et al. (1989) for AA). The effect of AA on hemichannel opening is probably a consequence of membrane depolarisation (Contreras et al., 2003a) and synthesis of ROS (Ramachandran et al., 2007), while the effect on gap junctional coupling might be the consequence of alterations of the acyl chain of the lipids that surround gap junction channels (Burt et al., 1991).

## Chapter

### 6

***Connexin hemichannels and gap junction channels are differentially influenced by lipopolysaccharide and basic fibroblast growth factor***

Elke De Vuyst<sup>1</sup>, Elke Decrock<sup>1</sup>, Marijke De Bock<sup>1</sup>, Hiroshi Yamasaki<sup>2</sup>, Christian C. Naus<sup>3</sup>, W. Howard Evans<sup>4</sup>, and Luc Leybaert<sup>1</sup>

<sup>1</sup> Department of Physiology and Pathophysiology, Faculty of Medicine and Health Sciences, Ghent University, Ghent, Belgium

<sup>2</sup> Department of Bioscience, School of Science and Technology, Kwansai Gakuin University, Gakuin, Sanda 669-13, Japan

<sup>3</sup> Department of Cellular and Physiological Sciences, Faculty of Medicine, University of British Columbia, Vancouver, BC, Canada

<sup>4</sup> Department of Medical Biochemistry and Immunology, Cardiff University School of Medicine, Cardiff, UK

Published in *Mol. Biol. Cell* **18**(1): 34–46 (2007)

Text and illustrations are modified from the published version

Descriptive anatomy is to physiology, what geography is to history  
-Louis Pasteur-

---

## Abstract

Gap junction channels are formed by two hemichannels, each contributed by the cells taking part in this direct cell-cell communication conduit. Hemichannels that do not interact with their counterparts on neighboring cells feature as a release pathway for small paracrine messengers such as nucleotides, glutamate, and prostaglandins. Connexins are phosphorylated by various kinases, and we compared the effect of various kinase activating stimuli on gap junction channels and hemichannels. Using peptides identical to a short connexin amino acid sequence to specifically block hemichannels, we found that protein kinase C (PKC), c-Src, and L- $\alpha$ -lysophosphatidic acid (LPA) inhibited gap junctions and hemichannel mediated ATP (adenosine triphosphate) release in Cx43 (connexin 43) expressing C6 glioma cells (C6-Cx43). Lipopolysaccharide (LPS) and basic fibroblast growth factor (bFGF) inhibited gap junctions, but they stimulated ATP release via hemichannels in C6-Cx43. LPS and bFGF inhibited hemichannel mediated ATP release in HeLa-Cx43 cells, but they stimulated it in HeLa-Cx43 with a truncated carboxyterminal domain (HeLa-Cx43 $\Delta$ C) or in HeLa-Cx26, which has a very short carboxyterminus. Hemichannel potentiation by LPS was inhibited by blockers of the arachidonic acid (AA) metabolism, and AA had a potentiating effect like LPS and bFGF. We conclude that gap junction channels and hemichannels display similar or oppositely directed responses to modulatory influences, depending on the balance between kinase activity and the activity of the AA pathway. Distinctive hemichannel responses to pathological stimulation with LPS or bFGF may serve to optimize the cell response, directed at strictly controlling cellular ATP release, switching from direct gap junctional communication to indirect paracrine signaling.

## 6.1 Introduction

Gap junctions are specialized structures that directly connect adjacent cells to allow the passage of small molecules such as amino acids, ions, and second messengers. Vertebrate gap junction channels are composed of proteins encoded by the connexin gene family (Sohl and Willecke, 2004). Connexins span the membrane four times, are endowed with a single cytoplasmic loop and two extracellular loops, and have their amino- and carboxyterminal domains inside the cell. Most of the connexins are phosphorylated *in vivo*, primarily on serine residues and to a lesser extent on threonine and tyrosine residues located in the carboxyterminal domain. Cx43 is a ubiquitously expressed connexin that has been well characterized in terms of phosphorylation sites and effects. A basal degree of phosphorylation on five serine residues seems to be required for the assembly and functioning of gap junctions composed of Cx43 (Musil and Goodenough, 1991; Laird et al., 1995; Cooper et al., 2000). Numerous studies have demonstrated the influence of growth factors, oncogene protein kinases, hormones, and inflammatory mediators on gap junctional communication via phosphorylations on the carboxyterminal domain of the protein (amino acid 236 - 382; Maldonado et al. (1988); Crow et al. (1990); Filson et al. (1990); Swenson et al. (1990); Kurata and Lau (1994); Matesic et al. (1994)). Several serine kinases have been identified, including PKC (S368 and S372), mitogen-activated protein kinases (MAP kinases - S255, S279, and S282), p34<sup>cdc2</sup>/cyclin B (S255 and S262), and casein kinase 1 (S325, S328, and S330 - Lampe and Lau (2004)).

Gap junction channels are composed of two hemichannels, each contributed by the cells that share this junctional communication channel. Hemichannels are hexameric high-conductance plasma membrane channels that are normally closed and can act as a conduit to release paracrine signaling molecules such as ATP, NAD<sup>+</sup> (nicotinamide adenine dinucleotide), glutamate, glutathione, and prostaglandins when opened (Bruzzone et al., 2001b; Bennett et al., 2003; Ebihara, 2003; Goodenough and Paul, 2003; Ye et al., 2003; Cherian et al., 2005; Rana and Dringen, 2007). Hemichannels are closed at physiological millimolar extracellular [Ca<sup>2+</sup>], but they open in response to lowering extracellular [Ca<sup>2+</sup>] (alone or in combination with a lowering of other extracellular divalent cations - Li et al. (1996); Pfahnl and Dahl (1999); Quist et al. (2000); Kamermans et al. (2001); Muller et al. (2002); Stout and Charles (2003); Ye et al. (2003); Thimm et al. (2005); Srinivas et al. (2006)), strong membrane depolarization (Trexler et al., 1996), mechanical stimulation (Bao et al., 2004b; Gomes et al., 2005), extracellular UTP (uridine triphosphate - Cotrina et al. (1998b)), metabolic inhibition (John et al., 1999; Kondo et al., 2000; Contreras et al., 2002; Vergara et al., 2003a; Vergara et al., 2003b), shigella infection (Tran Van Nhieu et al., 2003), and most recently also in response to an increase of cytoplasmic Ca<sup>2+</sup> (Pearson et al., 2005; De Vuyst et al., 2006).

Hemichannels have been reported to be inhibited by kinases such as PKC or v-/c-Src (Li et al., 1996; Bruzzone et al., 2001a; Bao et al., 2004c). The purpose of the present study was to determine whether gap junction channels and hemichannels are similarly or differentially influenced by various kinases or kinase activating stimuli. Both channels and hemichannels are composed of the same connexin building blocks and would, at first glance, be expected to respond similarly to phosphorylations. Both channel types are, however, differentially regulated to start with, gap junctions being open under resting conditions and hemichannels being closed to prevent cell leakage.

Our work demonstrates that although channels and hemichannels are influenced in the same direction by certain stimuli, e.g., PKC activation, c-Src, or LPA, both channels are differentially influenced by LPS and bFGF, depending on the cell type and the presence or absence of the carboxyterminal domain. In C6-Cx43 cells, LPS and bFGF potentiated ATP release via hemichannels, whereas in HeLa-Cx43 cells both substances inhibited these responses. Removal of the carboxyterminal domain in HeLa-Cx43 cells (HeLa-Cx43 $\Delta$ C) reduced the ATP release, but LPS or bFGF treatment potentiated the hemichannel mediated ATP response in these cells. Likewise, HeLa cells expressing Cx26, which has a short carboxyterminal domain, displayed hemichannel potentiation by LPS and bFGF. Antagonists of the AA metabolism inhibited LPS enhancement of ATP release, and AA itself mimicked the potentiation effect of LPS or bFGF. The cell specificity of hemichannel responses thus seemed to depend on the balance between phosphorylations (inhibition) and activation of the AA signaling cascade (stimulation). LPS and bFGF came up as the most versatile modulators of connexin channels that were tested, because they invariably inhibited gap junctions, but they inhibited or potentiated hemichannels depending on the dominance of kinase or AA effects. The immunostimulant LPS and the growth factor bFGF thus exert powerful control over the release of ATP via hemichannels, a purine messenger that has both immunomodulatory and mitogenic actions (Fields and Burnstock, 2006). In addition, hemichannels play, like gap junctions, a role in cell death signaling, either as an anti-apoptotic gate or a pathogenic pore (Plotkin et al., 2002; Hur et al., 2003; Kalvelyte et al., 2003; Krysko et al., 2005; Evans et al., 2006). Distinctive hemichannel responses may thus aim at optimizing cell-cell communication (stimulation of hemichannels compensating for the decreased gap junctional communication) or cell protection (inhibition of hemichannels), depending on the conditions and the cell type.

## 6.2 Materials and Methods

### 6.2.1 Cells and reagents

We used the following cell lines: C6 rat glioma cells stably transfected with Cx43 (C6-Cx43 - Zhu et al. (1991)), human epithelial HeLa cells stably transfected with Cx43 (HeLa-Cx43) or the truncated form of Cx43 (HeLa-Cx43 $\Delta$ C - Omori and Yamasaki (1999)), HeLa cells stably transfected with Cx26 (HeLa-Cx26 - Mesnil et al. (1996)) and human embryonic kidney (HEK293) stably transfected with P<sub>2</sub>X<sub>7</sub> (HEK293-P<sub>2</sub>X<sub>7</sub> - Humphreys et al. (1998)). C6-Cx43 was maintained in DMEM/Ham's F-12 (1:1), and the HeLa and HEK cell lines were maintained in DMEM. All media were supplemented with 10 % fetal bovine serum and 2 mM glutamine. All cell culture reagents were obtained from Invitrogen (Merelbeke, Belgium).

Six-carboxyfluorescein (6-CF; 0.4 mM), calcein-acetoxymethyl ester (calcein-AM; 5  $\mu$ M), and 5-carboxyfluorescein diacetate AM (5-CFDA-AM; 10  $\mu$ M) were from Invitrogen (Molecular Probes). Phorbol 12-myristate 13-acetate (PMA; 10 nM), LPA (10  $\mu$ M), LPS from *Escherichia coli* O111:B4 (100 ng/ml), bafilomycin A1 (100 nM), botulinum toxin B (1.5 nM), PD098.059 (50  $\mu$ M), U0126 (20  $\mu$ M), chelerythrine (250 nM), genistein (5  $\mu$ M), AA, indomethacin (50  $\mu$ M), adenosine 5'-triphosphate periodate oxidized sodium salt (ox-ATP; 100  $\mu$ M), and carbenoxolone (25  $\mu$ M) were obtained from Sigma (Bornem, Belgium). 4-Amino-5-(4-chlorophenyl)-7-(*t*-butyl)pyrazolo[3,4-*d*]pyrimidine (PP2; 10  $\mu$ M) was from BIOMOL Research Laboratories (Plymouth Meeting, MA), bFGF (10 ng/ml) was from Roche Diagnostics (Vilvoorde, Belgium), arachidonyl trifluoromethyl ketone (AACOCF<sub>3</sub>; 5  $\mu$ g/ml) and baicalein (30  $\mu$ M) were from Tocris Cookson (Avonmouth, United Kingdom), and ampicillin (100  $\mu$ g/ml) was from Invitrogen. The Gap peptides <sup>43</sup>Gap 26 (VCYDKSFPISHVR; 0.25 mg/ml) and <sup>43</sup>Gap 27 (SRPTEKTIFII; 0.25 mg/ml) were synthesized by Sigma-Genosys (Cambridge, United Kingdom).

### 6.2.2 Plasmid DNA purification and transfection

pcDNA constructs containing dominant-negative and dominant-positive mutants of the c-Src kinase were kindly provided by Dr. W. H. Moolenaar (Division of Cellular Biochemistry and Center for Biomedical Genetics, The Netherlands Cancer Institute, Amsterdam, The Netherlands - Giepmans et al. (2001)). Constructs (pcDNA3.1, pcDNA-SrcK<sup>+</sup>, pcDNA-SrcK<sup>-</sup>, and pDSRed - used as a marker for transfection efficiency) were transformed to DH5 $\alpha$  heat-shock competent bacteria and grown overnight on Luria Broth (LB) agar plates. A single colony was picked up and grown in liquid LB media supplemented with ampicillin overnight. The next day, bacteria were harvested by centrifugation, and DNA was isolated using Midi kits (QIAGEN, Benelux, The Netherlands).

Cells were seeded at a density of 25,000 cells/cm<sup>2</sup> and transfected 6 h after seeding with 0.45 µg of pcDNA plasmid and 0.05 µg of pDSRed plasmid/cm<sup>2</sup> by using Transfectin lipid reagent (Biorad, Nazareth, Belgium), except for ATP measurements where pDSRed was excluded.

### 6.2.3 Gap junctional communication

Gap junctional dye coupling was determined with fluorescence recovery after photobleaching (FRAP) or scrape loading and dye transfer (SLDT). For FRAP, confluent monolayer cultures grown on glass bottom microwell plates (MatTek, Ashland, MA) were loaded with 10 µM 5-CFDA-AM or 5 µM calcein-AM (used for HeLa-Cx26) in Hanks' balanced salt solution (HBSS)-HEPES for 45 min at room temperature, followed by a 30 min de-esterification period. Fluorescence within a single cell was photobleached by spot exposure to the 488 nm line of an Argon laser and imaging (again at 488 nm excitation) was done with a custom-made video-rate confocal laser scanning microscope (Leybaert et al., 2005) with a x 40 oil immersion objective (CFI Plan Fluor; Nikon, Tokyo, Japan). For SLDT, confluent monolayer cultures were washed three times with (nominally Ca<sup>2+</sup>-free) CF-HBSS-HEPES. Cells were incubated during 1 min in CF-HBSS-HEPES containing 0.4 mM 6-CF; a linear scratch (one per culture) was made across the culture by using a syringe needle, and the cells were left for another minute in the same solution. Cultures were then washed four times with HBSS-HEPES, left for 15 min at room temperature, and images were taken with a Nikon TE300 inverted microscope in epifluorescence mode (FITC excitation/emission) with a x 10 objective and a Nikon DS-5M camera (Analis, Namur, Belgium). A fluorescence diffusion profile was derived from the images, fitted to an exponential decaying function, and the spatial constant of intercellular dye spread was determined.

### 6.2.4 Cellular ATP release

ATP release was measured with an ATP bioluminescent luciferin/luciferase assay kit (Sigma) in combination with a luminometer plate reader (Victor3 1420 multi label counter; Perkin-Elmer, Zaventem, Belgium) on subconfluent cultures grown on 24-well plates (BD Bioscience, Erembodegem, Belgium). Cells were seeded at a density of 25,000 cells/cm<sup>2</sup> and used the next day for experiments. ATP release was triggered with divalent-free (DF) HBSS-HEPES (Ca<sup>2+</sup> and Mg<sup>2+</sup> replaced with 4.4 mM EGTA), and ATP was accumulated over a 2.5 min stimulation period. Baseline measurements were done according to the same procedure but with standard HBSS-HEPES instead. ATP assay mix (75 µl), prepared in HBSS-HEPES (at 5-fold dilution), was added to 150 µl of solution bathing the cells, and the photon flux was counted over a 10 s period at the end of the 2.5 min stimulation period. Average ATP release in C6-Cx43 cells was 23.5 ± 2.4 pmoles (n = 176) in baseline and 46.2 ± 3.4 pmoles (n = 183) with DF-stimulation. All pharmacological agents were pre-incubated for the times indicated,



in HBSS-HEPES at room temperature or in culture medium at 37 °C for incubations lasting 30 min or longer, and were absent during the 2.5 min stimulation.

### 6.2.5 Western blotting

Cell protein lysates were extracted by treatment of confluent cultures with RIPA (radio immunoprecipitation assay buffer - 25 mM Tris, 50 mM NaCl, 0.5 % NP-40, 0.5 % deoxycholate, 0.1 % SDS, 5.5 %  $\beta$ -glycerophosphate, 1 mM dithiothreitol, 2 % phosphatase inhibitor cocktail, and 2 % mini EDTA-free protease inhibitor cocktail) and sonicated by three 10 s pulses. Separation of Triton X-100-soluble and -insoluble material was done essentially according to the method of Cooper and Lampe (2002). After appropriate treatment, cells from 75 cm<sup>2</sup> culture flasks were washed two times with phosphate-buffered saline (PBS; 137 mM NaCl, 2.68 mM KCl, 0.90 mM CaCl<sub>2</sub>, 0.334 mM MgCl<sub>2</sub>·6H<sub>2</sub>O, 1.47 mM KH<sub>2</sub>PO<sub>4</sub>, 6.46 mM Na<sub>2</sub>HPO<sub>4</sub>·2H<sub>2</sub>O, pH 7.4). Cells were harvested in ice-cold 1 % Triton X-100 (Tx-100) in PBS supplemented with 50 mM NaF, 1 mM Na<sub>3</sub>VO<sub>4</sub>, 1 % protease inhibitor cocktail, 1 % phosphatase inhibitor cocktail 1 and 2 (Sigma), and 1 x mini-EDTA-free protease inhibitor cocktail (Roche Diagnostics). These samples were separated into Triton X-100-soluble and -insoluble fractions by centrifugation at 16,000 x g for 10 min. Triton-insoluble fractions (pellets) were resuspended in 1 x Laemmli sample buffer (10 % glycerol, 2.3 % SDS and 125 mM Tris pH 6.8 - Laemmli (1970)) and sonicated by five 10 s pulses. Protein concentration was determined with a Biorad DC protein assay kit, and absorbance was measured on a plate reader with a 590 nm long-pass filter. Proteins were separated by electrophoresis on a 10 % SDS-poly-acrylamide gel and transferred to a nitrocellulose membrane (GE Healthcare, Little Chalfont, Buckinghamshire, United Kingdom). Blots were probed with a rabbit polyclonal anti-rat Cx43 antibody (1/10,000; Sigma), a rabbit polyclonal anti-rat  $\beta$ -tubulin antibody (1/5,000, loading control; Abcam, Cambridge, United Kingdom), a mouse monoclonal anti-rat Cx43 antibody (1/500, epitope located at the intracellular loop; Upstate Cell Signaling, Huissen, The Netherlands), a rabbit polyclonal anti-rat Cx26 (1/2,000; Zymed, Invitrogen), or a rabbit polyclonal anti-rat P<sub>2</sub>X<sub>7</sub> antibody (1/1,000; Alomone Labs, Jerusalem, Israel) followed by alkaline phosphatase conjugated goat anti-rabbit IgG or goat anti-mouse IgG (1/8,000-1/4,000; Sigma), and detection was done with nitro blue tetrazolium/5-bromo-4-chloro-3-indolyl phosphate reagent (Zymed, Invitrogen). Specificity of the P<sub>2</sub>X<sub>7</sub> receptor antibody was confirmed by competition experiments with an antigenic peptide corresponding to amino acids 576 - 595 of the rat P<sub>2</sub>X<sub>7</sub> receptor. ImageJ (<http://rsb.info.nih.gov/ij/>) was used to quantify Western blot signals. A rectangular measurement window was drawn around the nonphosphorylated (P<sub>0</sub>) and phosphorylated bands (P<sub>1+2</sub>), and their respective intensities were determined. The same windows were used to measure the background signal in nitrocellulose membrane zones where no protein was present; this background was subtracted from the P<sub>0</sub>

and  $P_{1+2}$  signals. The degree of phosphorylation was then calculated as the ratio between  $P_{1+2}$  and  $P_0$ , which was set to 100 % for the control condition.

### 6.2.6 Data analysis and statistics

The data are expressed as mean  $\pm$  S.E.M. with 'n' (indicated on the bar graphs) denoting the number of experiments. Comparison of two groups was done with a one-tailed unpaired t-test with a p value below 0.05 indicating significance. Comparison of more than two groups was done with one-way analysis of variance (ANOVA) and a Bonferroni post test. Statistical significance is indicated in the graphs with a single symbol (\* or #) for  $p < 0.05$ , two symbols for  $p < 0.01$ , and three symbols for  $p < 0.001$ . Some substances or treatments also influenced the baseline signal, but these effects most often did not reach significance with ANOVA. Selected comparisons for baseline effects were redone with a t-test, and significant differences, if relevant, are given in the figure legend.

## 6.3 Results

### 6.3.1 ATP release triggered in Cx43 transfected cells by divalent-free extracellular conditions is related to hemichannel opening

Exposing C6 glioma cells stably transfected with Cx43 (C6-Cx43 - Zhu et al. (1991) to DF solutions triggered ATP release that was significantly above baseline (Figure 57 and Arcuino et al. (2002); Stout and Charles (2003); Ye et al. (2003)). DF-triggered ATP release in C6-Cx43 was significantly suppressed by the gap junction blocker carbenoxolone (25  $\mu$ M; 15 min),  $^{43}$ Gap 26 (0.25 mg/ml; amino acids 64 - 76 on the first extracellular loop of Cx43), and  $^{43}$ Gap 27 (0.25 mg/ml; amino acids 201 - 211 on the second extracellular loop - Figure 57). These peptides also significantly reduced baseline ATP release (Figure 57), indicating the presence of open hemichannels without DF stimulation.

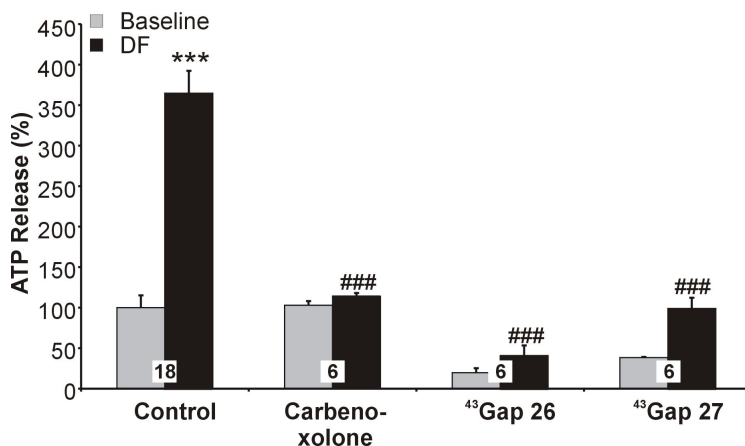


#### **Figure 57: DF-triggered ATP release is blocked by hemichannel inhibitors in C6-Cx43**

Exposure to DF conditions triggered significant ATP release that was blocked by carbenoxolone and  $^{43}$ Gap 26 and  $^{43}$ Gap 27. These peptides also significantly depressed baseline ATP release ( $p < 0.001$  and  $< 0.02$  respectively; t-test; not indicated on the graph). Star signs indicate significance compared to the corresponding baseline, while number signs represent significance compared to the control.

The action of these Gap peptides was specific for Cx43 hemichannels and not for gap junction channels when applied 30 min at 0.25 mg/ml (161  $\mu$ M for  $^{43}$ Gap 26 and 191  $\mu$ M for  $^{43}$ Gap 27 - Figure 58 and Braet et al. (2003a,b); Leybaert et al. (2003); Evans et al. (2006)).

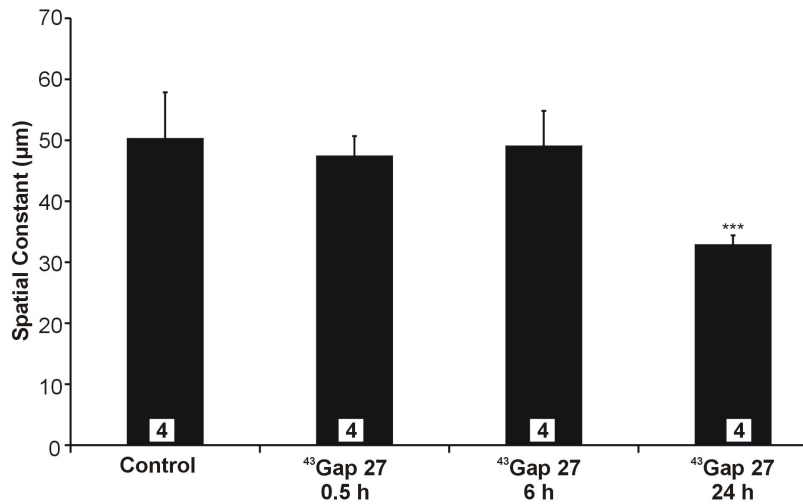


**Figure 58: Effect of  $^{43}$ Gap 27 on gap junctional coupling in C6-Cx43**

$^{43}$ Gap 27 had no effect on gap junctional communication after 0.5 h or after 6 h. Coupling was only inhibited after 24 h of incubation. Star signs indicate significance compared to control.

Botulinum toxin B (1.5 nM; 24 h), a blocker of vesicular release that cleaves synaptobrevin (Schiavo et al., (1992)) or bafilomycin A1 (100  $\mu$ M; 1 h), a v-ATPase inhibitor known to inhibit ATP storage (Coco et al., 2003), did not diminish DF-triggered ATP release (Figure 59). Botulinum toxin B even significantly stimulated DF-triggered ATP release.

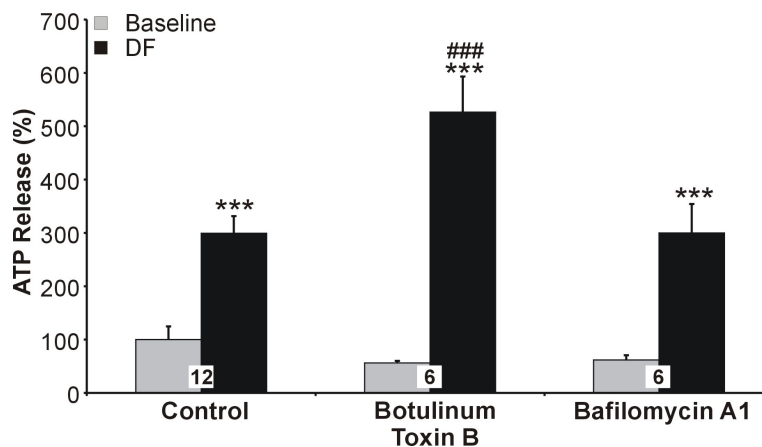


**Figure 59: Exocytosis is not involved in DF-triggered ATP release in C6-Cx43**

Botulinum toxin B and bafilomycin A1 had no inhibitory effects; botulinum toxin B even stimulated DF-triggered ATP release. Star signs indicate significance compared to the corresponding baseline, while number signs represent significance compared to control.

Activation of the  $P_2X_7$  receptor with subsequent opening of a large ATP permeable pore is another ATP releasing pathway (Chessell et al., 1997; Duan et al., 2003), but Western blot

analysis did not indicate  $P_2X_7$  receptor expression in the cell lines used in our study (Figure 60A), and exposure to the  $P_2X_7$  receptor pore inhibitors KN62 (1  $\mu$ M; 1 h) and ox-ATP (100  $\mu$ M; 1 h) did not significantly affect DF-triggered ATP release in C6-Cx43 cells ( $p = 0.3979$  for KN62 and  $p = 0.0823$  for Ox-ATP respectively using an unpaired t-test - Figure 60B). DF conditions also triggered ATP release in HeLa-Cx43 cells (Figure 61A), and this response was, like in C6-Cx43, blocked by  $^{43}$ Gap 27 and not influenced by botulinum toxin B (Figure 67A).

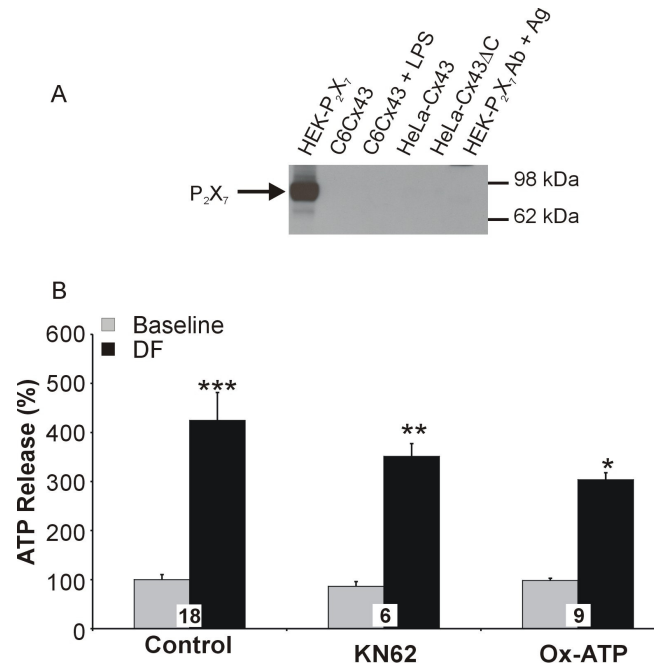


**Figure 60: Involvement of the  $P_2X_7$  receptor pore in DF-triggered ATP release**

(A) Western blots illustrating the absence of  $P_2X_7$  protein expression in the various cell lines and conditions used in this study. The specificity of the antibody was confirmed by pre-incubating the antibody with the antigenic peptide (1h; room temperature). (B) The  $P_2X_7$  receptor pore antagonists, KN62 and Ox-ATP showed a slight, but nonsignificant inhibition on DF-triggered ATP release in C6-Cx43. Star signs indicate significance compared to the corresponding baseline.

### 6.3.2 Carboxyterminal truncation of Cx43 does not affect gap junctional communication but abolishes ATP responses in HeLa-Cx43

The carboxyterminus of Cx43 is known to contain multiple consensus phosphorylation sites for PKC, Src, and MAP kinase (Warn-Cramer and Lau, 2004). To determine the gross effect of phosphorylations at these sites, we performed experiments on HeLa-Cx43 with the carboxyterminus truncated at position 239 (HeLa-Cx43 $\Delta$ C - Omori and Yamasaki (1999)). HeLa-Cx43 cells were well dye-coupled in FRAP experiments, and the level of coupling was not different in HeLa-Cx43 $\Delta$ C (Figure 61A-C and Omori and Yamasaki (1999)). In contrast, DF-triggered ATP release was reduced to baseline levels in HeLa-Cx43 $\Delta$ C, and the baseline level itself was also significantly lower when compared to HeLa-Cx43 cells (Figure 61D).

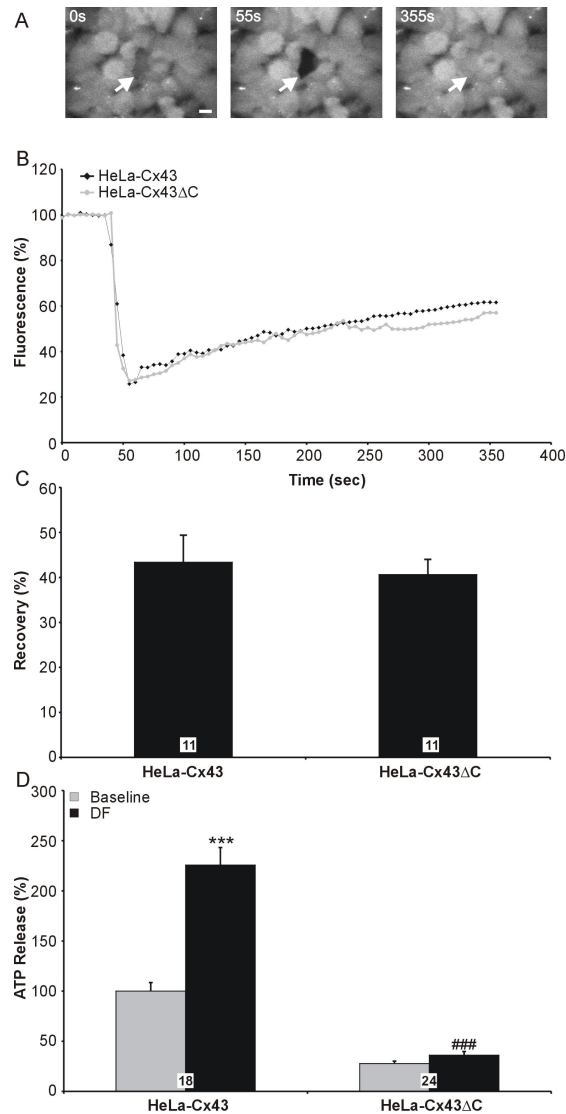


**Figure 61: Effect of carboxyterminal truncation on gap junctional coupling and ATP release in HeLa-Cx43 cells**

(A) Example pictures of FRAP experiments, 0 s: pre-bleach; 55 s: just after bleaching; 355 s: fluorescence at the end of the registration period. The white arrow points to the photobleached cell. The white scale bar measures 10  $\mu$ m. (B) Average FRAP recovery traces of the data presented in C. (C) Summary of FRAP recovery data determined by averaging data points over the last 25 s. Carboxyterminal truncation had no effect on gap junctional coupling (n is the number of photobleached cells in two different cultures). (D) Carboxyterminal truncation largely depressed baseline and triggered ATP release. Baseline in HeLa-Cx43ΔC was significantly below baseline in HeLa-Cx43 ( $p < 0.0001$ ; t-test). Star signs indicate significance compared to the corresponding baseline, while number signs indicate significance compared to the DF-trigger in HeLa-Cx43 cells.

Subsequent experiments on these cells confirmed the absence of DF-triggered ATP release in HeLa-Cx43ΔC (Figure 67B, Figure 68D, and Figure 71E), but in one series (Figure 71B) a small significant release component was apparent. In sum, removal of the Cx43 carboxyterminus inhibits hemichannel opening and does not affect gap junctions in HeLa cells. The intact gap junctional communication as shown in our experiments and by Omori and Yamasaki (1999) indicates the presence of Cx43ΔC at the plasma membrane and the

formation of functional gap junctions. This was confirmed with Western blot analysis after Tx-100 extraction, separating Cx43 present in the gap junctional plaque from all other fractions (Figure 67D and Omori and Yamasaki (1999)).

### 6.3.3 Activation of PKC and c-Src reduces gap junctional communication and ATP responses in C6-Cx43

PMA (10 nM; 2 h), a known PKC activator (Lampe, 1994; Malfait et al., 2001), significantly reduced dye coupling (FRAP) in C6-Cx43 (Figure 62A and B). Washing out PMA during 30 min or co-incubating the cells with the PKC inhibitor chelerythrin (250 nM; 30 min pre-incubation followed by 2 h co-incubation with PMA (Herbert et al., 1990) abolished the PMA effect. PMA also significantly reduced DF-triggered ATP release, and this was reversed by chelerythrin (Figure 62C). Furthermore, PMA induced a slight increase (+ 32 %) in the phosphorylation degree of Cx43 in C6-Cx43 cells (Figure 62D).

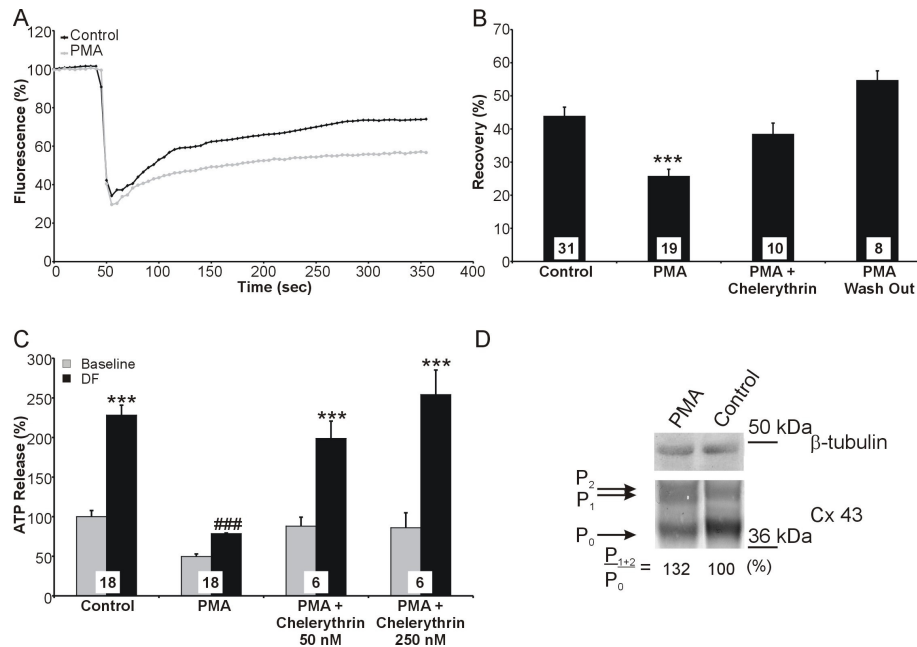


**Figure 62:** Effect of PMA treatment of C6-Cx43 cells

(A) Average FRAP recovery traces in control (n = 31) and after PKC activation with PMA (n = 19). (B) FRAP summary data, showing inhibition of dye coupling by PMA and reversal by chelerythrin or PMA washout (30 min - n is the number of photobleached cells on 3 different cultures for control and 2 different cultures for all other conditions). (C) DF-triggered ATP release was inhibited by PMA, an effect that was reversed by chelerythrin, in a dose-dependent manner. PMA significantly depressed baseline ATP release in C (p<0.001; t-test). (D) Western blot analysis showing the influence of PMA on the phosphorylation status of Cx43 in C6-Cx43 cells. The ratio of nonphosphorylated versus phosphorylated Cx43 is given under each lane, and the ratio for control conditions has been set to 100 % (n = 3). Star signs indicate significance compared to control condition in (B) and compared to the corresponding baseline signal in (C), while number signs indicate significance compared to control condition.

The effect of c-Src was investigated by transient transfection of C6-Cx43 with a vector containing constitutively active or inactive c-Src. Mock transfection or transfection with the inactive c-Src mutant (c-SrcK<sup>-</sup>; K295M; mutation of this residue interferes with the formation of ion-pairs between K295 and the  $\alpha$ - and  $\beta$ -phosphates of ATP - Roskoski (2004)) had no significant effect on gap junctional communication (SLDT), but transfection with the constitutively active mutant (c-SrcK<sup>+</sup>; Y527A; Y527 is largely phosphorylated under basal conditions and forms an intramolecular binding with the Src SH2 domain, resulting in the stabilization of the dormant form - Roskoski (2005)) significantly inhibited dye transfer between the cells (Figure 63A and B). Triggered ATP release was affected in a similar manner, with a significantly decreased ATP response in c-SrcK<sup>+</sup> transfected cells (Figure 63C). C6-Cx43 cells transfected with c-SrcK<sup>+</sup> showed an increase in the phosphorylated (P<sub>1+2</sub>) form (+ 44 %), when compared with cells transfected with c-SrcK<sup>-</sup> (Figure 63D).

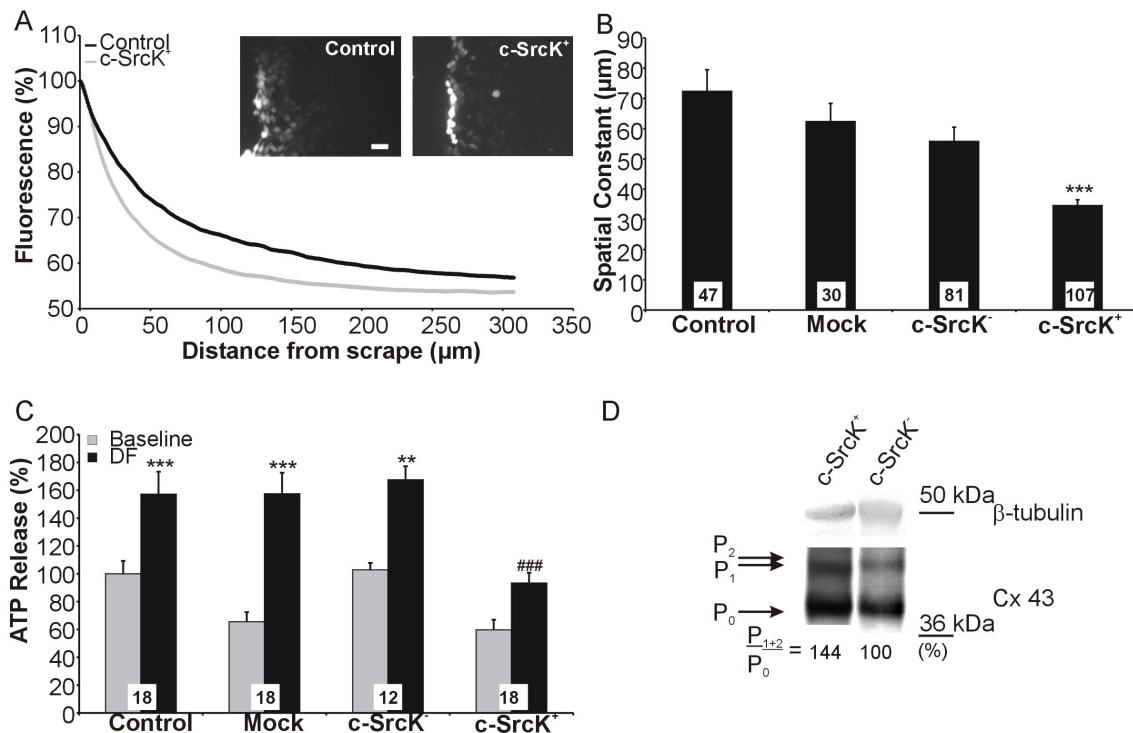


**Figure 63: Effect of c-SrcK<sup>-</sup> and c-SrcK<sup>+</sup> transfection of C6-Cx43 cells**

(A) Example pictures illustrating SLDT in control and c-SrcK<sup>+</sup>-transfected cells. The right border of the scrape is visible as the row of strongly 6-CF-stained cells, and dye spread proceeded from there to the right (scalebar: 100  $\mu\text{m}$ ). Average fluorescence intensity profiles were derived, and the spatial constant of exponential decay was determined. (B) Summary data of SLDT experiments. Dye coupling was not significantly affected by mock or c-SrcK<sup>-</sup> transfection, but it was significantly inhibited in c-SrcK<sup>+</sup> (n is the number of SLDT images obtained in 4 different cultures for control and 2 different cultures for all other conditions). (C) DF-triggered ATP release was not affected in mock or c-SrcK<sup>-</sup> transfected cells, but it was significantly depressed in c-SrcK<sup>+</sup>. (D) Western blot analysis indicated an increased phosphorylation of Cx43 after c-SrcK<sup>+</sup> transfection. The data are representative for three different experiments. Star signs indicate significance compared to control condition in (B) and compared to the corresponding baseline signal in (C), while number signs indicate significance compared to control condition.

### 6.3.4 LPA inhibits gap junctional coupling and ATP responses in C6-Cx43, whereas LPS inhibits coupling but stimulates ATP release

LPA activates various kinases, including PKC (Takeda et al., 1999; Kelley et al., 2006), c-Src kinase (Takeda et al., 1998; Kranenburg and Moolenaar, 2001), and the MAP kinase family (Takeda et al., 1999; Kranenburg and Moolenaar, 2001). In C6-Cx43, LPA (10  $\mu$ M; 1 h) significantly inhibited gap junctional coupling (FRAP) and DF-triggered ATP release (Figure 64). Both LPA effects were abolished with the Src inhibitor PP2 (10  $\mu$ M; 15 min pre-incubation followed by 1 h co-incubation with LPA - Figure 64 or with the MEK1/2 inhibitor U0126 (20  $\mu$ M; 1 h pre-incubation followed by 1 h co-incubation with LPA - Figure 64). The MEK1/2 inhibitor PD098.059 (50  $\mu$ M; same protocol as for U0126) had no significant effect, nor did the PKC inhibitor chelerythrin (Figure 64). LPA treatment of C6-Cx43 cells increased the phosphorylation status of Cx43 by 47 %, but did not induce a redistribution of Cx43 between the plasma membrane and the cytoplasm (Figure 64).

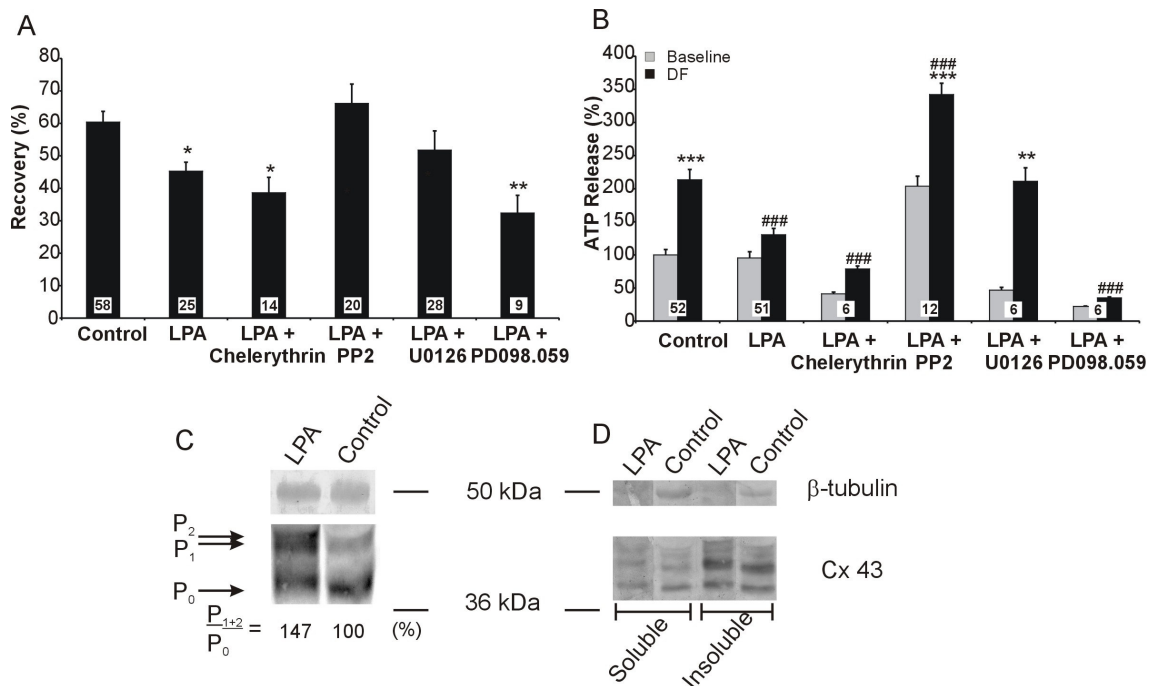


**Figure 64: Effects of LPA treatment in C6-Cx43**

(A) Gap junctional coupling (FRAP) was significantly inhibited by LPA, and this was reversed by PP2 and U0126 but not by chelerythrin or PD098.059 (n is the number of photobleached cells in 5 different cultures for control and 2 different cultures for all other conditions). (B) DF-triggered ATP release was significantly inhibited by LPA, an effect that was reversed by PP2 and U0126, but not by chelerythrin and PD098.059. (C) Western blot showing an increased Cx43 phosphorylation after LPA treatment (n = 3). (D) Western blot illustrating the separation of Triton X-100-soluble and -insoluble connexin fractions in C6-Cx43. Star signs indicate significance compared to control condition in (A) and compared to the corresponding baseline signal in (B), while number signs indicate significance compared to control condition.

LPS is another broad-spectrum kinase activator, which binds to the Toll-like receptor and the co-receptor CD14 (Ulevitch, 1993) and thereby activates PKC, c-Src, and the MAP kinase



signaling pathway (Lidington et al., 2000; Lidington et al., 2002; Schorey and Cooper, 2003). LPS (100 ng/ml; 1 h) inhibited dye coupling (like LPA), but (unlike LPA) stimulated DF-triggered ATP release (Figure 65A and B). Both LPS effects were reversed by PP2 and U0126 but not by chelerythrine or PD098.059.  $^{43}\text{Gap}$  27 blocked the LPS-enhanced ATP release (Figure 65C), to a similar extent as observed without LPS stimulation (Figure 57), whereas bafilomycin A1 had no effect on LPS enhanced DF-triggered ATP release (Figure 65D). LPS can upregulate  $\text{P}_2\text{X}_7$  receptor expression in macrophages (Le Feuvre et al., 2002), but Western blot experiments did not show any evidence for such effect in C6-Cx43 (Figure 60A). Together, LPA and LPS have opposing effects on DF-triggered ATP release and similar effects on gap junctional coupling. These influences involve c-Src and MEK1/2 activation and are exerted at the level of hemichannel gating. Figure 66A illustrates an increase in Cx43 phosphorylation (with 169 %), but the Cx43 localization at the plasma membrane did not change after LPS treatment.

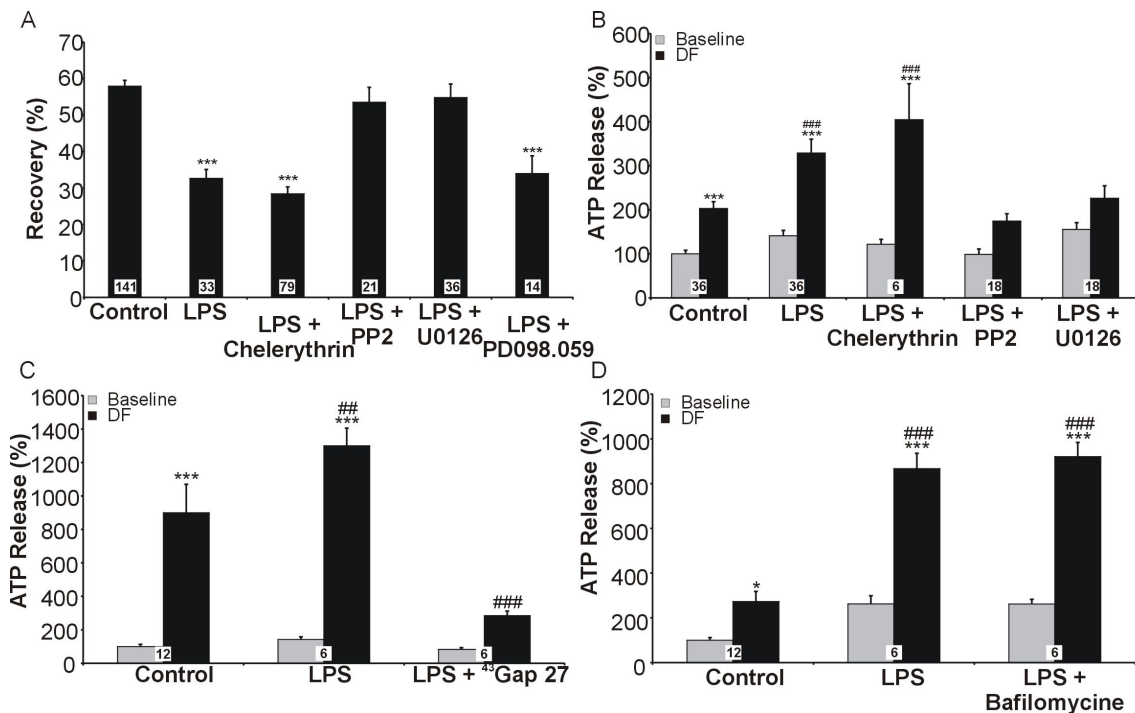
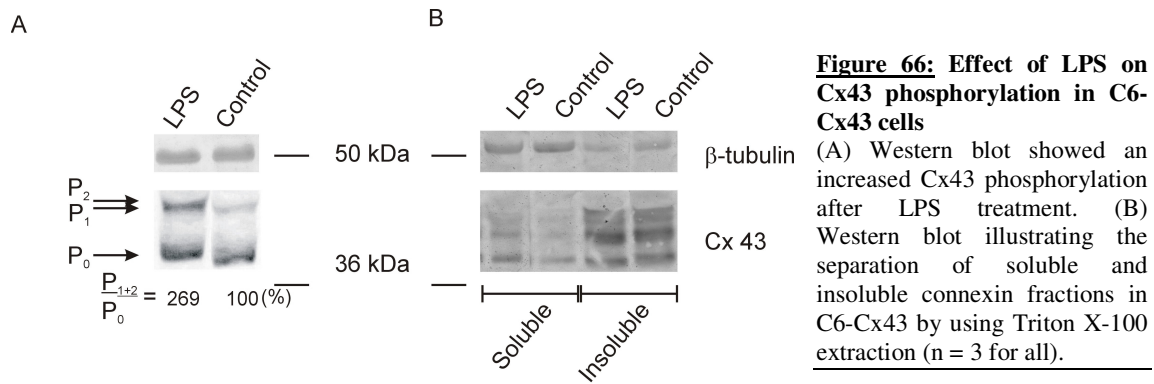


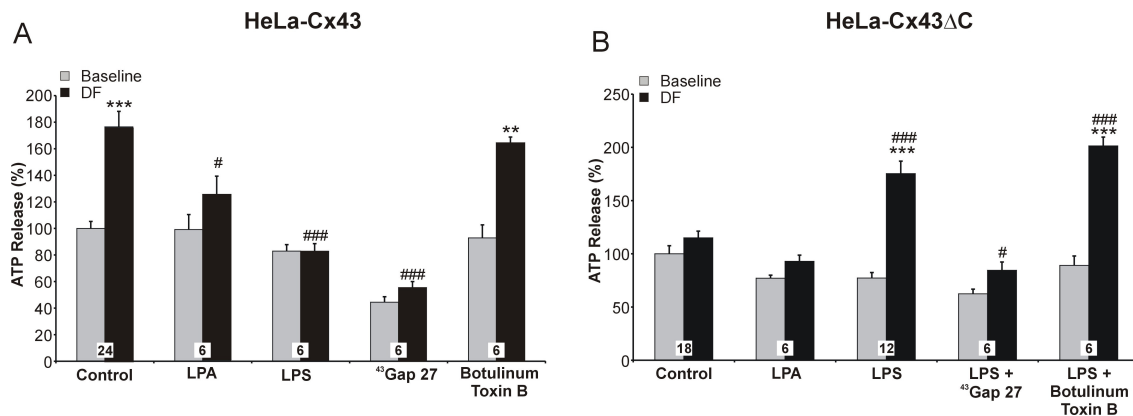
**Figure 65: Effects of LPS treatment in C6-Cx43 cells**

(A) Gap junctional coupling (FRAP) was inhibited by LPS, and this was reversed by PP2 and U0126, but not by chelerythrine or PD098.059 (n is the number of photobleached cells in 5 different cultures for control and 2 different cultures for all other conditions). (B) DF-triggered ATP release was significantly enhanced by LPS, an effect that was reversed by PP2 and U0126, but not by chelerythrine. (C) LPS enhancement of DF-triggered ATP release was strongly inhibited by  $^{43}\text{Gap}$  27, to an extent comparable to that in Figure 57. (D) Bafilomycin A1 had no effect on the LPS stimulated ATP release. LPS also significantly stimulated baseline ATP release ( $p < 0.001$  in B,  $< 0.05$  in C, and  $< 0.001$  in D; t-test). Star signs indicate significance compared to control condition in (A) and compared to the corresponding baseline signal in (B-D), while number signs indicate significance compared to control condition.



### 6.3.5 LPA and LPS inhibit ATP responses in HeLa-Cx43, but LPS potentiates these responses in carboxyterminal truncated HeLa-Cx43

To determine whether the opposing effects of LPA and LPS on DF-triggered ATP release were perhaps specific for C6-Cx43, we repeated these experiments in HeLa-Cx43. LPA and LPS inhibited DF-triggered ATP release in HeLa-Cx43 (Figure 67A) in contrast to C6-Cx43 where LPA inhibited and LPS potentiated these responses. No effect of LPA was found in HeLa-Cx43 $\Delta$ C, but quite remarkably, LPS restored the DF-triggered ATP response in these cells (while giving inhibition in HeLa-Cx43 cells - Figure 67). LPS-enhanced ATP release in HeLa-Cx43 $\Delta$ C was blocked by  $^{43}$ Gap 27 and not affected by botulinum toxin B (Figure 67B). The potentiation of DF-triggered ATP release by LPS is thus, as in C6-Cx43, the consequence of hemichannel stimulation.



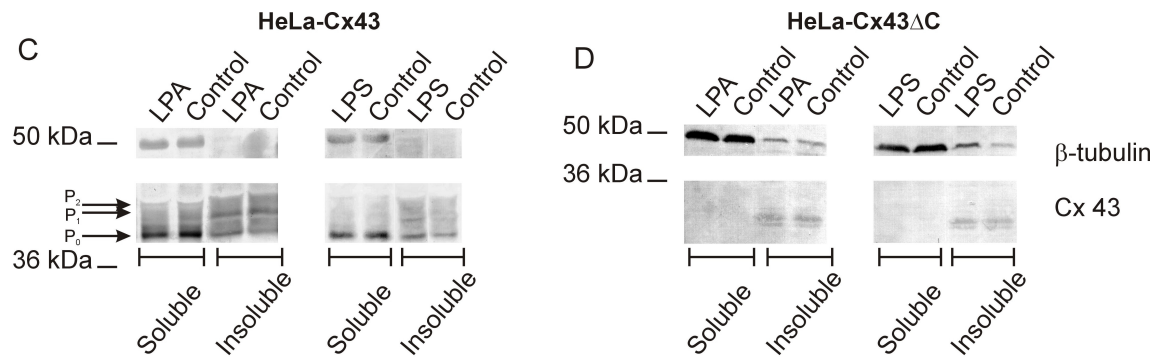
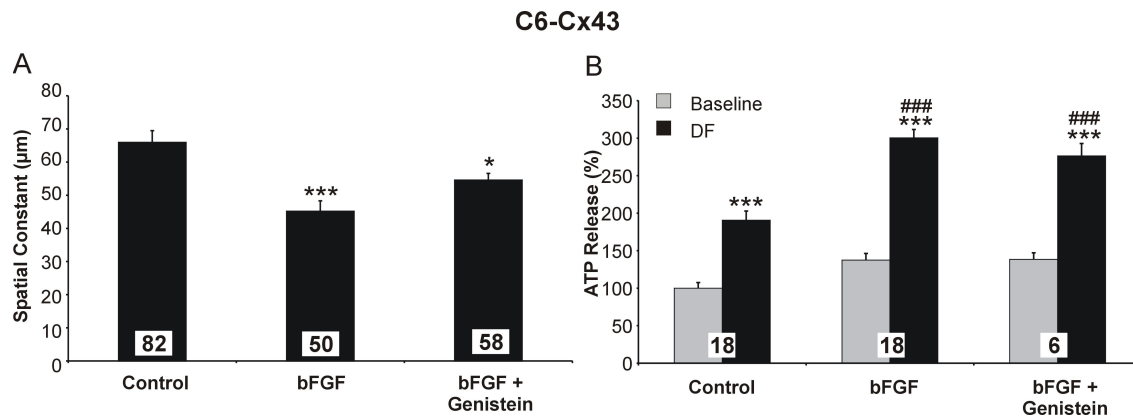


**Figure 67: Effect of LPA and LPS on DF-triggered ATP release in HeLa-Cx43 cells**

(A) Experiments in HeLa-Cx43 showed inhibition of DF-triggered ATP release by LPA and LPS.  $^{43}\text{Gap}$  27 blocked the DF-triggered ATP release, whereas botulinum toxin B had no effect ( $^{43}\text{Gap}$  27 also inhibited baseline ATP release,  $p < 0.0001$ ). (B) Experiments on HeLa-Cx43 $\Delta$ C cells illustrate the absence of DF-triggered ATP release in these cells, no effect of LPA, but significant stimulation of DF-triggered ATP release after LPS treatment.  $^{43}\text{Gap}$  27 blocked the LPS-enhanced ATP response, but botulinum toxin B had no effect, similar to the experiments in C6-Cx43 illustrated in Figure 65C and D. (C-D) There was no significant alteration in the distribution of Cx43 in HeLa-Cx43 and HeLa-Cx43 $\Delta$ C cells after LPA or LPS treatment ( $n = 3$ ). Star signs indicate significance compared to the corresponding baseline signal, while number signs indicate significance compared to control condition.

### 6.3.6 bFGF has similar effects as LPS

Basic FGF is another broad-spectrum kinase activator (Shiokawa-Sawada et al., 1997; Mergler et al., 2003); this growth factor (10 ng/ml in serum-free medium for 6 h), like LPS and LPA, significantly inhibited dye coupling (SLDT) in C6-Cx43. This effect was partly reversed by the tyrosine kinase blocker genistein (1 h pre-incubation, followed by 6 h co-incubation with bFGF - Figure 68A). The bFGF effects on DF-triggered ATP release were similar to those of LPS, that is, stimulation of ATP release in C6-Cx43 and HeLa-Cx43 $\Delta$ C and inhibition in HeLa-Cx43 (Figure 68B-D). Stimulation of DF-triggered ATP release by bFGF in C6-Cx43 was not reduced by genistein, indicating involvement of other pathways. Figure 69 illustrates a minor increase in Cx43 phosphorylation in C6-Cx43 cells after bFGF exposure, but the presence of Cx43 at the plasma membrane was unaffected.



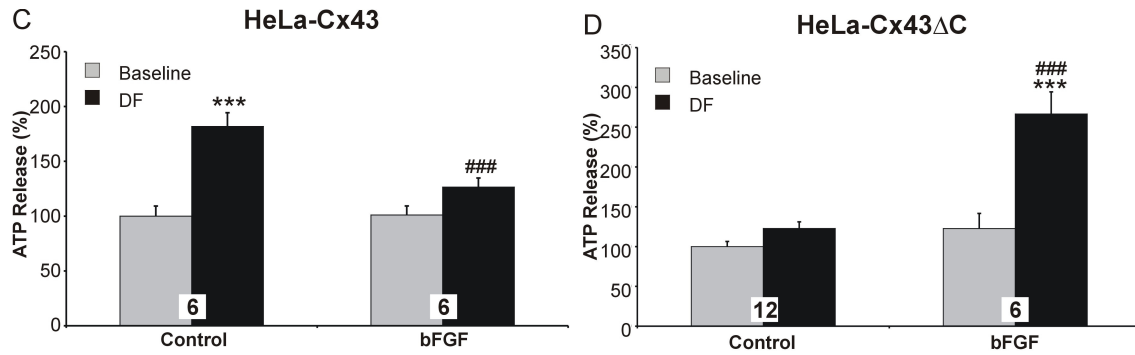


**Figure 68: Effects of bFGF on gap junctional communication and DF-triggered ATP release**

(A) bFGF significantly inhibited gap junctional coupling (SLDT) in C6-Cx43, and this effect was partly reversed by genistein (n is the number of SLDT images in 4 different cultures). (B) bFGF significantly stimulated DF-triggered ATP release in C6-Cx43, but this could not be reversed by genistein. (C) bFGF significantly inhibited the DF-triggered ATP release in HeLa-Cx43. (D) bFGF significantly stimulated DF-triggered ATP release in HeLa-Cx43ΔC cells. Star signs indicate significance compared to control condition in (A) and compared to the corresponding baseline signal in (B-D), while number signs indicate significance compared to control condition.

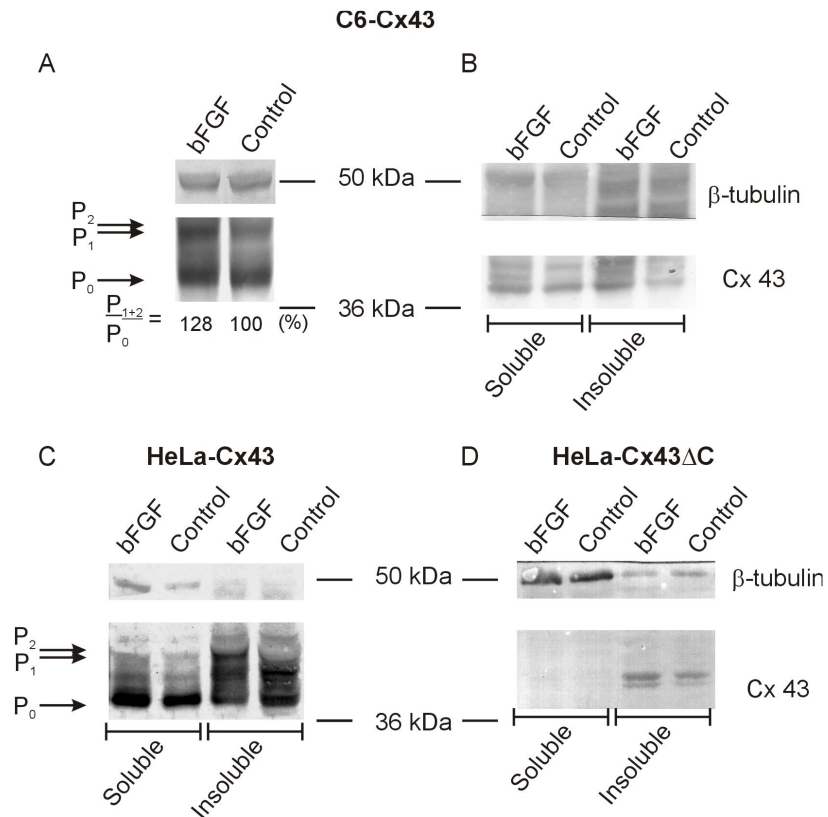
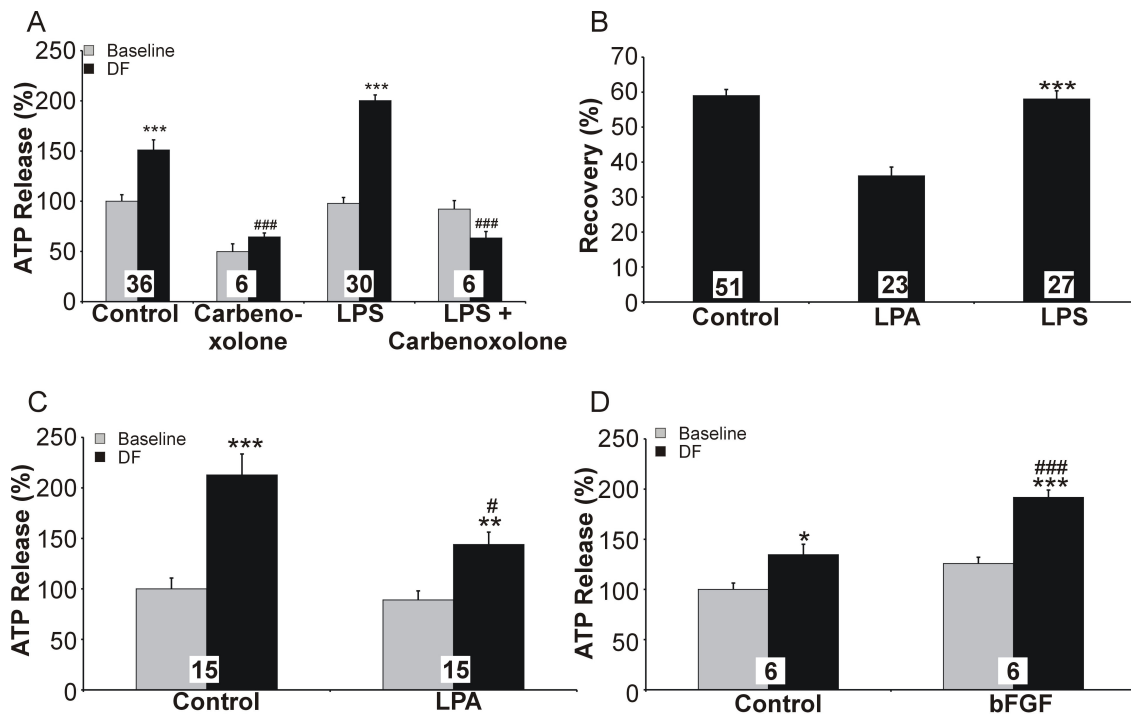


**Figure 69: Western blot analysis showing the effect of bFGF treatment on Cx43 phosphorylation**

(A) bFGF treatment in C6-Cx43 cells resulted in a small increase in the phosphorylation status of Cx43. (B-D) No major shifts between the Tx-100-soluble and -insoluble phases could be observed after bFGF treatment in C6-Cx43 cells, in HeLa-Cx43 cells or in HeLa-Cx43ΔC cells (n = 3).

### 6.3.7 bFGF and LPS potentiate DF-triggered ATP release in HeLa-Cx26

We next performed experiments on HeLa cells expressing Cx26, which is a connexin with a very short carboxyterminal domain of only 11 amino acids, and the only connexin known not to be phosphorylated (Traub et al., 1989; Lampe and Lau, 2000). Gap junctional communication was inhibited by LPA and not affected by LPS in HeLa-Cx26 (Figure 70A). DF conditions triggered ATP release significantly above baseline, and this was potentiated by LPS and bFGF (Figure 70B and C), as observed in HeLa-Cx43ΔC. No Gap peptides are currently available to block Cx26 hemichannels, so we applied carbenoxolone, which inhibited DF-triggered ATP release, both in control and after potentiation with LPS (Figure 70B). LPA inhibited the DF-triggered ATP release (Figure 70C). LPS and bFGF (Figure 70D) thus potentiate DF-triggered ATP release via hemichannels in C6-Cx43, HeLa-Cx43ΔC, and HeLa-Cx26 cells.



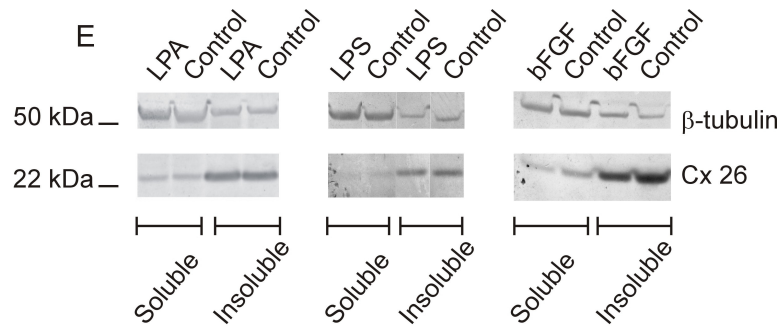


**Figure 70: Effect of LPA, LPS, and bFGF in HeLa-Cx26 cells**

(A) Effect of LPA and LPS on gap junctional coupling in HeLa-Cx26 cells as measured via FRAP, using calcein-AM as a gap junctional permeable dye ( $n$  is the number of photobleached cells in 2 different cultures). (B) DF conditions triggered significant ATP release that was stimulated by LPS and inhibited by carbenoxolone. Carbenoxolone alone also significantly depressed the baseline signal ( $p < 0.05$  with a t-test). (C) LPA inhibited DF-triggered ATP release. (D) bFGF slightly but significantly stimulated DF-triggered ATP release. (E) Western blots illustrating the separation of Tx-100-soluble and -insoluble connexin fractions in HeLa-Cx26. No gross and consistent shifts were however observed over three different experiments. Star signs indicate significance compared to control condition in (A) and compared to the corresponding baseline signal in (B-D), while number signs indicate significance compared to control condition.

### 6.3.8 LPS potentiation of ATP responses involves AA signaling

The kinases activated by LPS: c-Src, and MEK1/2 can lead to phosphorylation and activation of cytosolic/ $\text{Ca}^{2+}$ -dependent phospholipase  $\text{A}_2$  (cPLA $_2$ ) and  $\text{Ca}^{2+}$ -independent phospholipase  $\text{A}_2$  (iPLA $_2$  - Luo et al. (2005)) with subsequent production of AA, a proposed candidate for hemichannel activation (Contreras et al., 2002). We investigated the involvement of AA and its downstream products with the cPLA $_2$  and iPLA $_2$  inhibitor AACOCF3 (5  $\mu\text{g}/\text{ml}$ ; 1 h pre-incubation followed by 1 h co-incubation with LPS - Riendeau et al. (1994); Chakraborti et al. (2004)), the lipoxygenase inhibitor baicalein (30  $\mu\text{M}$ ; same protocol as for AACOCF3 - Vivancos and Moreno (2002)), and the cyclooxygenase inhibitor indomethacin (50  $\mu\text{M}$ ; same protocol as for AACOCF3 and baicalein - Fujiwara et al. (2006)). All these substances significantly suppressed the LPS potentiated effect on DF-triggered ATP release in C6-Cx43, HeLa-Cx43 $\Delta\text{C}$ , and HeLa-Cx26 cells (Figure 71A-C). In addition, exposure to AA significantly enhanced DF-triggered ATP release in these cell lines (Figure 71D-F).

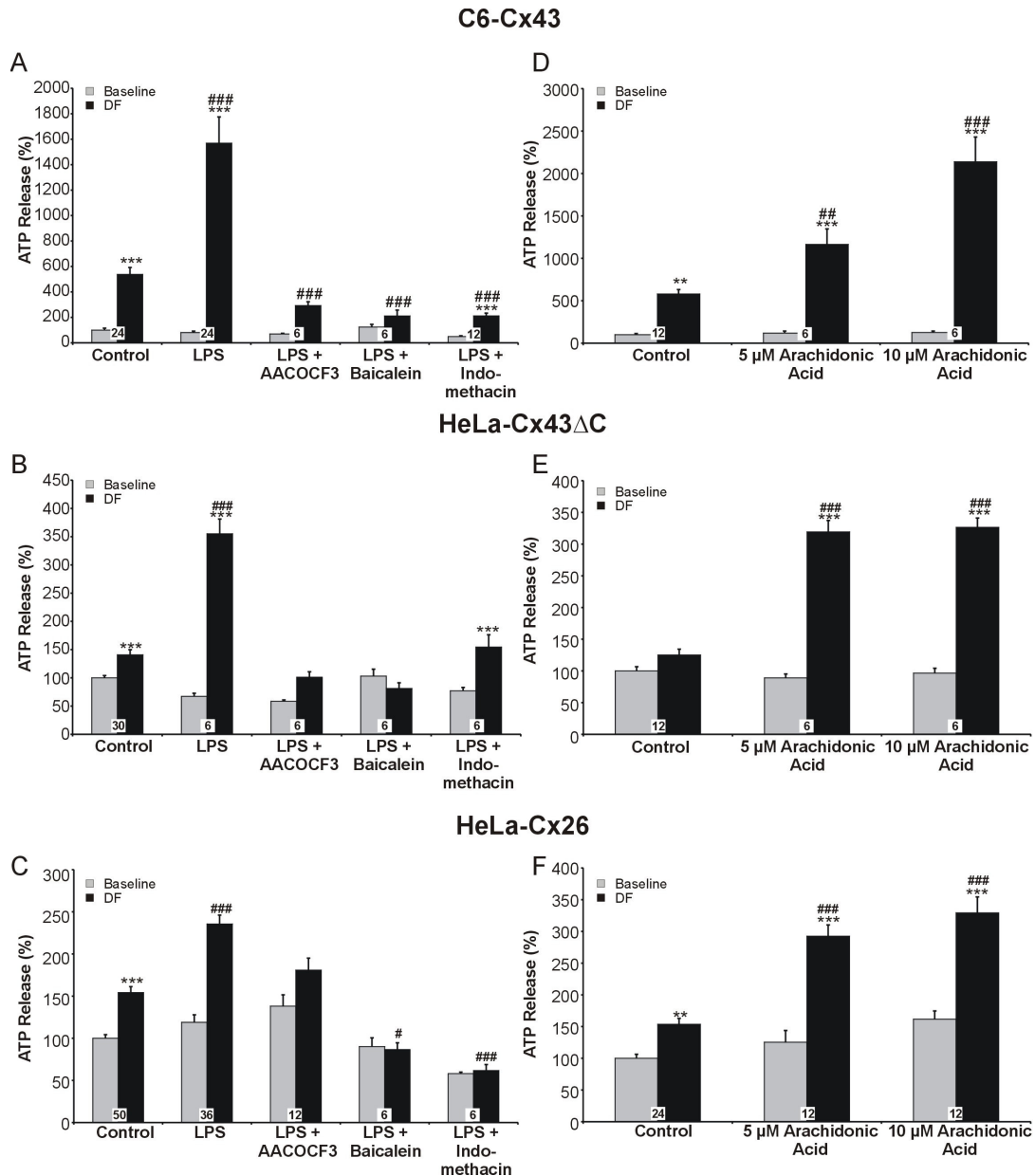


**Figure 71: AA metabolism and LPS enhancement of DF-triggered ATP release**

(A) Inhibition of AA release with AACOCF3, of lipoxygenase with baicalein, or of cyclooxygenase with indomethacin all drastically suppressed LPS enhancement of DF-triggered ATP release in C6-Cx43. Similar results were observed in HeLa-Cx43ΔC cells (B) and HeLa-Cx26 cells (C). (D–F) Exogenously applied AA potentiated DF-triggered ATP release in C6-Cx43 (D), HeLa-Cx43ΔC (E), and HeLa-Cx26 (F). Star signs indicate significance compared to the corresponding baseline signal and number signs indicate significance compared to control condition.

## 6.4 Discussion

Exposure to DF conditions is a well-known trigger for hemichannel opening, and ATP release provoked in this way proceeded through hemichannels, because it was strongly inhibited by the hemichannel blockers  $^{43}\text{Gap 26}$  and  $^{43}\text{Gap 27}$  (Braet et al., 2003a; Braet et al., 2003b; Leybaert et al., 2003; Gomes et al., 2005; Pearson et al., 2005; Evans et al., 2006). A substantial contribution of other ATP releasing mechanisms is unlikely because of the potency of the suppressive effect of the Gap peptides, the absence of inhibition by the vesicular release inhibitors botulinum toxin B (which unexpectedly potentiated the release for unknown reasons) and bafilomycin A1, the lack of  $\text{P}_2\text{X}_7$  receptor expression, and the absence of significant effects of  $\text{P}_2\text{X}_7$  receptor antagonists.

Truncation of the carboxyterminal tail of Cx43 at position 239 (HeLa-Cx43 $\Delta\text{C}$ ) did not influence gap junctional coupling, indicating that the carboxyterminus is not essential for the assembly and membrane insertion of gap junction channels. This confirms previous work on the same cell line (Omori and Yamasaki, 1999) and is in line with observations on carboxyterminal truncations at slightly different positions: position 244 (Fishman et al., 1991) or 257 (Liu et al., 1993; Hur et al., 2003). PKC activation depressed gap junctional coupling and ATP release via hemichannels in C6-Cx43, in line with other studies reporting inhibition of dye uptake (Li et al., 1996) and  $\text{NAD}^+$  release (Bruzzone et al., 2001a; Bruzzone et al., 2001b) via hemichannels. Recent work shows that inhibition occurs via phosphorylations on S262 and S368 of Cx43 (Bao et al., 2004c). c-Src kinase inhibits gap junctions via phosphorylations at Y265 and Y247 of Cx43 (Goldberg and Lau, 1993; Kanemitsu et al., 1997; Giepman et al., 2001; Lin et al., 2001), and hemichannel inhibition has also been reported (Li et al., 1996). In line with this, c-Src transfection inhibited both gap junctions and hemichannels in C6-Cx43. The phospholipid mediator LPA activates various protein kinases, including PKC, c-Src, and the MAP kinase family (Takeda et al., 1998; Takeda et al., 1999; van Leeuwen et al., 2003; Kelley et al., 2006). LPA inhibited gap junction channels and hemichannels, and experiments with the inhibitors PP2 (Src-inhibitor) and U0126 (MEK1/2 inhibitor) indicated involvement of c-Src and MEK1/2, respectively (absence of effect of the MEK1/2 inhibitor PD098.059 is probably related to its poor solubility - Davies et al. (2000); Ahn et al. (2001)). MAP kinases are known to inhibit gap junctions (Kim et al., 1999), and our work indicates that MEK1/2 (a MAP kinase kinase family member) has a similar action on hemichannels.

LPS, a glycolipid immunostimulant from Gram-negative bacteria, is another activator of PKC, c-Src, and the MAP kinase signaling pathway (Lidington et al., 2000; Lidington et al., 2002; Schorey and Cooper, 2003). LPS may also stimulate NO production, but this needs exposures longer than the 1 h used here (Shin et al., 2001). LPS reduced gap junctional coupling but



stimulated DF-triggered ATP release in C6-Cx43, and these opposite actions involved c-Src and MEK1/2 (reversed by PP2 and U0126, respectively). An enhancement of ATP release may result from the stimulation of hemichannels or the recruitment of other release mechanisms. LPS enhanced ATP release was suppressed by <sup>43</sup>Gap 27, to an equal and drastic extent as observed under control conditions. The strong inhibition by the Gap peptides together with the lack of any effect of bafilomycin A1 or botulinum toxin B, and the absence of P<sub>2</sub>X<sub>7</sub> receptor up-regulation in response to LPS, indicate that the enhancement of triggered ATP release is most likely due to stimulation of hemichannels.

LPS inhibited DF-triggered ATP release via hemichannels in HeLa-Cx43, and surprisingly, inhibition was turned into stimulation in HeLa-Cx43ΔC cells. bFGF, acting on membrane-bound tyrosine kinase receptors (Shiokawa-Sawada et al., 1997), had similar effects, i.e., depression of gap junctional coupling in C6-Cx43, stimulation of ATP release in C6-Cx43 and HeLa-Cx43ΔC cells, and inhibition of ATP release in HeLa-Cx43. LPS and bFGF also potentiated DF-triggered ATP release in HeLa-Cx26, a connexin with a very short carboxyterminal domain. In sum, in HeLa cells, the carboxyterminal domain seems to be necessary for hemichannel opening, whereas its absence is required for hemichannel stimulation by LPS or bFGF (Figure 72C).

The different effects of LPS and bFGF on different connexins implicate the involvement of other signaling pathways. LPS and bFGF can, either directly or indirectly, via intermediate kinases (Luo et al., 2005), lead to activation of cPLA<sub>2</sub> and/or iPLA<sub>2</sub> (Vivancos and Moreno, 2002; Antoniotti et al., 2003) with subsequent release of AA (Figure 72A). Treatment with AA indeed mimicked the effects of LPS and bFGF in C6-Cx43, HeLa-Cx43ΔC, and HeLa-Cx26, and inhibitors of AA release and metabolism furthermore reduced the potentiating effect of LPS. Stimulation of hemichannels by LPS and bFGF is thus related to the activation of the AA signaling pathway. In C6-Cx43, this pathway is presumably more active and overrides the inhibition of hemichannels by phosphorylations at the carboxyterminus. At the level of gap junctions, the two pathways lead to inhibition, as reported here for LPS and bFGF and by others for AA (Giaume et al., 1989; Criswell and Loch-Caruso, 1995; Velasco et al., 2000). The soluble and insoluble fractions were not grossly or systematically changed after LPA, LPS or bFGF treatments. Hemichannel modulation by LPS and bFGF is therefore likely to be mediated by effects at the level of hemichannel functioning (such as its gating) rather than by introducing shifts in the distribution of gap junction channels and hemichannels.

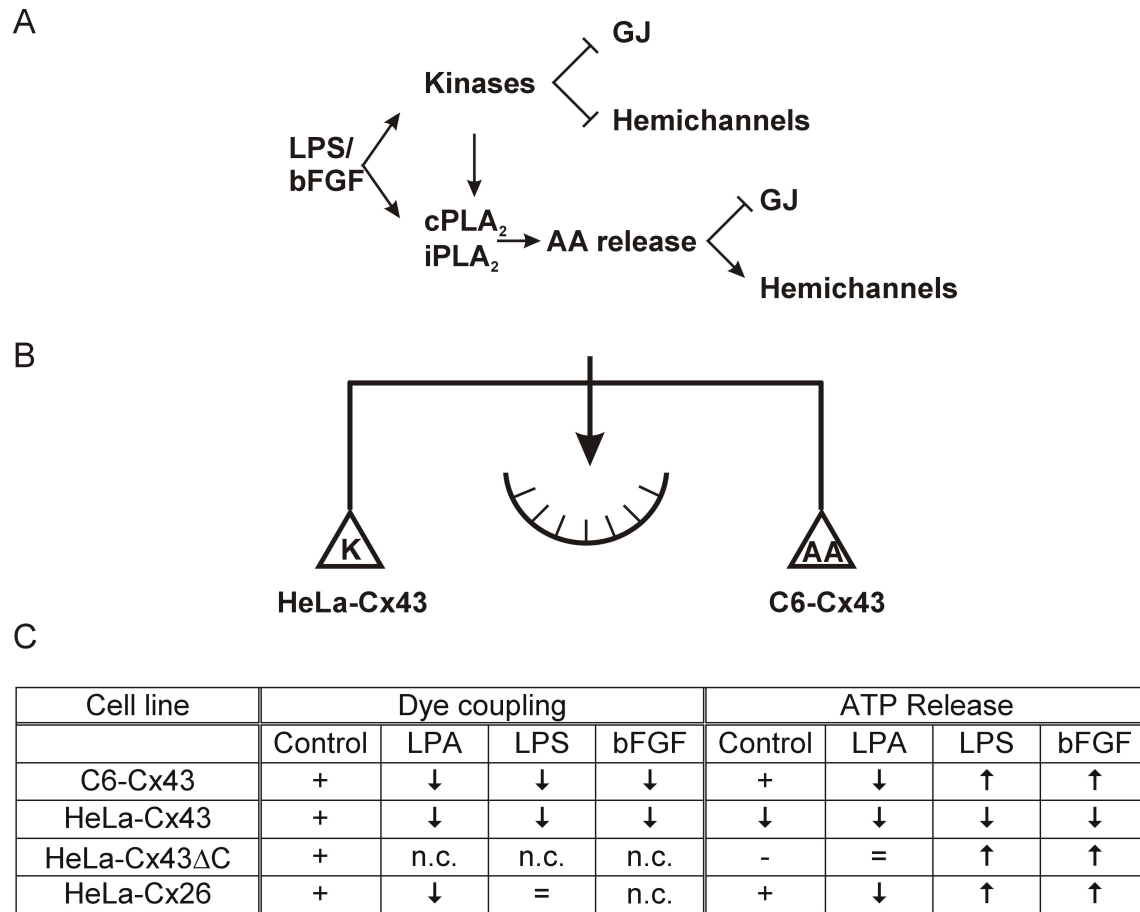


**Figure 72: Scheme summarizing the major findings of this study**

(A) LPS and bFGF activate various kinases that suppress gap junctions and hemichannel mediated ATP release. In addition, both substances also trigger the production of AA via activation of cPLA<sub>2</sub> and iPLA<sub>2</sub>. AA is known to inhibit gap junctions, and the present study demonstrates that it stimulates hemichannel mediated ATP release. (B) We conclude that the net effect of LPS and bFGF depends on the balance between activation of kinases (inhibition of hemichannels), and activation of the AA metabolic pathway (stimulating hemichannel mediated ATP release). In HeLa-Cx43 cells the kinase component predominates, whereas in C6-Cx43 it is the AA pathway that adds most weight. Truncation of the carboxyterminus in HeLa-Cx43 cells removes inhibition by kinases and thereby reveals the AA component. (C) Table summarizing the major findings of this chapter. n.c. indicates that these effects were not studied in this manuscript.

Our work demonstrates that gap junction channels and hemichannels, although composed of the same connexins, can be differentially modulated. The factors determining the hemichannel responses are related to the applied stimulus, the cell type, and the carboxyterminal domain containing the phosphorylation consensus sites, and they depend on the balance between connexin phosphorylations and activation of the AA pathway (Figure 72B).

The role of oppositely directed responses of gap junctions and hemichannels is not known, but they may serve cell-protective and restorative purposes. Gap junctions close under pathological conditions, for example, in response to bFGF released after brain trauma and ischemia (Logan et al., 1992) or in response to LPS present during bacterial infection

(Campos de Carvalho et al., 1998), and this may help to prevent the spread of cell death promoting factors to neighboring cells (Krysko et al., 2005). In this case, paracrine ATP signaling via hemichannels may be solicited to compensate for the lost gap junctional communication. Moreover, ATP released via hemichannels may stimulate the recovery of injured tissues (e.g., brain and liver) by its mitogenic actions (Thevananther et al., 2004; Pearson et al., 2005) and its vasodilatory and neuroprotective degradation product adenosine (Erlinge, 1998; Burnstock, 2002; Stone, 2002). Hemichannels can, however, also be considered as pathogenic pores promoting cell death (Evans et al., 2006), and closure of both gap junctions and hemichannels may thus be preferred when cell protection is the primary target. We conclude that the immunostimulant LPS and the growth factor bFGF exert a powerful control over hemichannel ATP release, with inhibition or stimulation being determined by the cell type, the intracellular signaling machinery, and the connexin type present. Given the pleiotropic effects of extracellular ATP, these results suggest that the final effect of LPS and bFGF may, in addition to the various intracellular cascades activated by these agents, also depend on hemichannel modulation.



## Chapter

### 7

# ***In situ bipolar electroporation for localized cell loading with reporter dyes and investigating gap junctional coupling***

Elke De Vuyst<sup>1</sup>, Marijke De Bock<sup>1</sup>, Elke Decrock<sup>1</sup>, Marijke Van Moorhem<sup>1</sup>, Christian C. Naus<sup>2</sup>, Cyriel Mabilde<sup>1</sup>, and Luc Leybaert<sup>1</sup>

<sup>1</sup> Department of Physiology and Pathophysiology, Faculty of Medicine and Health Sciences, Ghent University, Ghent, Belgium

<sup>2</sup> Department of Cellular and Physiological Sciences, Faculty of Medicine, University of British Columbia, Vancouver, BC, Canada

Published in *Biophys. J.* **94**(2):469-479 (2007)

Text and illustrations are modified from the published version

Eternity is a terrible thought. I mean, where is it going to end?

-Tom Stoppard-

## Abstract

Electroporation is generally used to transfect cells in suspension, but the technique can also be applied to load a defined zone of adherent cells with substances that normally do not permeate the plasma membrane. In this study a pulsed high-frequency oscillating electric field is applied over a small two-wire electrode positioned close to the cells. We compared unipolar and bipolar electroporation pulse protocols and found that the latter was ideally suited to efficiently load a narrow longitudinal strip of cells in a monolayer of cell culture. We further explored this property to determine whether electroporation loading was useful to investigate the extent of dye spread between cells coupled by gap junctions, by comparing wild type and stably transfected C6 glioma cells expressing Cx32 (connexin 32) or Cx43. Our investigations show that the spatial spread of 6-carboxyfluorescein (6-CF) loaded via electroporation, and quantified by the standard deviation of Gaussian dye spread or the spatial constant of exponential dye spread, was a reliable approach to investigate the degree of cell-cell coupling. The spread of reporter dye between coupled cells was significantly larger with electroporation loading than with scrape loading, a widely used method for dye coupling studies. We conclude that electroporation loading and dye transfer (ELDT) is a robust technique to investigate gap junctional coupling that combines minimal cell damage with accurate measurement of the degree of cell-cell communication.

## 7.1 Introduction

Electroporation is an efficient and versatile technique to bring plasma membrane impermeable compounds into biological cells. It has been extensively applied for gene transfer, as an alternative to viral vectors (Golzio et al., 2004), and it currently experiences a renewed and vigorous interest for its use as a safe method to increase the efficiency of anti-tumor treatments (electrochemotherapy - Gothelf et al. (2003)) or a promising tool for gene therapy (electroporation gene therapy - Li (2004); Wells (2004)). The spectrum of biological preparations to which electroporation has been applied ranges from single cells (Olofsson et al., 2003), over adherent cells (Teruel et al., 1999), brain slice preparations (Murphy and Messer, 2001), embryonic tissues (Inoue and Krumlauf, 2001; Krull, 2004), skin (Denet et al., 2004), up to whole tissues such as liver, lung and muscle (Aihara and Miyazaki, 1998; Mir et al., 1999; Dean et al., 2003; Matsuno et al., 2003). Electroporation is also well-suited to specifically load a geometrically defined zone in two-dimensional cell arrays, e.g. monolayer cell cultures or viable tissue slices, with membrane impermeable messengers and inhibitor substances to investigate intracellular signaling (Boitano et al., 1992; Braet et al., 2004). The advantage of this technique is the availability of a non-loaded zone in which control cellular responses can be recorded and compared to responses in the loaded zone, according to a paired experimental paradigm. Loading of a restricted zone is done with a special two-wire electrode positioned close to cells (Figure 73A) to which a pulsed high-frequency (50 kHz) oscillating electric field (as opposed to a single high-amplitude pulse) is applied to combine high efficiency and cell survival (Tekle et al., 1991; Boitano et al., 1992; Leybaert and Sanderson, 2001). The efficiency of cell loading is dependent on many factors including the time course and magnitude of the electric field, the composition of the solutions bathing the cells and the cell type and geometry (Cegovnik and Novakovic, 2004). Pulsed high-frequency electric fields can in principle be applied with or without an accompanying net DC (direct current) component, according to a unipolar or bipolar protocol respectively (Chang, 1989). Unipolar electroporation can improve the loading of charged substances by electrophoresis (Satkuskas et al., 2002; Muller et al., 2003), but can also introduce toxicity by current flow and subsequent cell heating (Pliquett, 2003), or the formation of electrolytic side products like oxygen gas and metal ions released from the electrode (Kotnik et al., 2001a). Bipolar electroporation may, on the other hand, be more efficient because it results in poration of the plasma membrane at two opposing sides of the cell while the unipolar protocol porates preferentially at the side where the net DC electric field sums with the local field of the membrane potential (Kotnik et al., 2001b). Uni- and bipolar electroporation have been compared for efficiency and cell survival in transfection experiments (Tekle et al., 1991) and cell suspensions (Kotnik et al., 2001b; Kotnik et al., 2003), but no information is available for its use with monolayer cell cultures and acute loading with reporter dyes or intracellular

messengers for functional studies. While some degree of cell death may be acceptable for transfection purposes (cells will recover and divide during the expression interval), cell death must be extremely low for functional studies. In addition, other parameters like the surface area of loaded cells are important when considering electroporation performance in adherent cell layers. Most studies performed hitherto with pulsed high-frequency electroporation of cell monolayers have been performed with the unipolar protocol (Boitano et al., 1992; Braet et al., 2001; Leybaert and Sanderson, 2001; Braet et al., 2003a; Braet et al., 2004; Vandamme et al., 2004).

The purpose of this study was to compare uni- and bipolar electroporation of monolayer cell cultures in terms of loading efficiency, size of the loaded zone and cell death in this zone. Our results show that bipolar electroporation combines the best loading efficiency with the lowest degree of cell death. In addition, the bipolar protocol allowed to safely load a narrow strip of cells within a culture and we further explored this property to load a restricted zone of cells with a gap junction permeable dye to study dye transfer between the cells via gap junctions. Electroporation loading and dye transfer (ELDT) appeared to be a promising method as an alternative to the widely used scrape loading and dye transfer (SLDT - el-Fouly et al. (1987); Meda (2001)). The advantage of both ELDT and SLDT is that quantification of dye coupling takes place over a large population of cells as opposed to fluorescence recovery after photobleaching (FRAP - Deleze et al. (2001)) or local activation of a molecular fluorescent probe (LAMP - Dakin et al. (2005)) that investigate dye coupling in a single cell (or a small group of cells). ELDT has the advantage that it is associated with minimal cell death, as opposed to SLDT that involves mechanical disruption of the plasma membrane to get the fluorescent reporter dye into the cells. Our results demonstrate that the level of dye coupling determined with ELDT is significantly above the level monitored with SLDT and may thus better reflect the normal degree of cell-cell coupling.

## **7.2 Material and Methods**

### **7.2.1 Cell cultures**

Initial experiments aimed at finding the best electroporation settings were done on ECV304 cells (bladder cancer epithelial cells - ECACC, Salisbury, UK) grown as monolayers on Nunclon 4-well plates (NUNC Brand products, Denmark). ECV304 cells were maintained in Medium-199 (Invitrogen, Merelbeke, Belgium) with 10 % fetal bovine serum and 2 mM glutamine. Experiments were done on confluent cultures (cell density  $2100 \pm 50$  cells/mm<sup>2</sup>; n = 4) with the cells bathed in Hanks' balanced salt solution buffered with 25 mM HEPES (HBSS-HEPES, pH 7.4) and at room temperature. Further experiments on dye coupling were performed on C6 glioma cells either as WT or stably transfected with Cx32 (C6-Cx32 - Bond



et al., 1994) or Cx43 (C6-Cx43 - Zhu et al., 1991). C6 was grown to confluency in DMEM-Ham's F12 (1:1) with 10 % FBS and 2 mM glutamine.

## 7.2.2 Electroporation procedure

Electroporation loading was done with the cells on the microscope stage and using a special electrode consisting of two parallel wires (Pt-Ir) supported by a holder (Figure 73A). All electroporation experiments were done at room temperature. Cultures were washed twice with a special electroporation buffer with low electrical conductivity (300 mM sorbitol, 4.2 mM  $\text{KH}_2\text{PO}_4$ , 10.8 mM  $\text{K}_2\text{HPO}_4$ , 1 mM  $\text{MgCl}_2$  and 2 mM HEPES, pH 7.20). After complete removal of this solution, a small volume (10  $\mu\text{l}$ ) of electroporation buffer containing the fluorescent dye was pipetted on the electrode wires. The applied solution settled between the electrode wires and the cells just underneath by capillary forces. The dyes used were 6-CF and dextran fluoresceins of 3, 10 and 40 kDa molecular weight, all from Molecular Probes (Invitrogen). The net charge of the applied probes was -2 for 6-CF and -1 for the dextran fluoresceins. Unipolar or bipolar electroporation pulses were applied to the electrode in a gated manner, delivering repeated trains of 2 ms pulses as depicted in Figure 73C and D. The voltage amplitude of the electroporation pulses was expressed as the peak value measured relative to the zero level (Figure 73). The electroporation signal was a 50 kHz signal going either in positive direction only, resulting in a net DC component, or alternating between positive and negative polarity without a net DC component. The choice of this particular frequency was based on the study performed by Tekle et al. (1991) and on follow-up work with similar settings in the study of Boitano et al. (1992). After electroporation, the cultures were washed with HBSS-HEPES and images were taken after 15 min unless otherwise indicated in the figure legends. Images were acquired on a Nikon TE300 inverted microscope equipped with a x 2 (CFI Plan Apo, NA 0.1) or x 10 objective (CFI Fluor, NA 0.5) and DS-5M camera head (Nikon Benelux, Brussels, Belgium), and were analyzed with custom-developed software written in Visual C++ (Fluoroframes program). Cell viability after electroporation was assayed 10 min after application of the procedure, by incubating the cells for another 10 min in a 0.4 % trypan blue solution (Sigma, Bornem, Belgium) followed by 3 washes in HBSS-HEPES and counting the number of trypan positive cells in four images of 0.49 by 0.37 mm (trans-illumination, Nikon x 10 objective, CFI 6 Fluor, NA 0.5). The number of trypan blue positive cells was zero in non-electroporated cell zones.

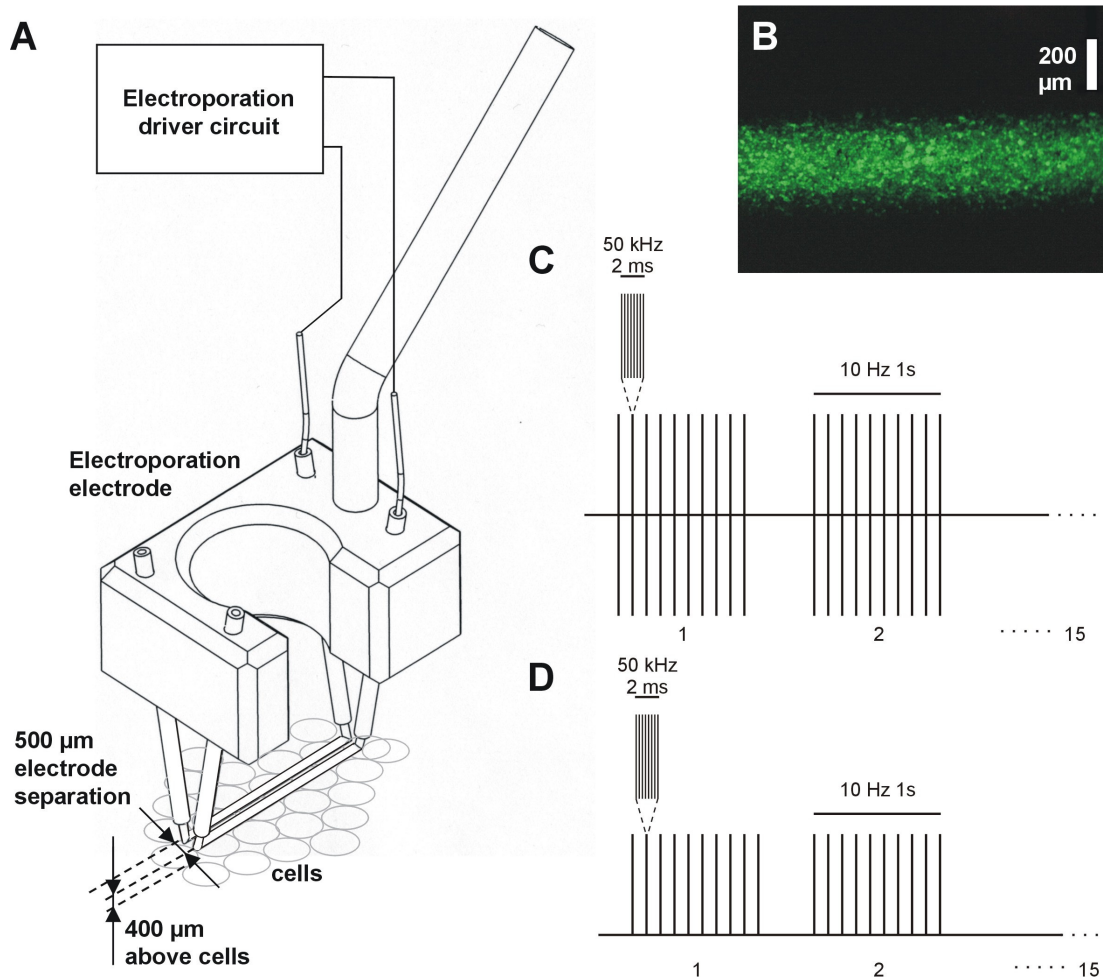


**Figure 73: Electroporation set-up**

(A) General set-up with the electroporation electrode positioned above the cell monolayer. (B) Illustration of a 6-CF loaded zone in confluent ECV304 cells. (C) Pulse protocol for bipolar electroporation. (D) Unipolar pulse protocol. The total duration of electroporation in these protocols was 15 s.

The electronic drive circuits to deliver uni- or bipolar electroporation signals are schematically depicted in Figure 74. These devices are not commercially available (a review of various drive circuits can be found in Puc et al. (2004)). Figure 74 illustrates a generator circuit built around an NE555 timer configured as a gatable, astable multivibrator delivering trains of 50 kHz 50 % duty cycle pulses. Positive, negative and bipolar output is obtained by weighted subtraction of the 50 kHz input signal. The gate is controlled by one of the output lines of the LPT port from a PC, with a small C-program running under Windows (with all interrupts disabled to allow correct timing) functioning as a programmable pulse generator. Two amplifier circuits were used in the experiments described in this paper: a true DC high voltage amplifier and a fully symmetrical mosfet amplifier with a toroidal step-up transformer at the output stage (Figure 74). The transformer-based amplifier has the advantage of a floating high voltage output and a true mean zero signal over the pulse trains, so as to minimize the DC component applied to the electrode. The frequency response of the two

amplifiers was characterized by a -3 dB point at 90 kHz and 55 kHz respectively (electrode connected and immersed into electroporation solution).

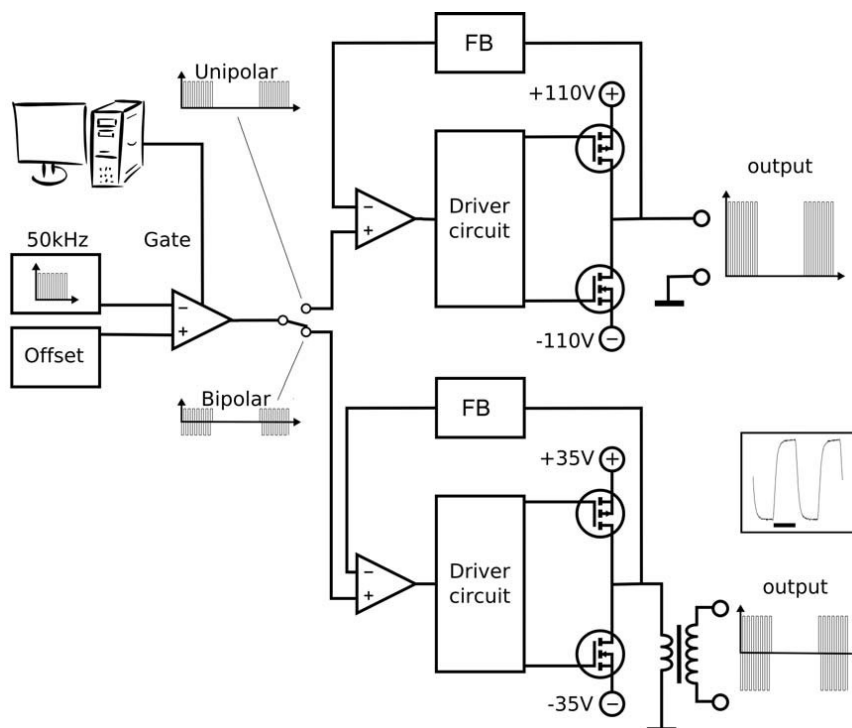


**Figure 74:** Schematic overview of the generator and amplifier set-up used for unipolar and bipolar electroporation

The scheme in the upper half demonstrates a true DC high voltage amplifier used for unipolar electroporation (FB signifies feed-back circuit). This amplifier can in principle be used for bipolar electroporation but to minimize the DC component, we developed an amplifier with a transformer output, depicted in the lower half. The inset illustrates the first two periods of the bipolar output of the transformer-based amplifier - the peak amplitude was 50 V (100 V total swing) and the scale bar delineates 10  $\mu\text{s}$ . Pulse flanks had an exponential time course characterized by a time constant of 1.75  $\mu\text{s}$  on average for the unipolar amplifier and 2.86  $\mu\text{s}$  for the bipolar amplifier.

### 7.2.3 Scrape loading and dye transfer

Confluent monolayer cultures were washed two times with nominally  $\text{Ca}^{2+}$ -free HBSS-HEPES (CF-HBSS-HEPES, same  $\text{Ca}^{2+}$ -composition as in electroporation buffer). Cells were incubated during 1 min in CF-HBSS-HEPES containing 0.4 mM 6-CF; a linear scratch (one per culture) was made across the cell layer using a syringe needle and the cells were left for another minute in the same solution. Cultures were then washed four times with HBSS-HEPES, left for 15 min at room temperature and images were taken as described for electroporation loading. For the combined ELDT/SLDT experiments illustrated in Figure 81F, cells were washed 2 times with electroporation buffer and a scratch was applied after removal of the buffer, immediately followed by electroporation of the culture with 0.4 mM 6-CF.

### 7.2.4 Fluorescence recovery after photobleaching

Confluent monolayer cultures grown on glass bottom microwell plates (MatTek Corporation, Ashwood, MA) were loaded with 5-CFDA-AM (10  $\mu$ M carboxyfluorescein diacetate acetoxy methylester) in HBSS-HEPES for 45 min at room temperature, followed by a 30 min de-esterification period. Fluorescence within a single cell was photobleached by spot exposure to the 488 nm line of an Argon laser and imaging (again at 488 nm excitation) was done with a custom-made video-rate confocal laser scanning microscope (Leybaert et al., 2005) with a x 40 oil immersion objective (CFI Plan Fluor, NA 1.4, Nikon Benelux, Brussels, Belgium) and recovery was measured over a 5 min time period after photobleaching. In the experiments where supernatant of scraped cultures was used, the supernatant was obtained 1 min after the scratch (conditions as described higher) and acceptor cultures were exposed for 10 min before the start of the FRAP experiments.

### 7.2.5 Western blotting

Cell protein lysates were extracted by treatment of confluent cultures with radio immuno precipitation assay buffer (RIPA - 25 mM Tris, 50 mM NaCl, 0.5 % NP40, 0.5 % deoxycholaat, 0.1 % SDS, 5.5 %  $\beta$ -glycerophosphate, 1 mM DTT, 2 % phosphatase inhibitor cocktail, 2 % mini EDTA-free protease inhibitor cocktail) and sonicated by three 10 s pulses. Separation of Triton X-100-soluble and -insoluble material was done essentially according to the method described by Cooper and Lampe (2002). Cells from 75 cm<sup>2</sup> culture flasks were washed 3 times with phosphate buffered saline (PBS; 137 mM NaCl, 2.68 mM KCl, 0.90 mM CaCl<sub>2</sub>, 0.334 mM MgCl<sub>2</sub>.6H<sub>2</sub>O, 1.47 mM KH<sub>2</sub>PO<sub>4</sub>, 6.46 mM Na<sub>2</sub>HPO<sub>4</sub>.2H<sub>2</sub>O, pH 7.4) and harvested in ice cold 1 % Triton X-100 in PBS supplemented with 50 mM NaF, 1 mM Na<sub>3</sub>VO<sub>4</sub>, 1 % protease inhibitor cocktail (Sigma), 1 % phosphatase inhibitor cocktail 1 and 2 (Sigma) and 1 % mini-EDTA-free protease inhibitor cocktail (Roche Diagnostics). Samples were separated into Triton X-100-soluble and -insoluble fractions by centrifugation at 16,000 x g for 10 min. Triton X-100-insoluble fractions (pellets) were resuspended in 1 x Laemmli sample buffer (10 % glycerol, 2.3 % SDS, 125 mM Tris, pH 6.8 - Laemmli (1970)) and sonicated by five 10 s pulses. Protein concentration was determined with a biorad DC protein assay kit (Biorad), and absorbance was measured on a plate reader with a 590 nm long-pass filter. Proteins were separated on a 10 % SDS-poly-acrylamide gel and transferred to a nitrocellulose membrane (GE Healthcare, Little Chalfont, Buckinghamshire, UK). Blots were probed with a rabbit polyclonal anti-rat Cx43 antibody (Sigma, 1/10,000), a rabbit polyclonal anti-rat Cx32 (Sigma, 1/500) or a rabbit polyclonal anti-rat  $\beta$ -tubulin (Abcam, Cambridge, UK; 1/5,000; loading control) followed by alkaline phosphatase conjugated goat anti-rabbit IgG (Sigma, 1/8,000) and detection was done with nitro blue tetrazolium/5-bromo-4-chloro-3-indolyl phosphate reagent (Zymed, Invitrogen).

### 7.2.6 Immunocytochemistry

Cells grown on glass coverslips were fixed with 4 % paraformaldehyde in PBS (10 min, room temperature) and subsequently permeabilized with 0.2 % Triton X-100 in PBS (10 min, room temperature). Cells were incubated for 1 h with primary antibody (rabbit polyclonal anti-rat Cx32 (Sigma, 1/1,000) and a rabbit polyclonal anti-rat Cx43 (Sigma, 1/10,000)) diluted in blocking solution (0.4 % gelatin in PBS), washed three times with PBS and incubated for 1 h with the secondary antibody coupled to an Alexa fluorophore 488 (goat anti-rabbit IgG antibody; Molecular Probes, 1/500). Cell nuclei were stained with DAPI (4',6-diamidino-2-phenylindole - 1 µg/ml) and the preparations were then mounted in Vectashield (Vector Laboratories) to prevent photobleaching. Images were acquired as described for electroporation treated cultures, but with a x 100 oil immersion objective (Fluor, NA 1.3, Nikon Belux, Brussels, Belgium) instead.

### 7.2.7 Data analysis and statistics

For measurements of the fluorescence intensity in the electroporation zone, images were first thresholded. The threshold corresponded to the upper level of the background noise and was determined from the fluorescence histogram of non-electroporated cells (cells outside the electroporation zone) as the fluorescence intensity at the right flank of the distribution where the frequency was half-maximal. The average value of above threshold pixels was then calculated. This value was subsequently converted to a relative fluorescence intensity by dividing it by the fluorescence intensity of a thin layer of the loading solution sandwiched between two coverslips. The thickness of the layer was adjusted to approximate the thickness of monolayer cell cultures, which was  $20 \pm 2.2 \mu\text{m}$  ( $n = 9$ ) as determined by inspection of fluo-3 loaded ECV304 cultures with a confocal laser scanning microscope. The size of the electroporation zone was determined by applying a threshold to the images (as described above) and calculating the surface area of above threshold pixels. Fluorescence intensity profiles perpendicular to the main axis of the electroporation loaded strip were determined by averaging all picture lines in this direction into an array of line width, using software written in Visual C++. Curve fitting of the Gaussian intensity profiles was done with the program Prism 3.0 (Graphpad Software, San Diego, CA) according to the following equation:

$$y = y_{\text{off}} + y_{\text{max}} \cdot e^{-1/2 \cdot (x - x_{\text{max}})^2 / \sigma^2}$$

Where  $y$  is the fluorescence intensity,  $y_{\text{off}}$  the y-offset,  $y_{\text{max}}$  the peak value minus  $y_{\text{off}}$ ,  $x$  the distance,  $x_{\text{max}}$  the x-coordinate of the peak, and  $\sigma$  the standard deviation of the Gaussian relation.

The spatial constant  $\lambda$  of dye spread was determined from the exponentially decreasing portion of the diffusion profiles obtained in ELDT or SLDT experiments. A single  $\lambda$  value was determined from both the right and left flanks in each experiment. The data are expressed as mean  $\pm$  s.e.m. with 'n' denoting the number of experiments on different cell cultures. Comparison of two groups was done using a one-tailed unpaired t-test with a p-value below 0.05 indicating significance. Comparison of more than two groups was done with one-way ANOVA and a Bonferroni post test. Statistical significance is indicated in the graphs with a single symbol (\* or #) for  $p < 0.05$ , 2 symbols for  $p < 0.01$  and 3 symbols in case  $p < 0.001$ .

## 7.3 Results

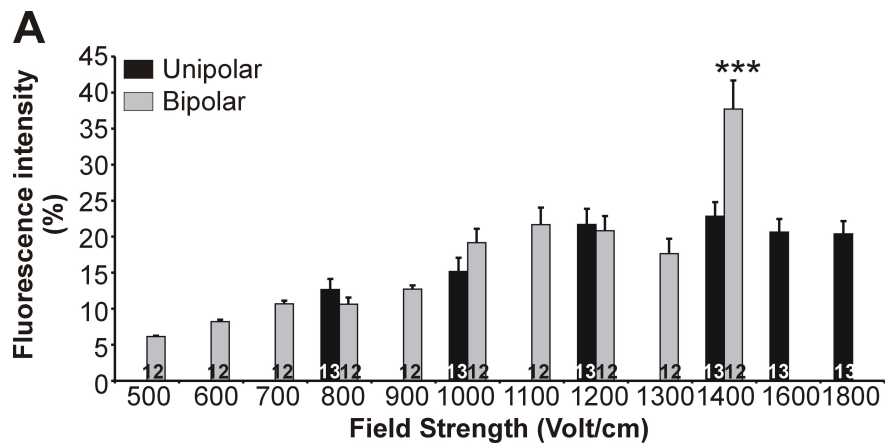
Electroporation of confluent ECV304 monolayer cell cultures was performed with an electrode consisting of two parallel wires placed on the microscope stage and positioned such that the electrode wires were in close apposition to the cells (Figure 73A). Application of the electroporation procedure in the presence of the fluorescent reporter dye 6-CF (100  $\mu$ M) resulted in the loading of a band-like cell zone beneath the electrode wires (Figure 73B). To quantify the efficiency of cell loading with the reporter dye, we determined the size of the electroporation loaded zone and the average fluorescence intensity within this zone. The fluorescence intensity was expressed relative to the fluorescence intensity of a layer of cell thickness of the loading solution, thus giving an estimate of the efficiency of the loading procedure. The size of the loaded zone was determined by measuring the surface area of cells that displayed a fluorescence intensity above the background level determined in non-loaded cell zones within the same culture (see section 7.2).

### 7.3.1 Experiments with a low molecular weight dyes

We investigated the fluorescence intensity and the size of the loaded zone with 6-CF as a reporter dye making use of uni- and bipolar electroporation. The pulse protocols for the two methods are illustrated in Figure 73C and D and the performance for both methods is depicted in Figure 75. Field strengths below 400 V/cm (i.e. 20 V peak amplitude applied over electrode wires separated over 0.5 mm - see Figure 73) did not result in significant cell loading. Above this field strength, both uni- and bipolar electroporation resulted in loading efficiencies that increased with the field strength (Figure 75A). Unipolar electroporation gave loading efficiencies in the order of 20 - 25 % in the 1,200 - 1,800 V/cm range and similar values were obtained for bipolar electroporation in the 1,000 - 1,300 V/cm range. None of the bars in these two voltage ranges showed significant differences upon comparison with analysis of variance (average loading efficiency of 21.4 % over the former and 19.8 % over the latter range).

Increasing the field strength of unipolar electroporation in the 1,200 - 1,800 V/cm range did not result in better loading efficiencies, but was associated with increased cell death (Figure 75B). For bipolar electroporation, increasing the field strength above 1,300 V/cm further increased the loading efficiency and at 1,400 V/cm the efficiency was ~ 38 % (Figure 75A), significantly above the efficiency observed for unipolar electroporation with any of the applied field strengths ( $p < 0.001$ ). At this setting, cell death associated with the bipolar protocol attained values in the order of what was observed in unipolar mode (~ 90 cells on a total of 2,100 cells/mm<sup>2</sup> in the electroporated zone, i.e. ~ 4 % of the electroporated cells). Thus, for the same degree of cell death, bipolar electroporation allowed more efficient loading.

Analysis of the size of the electroporation-loaded zone gave a somewhat different picture. The surface area of loaded cells increased with the field strength for both uni- and bipolar electroporation but the unipolar protocol yielded larger loading zones as compared to the bipolar protocol (Figure 75C). For unipolar electroporation the loaded zone measured around 2 mm<sup>2</sup> at 1,600 - 1,800 V/cm, corresponding to approximately 40 % of the surface area delineated by the electrode wires. In sum, the surface area of loaded cells was larger with unipolar as compared to bipolar electroporation (Figure 75C). Thus bipolar electroporation was better suited to load a narrow strip of cells, with a full-width at half-maximum in the order of 250  $\mu$ m (for an electrode wire separation of 500  $\mu$ m).



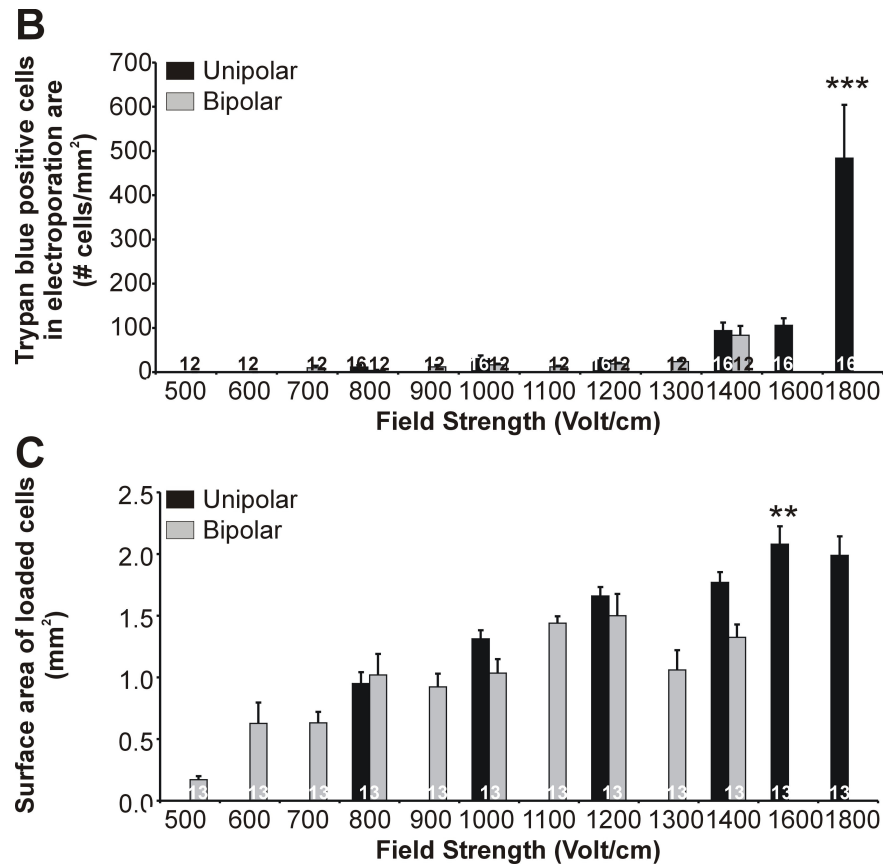


**Figure 75: Comparison of uni- and bipolar electroporation in ECV304 cells**

(A) Loading efficiency for 6-CF electroporation in function of the electric field strength. The three star symbols indicate a significant difference with  $p < 0.001$ , compared to all other bars in this graph. (B) Cell death in function of the electric field strength, as determined with trypan blue. Stars indicate significancies with  $p < 0.001$  compared to all the other unipolar data (other significant differences are given in the text). (C) Size of the electroporation loaded cell zone in function of electric field strength. The star symbol represents a significant difference with  $p < 0.01$  compared to all bipolar data.

### 7.3.2 Experiments with higher molecular weight dyes

The electroporation performance was further investigated with fluorescent probes of 3 and 40 kDa molecular weights (100  $\mu\text{M}$ ). We chose 1,200 V/cm for both unipolar and bipolar electroporation for the higher molecular weight dye, based on the fact that this setting combined a low degree of cell death with acceptable loading efficiency. With this setting, cell death in the electroporation zone averaged  $28 \pm 4$  cells per  $\text{mm}^2$  ( $n = 21$ ) for unipolar and  $18 \pm 3$  cells per  $\text{mm}^2$  ( $n = 16$ ) for bipolar electroporation (Figure 75B), corresponding to 1.3 and 0.8 % of the total number of cells in this zone respectively (both values were significantly different from each other with  $p < 0.05$  using a t-test).



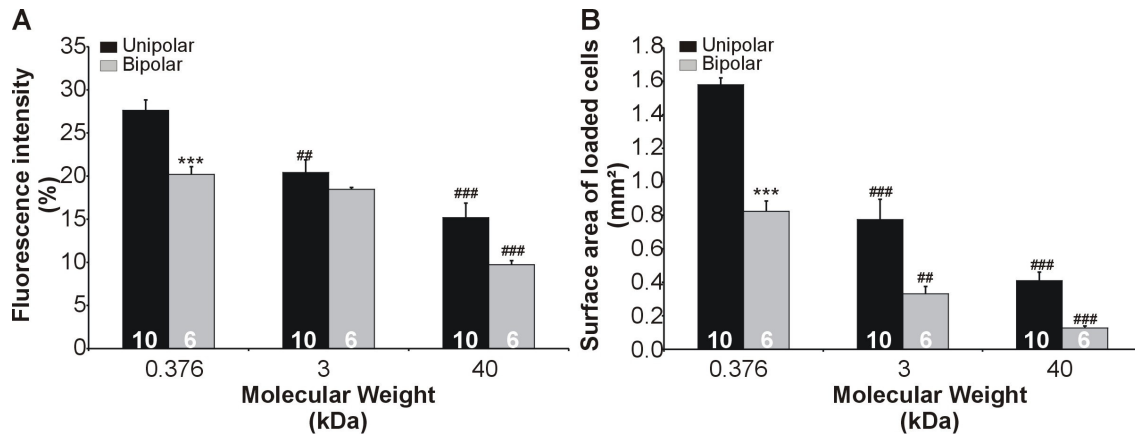


**Figure 76: Uni- and bipolar electroporation performance for various fluorescent reporter dyes in ECV304** (A) Electroporation loading efficiency in function of molecular weight. (B) Size of the electroporation loaded cell zone in function of molecular weight. Stars indicate significancies as compared to the corresponding unipolar condition; number signs indicate significancies compared to the corresponding bar for 0.376 kDa (6-CF).

The fluorescence intensity and the size of the electroporation-loaded zone in function of the molecular weight of the reporter dye are illustrated in Figure 76 for unipolar and bipolar electroporation. The experiments demonstrate decreased loading performance for probes with larger molecular weights, as expected because of slower diffusion. With the electroporation settings chosen, unipolar pulses were better than bipolar pulses in terms of loading efficiencies and size of the loaded zones for the various fluorescent probes used. The larger loading zone observed with the 0.376 kDa 6-CF (Figure 76B) was not due to spreading of the dye via gap junctions between cells (allowing the passage of substances below  $\leq 1.2$  kDa), because the ECV304 subclone used in these experiments did not express the major connexins 32 or 43 (Figure 77).

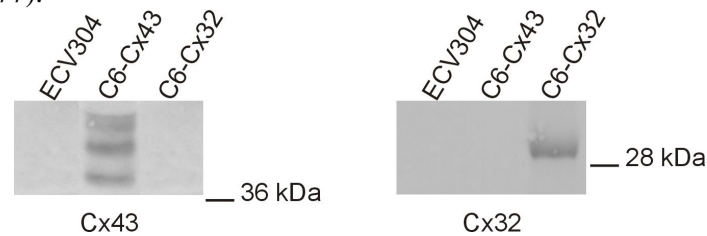


**Figure 77: Western blot analysis of connexin expression**

Western blots illustrating connexin 43 and 32 expression patterns in ECV304, C6-Cx32 and C6-Cx43.

### 7.3.3 Experiments on cells coupled by gap junctions

We further performed experiments with bipolar electroporation (1,000 V/cm field strength for C6 cells) to investigate dye spread from the loaded cell strip to non-loaded zones in cells that are coupled by gap junctions. We used C6 glioma cells stably transfected with Cx32 (C6-Cx32 - Bond et al. (1994)) or Cx43 (C6-Cx43 - Zhu et al. (1991)) for this purpose. Both cell

lines displayed significantly stronger expression of their respective connexins as compared to wild type C6 cells (C6-WT) in Western blot analysis (Figure 78A and B). The majority of the connexins was present in the Triton X-100-insoluble fraction, which corresponds to the fraction that contains the gap junctional plaque (Musil and Goodenough, 1991; Musil and Goodenough, 1993). Immunocytochemistry showed immunopositive dots and plaques at cell-cell interfaces (Figure 78C).

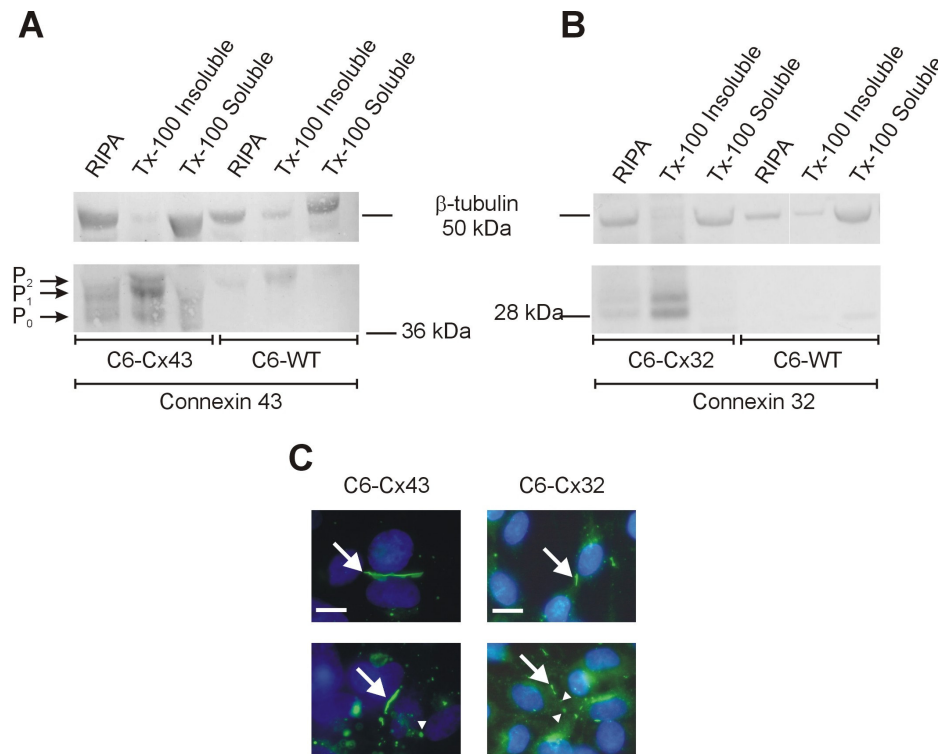


**Figure 78: Connexin expression in C6-Cx43 and C6-Cx32 cells**

(A - B) Western blots displaying connexin expression in total protein lysates (RIPA) and Tx-100-soluble and -insoluble fractions. The majority of connexins were present in the Triton X-100-insoluble phase, indicating incorporation into gap junctions. (C) Numerous immunopositive plaques and dots were observed at cell-cell interfaces - nuclei were stained with DAPI. The arrows point to large gap junctional plaques, arrowheads to immunopositive dots. Scale bar represents 100  $\mu$ m.

In FRAP experiments, C6-Cx32 and C6-Cx43 showed significantly higher cell-cell coupling when compared to C6-WT, as illustrated in Figure 79.

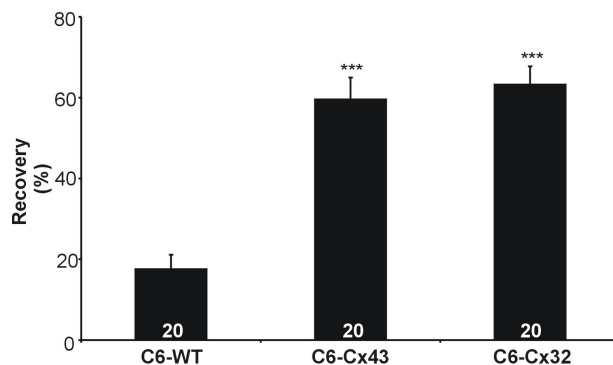


**Figure 79: Gap junctional coupling in C6-WT, C6-Cx43 and C6-Cx32 cells**

Connexin expressing cells showed significant higher average recovery (measured with FRAP) when compared to C6-WT cells. Star signs indicate significance compared to C6-WT cells.

Accordingly, electroporation with the gap junction permeable dye 6-CF (400  $\mu$ M) resulted in a significantly larger fluorescent zone in C6-Cx32 and Cx43 as compared to C6-WT (Figure 80A), illustrating dye transfer from the electroporation loaded zone to neighboring cells via gap junction channels. The surface area of fluorescently loaded cells of C6-WT cells was comparable with the surface area of ECV304 cells that did not express any of the major connexins (Cx32 and Cx43). Electroporation of C6-Cx32 and C6-Cx43 with the gap junction impermeable dye, 3 or 10 kDa dextran fluoresceins (0.4 mM), yielded very small zones of loaded cells as illustrated in Figure 80A for C6-Cx32, but because the loading efficiency of these higher molecular weight probes was intrinsically different from 6-CF (see Figure 76) these data cannot be directly compared to the 6-CF data. We evaluated another parameter indicative of dye spread that is independent on the loading efficiency of the fluorescent reporter. The profile of the fluorescence intensity along an axis perpendicular to the length axis of the loaded strip was bell-shaped, as illustrated in Figure 80B, and could reliably be fitted to a Gaussian curve with standard deviation sigma ( $\sigma$ ). This is an intrinsic parameter of dye spread and corresponds to the distance over which 68.3 % of the dye molecules have diffused in both directions from the initial loading strip. Figure 80C demonstrates that  $\sigma$  for 6-CF spread was significantly larger in C6-Cx32 cells and C6-Cx43 cells as compared to C6-WT. Treatment of the cells with the gap junction blocker carbenoxolone (25  $\mu$ M, 30 min) significantly reduced  $\sigma$ . This parameter was also strongly reduced when dye spread was probed with the gap junction impermeable 3 or 10 kDa dextran fluoresceins (Figure 80C).

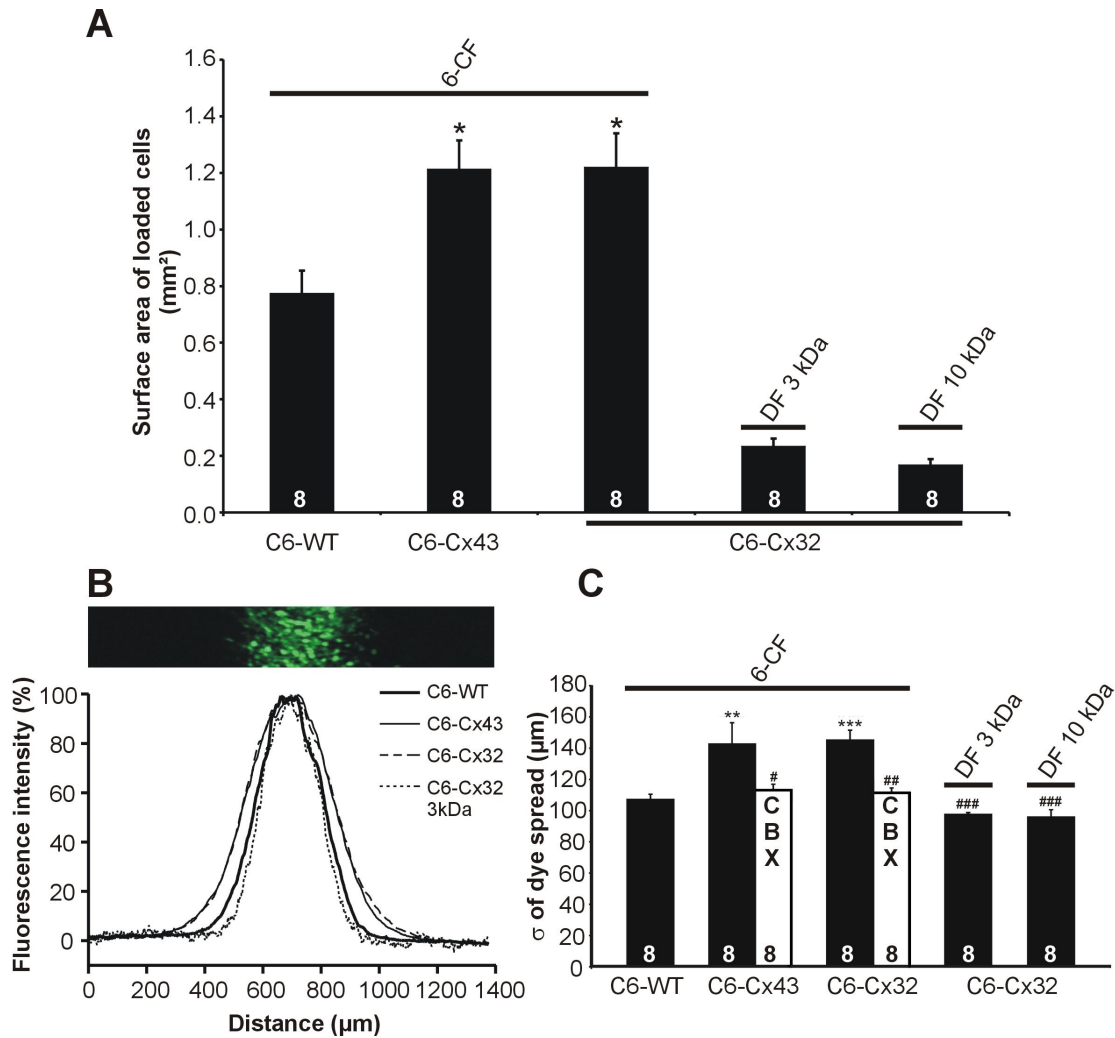


**Figure 80: Bipolar electroporation loading and dye transfer via gap junctions in C6 glioma cells**

(A) Size of the 6-CF loaded cell zone in C6-WT, C6-Cx32, and C6-Cx43, 30 min after electroporation. The size of the loaded zone in C6-WT was not different from ECV304, as can be appreciated by comparison to Figure 76B. In C6-Cx43 and C6-Cx32 the loaded zone was significantly larger than in C6-WT. Electroporation loading with the gap junction impermeable dyes 3 or 10 kDa dextran fluorescein (DF) resulted in very small zones, due to the low loading efficiency of these high molecular weight probes into the cells when compared to 6-CF (Figure 76A). (B) Example traces of the fluorescence intensity profile for the conditions indicated, 30 min after electroporation. The fluorescence intensity in the ordinate was normalized to the peak of the intensity profile ( $n = 8$ ). The image on top of the graph illustrates a representative example of 6-CF loading in C6-WT. (C) Averaged data for the standard deviation of dye spread,  $\sigma$ , as determined by fitting individual intensity profiles to a Gaussian equation. The  $\sigma$  of 6-CF spread was significantly larger in C6-Cx43 and C6-Cx32 as compared to C6-WT. Carbenoxolone (CBX) treatment (25  $\mu$ M, 30 min) significantly reduced  $\sigma$  and an even lower  $\sigma$  was observed when the C6-Cx32 cells were loaded with the gap junction impermeable 3 or 10 kDa dextran fluoresceins. Star signs indicate significancies as compared to C6-WT and number signs reflect significancies compared to 6-CF.

*In situ* electroporation loading appeared to be useful to investigate gap junctional coupling between cells and will further be referred to as electroporation loading and dye transfer (ELDT), analogous to the scrape loading and dye transfer (SLDT) method. In SLDT, a linear scratch is made over the culture with a needle, followed by dye uptake in disrupted cells and

dye transfer via gap junctions to neighboring cells (el-Fouly et al., 1987; Meda, 2001). The dye diffusion profiles obtained in SLDT experiments are difficult to fit by a Gaussian relation, because of the presence of a central dip where the cells are removed as a result of scraping. We therefore compared ELDT and SLDT by analyzing the spatial constant  $\lambda$  of dye spread, as determined by fitting the flanks of the diffusion profiles by an exponentially decaying function (Figure 81).  $\lambda$  corresponds to the distance where the dye fluorescence has decreased by a factor  $1/e$  and is, like  $\sigma$ , an intrinsic parameter of dye spread not affected by the absolute fluorescence levels. Figure 81A-D illustrates a significantly larger  $\lambda$  in cells transfected with Cx32 or Cx43 when compared to C6-WT, as expected. Moreover, the  $\lambda$  obtained in ELDT experiments was approximately twice as large as with the SLDT procedure. This difference may in part be related to the fact that the flanks of the electroporation loaded profiles are less sharply defined as those obtained with scrape loading, as a consequence of a gradual fall-off of the electric field strength away from the electrode. However, a closer look to Figure 81B shows that the change in diffusion profile from WT to connexin expressing cells is much more apparent in ELDT as compared to SLDT and this is also clear from Figure 81C and D (note that the ordinates have different calibrations in C and D). The increase of  $\lambda$  in connexin expressing cells as compared to WT cells, symbolized by  $\lambda_{Cx} - \lambda_{WT}$ , is depicted in Figure 81E, illustrating that this parameter is more than twice as large when probed with ELDT as compared to SLDT (40 - 50  $\mu\text{m}$  range for ELDT and below 20  $\mu\text{m}$  for SLDT). These data indicate that the degree of coupling determined with ELDT is significantly larger than with SLDT. Cell scraping as performed in SLDT involves strong mechanical stimulation with plasma membrane rupture, leakage of cell contents into the medium and activation of various signaling cascades. We tested whether dye spread measured with ELDT was influenced by the SLDT procedure, by applying the SLDT scrape immediately before the start of ELDT, as illustrated in Figure 81F. These experiments showed that  $\lambda_{Cx} - \lambda_{WT}$  determined from ELDT experiments was significantly lower in cultures that had received the SLDT scratch. In a further step, we tested whether supernatant obtained from SLDT-treated cultures influenced dye coupling in acceptor cultures as measured in FRAP experiments. FRAP recovery in supernatant exposed cultures was mildly but not significantly depressed in C6-Cx43 and not affected in C6-Cx32 (Figure 82) indicating that decreased dye coupling observed with SLDT is caused by intracellular factors rather than by factors released into the medium.

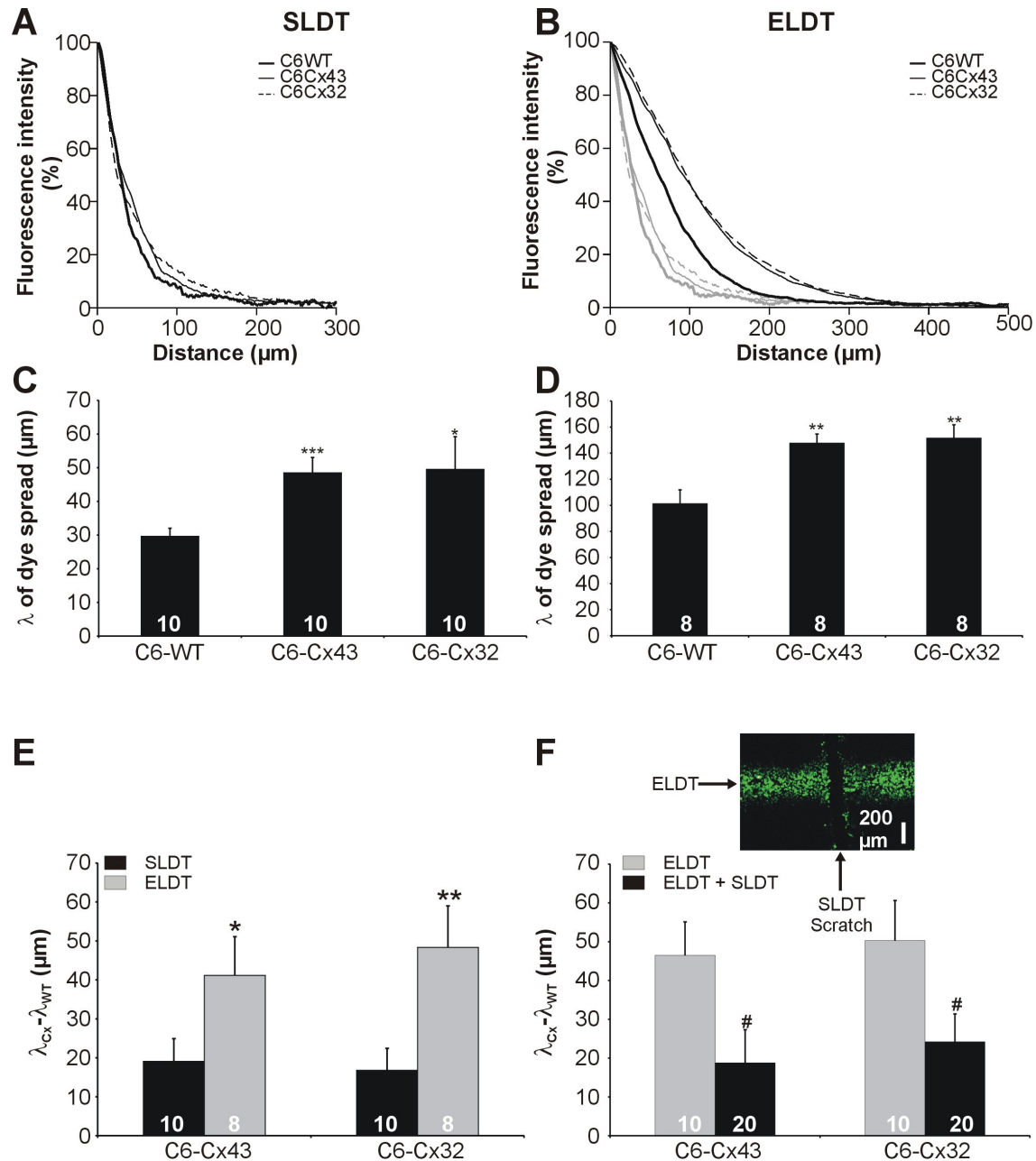


**Figure 81: Comparison of SLDT and ELDT**

(A) Examples of exponential diffusion profiles obtained in C6-WT, C6-Cx32, and C6-Cx43 cells after scrape loading (n = 10). (B) Diffusion profiles obtained with electroporation loading (n = 8). The gray curves are copies of the curves illustrated in A, added for comparison. (C and D) Summary graphs of the spatial constant of dye spread ( $\lambda$ ) determined in the experiments illustrated in A and B respectively. Star signs give significancies as compared to C6-WT. (E) Increase of  $\lambda$  in connexin expressing C6 cells as compared to WT with the two loading protocols. Dye spread was more than twice as large in ELDT as compared to SLDT experiments. Stars show significancies as compared to SLDT. (F) Decrease of  $\lambda$  determined with ELDT in cultures that received a SLDT scratch prior to electroporation. The picture illustrates the horizontal ELDT strip and the vertical SLDT scratch applied just before electroporation. Dye spread decreased to the level observed in SLDT when ELDT was done in cultures that received the SLDT scratch. Number signs indicate significancies as compared to ELDT.

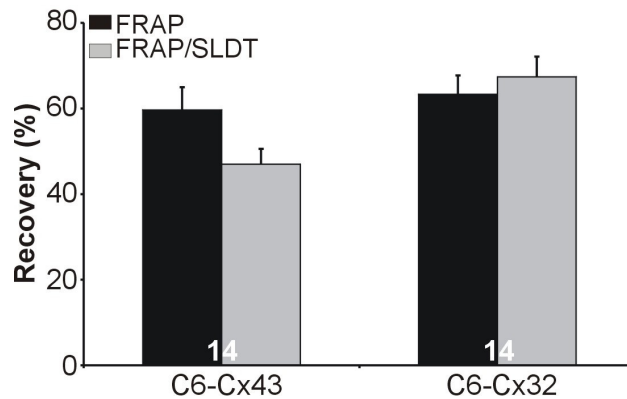


**Figure 82: FRAP recovery in C6-Cx43 and C6-Cx32 cells**

Fluorescence recovery was only minor influenced by exposing the cells to supernatant of cultures that received SLDT treatment.

## 7.4 Discussion

Electroporation is a technique that uses electrical pulses to create transient aqueous pores in the plasma membrane that act as a conduit for the delivery of cell-impermeable substances (reviewed in Gehl (2003)). The molecular processes taking place during permeabilization are currently not fully understood but various aspects of pore formation have been experimentally investigated and mathematically modeled (Krassowska and Filev, 2007). Pore formation happens on a time scale of microseconds and is followed by membrane resealing that is very much slower and proceeds on a time scale of minutes (Gehl, 2003). If the field strength becomes too strong, pore resealing may be hampered, resulting in cell death. Recent work indicates that pore formation depends on the time during which the electroporation pulses exceed a certain threshold value (Weaver, 1995a; Weaver, 1995b; Weaver, 1995c; Kotnik et al., 2003). For this reason, care should be taken in comparing unipolar and bipolar electroporation protocols as applied in the present study. Several differences between the two protocols make comparisons at the level of field strength intensity difficult: first, the unipolar pulses had a duty cycle of 50 %, i.e. the pulse was ON for 10  $\mu$ sec and OFF for the next 10  $\mu$ sec in the 50 kHz bursts while the OFF period was lacking in the bipolar protocol (which switched from 10  $\mu$ sec positive deflection to 10  $\mu$ sec negative deflection without OFF period). Second, small differences in the response time of the two amplifiers may result in slightly different above threshold voltage profiles and thus loading efficiencies. In addition, the reported field strengths should only be taken as indicative numbers: electroporation behavior depends on numerous influences, with cell geometry, electrode position, temperature, electroporation solution as some of the most obvious influences that may vary substantially between different set-ups. Notwithstanding these considerations, the aim of the present work was to establish whether *in situ* electroporation with oscillating electric fields could be applied for functional studies on cell-cell dye coupling via gap junctions. All previous work (from our

group and others) with *in situ* electroporation of adherent cell monolayers has been done with unipolar pulse protocols (Boitano et al., 1992; Braet et al., 2001; Leybaert and Sanderson, 2001; Braet et al., 2003a; Braet et al., 2004; Vandamme et al., 2004). Comparison of unipolar and bipolar electroporation is done in the context of cell transfection in suspension cultures (Tekle et al., 1991; Kotnik et al., 2001b), but not for functional studies where cell death is an important issue. Taken over the range of applied electric field strengths, the efficiency of bipolar loading of the low molecular weight probe 6-CF was on average comparable to unipolar loading (Figure 75A). At 1,400 V/cm, the bipolar protocol gave a significantly higher loading efficiency in the order of almost 40 %. Unipolar electroporation loaded the largest zone of cells (Figure 75C), but was associated with sharply increasing cell death (Figure 75B). Cell death with the bipolar protocol was comparable with unipolar electroporation but for the same amount of cell death, bipolar electroporation gave better loading efficiency at 1,400 V/cm. A field strength of 1,200 V/cm combined good loading with an acceptable degree of cell death for the unipolar and bipolar protocols. Electroporation loading of higher molecular weight dyes with these settings showed superior loading in terms of efficiency and size of the loaded zone with the unipolar as compared to the bipolar protocol. Efficiencies approximately halved between 0.376 and 40 kDa molecular weights (Figure 76A) and the decline was much more pronounced for the size of the loaded zone (Figure 76B).

Few researchers have compared uni- and bipolar protocols for *in situ* electroporation of monolayer cultures, for reasons delineated by Kotnik et al. (2001a, b), mainly related to the lack of commercially available devices that generate a bipolar output. These authors compared uni- and bipolar protocols on cell suspensions but the applied electroporation signals were pulses rather than a high-frequency oscillating signal. Nevertheless, bipolar electroporation yielded more efficient uptake of a reporter dye but no gain at the level of cell death (Kotnik et al., 2001b). Tekle et al. (1991) reported data performed with high-frequency oscillating fields applied to adherent cells. These authors found bipolar electroporation to be more efficient than its unipolar variant for DNA transfection of NIH 3T3 fibroblasts, but the conditions investigated were much more extreme as cell death levels ranging from 3 up to 99 % were reported. Clearly, cell death may be extensive for transfection experiments as the cells will recover and grow over the hours or days after which the expression efficiency is evaluated. The goal of electroporation for transfection purposes is indeed to maximize efficiency, while the goal in the present experiments was to identify conditions combining an absolute minimum of cell death with a realistic efficiency, so as to allow subsequent functional studies. Bipolar electroporation was an excellent method to load a narrow (~ 250  $\mu\text{m}$  wide) strip-like cell zone within a confluent monolayer and we further investigated whether this loading method could be used to estimate the degree of functional coupling and dye transfer between cells via gap junctions. Analysis of a simple parameter like the size of



the zone with suprathreshold fluorescence was sufficient to distinguish connexin expressing cells from WT non-coupled cells (Figure 80A). More sophisticated analysis was necessary to interpret the data obtained with higher molecular weight, non-gap junction permeable probes because of intrinsically different loading properties of higher molecular weight molecules. The standard deviation of Gaussian dye spread  $\sigma$  proved to be a useful and robust parameter (independent of the actual fluorescence levels) to evaluate the transfer of various reporter dyes between cells in the monolayer (Figure 80B and C). SLDT is a well known and widely used method to investigate dye coupling via gap junctions (el-Fouly et al., 1987; Meda, 2001) and we compared the performance of ELDT and SLDT in terms of dye spread quantified by the spatial constant  $\lambda$ . Both methods clearly demonstrated increased dye coupling in transfected and coupled cells as compared to WT cells. The most prominent difference was, however, that the change of  $\lambda$  from WT to coupled cells was more than twice as large in ELDT as compared to SLDT (Figure 81E), indicating an underestimation of the degree of dye coupling with SLDT. An obvious reason for this difference may reside in the nature of the cell loading protocol. SLDT is done by applying a linear scrape ('scratch') whereby plasma membranes are disrupted and the reporter dye leaks into the damaged cells. Cell death is one major difference between the two loading protocols and the first part of this study was devoted to adjust the electroporation settings to obtain minimal cell death in the loading zone. A consequence of traumatic cell loading is the release of cellular components into the medium and the activation of intracellular signalization cascades that may influence the degree of cell-cell coupling via gap junctions. Application of the SLDT scratch followed by ELDT showed that ELDT dye spread was significantly reduced to the level observed with SLDT (Figure 81F). The FRAP experiments on cells that received supernatant from scraped cultures indicate that an extracellular factor is probably not the major cause of decreased coupling in SLDT. Presumably, SLDT triggers intracellular signals that act to decrease transfer via gap junctions. One possibility is the generation of large intercellular  $\text{Ca}^{2+}$ -waves that increase the cytoplasmic  $\text{Ca}^{2+}$ -concentration (mostly by releasing  $\text{Ca}^{2+}$  from the endoplasmic reticulum - Dupont et al. (2007)) to a level that depresses gap junctional coupling (Peracchia, 2004; Dakin et al., 2005). We conclude from this study that bipolar pulsed high-frequency electroporation combines good loading performance with safety in terms of cell death and is the preferred method to load a narrow longitudinal strip of cells for subsequent studies on the temporal and spatial spread of reporter dyes via gap junctions. ELDT is an alternative for SLDT associated with low levels of cell death and better reflects the true level of cell-cell coupling via gap junctions. In comparison with FRAP and LAMP that represent point measurements of cell-cell coupling, ELDT has the advantage to report an average degree of coupling in a large population of cells. Studies on the evolution of the dye spread parameter  $\sigma$  in function of time in principle allow to establish an apparent diffusion constant ( $\sigma^2 = 2 \times D \times t$ ; where D is the diffusion constant and t is the time) for the movement of reporter dye

molecules in and between the cells. Future work will be directed to fully exploit the possibilities of this method.

**Chapter**

**8**

***Discussion and Perspectives***

A mouse is an animal that, if killed in sufficiently many and creative ways, will generate a PhD  
-Anonymous-

## 8.1 Discussion

### 8.1.1 Intracellular $\text{Ca}^{2+}$ -changes trigger Cx32 hemichannel opening

Previous studies showed that elevating 1,4,5-InsP<sub>3</sub> in connexin expressing cells triggered the release of ATP (Braet et al., 2003a; Braet et al., 2003b). The release mechanism was dependent on changes in  $[\text{Ca}^{2+}]_i$ , since buffering cytoplasmic  $\text{Ca}^{2+}$  with BAPTA suppressed ATP release to baseline levels. The responses were furthermore inhibited by the Gap peptides, <sup>43</sup>Gap 26 and <sup>43</sup>Gap 27 (Braet et al., 2003b), suggesting the involvement of connexins, presumably under the form of hemichannels. In this study, our aim was to investigate the regulation of hemichannels by changes in  $[\text{Ca}^{2+}]_i$  in more detail. To that purpose, we used Cx32 expressing cells and studied hemichannel opening indirectly, based on ATP release and dye uptake.

In [chapter 4](#), we showed that elevation of  $[\text{Ca}^{2+}]_i$  by either photoliberating  $\text{Ca}^{2+}$  from the NP-EGTA probe, or applying the  $\text{Ca}^{2+}$ -ionophore (A23187) to the cells triggered the release of ATP and the uptake of propidium iodide into the cells. These  $\text{Ca}^{2+}$ -triggered responses were completely absent in cells that did not express Cx32, pointing to the involvement of hemichannels. The activation of this mechanism was further strengthened by the action of gap junction/hemichannel blockers such as carbenoxolone,  $\alpha$ -GA and peptides that mimicked a sequence on the intracellular (<sup>32</sup>Gap 24) and the second extracellular loop (<sup>32</sup>Gap 27) of Cx32. All these substances strongly inhibited the ATP release and dye uptake triggered by changes in  $[\text{Ca}^{2+}]_i$ . Other ATP release mechanisms, such as the P<sub>2</sub>X<sub>7</sub> receptor pore were not involved, but there was a small contribution of exocytosis. Various A23187 concentrations were used to construct a concentration-response curve for  $\text{Ca}^{2+}$ -triggered ATP release as shown in [Figure 83](#). The results indicated activation of ATP release within a narrow A23187 concentration range. Next, we plotted ATP release in function of  $[\text{Ca}^{2+}]_i$  and found a bell-shaped response curve. These results demonstrate that the magnitude of the  $\text{Ca}^{2+}$ -stimulus is critical, and that only  $[\text{Ca}^{2+}]_i$  above 200 nM and beneath 1000 nM are able to trigger ATP release. Blocking CaM activation by incubating the cells with W7, a CaM antagonist, completely suppressed  $\text{Ca}^{2+}$ -triggered ATP release, suggesting the involvement of CaM downstream of intracellular  $\text{Ca}^{2+}$ . Cx32 contains two CaM binding sites, and Cx43 contains one such site. In the next study, we switched to Cx43, which is expressed in a wide-range of cells (Laird, 2006), to further investigate the downstream signaling pathways in more detail.

### 8.1.2 Cx43 hemichannel regulation by intracellular $\text{Ca}^{2+}$ -changes: involvement of various signaling pathways

Cx43 is the most abundant connexin and is expressed at very high levels in several tissues and organs (Laird, 2006). In [chapter 5](#), we aimed to investigate the  $[\text{Ca}^{2+}]_i$ -sensitivity of

hemichannels composed of Cx43 and the downstream signaling pathways. The starting point here was a known interaction between Cx43 and CaM, as shown by Torok et al. (1997) and Zhou et al. (2007), suggesting the possibility that Cx43 hemichannels might also respond to changes  $[Ca^{2+}]_i$ .

Our results show that Cx43 hemichannel responses triggered by elevating  $[Ca^{2+}]_i$  were comparable, with respect to  $[Ca^{2+}]_i$ -sensitivity and effect of inhibitor substances, to the responses observed in Cx32 expressing cells. ATP responses in Cx43 expressing cells occurred, like in Cx32 expressing cells, between 200 nM and 1000 nM of  $[Ca^{2+}]_i$ , which is in the  $K_d$ -range for  $Ca^{2+}$ /CaM binding (Figure 83 - Chin and Means (2000)). Using a CaM agonist (CALP1) and a CaM antagonist (W7), we demonstrated that  $[Ca^{2+}]_i$ -triggered ATP release was mediated by active CaM. Our data show a sigmoidal relation between increasing CALP1 concentrations and ATP release responses, with half-maximal activation at 87  $\mu$ M, which corresponds to the  $K_d$ -value of 88  $\mu$ M for CALP1/CaM interactions (Villain et al., 2000). CALP1- and  $Ca^{2+}$ -triggered ATP responses were furthermore potently blocked by Cx43 siRNA treatment, and absent in wild type cells, further pointing to the involvement of Cx43 hemichannels.  $Ca^{2+}$ /CaM activate various downstream kinases, of which CaMK-II is the best known. Work with CaMK-II antagonists (KN62 and AIP) pointed to the involvement of this kinase. CaMK-II and increased  $[Ca^{2+}]_i$  activate cPLA<sub>2</sub>, leading to the production of arachidonic acid (AA - Chakraborti (2003)).  $Ca^{2+}$ -ions bind to cPLA<sub>2</sub> and mediate the translocation to the membrane, and CaMK-II phosphorylates the enzyme, increasing the intrinsic activity of the latter. The free AA is further metabolized by the action of lipoxygenases and cyclooxygenases, both of which are associated with the production of reactive oxygen species (ROS - Simonian and Coyle (1996)). These ROS can cause membrane depolarization, inducing the opening of Cx43 hemichannels (Ramachandran et al., 2007). Work with antagonists of the AA signaling pathway strongly inhibited  $Ca^{2+}$ - and CALP1-triggered ATP release. AA alone also triggered ATP release that was inhibited by the Gap peptides (<sup>43</sup>Gap 26 and 27), by Cx43 siRNA treatment, and absent in wild type cells, similar to the responses observed by intracellular  $Ca^{2+}$  and CALP1. Remarkably, both inhibition of lipoxygenases and cyclooxygenases caused complete disappearance of the ATP responses. We hypothesize that obstruction of one of these enzymes dims the downstream cascade to such an extent that the signal does not reach a level high enough for hemichannel activation. The ROS produced in the AA metabolic pathway can further stimulate the synthesis of NO by a yet unknown mechanism (Shimizu et al., 1997). The produced NO induces S-nitrosylation of cysteine residues located in the intracellular loop of Cx43 and this results in the opening of Cx43 hemichannels (Retamal et al., 2006). Incubating the cells with free radical scavengers and with inhibitors of NO synthesis completely inhibited  $Ca^{2+}$ -triggered ATP release, CALP1-triggered ATP release and AA-triggered ATP release. Our results demonstrate that the effect of  $[Ca^{2+}]_i$  is mediated by known activators of hemichannel

opening, such as the AA metabolic pathway (Contreras et al., 2002), the production of ROS (Ramachandran et al., 2007), and the synthesis of NO (Retamal et al., 2006), and not by a direct effect of  $[Ca^{2+}]_i$  on connexin hemichannels.

### **8.1.3 Connexin hemichannels and gap junction channels are differentially influenced by lipopolysaccharide and basic fibroblast growth factor**

The work presented in chapter 4 and chapter 5 indicate hemichannel opening with  $[Ca^{2+}]_i$  increases. On the other hand, it is well known, although poorly understood, and somewhat controversial, that gap junctions close with elevated  $[Ca^{2+}]_i$ . These observations point to a different regulation of gap junctions and hemichannels composed of the same connexin. An even more obvious difference is the fact that hemichannels are normally closed, while gap junctions are open. In [chapter 6](#), our aim was to investigate whether various kinase activating stimuli had differential effects on hemichannel functioning as compared to gap junctional coupling. In this study, we used a solution with low extracellular divalent cations (containing EGTA - referred to as DF-trigger) to induce hemichannel related ATP release in Cx43 expressing cells. Removing extracellular  $Ca^{2+}$  elicits a conformational change in connexin hemichannels, resulting in the opening of the channel pore (Thimm et al., 2005). A first interesting observation was that deletion of the carboxyterminal domain of Cx43 inhibited DF-triggered ATP release, while the level of gap junctional communication was indiscernible from wild type Cx43, already indicating different regulation and pointing to the fact that the carboxyterminal domain of Cx43 plays an important role in controlling hemichannel responses. The hemichannel involvement was determined by using the  $^{43}Gap$  26 and  $^{43}Gap$  27 peptides and by excluding the involvement of other release pathways, as was done in the two previous chapters.

PKC activation by PMA, transfection of constitutive active c-Src, and activation of different kinases with LPA all led to inhibition of DF-triggered ATP release and gap junctional channels composed of Cx43. The effect of the broad-spectrum kinase activators, LPS and bFGF, were dependent on the cell type and the presence of the carboxyterminal domain. LPS and bFGF inhibited gap junctional communication in C6-Cx43 cells, and stimulated DF-triggered ATP release. In HeLa-Cx43 cells, LPS and bFGF gave inhibition of DF-triggered ATP release and, surprisingly, carboxyterminal truncation of Cx43 turned inhibition into a potentiating effect. In line with this, LPS and bFGF also potentiated DF-triggered ATP release in cells expressing Cx26. The cell type specific effects of LPS and bFGF on DF-triggered ATP release and gap junctional coupling implicate the involvement of different signaling pathways. LPS and bFGF can either directly or indirectly via intermediate kinases (Luo et al., 2005), lead to activation and translocation of cPLA<sub>2</sub> and/or iPLA<sub>2</sub> (Vivancos and Moreno, 2002; Antoniotti et al., 2003) with subsequent release of AA. Treatment with exogenously

added AA mimicked the potentiating effects of LPS and bFGF on ATP release observed in C6-Cx43, HeLa-Cx43ΔC, and HeLa-Cx26, and inhibitors of the AA metabolic pathway reduced the potentiating effect of LPS. Stimulation of DF-triggered ATP release by LPS and bFGF is thus related to the activation of the AA signaling pathway. As discussed in chapter 5, AA metabolization by lipoxygenases and cyclooxygenases is associated with production of ROS, which can induce hemichannel opening due to membrane depolarization (Ramachandran et al., 2007). In C6-Cx43, the AA metabolic pathway is presumably more active, as compared to HeLa-Cx43 cells and this overrides the inhibition of the ATP responses as a consequence of phosphorylations at the carboxyterminal domain. At the level of gap junctional channels, the two pathways lead to inhibition, as reported here for LPS and bFGF and by others for AA (Giaume et al., 1989; Criswell and Loch-Caruso, 1995; Martinez and Saez, 1999; Velasco et al., 2000). In sum, our study thus clearly demonstrates different regulation of gap junctional coupling and hemichannel related responses in different cell lines.

#### **8.1.4 In situ bipolar electroporation for localized cell loading with reporter dyes and investigating gap junctional coupling**

Several methods for the study of gap junctional communication are available, such as electrophysiological measurement of the channel currents and conductance, microinjection of gap junctional permeable dyes, fluorescence recovery after photobleaching (FRAP - Wade et al. (1986)), local activation of a fluorescent molecular probe (LAMP - Dakin et al. (2005)), and scrape loading and dye transfer (SLDT - el-Fouly et al. (1987)).

Measuring the current through gap junction channels is the most sensitive method, but requires special equipment, such as two voltage-clamp amplifiers. In addition, this method can only be applied to cell pairs and not on confluent or subconfluent cultures. Microinjection has the major disadvantage that the cell membrane is disrupted, and this can change the level of gap junctional coupling due to  $\text{Ca}^{2+}$ -entry. FRAP and LAMP are two elegant techniques, but they measure the coupling of only a single cell to a limited number of surrounding cells at the same time. SLDT allows the quantification of gap junctional coupling in a large number of cells, but with this technique, the plasma membrane is drastically disrupted. A consequence of this traumatic cell loading is the possible release of cellular constituents into the medium and the activation of intracellular signals that may influence the degree of cell-cell coupling via gap junctions. One possibility is for example the generation of large intercellular  $\text{Ca}^{2+}$ -transients that increase  $[\text{Ca}^{2+}]_i$  to levels that might be sufficient to potentially reduce gap junctional coupling (Peracchia, 2004; Dakin et al., 2005; Dupont et al., 2007).

In [chapter 7](#), we investigated the possibility to use a more cell-friendly approach to load a defined cell zone with a fluorescent reporter dye for subsequent studies on dye coupling in a large population of cells. Cell loading was done with *in situ* electroporation of adherent cell cultures. We compared unipolar with bipolar electroporation and concluded that bipolar

electroporation was an excellent method to load a narrow (~ 250  $\mu\text{m}$  wide) strip-like cell zone within a confluent monolayer. The electroporation loading protocol was further optimized to induce minimal cell death in the loaded zone. In addition, electroporation loaded cells showed dye transfer to non loaded cells when Cx32 or Cx43 was expressed, and we therefore called this technique electroporation loading and dye transfer (ELDT). In a next step we compared the performance of ELDT and SLDT in terms of dye spread quantified by the spatial constant  $\lambda$ . Both methods clearly demonstrated increased dye coupling in connexin transfected as compared to WT cells. The most prominent difference was, however, that the difference of coupling between wild type and connexin expressing cells was more than twice as large in ELDT as compared to SLDT, indicating an underestimation of the degree of dye coupling with SLDT. Experiments where SLDT was applied before ELDT indeed confirmed the disturbing effect of cell injury due to cell scratching.

## 8.2 General discussion

Connexin-based channels provide a pathway for direct signaling between the cytoplasm of two adjacent cells (gap junctional communication) and between the cytoplasm and the extracellular environment (paracrine signaling via hemichannels) by the release of small molecules ( $\leq 1.2$  kDa). Other mechanisms, responsible for the release of substances in the extracellular environment are also present in the cells, so caution should be taken to distinguish the involvement of hemichannels from the activation of other pathways, with different properties (i.e. exocytosis) or properties comparable to hemichannels. Recently, criteria for the involvement of hemichannels were published by Spray et al. (2006). In our study, the following criteria were used to attribute the observed effects to hemichannel opening: (i) the effect of *gjal* gene silencing with siRNA, (ii) the use of Gap peptides, (iii) the use of connexin expressing cells versus non connexin expressing cells, (iv) the uptake of small fluorescent probes, indicating the bidirectionality of the pathway, (v) the use of  $\text{P}_2\text{X}_7$  receptor antagonists combined with the expression study of this protein, (vi) the study of Panx1 expression (possibly forming hemichannels that can be activated by increasing  $[\text{Ca}^{2+}]_i$ ), and (vii) the use of blockers of exocytosis. Taken all evidence together, we conclude that ATP release is mainly mediated via open hemichannels, with a small contribution of exocytosis, at least in our model system used in the studies presented in this thesis.

### 8.2.1 Gap peptides

Gap peptides are identical to a short amino acid sequence of the connexin subunit (intracellular loop <sup>32</sup>Gap 24, first extracellular loop <sup>43</sup>Gap 26, and the second extracellular loop <sup>32,43</sup>Gap 27 - Dahl et al. (1994); Warner et al. (1995)). Warner et al. (1995) showed that



the extracellular loop peptides delayed the formation of gap junctional channels (Warner et al., 1995). Since the first reports of Braet et al. (2003a,b), several other groups have confirmed the actions of Gap peptides (mainly <sup>43</sup>Gap 26, and to a lesser extent <sup>43</sup>Gap 27) on hemichannel responses. The inhibition of hemichannel responses was shown by different methods, including inhibition of dye uptake, inhibition of ATP release, inhibition of Ca<sup>2+</sup>-waves, and inhibition of hemichannel currents (Table 4).

Our work shows that it is possible to separate the effect on gap junctional coupling from hemichannel inhibition by varying the exposure time of the cells to these peptides: ATP responses were suppressed after exposure times of less than 30 min, while inhibition of gap junctional coupling required incubation times of more than 24 hours. The long incubation needed to inhibit gap junctions in our experimental settings differs somewhat from the findings of other groups that have reported Gap peptides to inhibit gap junctional coupling within minutes (15 min) of application (Chaytor et al., 1997; Eugenin et al., 1998; Boitano and Evans, 2000). Presumably, the kinetics of these peptides depend on the turn-over rate of connexins, which can differ between different cell types.

The specificity of the Gap peptides on hemichannel responses was recently questioned by Wang et al. (2007). These authors showed that scrambled peptides and <sup>10</sup>Panx1 (a Panx1 mimetic peptide), in addition to <sup>43</sup>Gap 26 and <sup>32</sup>Gap 24 significantly inhibited hemichannel currents in *Xenopus laevis* oocytes and this effect was ascribed to sterical inhibition of the pore (Wang et al., 2007). In addition, <sup>32</sup>Gap 24 appeared to block Panx1 hemichannel currents, rather than currents through open hemichannels. The approach of this study does rise some questions: a chimeric connexin protein, where the first extracellular loop of Cx32 was replaced by the first extracellular loop of Cx43, was used in stead of native Cx43. Previous work of this group showed that this chimeric protein has altered properties in comparison to the wild type connexin (Wang et al., 2007). Second, the study was performed in *Xenopus laevis* oocytes in which regulation of hemichannels may be different. Evidence for this comes from *Xenopus laevis* oocytes injected with Cx46 mRNA (Paul et al., 1991). Expression of Cx46 induced lysis of the oocytes 24 h after injection (Paul et al., 1991), while Cx46 expression in HeLa cells was without effect (Valiunas and Weingart, 2000). Third, this study suggested that the aspecific effects of the Gap peptides and the scrambled peptides involved steric block of the channel (Wang et al., 2007). This conclusion was based on the use of millimolar concentrations of polyethylene glycol to block hemichannel currents. In contrast, our work demonstrates that the effect of the Gap peptides is half-maximal at concentrations in the order of 150 - 200  $\mu$ M and characterized by a large Hill coefficient of three. This indicates a positive cooperative interaction with a receptor site, rather than steric block. Recently, an interaction between <sup>43</sup>Gap 26 and the extracellular loops of Cx43 was shown by atomic force microscopy. The scrambled form of this peptide (PSFDSRHCIWKYV) did not interact, pointing to a specific interaction between <sup>43</sup>Gap 26 and Cx43 (Liu et al., 2006). This

interaction may disturb the  $\beta$ -barrel formed by the extracellular loops, in this way prevent the docking of two hemichannels (Foote et al., 1998) and inhibit channel opening.

Reference	Peptide	Cell Type	Mechanism
Braet et al. (2003a)	<sup>43</sup> Gap 26/27	HeLa-Cx43 GP8	ATP Release Dye Uptake
Braet et al. (2003b)	<sup>43</sup> Gap 26	RBE4 SV-ARBEC ECV304	ATP Release Dye Uptake Ca <sup>2+</sup> -waves
Vandamme et al. (2004)	<sup>43</sup> Gap 26	GP8	ATP Release
Pearson et al. (2005)	<sup>43</sup> Gap 26	RPE	ATP Release Dye Uptake Ca <sup>2+</sup> -waves
Gomes et al. (2005)	<sup>43</sup> Gap 26	BCEC	ATP Release Dye Uptake Ca <sup>2+</sup> -waves
Eltzschig et al. (2006)	<sup>40,43</sup> Gap 27	Polymorphonuclear cells	ATP Release
Gomes et al. (2006)	<sup>43</sup> Gap 27	BCEC	Dye Uptake Ca <sup>2+</sup> -waves
Retamal et al. (2006)	<sup>43</sup> Gap 26	Astrocytes	Dye uptake
Retamal et al. (2007a)	<sup>43</sup> Gap 26	Microglia	Dye Uptake
D'hondt et al. (2007)	<sup>43</sup> Gap 26	BCEC	ATP Release Dye Uptake Ca <sup>2+</sup> -waves
Romanov et al. (2007)	<sup>43</sup> Gap 26	Taste bud cells	ATP Release Hemichannel currents
Dobrowolski et al. (2007)	<sup>43</sup> Gap 26	Cardiomyocytes	ATP Release

**Table 4: Overview of work performed with Gap peptides on hemichannel responses**

The table gives an overview of different studies that used <sup>43</sup>Gap 26/27 peptides to inhibit hemichannel responses. The last column specifies the assay method used to study hemichannel involvement. HeLa-Cx43: human carcinoma cell line stably transfected with Cx43, RBE4: rat brain endothelial cell line, GP8: rat brain endothelial cell line, SV-ARBEC: rat brain microvascular endothelial cell line, ECV304: epithelial bladder cell line, RPE: retinal pigment epithelial cells, BCEC: bovine corneal endothelial cells.

A significant finding in chapter 4 was that a peptide composed of an amino acid sequence of the intracellular loop of Cx32 (<sup>32</sup>Gap 24) also potently blocked ATP release and dye uptake triggered by DF conditions or changes in [Ca<sup>2+</sup>]<sub>i</sub>. Moreover, this peptide did not have any effect on gap junctional coupling, not even after prolonged exposure times. It remains an

enigma how  $^{32}\text{Gap 24}$  makes its way into the cell. Several possibilities exist: (i) entry through spontaneously open hemichannels, or other pore forming units, (ii) endocytosis, or (iii) the presence of a cell-penetrating peptide sequence (Zorko and Langel, 2005). This sequence is characterized by the presence of amphipatic and net positively charged amino acids, which allows the peptide to interact with the lipid membrane (Zorko and Langel, 2005).  $^{32}\text{Gap 24}$  does however not contain such sequence. Uptake of the peptide via the endocytotic machinery is unlikely, because the peptide would be present in the wrong cell compartment and would be unable to affect hemichannels. Recent, unpublished work with a peptide identical to a short sequence on the intracellular loop of Cx43 seems to confirm the findings with  $^{32}\text{Gap 24}$ , i.e. strong inhibition of the hemichannel responses and no effect on gap junctional coupling. Interestingly, this peptide contains a sequence that resembles a known, lysine-rich, membrane translocation motifs. Future work will be directed to the study of interactions of this peptide with Cx43.

### 8.2.2 Intracellular $\text{Ca}^{2+}$ : gap junctions versus hemichannels

An increase in  $[\text{Ca}^{2+}]_i$  is since long considered as a condition that closes gap junctions in cells of various origin (Rose and Loewenstein, 1975; Lazrak and Peracchia, 1993; Enkvist and McCarthy, 1994; Schirmacher et al., 1996; Cotrina et al., 1998a). However, the matter is controversial, because some studies have demonstrated that gap junctions are not blocked by  $[\text{Ca}^{2+}]_i$  elevation (Clair et al., 2001). Hereby  $[\text{Ca}^{2+}]_i$ -changes may pass from cell-to-cell as  $\text{Ca}^{2+}$ -waves by the diffusion of 1,4,5- $\text{InsP}_3$  via gap junctions, without closing the latter. Other studies have suggested the  $[\text{Ca}^{2+}]_i$  increases may stimulate gap junctional communication or that gap junctions may be stimulated by inhibition of CaM (Delage and Deleze, 1998). These results are in contradiction with the results published by Blödow et al. (2003) who showed that CaM antagonists diminished gap junctional communication (such as hemichannels in our study - Blödow et al. (2003)).

Dakin and Li (2006) showed that capacitative  $\text{Ca}^{2+}$ -influx through store-operated  $\text{Ca}^{2+}$ -channels induced cell uncoupling in connexin expressing cells. Global changes in  $[\text{Ca}^{2+}]_i$  (up to  $\mu\text{M}$  levels) were however unable to reduce gap junctional communication (Dakin and Li, 2006). This was confirmed by a study from Matchkov et al. (2007) where it was shown that elevating  $[\text{Ca}^{2+}]_i$  in microdomains along the plasma membrane uncoupled myocytes, while global increases in  $[\text{Ca}^{2+}]_i$  were without effect (Matchkov et al., 2007).

Several reports indicate that changes in  $[\text{Ca}^{2+}]_i$  are involved in ATP release mediated by connexin hemichannels. Cotrina et al. (1998) reported that exposing C6-Cx43 cells to UTP triggered ATP release that was mediated via hemichannels and this was dependent on changes in  $[\text{Ca}^{2+}]_i$  (Cotrina et al., 1998b). Arcuino et al. (2002) showed that spontaneous  $\text{Ca}^{2+}$ -transients were associated with point-source ATP release bursts and propidium iodide uptake in the same cell. This ATP release mode was blocked by the intracellular  $\text{Ca}^{2+}$ -chelator

BAPTA and absent in wild type cells. These results suggest the involvement of  $[Ca^{2+}]_i$ -changes and hemichannels (Arcuino et al., 2002). According to these results, Braet et al. (2003) showed that elevating 1,4,5-InsP<sub>3</sub> in rat brain endothelial cells and in an epithelial bladder cancer cell line triggered hemichannel related ATP release and dye uptake (Braet et al., 2003a; Braet et al., 2003b). Furthermore, Pearson et al. (2005) showed that spontaneous elevations of  $[Ca^{2+}]_i$  in the trigger cell of a  $Ca^{2+}$ -wave in retinal pigment epithelial cells were associated with propidium iodide uptake in this cell. Local ATP release detected via an ATP biosensor electrode was dependent on the expression of Cx43, which appeared to be located at the retinal face of the RPE cells, presumably under the form of hemichannels (Pearson et al., 2005). Our data presented in chapter 4 and 5 fit into the picture of  $[Ca^{2+}]_i$ -induced hemichannel responses, but further suggest  $[Ca^{2+}]_i$ -activation and -inactivation of these responses respectively below and above 500 nM. Taken together these data suggest a differential regulation of hemichannels and gap junction channels to  $[Ca^{2+}]_i$ -changes, with hemichannels opening in a low  $[Ca^{2+}]_i$ -range and both hemichannels and gap junction channels closing at more elevated  $[Ca^{2+}]_i$  levels. For gap junctions, the responses are further complicated by different effects depending on the  $Ca^{2+}$ -source leading to  $[Ca^{2+}]_i$ -changes. Our results, showing the  $[Ca^{2+}]_i$ -sensitivity of connexin hemichannel responses differs from the  $[Ca^{2+}]_i$ -sensitivity of Panx1 hemichannels (Figure 83 - Locovei et al. (2006b)). In this study, Panx1 hemichannel currents increased with elevating  $[Ca^{2+}]_i$ . These results point to differences of the responses of connexin hemichannels, as compared to Panx1 hemichannels.

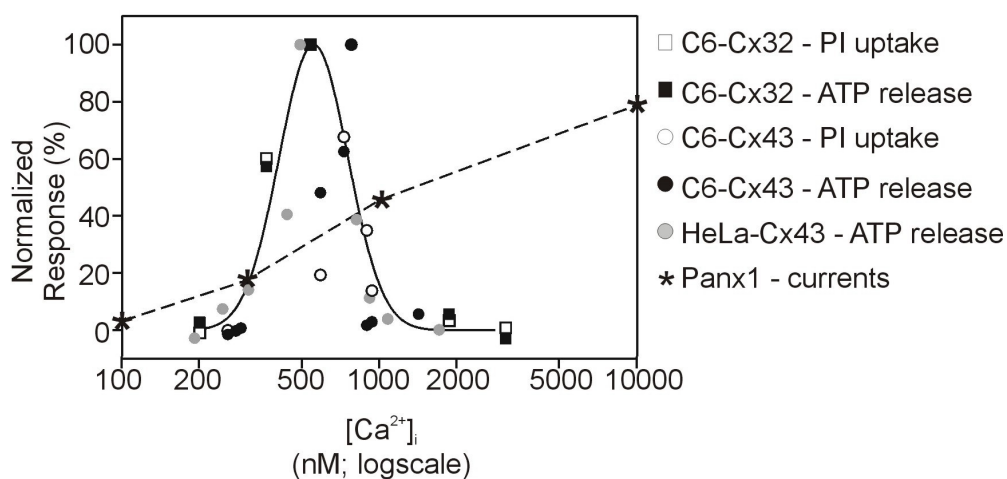


**Figure 83:  $[Ca^{2+}]_i$  induced opening of hemichannels composed of Panx1, Cx32, and Cx43**

The effect of increases in  $[Ca^{2+}]_i$  on the normalized hemichannel response recorded in oocytes injected with Panx1 mRNA (Locovei et al., 2006b) differs from the normalized hemichannel responses observed in C6-Cx32, C6-Cx43, and HeLa-Cx43. Panx1 hemichannel responses were registered by measuring hemichannel currents (Locovei et al., 2006b), while connexin hemichannel responses were observed either with propidium iodide (PI) uptake or ATP release. This curve is composed from data presented in Locovei et al. (2006b) for Panx1 and in chapters 4 and 5 for Cx32 and Cx43.

A better understanding of these complex effects may be obtained by considering  $[Ca^{2+}]_i$  microdomains, lipid rafts and caveolae. Proteins (including connexins) may translocate from and to lipid rafts allowing the cell a novel way of signal transduction (Zajchowski and Robbins, 2002). Lipid rafts are zones of the plasma membrane with a high sterol, glycolipid, and sphingolipid content forming very ordered structures with a low fluidity grade (Carter and Cheville, 1981). Caveolae are flask-shaped membrane invaginations that form lipid rafts by multimerization of caveolin. These domains are insoluble in cold non-ionic detergents. Several connexin isoforms (Cx43, Cx32, Cx36, and Cx46) are preferentially associated with caveolin-1, while others are excluded (Cx50 - Schubert et al. (2002)). The majority of the phosphorylated Cx43 ( $P_{1+2}$ ) form is found in gap junctional plaques, which are localized in lipid rafts forming Triton X-100-insoluble fractions, and are associated with caveolin-1, a marker for lipid rafts. The nonphosphorylated ( $P_0$ ) form of Cx43 is found in hemichannels outside the lipid rafts (Barth et al., 2005) and is localized in Triton X-100-soluble domains. In chapter 4, 5 and 6, we showed the presence of gap junctional plaques composed of Cx26, Cx32, Cx43 and the carboxyterminal truncated form of Cx43 in detergent-resistant membranes. Lipid rafts may delineate a micro-environment in the cytoplasm and in this way diminish the accessibility to  $[Ca^{2+}]_i$ . As such, higher global  $[Ca^{2+}]_i$  may be necessary to close gap junctions when compared to hemichannels. Weerth et al. (2007) showed that density gradient centrifugation of Triton X-100-solubilized glial cell membranes resulted in the co-sedimentation of proteins from the plasma membrane (TRPC-channels), the ER (1,4,5-InsP<sub>3</sub> receptor), and the cytosol with caveolin-1 (Weerth et al., 2007). This may explain the effect observed by Dakin and Li (2006), in that only capacitative  $Ca^{2+}$ -entry mediated by store-operated  $Ca^{2+}$ -channels was able to close gap junctions, and was related to the close proximity of the latter to TRPC-channels that are candidate store-operated channels (Ambudkar et al., 2007). Connexin hemichannels, on the other hand, are freely floating in the plasma membrane, which may lower the  $[Ca^{2+}]_i$  required for hemichannel closure.

A point of notice is the strong inhibitory effects often showing complete block (to baseline level) observed with many substances, including gap junction blockers, Gap peptides, CaM antagonists,  $Ca^{2+}$ -chelators, inhibitors of the AA metabolic pathway, ROS scavengers, NO inhibitors, and siRNA. This suggests the presence of positive feed-back loops, i.e. from AA back to  $[Ca^{2+}]_i$  at the beginning of the cascade illustrated in Figure 84. In addition, other influences may positively feed-back to  $[Ca^{2+}]_i$ , such as  $Ca^{2+}$ -entry via open hemichannels, or released ATP acting on P<sub>2</sub>Y receptors. A possibility is that an initial  $[Ca^{2+}]_i$ -triggered opening of hemichannels initiates ATP release that is further amplified by  $Ca^{2+}$ -entry via hemichannels (at least in the activation range of the response) and ATP-induced ATP release.

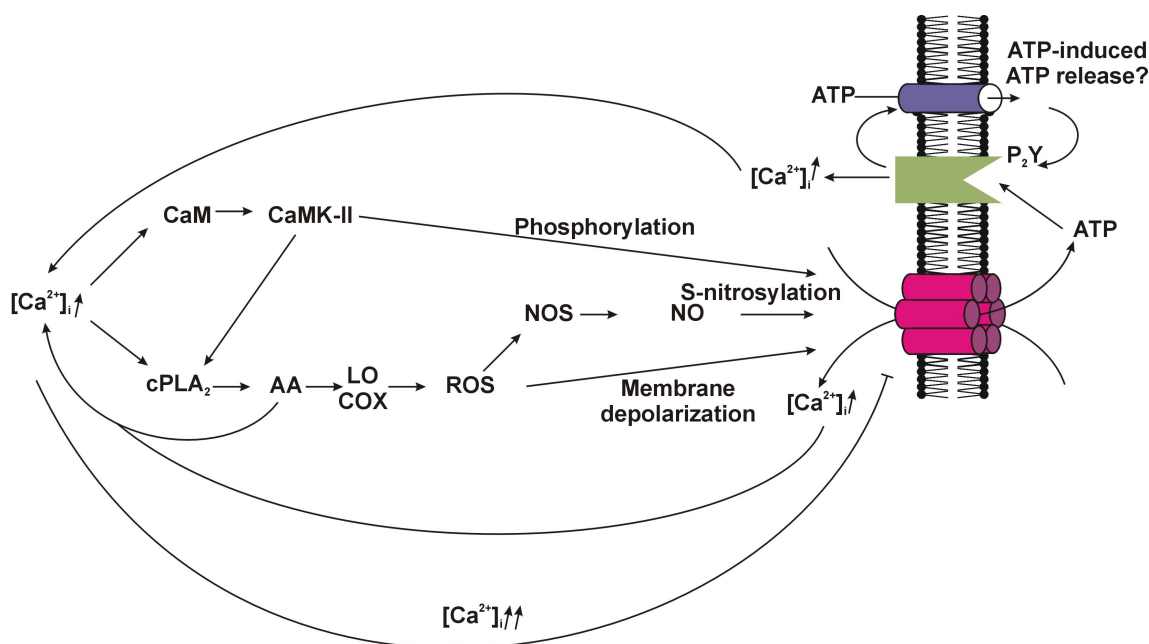


**Figure 84: Signaling pathways involved in the hemichannel responses observed in this thesis**

Elevating  $[Ca^{2+}]_i$  activates the AA signaling cascade that is associated with the production of ROS and with NO synthase activation. All these stimuli induce hemichannel opening, inducing a  $Ca^{2+}$ -influx from the extracellular environment activating the positive feed-back loop. The effect of Cx43 phosphorylation by CaMK-II has only been investigated on the level of gap junctional communication (de Pina-Benabou et al., 2005). Furthermore, the release of AA from the membrane induces also an increase in  $[Ca^{2+}]_i$ , again providing a positive feed-back loop. ATP-induced ATP release is most likely mediated via Panx1 hemichannels (Locovei et al., 2006b).

Because prolonged opening of hemichannels can result in the loss of ATP (Bodin and Burnstock, 2001), the energy substrate of the cells, and in the depolarization of the membrane potential (Contreras et al., 2003b), a negative feed-back is expected to be present as well. The disappearance of the hemichannel responses at high  $[Ca^{2+}]_i$ , which we call “inactivation”, as represented by the down-going flank of the bell-shaped dose-response relation, confirms the presence of a negative inhibitory action of  $[Ca^{2+}]_i$ . At sustained high  $[Ca^{2+}]_i$ , CaM activates the plasma membrane  $Ca^{2+}$ -pumps and the SR/ER  $Ca^{2+}$ -pumps terminating the  $Ca^{2+}$ -signal (Carafoli and Stauffer, 1994). At high  $[Ca^{2+}]_i$ , CaMK-II undergoes self-association, which restricts its access to substrates. Hereby, a cellular defense mechanism that limits CaMK-II activation during  $Ca^{2+}$ -overload is activated (Hudmon et al., 1996; Hudmon et al., 2005). In this way, the  $Ca^{2+}$ -induced hemichannel opening is terminated and prolonged opening of hemichannels prevented.

### 8.2.3 Distinct modulation of gap junctions and hemichannels: role of arachidonic acid

Work presented in chapter 6 not only demonstrated different responses of gap junctions and hemichannels following exposure to LPS and bFGF, but also pointed to opposite hemichannel responses depending on the cell type and on the presence of the carboxyterminal domain. The

main source of the different responses appeared to converge on the activation of the AA signaling pathway in certain cell types. AA is oxidized by the action of lipoxygenases and cyclooxygenases and this is associated with the formation of ROS (Simonian and Coyle, 1996). The production of free radicals induces membrane depolarization, leading to hemichannel opening (Ebihara and Steiner, 1993; Contreras et al., 2003a; Ramachandran et al., 2007), while membrane depolarization results in the closure of gap junction channels composed of Cx32 and Cx43 (Revilla et al., 2000; Gonzalez et al., 2007). This differential regulation by membrane depolarization is the consequence of different voltage sensors (see section 1.2.2) active in hemichannels as compared to gap junction channels. Apart from membrane depolarization, the effect of AA on gap junctional communication can also be mediated by alterations of the acyl chain of the lipids surrounding the connexin channels (Burt et al., 1991). An increase in the free intracellular AA content can change the membrane stiffness and fluidity of the lipid rafts in which the gap junctional plaques reside, and this can disturb gap junctional coupling. A possibility is that the fatty acids surrounding the hemichannels are less accessible for AA, because they are not incorporated into lipid rafts. In this way the lipid composition of the plasma membrane surrounding the hemichannels would not be changed, meaning that hemichannels may be influenced by membrane depolarization only, while gap junctions may be affected by both membrane depolarization and an altered lipid environment.

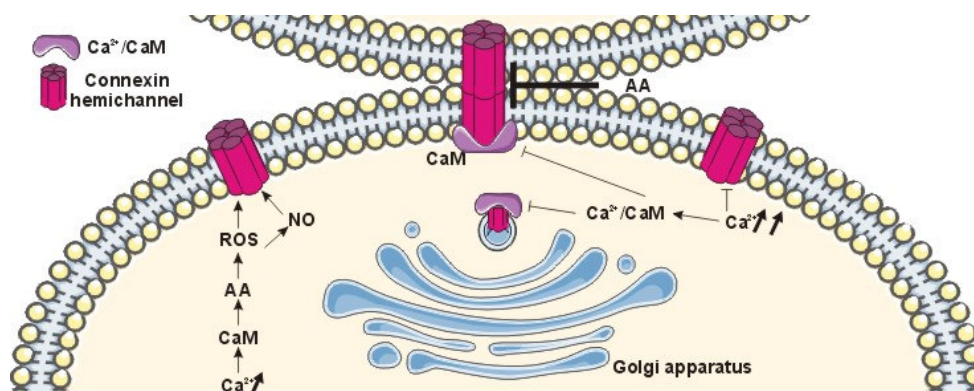


**Figure 85: Scheme summarizing the influence of intracellular  $\text{Ca}^{2+}$  on connexin channels**

CaM blocks hemichannel opening in the Golgi apparatus to maintain steep ion gradients between the cytoplasm and the interior of the organelle. Elevation of  $[\text{Ca}^{2+}]_i$  closes gap junctions in a CaM dependent way. Our work demonstrates that elevation of  $[\text{Ca}^{2+}]_i$  induces hemichannel opening through the CaM mediated activation of the AA metabolic pathway, which is associated with ROS production and NO synthesis. Some stimuli, such as AA and intracellular  $\text{Ca}^{2+}$  thus have opposing effects on hemichannels and gap junctions, although these two types of channels are composed of the same protein.

Evidence is accumulating that hemichannels and gap junctional channels are not necessarily regulated in the same way by some stimuli (Figure 85). It was shown that metabolic inhibition inhibits gap junctional communication (Contreras et al., 2002; Retamal et al., 2006), but induces an increase in the levels of Cx43 hemichannels present at the plasma membrane

(Retamal et al., 2006). Inflammatory conditions also induce the opening of hemichannels (as measured by dye uptake and single channel conductance), but at the same time reduce gap junctional communication (Retamal et al., 2007a). This process is mediated by the activation of the p38 MAP kinase by IL-1 $\beta$  and TNF- $\alpha$  (Winston et al., 1997; Retamal et al., 2007a). p38 kinase activation induces NO synthesis (Cheng et al., 2001a) and this induces hemichannel opening through Cx43 S-nitrosylation (Retamal et al., 2006). The authors showed that the disruption of gap junctional coupling induced by p38 activation is mediated by a different signaling pathway, but the exact cascade involved was however not elucidated. The different regulated responses of gap junctions and hemichannels are most likely cell-protective. Gap junctions close under pathological conditions, for example, in response to bFGF released after brain trauma and ischemia (Logan et al., 1992), in response to LPS present during bacterial infection (Campos de Carvalho et al., 1998), in response to an increase in  $[Ca^{2+}]_i$  after stroke (Friedman, 2006), in response to oxidative stress (Martinez and Saez, 1999), or in response to inflammation (Retamal et al., 2007a). This may help to prevent the spread of cell death-promoting factors to neighboring cells (Krysko et al., 2005). To assure cell-cell communication after uncoupling, the cells may activate paracrine signaling by releasing messengers via open hemichannels, and possible other mechanisms. Moreover, paracrine signaling, mediated by ATP release may stimulate the recovery of injured tissues (e.g., brain and liver) by its mitogenic actions (Thevananther et al., 2004; Pearson et al., 2005) and its vasodilatory and neuroprotective degradation product adenosine (Erlinge, 1998; Burnstock, 2002; Stone, 2002). Opening of unapposed hemichannels can also be harmful for cells due to the unregulated influx of  $Na^+$  and  $Ca^{2+}$ , and the loss of ATP (Evans et al., 2006). The loss of intracellular glutathione, a primary endogenous antioxidant, through open hemichannels, is also harmful when excessive ROS are generated (Rana and Dringen, 2007). In this way open hemichannels may possibly contribute to cell death.

### 8.3 Future perspectives

The work presented in this thesis generated important mechanistic questions that are the starting points for future follow-up studies. Two major topics require specific attention:  $[Ca^{2+}]_i$  influences on hemichannels and interactions and modulation of hemichannels by the Gap peptides.

In a first step the hypothesis of intracellular  $Ca^{2+}$ -microdomains in proximity to the hemichannels and gap junction channels will be studied. A construct in which Cx43 is fused to aequorin can be used to measure  $[Ca^{2+}]_i$  in proximity of the connexin protein (George et al., 1998). Although, this construct is already available, this method is technically difficult and requires the use of a very sensitive, liquid nitrogen cooled camera. An alternative has recently become available and consists of the  $Ca^{2+}$ -green fAsH probe coupled to the connexin protein



(Tour et al., 2007). This molecule is a triple hybrid that combines a fluorescein moiety (with bi-arsenical substituents) and a BAPTA-like chelator. The upper domain provides  $\text{Ca}^{2+}$ -binding, the middle fluorescein structure is the fluorophore, and the bottom domain contains two arsenic atoms that prevent photo-induced electron transfer quenching of the fluorescein group. This approach allows the registration of small  $[\text{Ca}^{2+}]_i$  changes, which are located in microdomains in close proximity of the plasma membrane. Hemichannel responses will be studied with electrophysiological methods instead of the indirect approach based on ATP release and dye uptake. This allows the measurement of hemichannel currents in the whole-cell-recording mode. This method is more direct and also reports detailed information like open probability of the channel and gating kinetics. Preliminary work in collaboration with the group of Prof. Dr. Bukauskas (AECOM, New York, USA) indicates that single hemichannel events can readily be observed in whole-cell recordings of Cx43 expressing cells.

In a second step, the mechanism of the intracellular loop Gap peptides will be studied in detail. We will focus this work on a new peptide that is identical to a short sequence on the intracellular loop of Cx43 and for which we have evidence that it blocks hemichannel responses but not gap junctional coupling. We will investigate the interactions of this peptide with Cx43. This will be performed using a construct that contains the peptide sequence coupled to a tag, followed by co-immunoprecipitation and co-localization studies. In a next step, a construct that contains the peptide sequence and the sequence coding for the green fluorescent protein will be transfected into the cells. It is of note, that we will not use a Gap-GFP fusion protein, this might render the peptide inactive. A first possibility is that the sequence of the peptide is separated from the sequence of the GFP protein via an IRES (internal ribosome entry site), or that the two sequences are under the control of two different promoters. This allows the identification of cells that contain the peptide, and in this cell the hemichannel responses will be quantified by electrophysiological measurements.



**Chapter****9*****References***

It is terrifying to think how much research is needed to determine the truth of even the most unimportant fact

-Stendhal-

- Aarden, E.M., Burger, E.H. and Nijweide, P.J. (1994) Function of osteocytes in bone. *J Cell Biochem*, **55**, 287-299.
- Abraham, E.H., Okunieff, P., Scala, S., Vos, P., Oosterveld, M.J., Chen, A.Y. and Shrivastav, B. (1997) Cystic fibrosis transmembrane conductance regulator and adenosine triphosphate. *Science*, **275**, 1324-1326.
- Agell, N., Bachs, O., Rocamora, N. and Villalonga, P. (2002) Modulation of the Ras/Raf/MEK/ERK pathway by Ca(2+), and calmodulin. *Cell Signal*, **14**, 649-654.
- Agteresch, H.J., Dagnelie, P.C., van den Berg, J.W. and Wilson, J.H. (1999) Adenosine triphosphate: established and potential clinical applications. *Drugs*, **58**, 211-232.
- Ahmad, S., Martin, P.E. and Evans, W.H. (2001) Assembly of gap junction channels: mechanism, effects of calmodulin antagonists and identification of connexin oligomerization determinants. *Eur J Biochem*, **268**, 4544-4552.
- Ahn, N.G., Nahreini, T.S., Tolwinski, N.S. and Resing, K.A. (2001) Pharmacologic inhibitors of MKK1 and MKK2. *Methods Enzymol*, **332**, 417-431.
- Aihara, H. and Miyazaki, J. (1998) Gene transfer into muscle by electroporation in vivo. *Nat Biotechnol*, **16**, 867-870.
- Alexander, D.B. and Goldberg, G.S. (2003) Transfer of biologically important molecules between cells through gap junction channels. *Curr Med Chem*, **10**, 2045-2058.
- Alexopoulos, H., Bottger, A., Fischer, S., Levin, A., Wolf, A., Fujisawa, T., Hayakawa, S., Gojobori, T., Davies, J.A., David, C.N. and Bacon, J.P. (2004) Evolution of gap junctions: the missing link? *Curr Biol*, **14**, R879-880.
- Allbritton, N.L., Meyer, T. and Stryer, L. (1992) Range of messenger action of calcium ion and inositol 1,4,5-trisphosphate. *Science*, **258**, 1812-1815.
- Allue, I., Gandelman, O., Dementieva, E., Ugarova, N. and Cobbold, P. (1996) Evidence for rapid consumption of millimolar concentrations of cytoplasmic ATP during rigor-contraction of metabolically compromised single cardiomyocytes. *Biochem J*, **319** ( Pt 2), 463-469.
- Altevogt, B.M., Kleopa, K.A., Postma, F.R., Scherer, S.S. and Paul, D.L. (2002) Connexin29 is uniquely distributed within myelinating glial cells of the central and peripheral nervous systems. *J Neurosci*, **22**, 6458-6470.
- Ambudkar, I.S., Ong, H.L., Liu, X., Bandyopadhyay, B. and Cheng, K.T. (2007) TRPC1: the link between functionally distinct store-operated calcium channels. *Cell Calcium*, **42**, 213-223.
- Anderson, C.M., Bergher, J.P. and Swanson, R.A. (2004) ATP-induced ATP release from astrocytes. *J Neurochem*, **88**, 246-256.
- Anderson, M.E., Underwood, M., Bridges, R.J. and Meister, A. (1989) Glutathione metabolism at the blood-cerebrospinal fluid barrier. *Faseb J*, **3**, 2527-2531.
- Anderson, M.P., Berger, H.A., Rich, D.P., Gregory, R.J., Smith, A.E. and Welsh, M.J. (1991) Nucleoside triphosphates are required to open the CFTR chloride channel. *Cell*, **67**, 775-784.
- Angst, B.D., Khan, L.U., Severs, N.J., Whitely, K., Rothery, S., Thompson, R.P., Magee, A.I. and Gourdie, R.G. (1997) Dissociated spatial patterning of gap junctions and cell adhesion junctions during postnatal differentiation of ventricular myocardium. *Circ Res*, **80**, 88-94.
- Antoniotti, S., Fiorio Pla, A., Pregnolato, S., Mottola, A., Lovisolio, D. and Munaron, L. (2003) Control of endothelial cell proliferation by calcium influx and arachidonic acid metabolism: a pharmacological approach. *J Cell Physiol*, **197**, 370-378.
- Anumonwo, J.M., Taffet, S.M., Gu, H., Chanson, M., Moreno, A.P. and Delmar, M. (2001) The carboxyl terminal domain regulates the unitary conductance and voltage dependence of connexin40 gap junction channels. *Circ Res*, **88**, 666-673.

- Arcuino, G., Lin, J.H., Takano, T., Liu, C., Jiang, L., Gao, Q., Kang, J. and Nedergaard, M. (2002) Intercellular calcium signaling mediated by point-source burst release of ATP. *Proc Natl Acad Sci U S A*, **99**, 9840-9845.
- Askham, J.M., Vaughan, K.T., Goodson, H.V. and Morrison, E.E. (2002) Evidence that an interaction between EB1 and p150(Glued) is required for the formation and maintenance of a radial microtubule array anchored at the centrosome. *Mol Biol Cell*, **13**, 3627-3645.
- Atkinson, M.M., Lampe, P.D., Lin, H.H., Kollander, R., Li, X.R. and Kiang, D.T. (1995) Cyclic AMP modifies the cellular distribution of connexin43 and induces a persistent increase in the junctional permeability of mouse mammary tumor cells. *J Cell Sci*, **108** (Pt 9), 3079-3090.
- Ayad, W.A., Locke, D., Koreen, I.V. and Harris, A.L. (2006) Heteromeric, but not homomeric, connexin channels are selectively permeable to inositol phosphates. *J Biol Chem*, **281**, 16727-16739.
- Banach, K. and Weingart, R. (2000) Voltage gating of Cx43 gap junction channels involves fast and slow current transitions. *Pflugers Arch*, **439**, 248-250.
- Banrud, H., Mikalsen, S.O., Berg, K. and Moan, J. (1994) Effects of ultraviolet radiation on intercellular communication in V79 Chinese hamster fibroblasts. *Carcinogenesis*, **15**, 233-239.
- Bao, L., Locovei, S. and Dahl, G. (2004a) Pannexin membrane channels are mechanosensitive conduits for ATP. *FEBS Lett*, **572**, 65-68.
- Bao, L., Sachs, F. and Dahl, G. (2004b) Connexins are mechanosensitive. *Am J Physiol Cell Physiol*, **287**, C1389-1395.
- Bao, L., Samuels, S., Locovei, S., Macagno, E.R., Muller, K.J. and Dahl, G. (2007) Innexins form two types of channels. *FEBS Lett*, **581**, 5703-5708.
- Bao, X., Altenberg, G.A. and Reuss, L. (2004c) Mechanism of regulation of the gap junction protein connexin 43 by protein kinase C-mediated phosphorylation. *Am J Physiol Cell Physiol*, **286**, C647-654.
- Bao, X., Lee, S.C., Reuss, L. and Altenberg, G.A. (2007) Change in permeant size selectivity by phosphorylation of connexin 43 gap-junctional hemichannels by PKC. *Proc Natl Acad Sci U S A*, **104**, 4919-4924.
- Baranova, A., Ivanov, D., Petrash, N., Pestova, A., Skoblov, M., Kelmanson, I., Shagin, D., Nazarenko, S., Geraymovych, E., Litvin, O., Tiunova, A., Born, T.L., Usman, N., Staroverov, D., Lukyanov, S. and Panchin, Y. (2004) The mammalian pannexin family is homologous to the invertebrate innexin gap junction proteins. *Genomics*, **83**, 706-716.
- Barbe, M.T., Monyer, H. and Bruzzone, R. (2006) Cell-cell communication beyond connexins: the pannexin channels. *Physiology (Bethesda)*, **21**, 103-114.
- Barrett, C.F., Liu, L. and Rittenhouse, A.R. (2001) Arachidonic acid reversibly enhances N-type calcium current at an extracellular site. *Am J Physiol Cell Physiol*, **280**, C1306-1318.
- Barrio, L.C., Capel, J., Jarillo, J.A., Castro, C. and Revilla, A. (1997) Species-specific voltage-gating properties of connexin-45 junctions expressed in *Xenopus* oocytes. *Biophys J*, **73**, 757-769.
- Barth, K., Gentsch, M., Blasche, R., Pfuller, A., Parshyna, I., Koslowski, R., Barth, G. and Kasper, M. (2005) Distribution of caveolin-1 and connexin43 in normal and injured alveolar epithelial R3/1 cells. *Histochem Cell Biol*, **123**, 239-247.
- Bauer, R., Lehmann, C., Martini, J., Eckardt, F. and Hoch, M. (2004) Gap junction channel protein innexin 2 is essential for epithelial morphogenesis in the *Drosophila* embryo. *Mol Biol Cell*, **15**, 2992-3004.

- Bauer, R., Loer, B., Ostrowski, K., Martini, J., Weimbs, A., Lechner, H. and Hoch, M. (2005) Intercellular communication: the *Drosophila* innexin multiprotein family of gap junction proteins. *Chem Biol*, **12**, 515-526.
- Beardslee, M.A., Laing, J.G., Beyer, E.C. and Saffitz, J.E. (1998) Rapid turnover of connexin43 in the adult rat heart. *Circ Res*, **83**, 629-635.
- Beblo, D.A. and Veenstra, R.D. (1997) Monovalent cation permeation through the connexin40 gap junction channel. Cs, Rb, K, Na, Li, TEA, TMA, TBA, and effects of anions Br, Cl, F, acetate, aspartate, glutamate, and NO<sub>3</sub>. *J Gen Physiol*, **109**, 509-522.
- Belozerskaya, T.A. (1998) Cell-to-cell communication in differentiation of mycelial fungi. *Membr Cell Biol*, **11**, 831-840.
- Bennett, M.V., Contreras, J.E., Bukauskas, F.F. and Saez, J.C. (2003) New roles for astrocytes: Gap junction hemichannels have something to communicate. *Trends Neurosci*, **26**, 610-617.
- Benz, R. (1994) Permeation of hydrophilic solutes through mitochondrial outer membranes: review on mitochondrial porins. *Biochim Biophys Acta*, **1197**, 167-196.
- Berman, R.S., Martin, P.E., Evans, W.H. and Griffith, T.M. (2002) Relative contributions of NO and gap junctional communication to endothelium-dependent relaxations of rabbit resistance arteries vary with vessel size. *Microvasc Res*, **63**, 115-128.
- Berridge, M.J. (1997) Elementary and global aspects of calcium signalling. *J Physiol*, **499** ( Pt 2), 291-306.
- Berridge, M.J., Lipp, P. and Bootman, M.D. (2000) The versatility and universality of calcium signalling. *Nat Rev Mol Cell Biol*, **1**, 11-21.
- Berthoud, V.M., Beyer, E.C., Kurata, W.E., Lau, A.F. and Lampe, P.D. (1997) The gap-junction protein connexin 56 is phosphorylated in the intracellular loop and the carboxy-terminal region. *Eur J Biochem*, **244**, 89-97.
- Berthoud, V.M., Beyer, E.C. and Seul, K.H. (2000) Peptide inhibitors of intercellular communication. *Am J Physiol Lung Cell Mol Physiol*, **279**, L619-622.
- Berthoud, V.M., Ledbetter, M.L., Hertzberg, E.L. and Saez, J.C. (1992) Connexin43 in MDCK cells: regulation by a tumor-promoting phorbol ester and Ca<sup>2+</sup>. *Eur J Cell Biol*, **57**, 40-50.
- Bevans, C.G. and Harris, A.L. (1999) Direct high affinity modulation of connexin channel activity by cyclic nucleotides. *J Biol Chem*, **274**, 3720-3725.
- Bevans, C.G., Kordel, M., Rhee, S.K. and Harris, A.L. (1998) Isoform composition of connexin channels determines selectivity among second messengers and uncharged molecules. *J Biol Chem*, **273**, 2808-2816.
- Bittman, K.S. and LoTurco, J.J. (1999) Differential regulation of connexin 26 and 43 in murine neocortical precursors. *Cereb Cortex*, **9**, 188-195.
- Bjorkman, N. (1962) A study of the ultrastructure of the granulosa cells of the rat ovary. *Acta Anat (Basel)*, **51**, 125-147.
- Blodow, A., Ngezahayo, A., Ernst, A. and Kolb, H.A. (2003) Calmodulin antagonists suppress gap junction coupling in isolated Hensen cells of the guinea pig cochlea. *Pflugers Arch*, **446**, 36-41.
- Blom, N., Gammeltoft, S. and Brunak, S. (1999) Sequence and structure-based prediction of eukaryotic protein phosphorylation sites. *J Mol Biol*, **294**, 1351-1362.
- Blomstrand, F., Venance, L., Siren, A.L., Ezan, P., Hanse, E., Glowinski, J., Ehrenreich, H. and Giaume, C. (2004) Endothelins regulate astrocyte gap junctions in rat hippocampal slices. *Eur J Neurosci*, **19**, 1005-1015.
- Boassa, D., Ambrosi, C., Qiu, F., Dahl, G., Gaietta, G. and Sosinsky, G. (2007) Pannexin1 channels contain a glycosylation site that targets the hexamer to the plasma membrane. *J Biol Chem*.

- Bodin, P. and Burnstock, G. (2001) Purinergic signalling: ATP release. *Neurochem Res*, **26**, 959-969.
- Bohley, P. and Seglen, P.O. (1992) Proteases and proteolysis in the lysosome. *Experientia*, **48**, 151-157.
- Boitano, S., Dirksen, E.R. and Sanderson, M.J. (1992) Intercellular propagation of calcium waves mediated by inositol trisphosphate. *Science*, **258**, 292-295.
- Boitano, S. and Evans, W.H. (2000) Connexin mimetic peptides reversibly inhibit Ca(2+) signaling through gap junctions in airway cells. *Am J Physiol Lung Cell Mol Physiol*, **279**, L623-630.
- Bond, S.L., Bechberger, J.F., Khoo, N.K. and Naus, C.C. (1994) Transfection of C6 glioma cells with connexin32: the effects of expression of a nonendogenous gap junction protein. *Cell Growth Differ*, **5**, 179-186.
- Bonifacino, J.S. and Dell'Angelica, E.C. (1999) Molecular bases for the recognition of tyrosine-based sorting signals. *J Cell Biol*, **145**, 923-926.
- Bosanac, I., Alattia, J.R., Mal, T.K., Chan, J., Talarico, S., Tong, F.K., Tong, K.I., Yoshikawa, F., Furuichi, T., Iwai, M., Michikawa, T., Mikoshiba, K. and Ikura, M. (2002) Structure of the inositol 1,4,5-trisphosphate receptor binding core in complex with its ligand. *Nature*, **420**, 696-700.
- Boudreault, F. and Grygorczyk, R. (2004) Cell swelling-induced ATP release is tightly dependent on intracellular calcium elevations. *J Physiol*, **561**, 499-513.
- Bours, M.J., Swennen, E.L., Di Virgilio, F., Cronstein, B.N. and Dagnelie, P.C. (2006) Adenosine 5'-triphosphate and adenosine as endogenous signaling molecules in immunity and inflammation. *Pharmacol Ther*, **112**, 358-404.
- Braet, K., Aspeslagh, S., Vandamme, W., Willecke, K., Martin, P.E., Evans, W.H. and Leybaert, L. (2003a) Pharmacological sensitivity of ATP release triggered by photoliberation of inositol-1,4,5-trisphosphate and zero extracellular calcium in brain endothelial cells. *J Cell Physiol*, **197**, 205-213.
- Braet, K., Mabilde, C., Cabooter, L., Rapp, G. and Leybaert, L. (2004) Electroporation loading and photoactivation of caged InsP<sub>3</sub>: tools to investigate the relation between cellular ATP release in response to intracellular InsP<sub>3</sub> elevation. *J Neurosci Methods*, **132**, 81-89.
- Braet, K., Paemeleire, K., D'Herde, K., Sanderson, M.J. and Leybaert, L. (2001) Astrocyte-endothelial cell calcium signals conveyed by two signalling pathways. *Eur J Neurosci*, **13**, 79-91.
- Braet, K., Vandamme, W., Martin, P.E., Evans, W.H. and Leybaert, L. (2003b) Photoliberating inositol-1,4,5-trisphosphate triggers ATP release that is blocked by the connexin mimetic peptide gap 26. *Cell Calcium*, **33**, 37-48.
- Braunstein, G.M., Roman, R.M., Clancy, J.P., Kudlow, B.A., Taylor, A.L., Shylonsky, V.G., Jovov, B., Peter, K., Jilling, T., Ismailov, II, Benos, D.J., Schwiebert, L.M., Fitz, J.G. and Schwiebert, E.M. (2001) Cystic fibrosis transmembrane conductance regulator facilitates ATP release by stimulating a separate ATP release channel for autocrine control of cell volume regulation. *J Biol Chem*, **276**, 6621-6630.
- Brissette, J.L., Kumar, N.M., Gilula, N.B., Hall, J.E. and Dotto, G.P. (1994) Switch in gap junction protein expression is associated with selective changes in junctional permeability during keratinocyte differentiation. *Proc Natl Acad Sci U S A*, **91**, 6453-6457.
- Bruzzone, R., Barbe, M.T., Jakob, N.J. and Monyer, H. (2005) Pharmacological properties of homomeric and heteromeric pannexin hemichannels expressed in *Xenopus* oocytes. *J Neurochem*, **92**, 1033-1043.

- Bruzzone, R., Hormuzdi, S.G., Barbe, M.T., Herb, A. and Monyer, H. (2003) Pannexins, a family of gap junction proteins expressed in brain. *Proc Natl Acad Sci U S A*, **100**, 13644-13649.
- Bruzzone, S., Franco, L., Guida, L., Zocchi, E., Contini, P., Bisso, A., Usai, C. and De Flora, A. (2001a) A self-restricted CD38-connexin 43 cross-talk affects NAD<sup>+</sup> and cyclic ADP-ribose metabolism and regulates intracellular calcium in 3T3 fibroblasts. *J Biol Chem*, **276**, 48300-48308.
- Bruzzone, S., Guida, L., Zocchi, E., Franco, L. and De Flora, A. (2001b) Connexin 43 hemichannels mediate Ca<sup>2+</sup>-regulated transmembrane NAD<sup>+</sup> fluxes in intact cells. *Faseb J*, **15**, 10-12.
- Bukauskas, F.F., Angele, A.B., Verselis, V.K. and Bennett, M.V. (2002) Coupling asymmetry of heterotypic connexin 45/ connexin 43-EGFP gap junctions: properties of fast and slow gating mechanisms. *Proc Natl Acad Sci U S A*, **99**, 7113-7118.
- Bukauskas, F.F., Elfgang, C., Willecke, K. and Weingart, R. (1995) Biophysical properties of gap junction channels formed by mouse connexin40 in induced pairs of transfected human HeLa cells. *Biophys J*, **68**, 2289-2298.
- Burnstock, G. (2002) Purinergic signaling and vascular cell proliferation and death. *Arterioscler Thromb Vasc Biol*, **22**, 364-373.
- Burnstock, G. (2006) Purinergic signalling. *Br J Pharmacol*, **147 Suppl 1**, S172-181.
- Burnstock, G. (2007) Purine and pyrimidine receptors. *Cell Mol Life Sci*, **64**, 1471-1483.
- Burr, G.S., Mitchell, C.K., Keflemariam, Y.J., Heidelberger, R. and O'Brien, J. (2005) Calcium-dependent binding of calmodulin to neuronal gap junction proteins. *Biochem Biophys Res Commun*, **335**, 1191-1198.
- Burt, J.M., Massey, K.D. and Minnich, B.N. (1991) Uncoupling of cardiac cells by fatty acids: structure-activity relationships. *Am J Physiol*, **260**, C439-448.
- Butterweck, A., Gergs, U., Elfgang, C., Willecke, K. and Traub, O. (1994) Immunochemical characterization of the gap junction protein connexin45 in mouse kidney and transfected human HeLa cells. *J Membr Biol*, **141**, 247-256.
- Calegari, F., Coco, S., Taverna, E., Bassetti, M., Verderio, C., Corradi, N., Matteoli, M. and Rosa, P. (1999) A regulated secretory pathway in cultured hippocampal astrocytes. *J Biol Chem*, **274**, 22539-22547.
- Cameron, S.J., Malik, S., Akaike, M., Lerner-Marmarosh, N., Yan, C., Lee, J.D., Abe, J. and Yang, J. (2003) Regulation of epidermal growth factor-induced connexin 43 gap junction communication by big mitogen-activated protein kinase1/ERK5 but not ERK1/2 kinase activation. *J Biol Chem*, **278**, 18682-18688.
- Campos de Carvalho, A.C., Roy, C., Hertzberg, E.L., Tanowitz, H.B., Kessler, J.A., Weiss, L.M., Wittner, M., Dermietzel, R., Gao, Y. and Spray, D.C. (1998) Gap junction disappearance in astrocytes and leptomeningeal cells as a consequence of protozoan infection. *Brain Res*, **790**, 304-314.
- Canfield, W.M., Johnson, K.F., Ye, R.D., Gregory, W. and Kornfeld, S. (1991) Localization of the signal for rapid internalization of the bovine cation-independent mannose 6-phosphate/insulin-like growth factor-II receptor to amino acids 24-29 of the cytoplasmic tail. *J Biol Chem*, **266**, 5682-5688.
- Cantiello, H.F. (2001) Electrodifusional ATP movement through CFTR and other ABC transporters. *Pflugers Arch*, **443 Suppl 1**, S22-27.
- Cao, F., Eckert, R., Elfgang, C., Nitsche, J.M., Snyder, S.A., DF, H.u., Willecke, K. and Nicholson, B.J. (1998) A quantitative analysis of connexin-specific permeability differences of gap junctions expressed in HeLa transfectants and *Xenopus* oocytes. *J Cell Sci*, **111 ( Pt 1)**, 31-43.



- Carafoli, E. and Stauffer, T. (1994) The plasma membrane calcium pump: functional domains, regulation of the activity, and tissue specificity of isoform expression. *J Neurobiol*, **25**, 312-324.
- Carter, J.K. and Cheville, N.F. (1981) Isolation of surface tubules of fowlpox virus. *Avian Dis*, **25**, 454-462.
- Castro, C., Gomez-Hernandez, J.M., Silander, K. and Barrio, L.C. (1999) Altered formation of hemichannels and gap junction channels caused by C-terminal connexin-32 mutations. *J Neurosci*, **19**, 3752-3760.
- Cegovnik, U. and Novakovic, S. (2004) Setting optimal parameters for in vitro electrotransfection of B16F1, SA1, LPB, SCK, L929 and CHO cells using predefined exponentially decaying electric pulses. *Bioelectrochemistry*, **62**, 73-82.
- Chakraborti, S. (2003) Phospholipase A(2) isoforms: a perspective. *Cell Signal*, **15**, 637-665.
- Chakraborti, S., Michael, J.R. and Chakraborti, T. (2004) Role of an aprotinin-sensitive protease in protein kinase Calpha-mediated activation of cytosolic phospholipase A2 by calcium ionophore (A23187) in pulmonary endothelium. *Cell Signal*, **16**, 751-762.
- Chang, D.C. (1989) Cell poration and cell fusion using an oscillating electric field. *Biophys J*, **56**, 641-652.
- Channon, J.Y. and Leslie, C.C. (1990) A calcium-dependent mechanism for associating a soluble arachidonoyl-hydrolyzing phospholipase A2 with membrane in the macrophage cell line RAW 264.7. *J Biol Chem*, **265**, 5409-5413.
- Chanson, M., Mollard, P., Meda, P., Suter, S. and Jongsma, H.J. (1999) Modulation of pancreatic acinar cell to cell coupling during ACh-evoked changes in cytosolic Ca<sup>2+</sup>. *J Biol Chem*, **274**, 282-287.
- Chanson, M., White, M.M. and Garber, S.S. (1996) cAMP promotes gap junctional coupling in T84 cells. *Am J Physiol*, **271**, C533-539.
- Charpentier, E., Cancela, J. and Meda, P. (2007) Beta cells preferentially exchange cationic molecules via connexin 36 gap junction channels. *Diabetologia*, **50**, 2332-2341.
- Chaytor, A.T., Evans, W.H. and Griffith, T.M. (1997) Peptides homologous to extracellular loop motifs of connexin 43 reversibly abolish rhythmic contractile activity in rabbit arteries. *J Physiol*, **503** ( Pt 1), 99-110.
- Chaytor, A.T., Martin, P.E., Evans, W.H., Randall, M.D. and Griffith, T.M. (1999) The endothelial component of cannabinoid-induced relaxation in rabbit mesenteric artery depends on gap junctional communication. *J Physiol*, **520 Pt 2**, 539-550.
- Cheewatrakoolpong, B., Gilchrist, H., Anthes, J.C. and Greenfeder, S. (2005) Identification and characterization of splice variants of the human P2X7 ATP channel. *Biochem Biophys Res Commun*, **332**, 17-27.
- Chen, X., Wang, L., Zhou, Y., Zheng, L.H. and Zhou, Z. (2005) "Kiss-and-run" glutamate secretion in cultured and freshly isolated rat hippocampal astrocytes. *J Neurosci*, **25**, 9236-9243.
- Cheng, A., Chan, S.L., Milhavet, O., Wang, S. and Mattson, M.P. (2001a) p38 MAP kinase mediates nitric oxide-induced apoptosis of neural progenitor cells. *J Biol Chem*, **276**, 43320-43327.
- Cheng, B., Kato, Y., Zhao, S., Luo, J., Sprague, E., Bonewald, L.F. and Jiang, J.X. (2001b) PGE(2) is essential for gap junction-mediated intercellular communication between osteocyte-like MLO-Y4 cells in response to mechanical strain. *Endocrinology*, **142**, 3464-3473.
- Cheng, H.L. and Louis, C.F. (2001) Functional effects of casein kinase I-catalyzed phosphorylation on lens cell-to-cell coupling. *J Membr Biol*, **181**, 21-30.

- Cherian, P.P., Cheng, B., Gu, S., Sprague, E., Bonewald, L.F. and Jiang, J.X. (2003) Effects of mechanical strain on the function of Gap junctions in osteocytes are mediated through the prostaglandin EP2 receptor. *J Biol Chem*, **278**, 43146-43156.
- Cherian, P.P., Siller-Jackson, A.J., Gu, S., Wang, X., Bonewald, L.F., Sprague, E. and Jiang, J.X. (2005) Mechanical Strain Opens Connexin 43 Hemichannels in Osteocytes: A Novel Mechanism for the Release of Prostaglandin. *Mol Biol Cell*.
- Chessell, I.P., Michel, A.D. and Humphrey, P.P. (1997) Properties of the pore-forming P2X7 purinoceptor in mouse NTW8 microglial cells. *Br J Pharmacol*, **121**, 1429-1437.
- Chin, D. and Means, A.R. (2000) Calmodulin: a prototypical calcium sensor. *Trends Cell Biol*, **10**, 322-328.
- Choudhury, G.G., Karamitsos, C., Hernandez, J., Gentilini, A., Bardgette, J. and Abboud, H.E. (1997) PI-3-kinase and MAPK regulate mesangial cell proliferation and migration in response to PDGF. *Am J Physiol*, **273**, F931-938.
- Clair, C., Chalumeau, C., Tordjmann, T., Poggioli, J., Erneux, C., Dupont, G. and Combettes, L. (2001) Investigation of the roles of Ca(2+) and InsP(3) diffusion in the coordination of Ca(2+) signals between connected hepatocytes. *J Cell Sci*, **114**, 1999-2007.
- Clapham, D.E. (1995) Calcium signaling. *Cell*, **80**, 259-268.
- Coco, S., Calegari, F., Pravettoni, E., Pozzi, D., Taverna, E., Rosa, P., Matteoli, M. and Verderio, C. (2003) Storage and release of ATP from astrocytes in culture. *J Biol Chem*, **278**, 1354-1362.
- Cole, W.C. and Garfield, R.E. (1986) Evidence for physiological regulation of myometrial gap junction permeability. *Am J Physiol*, **251**, C411-420.
- Colombini, M. (2004) VDAC: the channel at the interface between mitochondria and the cytosol. *Mol Cell Biochem*, **256-257**, 107-115.
- Contreras, J.E., Saez, J.C., Bukauskas, F.F. and Bennett, M.V. (2003a) Functioning of cx43 hemichannels demonstrated by single channel properties. *Cell Commun Adhes*, **10**, 245-249.
- Contreras, J.E., Saez, J.C., Bukauskas, F.F. and Bennett, M.V. (2003b) Gating and regulation of connexin 43 (Cx43) hemichannels. *Proc Natl Acad Sci U S A*, **100**, 11388-11393.
- Contreras, J.E., Sanchez, H.A., Eugenin, E.A., Speidel, D., Theis, M., Willecke, K., Bukauskas, F.F., Bennett, M.V. and Saez, J.C. (2002) Metabolic inhibition induces opening of unapposed connexin 43 gap junction hemichannels and reduces gap junctional communication in cortical astrocytes in culture. *Proc Natl Acad Sci U S A*, **99**, 495-500.
- Cooper, C.D. and Lampe, P.D. (2002) Casein kinase 1 regulates connexin-43 gap junction assembly. *J Biol Chem*, **277**, 44962-44968.
- Cooper, C.D., Solan, J.L., Dolejsi, M.K. and Lampe, P.D. (2000) Analysis of connexin phosphorylation sites. *Methods*, **20**, 196-204.
- Cotrina, M.L., Kang, J., Lin, J.H., Bueno, E., Hansen, T.W., He, L., Liu, Y. and Nedergaard, M. (1998a) Astrocytic gap junctions remain open during ischemic conditions. *J Neurosci*, **18**, 2520-2537.
- Cotrina, M.L., Lin, J.H., Alves-Rodrigues, A., Liu, S., Li, J., Azmi-Ghadimi, H., Kang, J., Naus, C.C. and Nedergaard, M. (1998b) Connexins regulate calcium signaling by controlling ATP release. *Proc Natl Acad Sci U S A*, **95**, 15735-15740.
- Cotrina, M.L., Lin, J.H., Lopez-Garcia, J.C., Naus, C.C. and Nedergaard, M. (2000) ATP-mediated glia signaling. *J Neurosci*, **20**, 2835-2844.
- Cottrell, G.T. and Burt, J.M. (2005) Functional consequences of heterogeneous gap junction channel formation and its influence in health and disease. *Biochim Biophys Acta*, **1711**, 126-141.

- Cottrell, G.T., Lin, R., Warn-Cramer, B.J., Lau, A.F. and Burt, J.M. (2003) Mechanism of v-Src- and mitogen-activated protein kinase-induced reduction of gap junction communication. *Am J Physiol Cell Physiol*, **284**, C511-520.
- Coux, O., Tanaka, K. and Goldberg, A.L. (1996) Structure and functions of the 20S and 26S proteasomes. *Annu Rev Biochem*, **65**, 801-847.
- Crippa, D., Schenk, U., Francolini, M., Rosa, P., Verderio, C., Zonta, M., Pozzan, T., Matteoli, M. and Carmignoto, G. (2006) Synaptobrevin2-expressing vesicles in rat astrocytes: insights into molecular characterization, dynamics and exocytosis. *J Physiol*, **570**, 567-582.
- Criswell, K.A. and Loch-Caruso, R. (1995) Lindane-induced elimination of gap junctional communication in rat uterine myocytes is mediated by an arachidonic acid-sensitive cAMP-independent mechanism. *Toxicol Appl Pharmacol*, **135**, 127-138.
- Crow, D.S., Beyer, E.C., Paul, D.L., Kobe, S.S. and Lau, A.F. (1990) Phosphorylation of connexin43 gap junction protein in uninfected and Rous sarcoma virus-transformed mammalian fibroblasts. *Mol Cell Biol*, **10**, 1754-1763.
- Crow, J.M., Atkinson, M.M. and Johnson, R.G. (1994) Micromolar levels of intracellular calcium reduce gap junctional permeability in lens cultures. *Invest Ophthalmol Vis Sci*, **35**, 3332-3341.
- Cruciani, V. and Mikalsen, S.O. (2002) Connexins, gap junctional intercellular communication and kinases. *Biol Cell*, **94**, 433-443.
- Cruciani, V. and Mikalsen, S.O. (2007) Evolutionary selection pressure and family relationships among connexin genes. *Biol Chem*, **388**, 253-264.
- Curran, J.E. and Woodruff, R.I. (2007) Passage of 17kDa calmodulin through gap junctions of three vertebrate species. *Tissue Cell*, **39**, 303-309.
- Curtin, K.D., Zhang, Z. and Wyman, R.J. (2002) Gap junction proteins are not interchangeable in development of neural function in the Drosophila visual system. *J Cell Sci*, **115**, 3379-3388.
- Dahl, G., Nonner, W. and Werner, R. (1994) Attempts to define functional domains of gap junction proteins with synthetic peptides. *Biophys J*, **67**, 1816-1822.
- Dakin, K. and Li, W.H. (2006) Local Ca<sup>2+</sup> rise near store operated Ca<sup>2+</sup> channels inhibits cell coupling during capacitative Ca<sup>2+</sup> influx. *Cell Commun Adhes*, **13**, 29-39.
- Dakin, K., Zhao, Y. and Li, W.H. (2005) LAMP, a new imaging assay of gap junctional communication unveils that Ca<sup>2+</sup> influx inhibits cell coupling. *Nat Methods*, **2**, 55-62.
- Damron, D.S. and Bond, M. (1993) Modulation of Ca<sup>2+</sup> cycling in cardiac myocytes by arachidonic acid. *Circ Res*, **72**, 376-386.
- Danbolt, N.C. (2001) Glutamate uptake. *Prog Neurobiol*, **65**, 1-105.
- Darrow, B.J., Fast, V.G., Kleber, A.G., Beyer, E.C. and Saffitz, J.E. (1996) Functional and structural assessment of intercellular communication. Increased conduction velocity and enhanced connexin expression in dibutyl cAMP-treated cultured cardiac myocytes. *Circ Res*, **79**, 174-183.
- Darrow, B.J., Laing, J.G., Lampe, P.D., Saffitz, J.E. and Beyer, E.C. (1995) Expression of multiple connexins in cultured neonatal rat ventricular myocytes. *Circ Res*, **76**, 381-387.
- Dasgupta, C., Martinez, A.M., Zuppan, C.W., Shah, M.M., Bailey, L.L. and Fletcher, W.H. (2001) Identification of connexin43 (alpha1) gap junction gene mutations in patients with hypoplastic left heart syndrome by denaturing gradient gel electrophoresis (DGGE). *Mutat Res*, **479**, 173-186.
- Davies, S.P., Reddy, H., Caivano, M. and Cohen, P. (2000) Specificity and mechanism of action of some commonly used protein kinase inhibitors. *Biochem J*, **351**, 95-105.

- De Flora, A., Zocchi, E., Guida, L., Franco, L. and Bruzzone, S. (2004) Autocrine and paracrine calcium signaling by the CD38/NAD<sup>+</sup>/cyclic ADP-ribose system. *Ann N Y Acad Sci*, **1028**, 176-191.
- De Maio, A., Gingalewski, C., Theodorakis, N.G. and Clemens, M.G. (2000) Interruption of hepatic gap junctional communication in the rat during inflammation induced by bacterial lipopolysaccharide. *Shock*, **14**, 53-59.
- De Maio, A., Vega, V.L. and Contreras, J.E. (2002) Gap junctions, homeostasis, and injury. *J Cell Physiol*, **191**, 269-282.
- de Pina-Benabou, M.H., Szostak, V., Kyrozis, A., Rempe, D., Uziel, D., Urban-Maldonado, M., Benabou, S., Spray, D.C., Federoff, H.J., Stanton, P.K. and Rozental, R. (2005) Blockade of gap junctions in vivo provides neuroprotection after perinatal global ischemia. *Stroke*, **36**, 2232-2237.
- De Vuyst, E., Decrock, E., Cabooter, L., Dubyak, G.R., Naus, C.C., Evans, W.H. and Leybaert, L. (2006) Intracellular calcium changes trigger connexin 32 hemichannel opening. *Embo J*, **25**, 34-44.
- De Vuyst, E., Decrock, E., De Bock, M., Yamasaki, H., Naus, C.C., Evans, W.H. and Leybaert, L. (2007) Connexin hemichannels and gap junction channels are differentially influenced by lipopolysaccharide and basic fibroblast growth factor. *Mol Biol Cell*, **18**, 34-46.
- Dean, D.A., Machado-Aranda, D., Blair-Parks, K., Yeldandi, A.V. and Young, J.L. (2003) Electroporation as a method for high-level nonviral gene transfer to the lung. *Gene Ther*, **10**, 1608-1615.
- Delage, B. and Deleze, J. (1998) Increase of the gap junction conductance of adult mammalian heart myocytes by intracellular calcium. In Werner, R. (ed.), *Gap junction conference*. IOS Press; The Netherlands, Key Largo, Florida, USA, pp. 72-75.
- Deleze, J., Delage, B., Hentati-Ksibi, O., Verrecchia, F. and Herve, J.C. (2001) Fluorescence recovery after photobleaching. *Methods Mol Biol*, **154**, 313-327.
- Delmar, M., Coombs, W., Sorgen, P., Duffy, H.S. and Taffet, S.M. (2004) Structural bases for the chemical regulation of Connexin43 channels. *Cardiovasc Res*, **62**, 268-275.
- Denet, A.R., Vanbever, R. and Preat, V. (2004) Skin electroporation for transdermal and topical delivery. *Adv Drug Deliv Rev*, **56**, 659-674.
- Dermietzel, R., Hwang, T.K., Buettner, R., Hofer, A., Dotzler, E., Kremer, M., Deutzmann, R., Thinner, F.P., Fishman, G.I., Spray, D.C. and et al. (1994) Cloning and in situ localization of a brain-derived porin that constitutes a large-conductance anion channel in astrocytic plasma membranes. *Proc Natl Acad Sci U S A*, **91**, 499-503.
- D'hondt, C., Srinivas, S.P., Vereecke, J. and Himpens, B. (2007) Adenosine opposes thrombin-induced inhibition of intercellular calcium wave in corneal endothelial cells. *Invest Ophthalmol Vis Sci*, **48**, 1518-1527.
- Di Virgilio, F. (2006) Purinergic signalling between axons and microglia. *Novartis Found Symp*, **276**, 253-258; discussion 259-262, 275-281.
- Diez, J.A., Ahmad, S. and Evans, W.H. (1999) Assembly of heteromeric connexons in guinea-pig liver en route to the Golgi apparatus, plasma membrane and gap junctions. *Eur J Biochem*, **262**, 142-148.
- Diez, J.A., Elvira, M. and Villalobo, A. (1995) Phosphorylation of connexin-32 by the epidermal growth factor receptor tyrosine kinase. *Ann N Y Acad Sci*, **766**, 477-480.
- Doble, B.W., Chen, Y., Bosc, D.G., Litchfield, D.W. and Kardami, E. (1996) Fibroblast growth factor-2 decreases metabolic coupling and stimulates phosphorylation as well as masking of connexin43 epitopes in cardiac myocytes. *Circ Res*, **79**, 647-658.
- Doble, B.W., Dang, X., Ping, P., Fandrich, R.R., Nickel, B.E., Jin, Y., Cattini, P.A. and Kardami, E. (2004) Phosphorylation of serine 262 in the gap junction protein

- connexin-43 regulates DNA synthesis in cell-cell contact forming cardiomyocytes. *J Cell Sci*, **117**, 507-514.
- Doble, B.W. and Kardami, E. (1995) Basic fibroblast growth factor stimulates connexin-43 expression and intercellular communication of cardiac fibroblasts. *Mol Cell Biochem*, **143**, 81-87.
- Dobrowolski, R., Sasse, P., Schrickel, J.W., Watkins, M., Kim, J.S., Rackauskas, M., Troatz, C., Ghanem, A., Tiemann, K., Degen, J., Bukauskas, F.F., Civitelli, R., Lewalter, T., Fleischmann, B.K. and Willecke, K. (2007) The conditional connexin43G138R mouse mutant represents a new model of hereditary oculodentodigital dysplasia in humans. *Hum Mol Genet*.
- Dora, K.A., Martin, P.E., Chaytor, A.T., Evans, W.H., Garland, C.J. and Griffith, T.M. (1999) Role of heterocellular Gap junctional communication in endothelium-dependent smooth muscle hyperpolarization: inhibition by a connexin-mimetic peptide. *Biochem Biophys Res Commun*, **254**, 27-31.
- Dringen, R. (2000) Metabolism and functions of glutathione in brain. *Prog Neurobiol*, **62**, 649-671.
- Dringen, R. and Hirrlinger, J. (2003) Glutathione pathways in the brain. *Biol Chem*, **384**, 505-516.
- Dringen, R., Pfeiffer, B. and Hamprecht, B. (1999) Synthesis of the antioxidant glutathione in neurons: supply by astrocytes of CysGly as precursor for neuronal glutathione. *J Neurosci*, **19**, 562-569.
- Duan, S., Anderson, C.M., Keung, E.C., Chen, Y. and Swanson, R.A. (2003) P2X7 receptor-mediated release of excitatory amino acids from astrocytes. *J Neurosci*, **23**, 1320-1328.
- Dubyak, G.R. and el-Moatassim, C. (1993) Signal transduction via P2-purinergic receptors for extracellular ATP and other nucleotides. *Am J Physiol*, **265**, C577-606.
- Duffy, H.S., Sorgen, P.L., Girvin, M.E., O'Donnell, P., Coombs, W., Taffet, S.M., Delmar, M. and Spray, D.C. (2002) pH-dependent intramolecular binding and structure involving Cx43 cytoplasmic domains. *J Biol Chem*, **277**, 36706-36714.
- Dupont, G., Combettes, L. and Leybaert, L. (2007) Calcium dynamics: spatio-temporal organization from the subcellular to the organ level. *Int Rev Cytol*, **261**, 193-245.
- Dykes, I.M., Freeman, F.M., Bacon, J.P. and Davies, J.A. (2004) Molecular basis of gap junctional communication in the CNS of the leech *Hirudo medicinalis*. *J Neurosci*, **24**, 886-894.
- Ebihara, L. (2003) New roles for connexons. *News Physiol Sci*, **18**, 100-103.
- Ebihara, L., Liu, X. and Pal, J.D. (2003) Effect of external magnesium and calcium on human connexin46 hemichannels. *Biophys J*, **84**, 277-286.
- Ebihara, L. and Steiner, E. (1993) Properties of a nonjunctional current expressed from a rat connexin46 cDNA in *Xenopus* oocytes. *J Gen Physiol*, **102**, 59-74.
- Eggermont, J., Trouet, D., Carton, I. and Nilius, B. (2001) Cellular function and control of volume-regulated anion channels. *Cell Biochem Biophys*, **35**, 263-274.
- Ek-Vitorin, J.F., Calero, G., Morley, G.E., Coombs, W., Taffet, S.M. and Delmar, M. (1996) PH regulation of connexin43: molecular analysis of the gating particle. *Biophys J*, **71**, 1273-1284.
- Elfgang, C., Eckert, R., Lichtenberg-Frate, H., Butterweck, A., Traub, O., Klein, R.A., Hulser, D.F. and Willecke, K. (1995) Specific permeability and selective formation of gap junction channels in connexin-transfected HeLa cells. *J Cell Biol*, **129**, 805-817.
- el-Fouly, M.H., Trosko, J.E. and Chang, C.C. (1987) Scrape-loading and dye transfer. A rapid and simple technique to study gap junctional intercellular communication. *Exp Cell Res*, **168**, 422-430.

- Ellis-Davies, G.C. and Kaplan, J.H. (1994) Nitrophenyl-EGTA, a photolabile chelator that selectively binds Ca<sup>2+</sup> with high affinity and releases it rapidly upon photolysis. *Proc Natl Acad Sci U S A*, **91**, 187-191.
- Eltzschig, H.K., Eckle, T., Mager, A., Kuper, N., Karcher, C., Weissmuller, T., Boengler, K., Schulz, R., Robson, S.C. and Colgan, S.P. (2006) ATP release from activated neutrophils occurs via connexin 43 and modulates adenosine-dependent endothelial cell function. *Circ Res*, **99**, 1100-1108.
- Enkvist, M.O. and McCarthy, K.D. (1994) Astroglial gap junction communication is increased by treatment with either glutamate or high K<sup>+</sup> concentration. *J Neurochem*, **62**, 489-495.
- Erlinge, D. (1998) Extracellular ATP: a growth factor for vascular smooth muscle cells. *Gen Pharmacol*, **31**, 1-8.
- Erriquez, J., Gilardino, A., Ariano, P., Munaron, L., Lovisolò, D. and Distasi, C. (2005) Calcium signals activated by arachidonic acid in embryonic chick ciliary ganglion neurons. *Neurosignals*, **14**, 244-254.
- Escobar, L.I., Salvador, C., Martinez, M. and Vaca, L. (1998) Maitotoxin, a cationic channel activator. *Neurobiology (Bp)*, **6**, 59-74.
- Eskandari, S., Zampighi, G.A., Leung, D.W., Wright, E.M. and Loo, D.D. (2002) Inhibition of gap junction hemichannels by chloride channel blockers. *J Membr Biol*, **185**, 93-102.
- Eugenin, E.A., Gonzalez, H., Saez, C.G. and Saez, J.C. (1998) Gap junctional communication coordinates vasopressin-induced glycogenolysis in rat hepatocytes. *Am J Physiol*, **274**, G1109-1116.
- Evans, J.H., Spencer, D.M., Zweifach, A. and Leslie, C.C. (2001) Intracellular calcium signals regulating cytosolic phospholipase A2 translocation to internal membranes. *J Biol Chem*, **276**, 30150-30160.
- Evans, W.H. and Boitano, S. (2001) Connexin mimetic peptides: specific inhibitors of gap-junctional intercellular communication. *Biochem Soc Trans*, **29**, 606-612.
- Evans, W.H., De Vuyst, E. and Leybaert, L. (2006) The gap junction cellular internet: connexin hemichannels enter the signalling limelight. *Biochem J*, in press.
- Falk, M.M. (2000) Connexin-specific distribution within gap junctions revealed in living cells. *J Cell Sci*, **113** ( Pt 22), 4109-4120.
- Fallon, R.F. and Goodenough, D.A. (1981) Five-hour half-life of mouse liver gap-junction protein. *J Cell Biol*, **90**, 521-526.
- Faria, R.X., Defarias, F.P. and Alves, L.A. (2005) Are second messengers crucial for opening the pore associated with P2X7 receptor? *Am J Physiol Cell Physiol*, **288**, C260-271.
- Ferrari, D., Pizzirani, C., Adinolfi, E., Lemoli, R.M., Curti, A., Idzko, M., Panther, E. and Di Virgilio, F. (2006) The P2X7 receptor: a key player in IL-1 processing and release. *J Immunol*, **176**, 3877-3883.
- Fields, R.D. and Burnstock, G. (2006) Purinergic signalling in neuron-glia interactions. *Nat Rev Neurosci*, **7**, 423-436.
- Filson, A.J., Azarnia, R., Beyer, E.C., Loewenstein, W.R. and Brugge, J.S. (1990) Tyrosine phosphorylation of a gap junction protein correlates with inhibition of cell-to-cell communication. *Cell Growth Differ*, **1**, 661-668.
- Finbow, M.E., Shuttleworth, J., Hamilton, A.E. and Pitts, J.D. (1983) Analysis of vertebrate gap junction protein. *Embo J*, **2**, 1479-1486.
- Firek, L. and Weingart, R. (1995) Modification of gap junction conductance by divalent cations and protons in neonatal rat heart cells. *J Mol Cell Cardiol*, **27**, 1633-1643.

- Fishman, G.I., Moreno, A.P., Spray, D.C. and Levinwand, L.A. (1991) Functional analysis of human cardiac gap junction channel mutants. *Proc Natl Acad Sci U S A*, **88**, 3525-3529.
- Fleming, I. (2007) Epoxyeicosatrienoic acids, cell signaling and angiogenesis. *Prost Lipid Med*, **82**, 60-67.
- Foote, C.I., Zhou, L., Zhu, X. and Nicholson, B.J. (1998) The pattern of disulfide linkages in the extracellular loop regions of connexin 32 suggests a model for the docking interface of gap junctions. *J Cell Biol*, **140**, 1187-1197.
- Francis, D., Stergiopoulos, K., Ek-Vitorin, J.F., Cao, F.L., Taffet, S.M. and Delmar, M. (1999) Connexin diversity and gap junction regulation by pHi. *Dev Genet*, **24**, 123-136.
- Friedman, L.K. (2006) Calcium: a role for neuroprotection and sustained adaptation. *Mol Interv*, **6**, 315-329.
- Fujimoto, K., Nagafuchi, A., Tsukita, S., Kuraoka, A., Ohokuma, A. and Shibata, Y. (1997) Dynamics of connexins, E-cadherin and alpha-catenin on cell membranes during gap junction formation. *J Cell Sci*, **110** ( Pt 3), 311-322.
- Fujiwara, S., Shimamoto, C., Nakanishi, Y., Katsu, K., Kato, M. and Nakahari, T. (2006) Enhancement of Ca<sup>2+</sup>-regulated exocytosis by indomethacin in guinea-pig antral mucous cells: arachidonic acid accumulation. *Exp Physiol*, **91**, 249-259.
- Furukawa, T., Ogura, T., Katayama, Y. and Hiraoka, M. (1998) Characteristics of rabbit CIC-2 current expressed in *Xenopus* oocytes and its contribution to volume regulation. *Am J Physiol*, **274**, C500-512.
- Gabriel, B. and Teissie, J. (1999) Time courses of mammalian cell electropermeabilization observed by millisecond imaging of membrane property changes during the pulse. *Biophys J*, **76**, 2158-2165.
- Gaietta, G., Deerinck, T.J., Adams, S.R., Bouwer, J., Tour, O., Laird, D.W., Sosinsky, G.E., Tsien, R.Y. and Ellisman, M.H. (2002) Multicolor and electron microscopic imaging of connexin trafficking. *Science*, **296**, 503-507.
- Gehl, J. (2003) Electroporation: theory and methods, perspectives for drug delivery, gene therapy and research. *Acta Physiol Scand*, **177**, 437-447.
- George, C.H., Kendall, J.M., Campbell, A.K. and Evans, W.H. (1998) Connexin-aequorin chimeras report cytoplasmic calcium environments along trafficking pathways leading to gap junction biogenesis in living COS-7 cells. *J Biol Chem*, **273**, 29822-29829.
- George, C.H., Kendall, J.M. and Evans, W.H. (1999) Intracellular trafficking pathways in the assembly of connexins into gap junctions. *J Biol Chem*, **274**, 8678-8685.
- Gerdes, H.H., Bukoreshtliev, N.V. and Barroso, J.F. (2007) Tunneling nanotubes: a new route for the exchange of components between animal cells. *FEBS Lett*, **581**, 2194-2201.
- Giaume, C., Randriamampita, C. and Trautmann, A. (1989) Arachidonic acid closes gap junction channels in rat lacrimal glands. *Pflugers Arch*, **413**, 273-279.
- Giepmans, B.N., Hengeveld, T., Postma, F.R. and Moolenaar, W.H. (2001) Interaction of c-Src with gap junction protein connexin-43. Role in the regulation of cell-cell communication. *J Biol Chem*, **276**, 8544-8549.
- Goldberg, G.S., Bechberger, J.F., Tajima, Y., Merritt, M., Omori, Y., Gawinowicz, M.A., Narayanan, R., Tan, Y., Sanai, Y., Yamasaki, H., Naus, C.C., Tsuda, H. and Nicholson, B.J. (2000) Connexin43 suppresses MFG-E8 while inducing contact growth inhibition of glioma cells. *Cancer Res*, **60**, 6018-6026.
- Goldberg, G.S., Lampe, P.D. and Nicholson, B.J. (1999) Selective transfer of endogenous metabolites through gap junctions composed of different connexins. *Nat Cell Biol*, **1**, 457-459.

- Goldberg, G.S. and Lau, A.F. (1993) Dynamics of connexin43 phosphorylation in pp60v-src-transformed cells. *Biochem J*, **295** ( Pt 3), 735-742.
- Goldberg, G.S., Moreno, A.P. and Lampe, P.D. (2002) Gap junctions between cells expressing connexin 43 or 32 show inverse permselectivity to adenosine and ATP. *J Biol Chem*, **277**, 36725-36730.
- Golzio, M., Rols, M.P. and Teissie, J. (2004) In vitro and in vivo electric field-mediated permeabilization, gene transfer, and expression. *Methods*, **33**, 126-135.
- Gomes, P., Srinivas, S.P., Van Driessche, W., Vereecke, J. and Himpens, B. (2005) ATP release through connexin hemichannels in corneal endothelial cells. *Invest Ophthalmol Vis Sci*, **46**, 1208-1218.
- Gomes, P., Srinivas, S.P., Vereecke, J. and Himpens, B. (2006) Gap junctional intercellular communication in bovine corneal endothelial cells. *Exp Eye Res*, **83**, 1225-1237.
- Gomez-Hernandez, J.M., de Miguel, M., Larrosa, B., Gonzalez, D. and Barrio, L.C. (2003) Molecular basis of calcium regulation in connexin-32 hemichannels. *Proc Natl Acad Sci U S A*, **100**, 16030-16035.
- Gonzalez, D., Gomez-Hernandez, J.M. and Barrio, L.C. (2006) Species specificity of mammalian connexin-26 to form open voltage-gated hemichannels. *Faseb J*, **20**, 2329-2338.
- Gonzalez, D., Gomez-Hernandez, J.M. and Barrio, L.C. (2007) Molecular basis of voltage dependence of connexin channels: An integrative appraisal. *Prog Biophys Mol Biol*.
- Goodenough, D.A. and Paul, D.L. (2003) Beyond the gap: functions of unpaired connexon channels. *Nat Rev Mol Cell Biol*, **4**, 285-294.
- Gothelf, A., Mir, L.M. and Gehl, J. (2003) Electrochemotherapy: results of cancer treatment using enhanced delivery of bleomycin by electroporation. *Cancer Treat Rev*, **29**, 371-387.
- Granot, I. and Dekel, N. (1994) Phosphorylation and expression of connexin-43 ovarian gap junction protein are regulated by luteinizing hormone. *J Biol Chem*, **269**, 30502-30509.
- Gregory, W.A. and Bennett, M.V. (1988) Gap junctions in goldfish preoptic ependyma: regional variation in cellular differentiation. *Brain Res*, **470**, 205-216.
- Gross, S.D. and Anderson, R.A. (1998) Casein kinase I: spatial organization and positioning of a multifunctional protein kinase family. *Cell Signal*, **10**, 699-711.
- Grygorczyk, R. and Hanrahan, J.W. (1997) CFTR-independent ATP release from epithelial cells triggered by mechanical stimuli. *Am J Physiol*, **272**, C1058-1066.
- Grygorczyk, R., Tabcharani, J.A. and Hanrahan, J.W. (1996) CFTR channels expressed in CHO cells do not have detectable ATP conductance. *J Membr Biol*, **151**, 139-148.
- Grynkiewicz, G., Poenie, M. and Tsien, R.Y. (1985) A new generation of Ca<sup>2+</sup> indicators with greatly improved fluorescence properties. *J Biol Chem*, **260**, 3440-3450.
- Gu, B.J., Zhang, W., Worthington, R.A., Sluyter, R., Dao-Ung, P., Petrou, S., Barden, J.A. and Wiley, J.S. (2001) A Glu-496 to Ala polymorphism leads to loss of function of the human P2X7 receptor. *J Biol Chem*, **276**, 11135-11142.
- Guan, X., Wilson, S., Schlender, K.K. and Ruch, R.J. (1996) Gap-junction disassembly and connexin 43 dephosphorylation induced by 18 beta-glycyrrhetic acid. *Mol Carcinog*, **16**, 157-164.
- Gudermann, T., Grosse, R. and Schultz, G. (2000) Contribution of receptor/G protein signaling to cell growth and transformation. *Naunyn Schmiedebergs Arch Pharmacol*, **361**, 345-362.
- Gusovsky, F. and Daly, J.W. (1990) Maitotoxin: a unique pharmacological tool for research on calcium-dependent mechanisms. *Biochem Pharmacol*, **39**, 1633-1639.



- Guthrie, P.B., Knappenberger, J., Segal, M., Bennett, M.V., Charles, A.C. and Kater, S.B. (1999) ATP released from astrocytes mediates glial calcium waves. *J Neurosci*, **19**, 520-528.
- Hare, J.F. and Taylor, K. (1991) Mechanisms of plasma membrane protein degradation: recycling proteins are degraded more rapidly than those confined to the cell surface. *Proc Natl Acad Sci U S A*, **88**, 5902-5906.
- Harris, A.L. (2001) Emerging issues of connexin channels: biophysics fills the gap. *Q Rev Biophys*, **34**, 325-472.
- Harris, A.L., Spray, D.C. and Bennett, M.V. (1981) Kinetic properties of a voltage-dependent junctional conductance. *J Gen Physiol*, **77**, 95-117.
- Hassinger, T.D., Guthrie, P.B., Atkinson, P.B., Bennett, M.V. and Kater, S.B. (1996) An extracellular signaling component in propagation of astrocytic calcium waves. *Proc Natl Acad Sci U S A*, **93**, 13268-13273.
- Hayashi, I., Wilde, A., Mal, T.K. and Ikura, M. (2005) Structural basis for the activation of microtubule assembly by the EB1 and p150Glued complex. *Mol Cell*, **19**, 449-460.
- He, L. and Wu, L. (2007) The debate on the kiss-and-run fusion at synapses. *Trends Neurosci*, **30**, 447-455.
- Herbert, J.M., Augereau, J.M., Gleye, J. and Maffrand, J.P. (1990) Chelerythrine is a potent and specific inhibitor of protein kinase C. *Biochem Biophys Res Commun*, **172**, 993-999.
- Hershko, A. and Ciechanover, A. (1998) The ubiquitin system. *Annu Rev Biochem*, **67**, 425-479.
- Hertlein, B., Butterweck, A., Haubrich, S., Willecke, K. and Traub, O. (1998) Phosphorylated carboxy terminal serine residues stabilize the mouse gap junction protein connexin45 against degradation. *J Membr Biol*, **162**, 247-257.
- Herve, J.C., Derangeon, M., Bahbouhi, B., Mesnil, M. and Sarrouilhe, D. (2007) The Connexin Turnover, an Important Modulating Factor of the Level of Cell-to-Cell Junctional Communication: Comparison with Other Integral Membrane Proteins. *J Membr Biol*.
- Hicke, L. (1999) Gettin' down with ubiquitin: turning off cell-surface receptors, transporters and channels. *Trends Cell Biol*, **9**, 107-112.
- Hicke, L. and Dunn, R. (2003) Regulation of membrane protein transport by ubiquitin and ubiquitin-binding proteins. *Annu Rev Cell Dev Biol*, **19**, 141-172.
- Hidaka, H. and Yokokura, H. (1996) Molecular and cellular pharmacology of a calcium/calmodulin-dependent protein kinase II (CaM kinase II) inhibitor, KN-62, and proposal of CaM kinase phosphorylation cascades. *Adv Pharmacol*, **36**, 193-219.
- Hill, C.S., Oh, S.Y., Schmidt, S.A., Clark, K.J. and Murray, A.W. (1994) Lysophosphatidic acid inhibits gap-junctional communication and stimulates phosphorylation of connexin-43 in WB cells: possible involvement of the mitogen-activated protein kinase cascade. *Biochem J*, **303 ( Pt 2)**, 475-479.
- Hille, B. (1978) Ionic channels in excitable membranes. Current problems and biophysical approaches. *Biophys J*, **22**, 283-294.
- Hirst-Jensen, B.J., Sahoo, P., Kieken, F., Delmar, M. and Sorgen, P.L. (2007) Characterization of the pH-dependent interaction between the gap junction protein connexin43 carboxyl terminus and cytoplasmic loop domains. *J Biol Chem*, **282**, 5801-5813.
- Hisadome, K., Koyama, T., Kimura, C., Droogmans, G., Ito, Y. and Oike, M. (2002) Volume-regulated anion channels serve as an auto/paracrine nucleotide release pathway in aortic endothelial cells. *J Gen Physiol*, **119**, 511-520.

- Hoebertz, A., Arnett, T.R. and Burnstock, G. (2003) Regulation of bone resorption and formation by purines and pyrimidines. *Trends Pharmacol Sci*, **24**, 290-297.
- Hofer, A.M. and Brown, E.M. (2003) Extracellular calcium sensing and signalling. *Nat Rev Mol Cell Biol*, **4**, 530-538.
- Homma, N., Alvarado, J.L., Coombs, W., Stergiopoulos, K., Taffet, S.M., Lau, A.F. and Delmar, M. (1998) A particle-receptor model for the insulin-induced closure of connexin43 channels. *Circ Res*, **83**, 27-32.
- Hossain, M.Z., Ao, P. and Boynton, A.L. (1998) Rapid disruption of gap junctional communication and phosphorylation of connexin43 by platelet-derived growth factor in T51B rat liver epithelial cells expressing platelet-derived growth factor receptor. *J Cell Physiol*, **174**, 66-77.
- Hossain, M.Z., Jagdale, A.B., Ao, P. and Boynton, A.L. (1999a) Mitogen-activated protein kinase and phosphorylation of connexin43 are not sufficient for the disruption of gap junctional communication by platelet-derived growth factor and tetradecanoylphorbol acetate. *J Cell Physiol*, **179**, 87-96.
- Hossain, M.Z., Jagdale, A.B., Ao, P., Kazlauskas, A. and Boynton, A.L. (1999b) Disruption of gap junctional communication by the platelet-derived growth factor is mediated via multiple signaling pathways. *J Biol Chem*, **274**, 10489-10496.
- Hua, V.B., Chang, A.B., Tchieu, J.H., Kumar, N.M., Nielsen, P.A. and Saier, M.H., Jr. (2003) Sequence and phylogenetic analyses of 4 TMS junctional proteins of animals: connexins, innexins, claudins and occludins. *J Membr Biol*, **194**, 59-76.
- Huang, X.D., Horackova, M. and Pressler, M.L. (1996) Changes in the expression and distribution of connexin 43 in isolated cultured adult guinea pig cardiomyocytes. *Exp Cell Res*, **228**, 254-261.
- Hudmon, A., Aronowski, J., Kolb, S.J. and Waxham, M.N. (1996) Inactivation and self-association of Ca<sup>2+</sup>/calmodulin-dependent protein kinase II during autophosphorylation. *J Biol Chem*, **271**, 8800-8808.
- Hudmon, A., Schulman, H., Kim, J., Maltez, J.M., Tsien, R.W. and Pitt, G.S. (2005) CaMKII tethers to L-type Ca<sup>2+</sup> channels, establishing a local and dedicated integrator of Ca<sup>2+</sup> signals for facilitation. *J Cell Biol*, **171**, 537-547.
- Humphreys, B.D., Virginio, C., Surprenant, A., Rice, J. and Dubyak, G.R. (1998) Isoquinolines as antagonists of the P2X7 nucleotide receptor: high selectivity for the human versus rat receptor homologues. *Mol Pharmacol*, **54**, 22-32.
- Hur, K.C., Shim, J.E. and Johnson, R.G. (2003) A potential role for cx43-hemichannels in staurosporin-induced apoptosis. *Cell Commun Adhes*, **10**, 271-277.
- Inoue, T. and Krumlauf, R. (2001) An impulse to the brain--using in vivo electroporation. *Nat Neurosci*, **4 Suppl**, 1156-1158.
- Isakson, B.E., Evans, W.H. and Boitano, S. (2001) Intercellular Ca<sup>2+</sup> signaling in alveolar epithelial cells through gap junctions and by extracellular ATP. *Am J Physiol Lung Cell Mol Physiol*, **280**, L221-228.
- Isakson, B.E., Seedorf, G.J., Lubman, R.L., Evans, W.H. and Boitano, S. (2003) Cell-cell communication in heterocellular cultures of alveolar epithelial cells. *Am J Respir Cell Mol Biol*, **29**, 552-561.
- Ishida, A., Kameshita, I., Okuno, S., Kitani, T. and Fujisawa, H. (1995) A novel highly specific and potent inhibitor of calmodulin-dependent protein kinase II. *Biochem Biophys Res Commun*, **212**, 806-812.
- Jamora, C. and Fuchs, E. (2002) Intercellular adhesion, signalling and the cytoskeleton. *Nat Cell Biol*, **4**, E101-108.

- Jee, W.S., Ueno, K., Deng, Y.P. and Woodbury, D.M. (1985) The effects of prostaglandin E<sub>2</sub> in growing rats: increased metaphyseal hard tissue and cortico-endosteal bone formation. *Calcif Tissue Int*, **37**, 148-157.
- Jentsch, T.J., Stein, V., Weinreich, F. and Zdebik, A.A. (2002) Molecular structure and physiological function of chloride channels. *Physiol Rev*, **82**, 503-568.
- Jiang, J.X. and Cherian, P.P. (2003) Hemichannels formed by connexin 43 play an important role in the release of prostaglandin E<sub>2</sub> by osteocytes in response to mechanical strain. *Cell Commun Adhes*, **10**, 259-264.
- Jiang, J.X. and Goodenough, D.A. (1998) Phosphorylation of lens-fiber connexins in lens organ cultures. *Eur J Biochem*, **255**, 37-44.
- Jiang, J.X., Paul, D.L. and Goodenough, D.A. (1993) Posttranslational phosphorylation of lens fiber connexin46: a slow occurrence. *Invest Ophthalmol Vis Sci*, **34**, 3558-3565.
- John, S.A., Kondo, R., Wang, S.Y., Goldhaber, J.I. and Weiss, J.N. (1999) Connexin-43 hemichannels opened by metabolic inhibition. *J Biol Chem*, **274**, 236-240.
- Jordan, K., Chodock, R., Hand, A.R. and Laird, D.W. (2001) The origin of annular junctions: a mechanism of gap junction internalization. *J Cell Sci*, **114**, 763-773.
- Jorgensen, N.R., Henriksen, Z., Sorensen, O.H., Eriksen, E.F., Civitelli, R. and Steinberg, T.H. (2002) Intercellular calcium signaling occurs between human osteoblasts and osteoclasts and requires activation of osteoclast P2X<sub>7</sub> receptors. *J Biol Chem*, **277**, 7574-7580.
- Kalvelyte, A., Imbrasaitė, A., Bukauskiene, A., Verselis, V.K. and Bukauskas, F.F. (2003) Connexins and apoptotic transformation. *Biochem Pharmacol*, **66**, 1661-1672.
- Kamermans, M., Fahrenfort, I., Schultz, K., Janssen-Bienhold, U., Sjoerdsma, T. and Weiler, R. (2001) Hemichannel-mediated inhibition in the outer retina. *Science*, **292**, 1178-1180.
- Kanemitsu, M.Y., Jiang, W. and Eckhart, W. (1998) Cdc2-mediated phosphorylation of the gap junction protein, connexin43, during mitosis. *Cell Growth Differ*, **9**, 13-21.
- Kanemitsu, M.Y. and Lau, A.F. (1993) Epidermal growth factor stimulates the disruption of gap junctional communication and connexin43 phosphorylation independent of 12-O-tetradecanoylphorbol 13-acetate-sensitive protein kinase C: the possible involvement of mitogen-activated protein kinase. *Mol Biol Cell*, **4**, 837-848.
- Kanemitsu, M.Y., Loo, L.W., Simon, S., Lau, A.F. and Eckhart, W. (1997) Tyrosine phosphorylation of connexin 43 by v-Src is mediated by SH2 and SH3 domain interactions. *J Biol Chem*, **272**, 22824-22831.
- Kardami, E., Stoski, R.M., Doble, B.W., Yamamoto, T., Hertzberg, E.L. and Nagy, J.I. (1991) Biochemical and ultrastructural evidence for the association of basic fibroblast growth factor with cardiac gap junctions. *J Biol Chem*, **266**, 19551-19557.
- Katsuki, H. and Okuda, S. (1995) Arachidonic acid as a neurotoxic and neurotrophic substance. *Prog Neurobiol*, **46**, 607-636.
- Kelley, G.G., Kaproth-Joslin, K.A., Reks, S.E., Smrcka, A.V. and Wojcikiewicz, R.J. (2006) G-protein-coupled receptor agonists activate endogenous phospholipase Cepsilon and phospholipase Cbeta3 in a temporally distinct manner. *J Biol Chem*, **281**, 2639-2648.
- Khakh, B.S. (2001) Molecular physiology of P2X receptors and ATP signalling at synapses. *Nat Rev Neurosci*, **2**, 165-174.
- Kim, D.Y., Kam, Y., Koo, S.K. and Joe, C.O. (1999) Gating connexin 43 channels reconstituted in lipid vesicles by mitogen-activated protein kinase phosphorylation. *J Biol Chem*, **274**, 5581-5587.
- Klee, C.B., Ren, H. and Wang, X. (1998) Regulation of the calmodulin-stimulated protein phosphatase, calcineurin. *J Biol Chem*, **273**, 13367-13370.

- Kojima, T., Sawada, N., Oyamada, M., Chiba, H., Isomura, H. and Mori, M. (1994) Rapid appearance of connexin 26-positive gap junctions in centrilobular hepatocytes without induction of mRNA and protein synthesis in isolated perfused liver of female rat. *J Cell Sci*, **107** ( Pt 12), 3579-3590.
- Kojima, T., Srinivas, M., Fort, A., Hopperstad, M., Urban, M., Hertzberg, E.L., Mochizuki, Y. and Spray, D.C. (1999) TPA induced expression and function of human connexin 26 by post-translational mechanisms in stably transfected neuroblastoma cells. *Cell Struct Funct*, **24**, 435-441.
- Komarov, A.G., Deng, D., Craigen, W.J. and Colombini, M. (2005) New insights into the mechanism of permeation through large channels. *Biophys J*, **89**, 3950-3959.
- Kondo, R.P., Wang, S.Y., John, S.A., Weiss, J.N. and Goldhaber, J.I. (2000) Metabolic inhibition activates a non-selective current through connexin hemichannels in isolated ventricular myocytes. *J Mol Cell Cardiol*, **32**, 1859-1872.
- Kotnik, T., Miklavcic, D. and Mir, L.M. (2001a) Cell membrane electropermeabilization by symmetrical bipolar rectangular pulses. Part II. Reduced electrolytic contamination. *Bioelectrochemistry*, **54**, 91-95.
- Kotnik, T., Mir, L.M., Flisar, K., Puc, M. and Miklavcic, D. (2001b) Cell membrane electropermeabilization by symmetrical bipolar rectangular pulses. Part I. Increased efficiency of permeabilization. *Bioelectrochemistry*, **54**, 83-90.
- Kotnik, T., Pucihar, G., Rebersek, M., Miklavcic, D. and Mir, L.M. (2003) Role of pulse shape in cell membrane electropermeabilization. *Biochim Biophys Acta*, **1614**, 193-200.
- Koval, M., Geist, S.T., Westphale, E.M., Kemendy, A.E., Civitelli, R., Beyer, E.C. and Steinberg, T.H. (1995) Transfected connexin45 alters gap junction permeability in cells expressing endogenous connexin43. *J Cell Biol*, **130**, 987-995.
- Kranenburg, O. and Moolenaar, W.H. (2001) Ras-MAP kinase signaling by lysophosphatidic acid and other G protein-coupled receptor agonists. *Oncogene*, **20**, 1540-1546.
- Krassowska, W. and Filev, P.D. (2007) Modeling electroporation in a single cell. *Biophys J*, **92**, 404-417.
- Kristian, T. and Siesjo, B.K. (1998) Calcium in ischemic cell death. *Stroke*, **29**, 705-718.
- Krull, C.E. (2004) A primer on using in ovo electroporation to analyze gene function. *Dev Dyn*, **229**, 433-439.
- Krysko, D.V., Leybaert, L., Vandenabeele, P. and D'Herde, K. (2005) Gap junctions and the propagation of cell survival and cell death signals. *Apoptosis*, **10**, 459-469.
- Kumar, N.M. and Gilula, N.B. (1996) The gap junction communication channel. *Cell*, **84**, 381-388.
- Kurata, W.E. and Lau, A.F. (1994) p130gag-fps disrupts gap junctional communication and induces phosphorylation of connexin43 in a manner similar to that of pp60v-src. *Oncogene*, **9**, 329-335.
- Kwak, B.R., Hermans, M.M., De Jonge, H.R., Lohmann, S.M., Jongsma, H.J. and Chanson, M. (1995a) Differential regulation of distinct types of gap junction channels by similar phosphorylating conditions. *Mol Biol Cell*, **6**, 1707-1719.
- Kwak, B.R. and Jongsma, H.J. (1999) Selective inhibition of gap junction channel activity by synthetic peptides. *J Physiol*, **516** ( Pt 3), 679-685.
- Kwak, B.R., van Veen, T.A., Analbers, L.J. and Jongsma, H.J. (1995b) TPA increases conductance but decreases permeability in neonatal rat cardiomyocyte gap junction channels. *Exp Cell Res*, **220**, 456-463.
- Labarthe, M.P., Bosco, D., Saurat, J.H., Meda, P. and Salomon, D. (1998) Upregulation of connexin 26 between keratinocytes of psoriatic lesions. *J Invest Dermatol*, **111**, 72-76.

- Laemmli, U.K. (1970) Cleavage of structural proteins during the assembly of the head of bacteriophage T4. *Nature*, **227**, 680-685.
- Lagostena, L., Ashmore, J.F., Kachar, B. and Mammano, F. (2001) Purinergic control of intercellular communication between Hensen's cells of the guinea-pig cochlea. *J Physiol*, **531**, 693-706.
- Lagostena, L. and Mammano, F. (2001) Intracellular calcium dynamics and membrane conductance changes evoked by Deiters' cell purinoceptor activation in the organ of Corti. *Cell Calcium*, **29**, 191-198.
- Lai, C.P., Bechberger, J.F., Thompson, R.J., MacVicar, B.A., Bruzzone, R. and Naus, C.C. (2007) Tumor-suppressive effects of pannexin 1 in C6 glioma cells. *Cancer Res*, **67**, 1545-1554.
- Laing, J.G., Westphale, E.M., Engelmann, G.L. and Beyer, E.C. (1994) Characterization of the gap junction protein, connexin45. *J Membr Biol*, **139**, 31-40.
- Laird, D.W. (1996) The life cycle of a connexin: gap junction formation, removal, and degradation. *J Bioenerg Biomembr*, **28**, 311-318.
- Laird, D.W. (2005) Connexin phosphorylation as a regulatory event linked to gap junction internalization and degradation. *Biochim Biophys Acta*, **1711**, 172-182.
- Laird, D.W. (2006) Life cycle of connexins in health and disease. *Biochem J*, **394**, 527-543.
- Laird, D.W., Castillo, M. and Kasprzak, L. (1995) Gap junction turnover, intracellular trafficking, and phosphorylation of connexin43 in brefeldin A-treated rat mammary tumor cells. *J Cell Biol*, **131**, 1193-1203.
- Laird, D.W., Puranam, K.L. and Revel, J.P. (1991) Turnover and phosphorylation dynamics of connexin43 gap junction protein in cultured cardiac myocytes. *Biochem J*, **273(Pt 1)**, 67-72.
- Lampe, P.D. (1994) Analyzing phorbol ester effects on gap junctional communication: a dramatic inhibition of assembly. *J Cell Biol*, **127**, 1895-1905.
- Lampe, P.D., Kurata, W.E., Warn-Cramer, B.J. and Lau, A.F. (1998) Formation of a distinct connexin43 phosphoisoform in mitotic cells is dependent upon p34cdc2 kinase. *J Cell Sci*, **111 ( Pt 6)**, 833-841.
- Lampe, P.D. and Lau, A.F. (2000) Regulation of gap junctions by phosphorylation of connexins. *Arch Biochem Biophys*, **384**, 205-215.
- Lampe, P.D. and Lau, A.F. (2004) The effects of connexin phosphorylation on gap junctional communication. *Int J Biochem Cell Biol*, **36**, 1171-1186.
- Lampe, P.D., TenBroek, E.M., Burt, J.M., Kurata, W.E., Johnson, R.G. and Lau, A.F. (2000) Phosphorylation of connexin43 on serine368 by protein kinase C regulates gap junctional communication. *J Cell Biol*, **149**, 1503-1512.
- Larsen, W.J., Tung, H.N., Murray, S.A. and Swenson, C.A. (1979) Evidence for the participation of actin microfilaments and bristle coats in the internalization of gap junction membrane. *J Cell Biol*, **83**, 576-587.
- Lau, A.F., Kanemitsu, M.Y., Kurata, W.E., Danesh, S. and Boynton, A.L. (1992) Epidermal growth factor disrupts gap-junctional communication and induces phosphorylation of connexin43 on serine. *Mol Biol Cell*, **3**, 865-874.
- Lauf, U., Giepmans, B.N., Lopez, P., Braconnot, S., Chen, S.C. and Falk, M.M. (2002) Dynamic trafficking and delivery of connexons to the plasma membrane and accretion to gap junctions in living cells. *Proc Natl Acad Sci U S A*, **99**, 10446-10451.
- Lazarowski, E.R., Boucher, R.C. and Harden, T.K. (2003) Mechanisms of release of nucleotides and integration of their action as P2X- and P2Y-receptor activating molecules. *Mol Pharmacol*, **64**, 785-795.
- Lazrak, A. and Peracchia, C. (1993) Gap junction gating sensitivity to physiological internal calcium regardless of pH in Novikoff hepatoma cells. *Biophys J*, **65**, 2002-2012.

- Le Feuvre, R.A., Brough, D., Iwakura, Y., Takeda, K. and Rothwell, N.J. (2002) Priming of macrophages with lipopolysaccharide potentiates P2X7-mediated cell death via a caspase-1-dependent mechanism, independently of cytokine production. *J Biol Chem*, **277**, 3210-3218.
- Lee, S.W., Tomasetto, C., Paul, D., Keyomarsi, K. and Sager, R. (1992) Transcriptional downregulation of gap-junction proteins blocks junctional communication in human mammary tumor cell lines. *J Cell Biol*, **118**, 1213-1221.
- Leech, C.A. and Habener, J.F. (1998) A role for Ca<sup>2+</sup>-sensitive nonselective cation channels in regulating the membrane potential of pancreatic beta-cells. *Diabetes*, **47**, 1066-1073.
- Leem, C.H., Lagadic-Gossmann, D. and Vaughan-Jones, R.D. (1999) Characterization of intracellular pH regulation in the guinea-pig ventricular myocyte. *J Physiol*, **517** ( Pt 1), 159-180.
- Leithe, E., Brech, A. and Rivedal, E. (2006) Endocytic processing of connexin43 gap junctions: a morphological study. *Biochem J*, **393**, 59-67.
- Leithe, E. and Rivedal, E. (2004) Epidermal growth factor regulates ubiquitination, internalization and proteasome-dependent degradation of connexin43. *J Cell Sci*, **117**, 1211-1220.
- Leithe, E. and Rivedal, E. (2007) Ubiquitination of Gap Junction Proteins. *J Membr Biol*.
- Leybaert, L., Braet, K., Vandamme, W., Cabooter, L., Martin, P.E. and Evans, W.H. (2003) Connexin channels, connexin mimetic peptides and ATP release. *Cell Commun Adhes*, **10**, 251-257.
- Leybaert, L., de Meyer, A., Mabilde, C. and Sanderson, M.J. (2005) A simple and practical method to acquire geometrically correct images with resonant scanning-based line scanning in a custom-built video-rate laser scanning microscope. *J Microsc*, **219**, 133-140.
- Leybaert, L. and Sanderson, M.J. (2001) Intercellular calcium signaling and flash photolysis of caged compounds. A sensitive method to evaluate gap junctional coupling. *Methods Mol Biol*, **154**, 407-430.
- Leykauf, K., Salek, M., Bomke, J., Frech, M., Lehmann, W.D., Durst, M. and Alonso, A. (2006) Ubiquitin protein ligase Nedd4 binds to connexin43 by a phosphorylation-modulated process. *J Cell Sci*, **119**, 3634-3642.
- Li, H., Liu, T.F., Lazrak, A., Peracchia, C., Goldberg, G.S., Lampe, P.D. and Johnson, R.G. (1996) Properties and regulation of gap junctional hemichannels in the plasma membranes of cultured cells. *J Cell Biol*, **134**, 1019-1030.
- Li, S. (2004) Electroporation gene therapy: new developments in vivo and in vitro. *Curr Gene Ther*, **4**, 309-316.
- Li, S., Dent, J.A. and Roy, R. (2003) Regulation of intermuscular electrical coupling by the *Caenorhabditis elegans* innexin *inx-6*. *Mol Biol Cell*, **14**, 2630-2644.
- Lidington, D., Ouellette, Y. and Tyml, K. (2000) Endotoxin increases intercellular resistance in microvascular endothelial cells by a tyrosine kinase pathway. *J Cell Physiol*, **185**, 117-125.
- Lidington, D., Tyml, K. and Ouellette, Y. (2002) Lipopolysaccharide-induced reductions in cellular coupling correlate with tyrosine phosphorylation of connexin 43. *J Cell Physiol*, **193**, 373-379.
- Ligon, L.A., Karki, S., Tokito, M. and Holzbaur, E.L. (2001) Dynein binds to beta-catenin and may tether microtubules at adherens junctions. *Nat Cell Biol*, **3**, 913-917.
- Lin, R., Martyn, K.D., Guyette, C.V., Lau, A.F. and Warn-Cramer, B.J. (2006) v-Src tyrosine phosphorylation of connexin43: regulation of gap junction communication and effects on cell transformation. *Cell Commun Adhes*, **13**, 199-216.

- Lin, R., Warn-Cramer, B.J., Kurata, W.E. and Lau, A.F. (2001) v-Src phosphorylation of connexin 43 on Tyr247 and Tyr265 disrupts gap junctional communication. *J Cell Biol*, **154**, 815-827.
- Liu, F., Arce, F.T., Ramachandran, S. and Lal, R. (2006) Nanomechanics of hemichannel conformations: connexin flexibility underlying channel opening and closing. *J Biol Chem*, **281**, 23207-23217.
- Liu, S., Taffet, S., Stoner, L., Delmar, M., Vallano, M.L. and Jalife, J. (1993) A structural basis for the unequal sensitivity of the major cardiac and liver gap junctions to intracellular acidification: the carboxyl tail length. *Biophys J*, **64**, 1422-1433.
- Locke, D. (1998) Gap junctions in normal and neoplastic mammary gland. *J Pathol*, **186**, 343-349.
- Locke, D., Stein, T., Davies, C., Morris, J., Harris, A.L., Evans, W.H., Monaghan, P. and Gusterson, B. (2004) Altered permeability and modulatory character of connexin channels during mammary gland development. *Exp Cell Res*, **298**, 643-660.
- Locovei, S., Bao, L. and Dahl, G. (2006a) Pannexin 1 in erythrocytes: function without a gap. *Proc Natl Acad Sci U S A*, **103**, 7655-7659.
- Locovei, S., Scemes, E., Qiu, F., Spray, D.C. and Dahl, G. (2007) Pannexin1 is part of the pore forming unit of the P2X(7) receptor death complex. *FEBS Lett*, **581**, 483-488.
- Locovei, S., Wang, J. and Dahl, G. (2006b) Activation of pannexin 1 channels by ATP through P2Y receptors and by cytoplasmic calcium. *FEBS Lett*, **580**, 239-244.
- Logan, A., Frautschy, S.A., Gonzalez, A.M. and Baird, A. (1992) A time course for the focal elevation of synthesis of basic fibroblast growth factor and one of its high-affinity receptors (flg) following a localized cortical brain injury. *J Neurosci*, **12**, 3828-3837.
- Loo, L.W., Berestecky, J.M., Kanemitsu, M.Y. and Lau, A.F. (1995) pp60src-mediated phosphorylation of connexin 43, a gap junction protein. *J Biol Chem*, **270**, 12751-12761.
- Loo, L.W., Kanemitsu, M.Y. and Lau, A.F. (1999) In vivo association of pp60v-src and the gap-junction protein connexin 43 in v-src-transformed fibroblasts. *Mol Carcinog*, **25**, 187-195.
- Luke, R.A. and Saffitz, J.E. (1991) Remodeling of ventricular conduction pathways in healed canine infarct border zones. *J Clin Invest*, **87**, 1594-1602.
- Lundy, P.M., Nelson, P., Mi, L., Frew, R., Minaker, S., Vair, C. and Sawyer, T.W. (2004) Pharmacological differentiation of the P2X7 receptor and the maitotoxin-activated cationic channel. *Eur J Pharmacol*, **487**, 17-28.
- Luo, S.F., Lin, W.N., Yang, C.M., Lee, C.W., Liao, C.H., Leu, Y.L. and Hsiao, L.D. (2005) Induction of cytosolic phospholipase A(2) by lipopolysaccharide in canine tracheal smooth muscle cells: Involvement of MAPKs and NF-kappaB pathways. *Cell Signal*.
- Lurtz, M.M. and Louis, C.F. (2003) Calmodulin and protein kinase C regulate gap junctional coupling in lens epithelial cells. *Am J Physiol Cell Physiol*, **285**, C1475-1482.
- Luttrell, L.M., Ferguson, S.S., Daaka, Y., Miller, W.E., Maudsley, S., Della Rocca, G.J., Lin, F., Kawakatsu, H., Owada, K., Luttrell, D.K., Caron, M.G. and Lefkowitz, R.J. (1999) Beta-arrestin-dependent formation of beta2 adrenergic receptor-Src protein kinase complexes. *Science*, **283**, 655-661.
- MacLeod, R.A., Dirks, W.G., Matsuo, Y., Kaufmann, M., Milch, H. and Drexler, H.G. (1999) Widespread intraspecies cross-contamination of human tumor cell lines arising at source. *Int J Cancer*, **83**, 555-563.
- Maienschein, V., Marxen, M., Volkandt, W. and Zimmermann, H. (1999) A plethora of presynaptic proteins associated with ATP-storing organelles in cultured astrocytes. *Glia*, **26**, 233-244.

- Maldonado, P.E., Rose, B. and Loewenstein, W.R. (1988) Growth factors modulate junctional cell-to-cell communication. *J Membr Biol*, **106**, 203-210.
- Malfait, M., Gomez, P., van Veen, T.A., Parys, J.B., De Smedt, H., Vereecke, J. and Himpens, B. (2001) Effects of hyperglycemia and protein kinase C on connexin43 expression in cultured rat retinal pigment epithelial cells. *J Membr Biol*, **181**, 31-40.
- Mambetisaeva, E.T., Gire, V. and Evans, W.H. (1999) Multiple connexin expression in peripheral nerve, Schwann cells, and Schwannoma cells. *J Neurosci Res*, **57**, 166-175.
- Manthey, D., Bukauskas, F., Lee, C.G., Kozak, C.A. and Willecke, K. (1999) Molecular cloning and functional expression of the mouse gap junction gene connexin-57 in human HeLa cells. *J Biol Chem*, **274**, 14716-14723.
- Martin, P.E., Blundell, G., Ahmad, S., Errington, R.J. and Evans, W.H. (2001) Multiple pathways in the trafficking and assembly of connexin 26, 32 and 43 into gap junction intercellular communication channels. *J Cell Sci*, **114**, 3845-3855.
- Martinez, A.D. and Saez, J.C. (1999) Arachidonic acid-induced dye uncoupling in rat cortical astrocytes is mediated by arachidonic acid byproducts. *Brain Res*, **816**, 411-423.
- Martinez-Francois, J.R., Morales-Tlalpan, V. and Vaca, L. (2002) Characterization of the maitotoxin-activated cationic current from human skin fibroblasts. *J Physiol*, **538**, 79-86.
- Matchkov, V.V., Gustafsson, H., Rahman, A., Briggs Boedtkjer, D.M., Gorintin, S., Hansen, A.K., Bouzinova, E.V., Praetorius, H.A., Aalkjaer, C. and Nilsson, H. (2007) Interaction between Na<sup>+</sup>/K<sup>+</sup>-pump and Na<sup>+</sup>/Ca<sup>2+</sup>-exchanger modulates intercellular communication. *Circ Res*, **100**, 1026-1035.
- Matesic, D.F., Rupp, H.L., Bonney, W.J., Ruch, R.J. and Trosko, J.E. (1994) Changes in gap-junction permeability, phosphorylation, and number mediated by phorbol ester and non-phorbol-ester tumor promoters in rat liver epithelial cells. *Mol Carcinog*, **10**, 226-236.
- Matsuno, Y., Iwata, H., Umeda, Y., Takagi, H., Mori, Y., Kosugi, A., Matsumoto, K., Nakamura, T. and Hirose, H. (2003) Hepatocyte growth factor gene transfer into the liver via the portal vein using electroporation attenuates rat liver cirrhosis. *Gene Ther*, **10**, 1559-1566.
- Mazet, F., Wittenberg, B.A. and Spray, D.C. (1985) Fate of intercellular junctions in isolated adult rat cardiac cells. *Circ Res*, **56**, 195-204.
- McKenna, M.C. (2003) Glutamate metabolism in primary cultures of rat brain astrocytes: rationale and initial efforts toward developing a compartmental model. *Adv Exp Med Biol*, **537**, 317-341.
- McKenna, M.C. (2007) The glutamate-glutamine cycle is not stoichiometric: fates of glutamate in brain. *J Neurosci Res*, **85**, 3347-3358.
- Means, A.R. (2000) Regulatory cascades involving calmodulin-dependent protein kinases. *Mol Endocrinol*, **14**, 4-13.
- Means, A.R. and Dedman, J.R. (1980) Calmodulin--an intracellular calcium receptor. *Nature*, **285**, 73-77.
- Mears, D., Sheppard, N.F., Jr., Atwater, I. and Rojas, E. (1995) Magnitude and modulation of pancreatic beta-cell gap junction electrical conductance in situ. *J Membr Biol*, **146**, 163-176.
- Meda, P. (2001) Assaying the molecular permeability of connexin channels. *Methods Mol Biol*, **154**, 201-224.
- Meiners, S., Baron-Epel, O. and Schindler, M. (1988) Intercellular Communication-Filling in the Gaps. *Plant Physiol*, **87**, 791-793.



- Meme, W., Ezan, P., Venance, L., Glowinski, J. and Giaume, C. (2004) ATP-induced inhibition of gap junctional communication is enhanced by interleukin-1 beta treatment in cultured astrocytes. *Neuroscience*, **126**, 95-104.
- Mergler, S., Dannowski, H., Bednarz, J., Engelmann, K., Hartmann, C. and Pleyer, U. (2003) Calcium influx induced by activation of receptor tyrosine kinases in SV40-transfected human corneal endothelial cells. *Exp Eye Res*, **77**, 485-495.
- Mese, G., Londin, E., Mui, R., Brink, P.R. and White, T.W. (2004) Altered gating properties of functional Cx26 mutants associated with recessive non-syndromic hearing loss. *Hum Genet*, **115**, 191-199.
- Mese, G., Richard, G. and White, T.W. (2007) Gap junctions: basic structure and function. *J Invest Dermatol*, **127**, 2516-2524.
- Mesnil, M., Piccoli, C., Tiraby, G., Willecke, K. and Yamasaki, H. (1996) Bystander killing of cancer cells by herpes simplex virus thymidine kinase gene is mediated by connexins. *Proc Natl Acad Sci U S A*, **93**, 1831-1835.
- Mir, L.M., Bureau, M.F., Gehl, J., Rangara, R., Rouy, D., Caillaud, J.M., Delaere, P., Branell, D., Schwartz, B. and Scherman, D. (1999) High-efficiency gene transfer into skeletal muscle mediated by electric pulses. *Proc Natl Acad Sci U S A*, **96**, 4262-4267.
- Mochizuki-Oda, N., Negishi, M., Mori, K. and Ito, S. (1993) Arachidonic acid activates cation channels in bovine adrenal chromaffin cells. *J Neurochem*, **61**, 1882-1890.
- Mongin, A.A. and Kimelberg, H.K. (2002) ATP potently modulates anion channel-mediated excitatory amino acid release from cultured astrocytes. *Am J Physiol Cell Physiol*, **283**, C569-578.
- Mongin, A.A., Reddi, J.M., Charniga, C. and Kimelberg, H.K. (1999) [3H]taurine and D-[3H]aspartate release from astrocyte cultures are differently regulated by tyrosine kinases. *Am J Physiol*, **276**, C1226-1230.
- Montana, V., Malarkey, E.B., Verderio, C., Matteoli, M. and Parpura, V. (2006) Vesicular transmitter release from astrocytes. *Glia*, **54**, 700-715.
- Montero, M., Alonso, M.T., Albillos, A., Cuchillo-Ibanez, I., Olivares, R., A, G.G., Garcia-Sancho, J. and Alvarez, J. (2001) Control of secretion by mitochondria depends on the size of the local [Ca<sup>2+</sup>] after chromaffin cell stimulation. *Eur J Neurosci*, **13**, 2247-2254.
- Moore, L.K., Beyer, E.C. and Burt, J.M. (1991) Characterization of gap junction channels in A7r5 vascular smooth muscle cells. *Am J Physiol*, **260**, C975-981.
- Moreno, A.P., Campos de Carvalho, A.C., Christ, G., Melman, A. and Spray, D.C. (1993) Gap junctions between human corpus cavernosum smooth muscle cells: gating properties and unitary conductance. *Am J Physiol*, **264**, C80-92.
- Moreno, A.P., Chanson, M., Elenes, S., Anumonwo, J., Scerri, I., Gu, H., Taffet, S.M. and Delmar, M. (2002) Role of the carboxyl terminal of connexin43 in transjunctional fast voltage gating. *Circ Res*, **90**, 450-457.
- Moreno, A.P. and Lau, A.F. (2007) Gap junction channel gating modulated through protein phosphorylation. *Prog Biophys Mol Biol*, **94**, 107-119.
- Morley, G.E., Taffet, S.M. and Delmar, M. (1996) Intramolecular interactions mediate pH regulation of connexin43 channels. *Biophys J*, **70**, 1294-1302.
- Muller, D.J., Hand, G.M., Engel, A. and Sosinsky, G.E. (2002) Conformational changes in surface structures of isolated connexin 26 gap junctions. *Embo J*, **21**, 3598-3607.
- Muller, K.J., Horbaschek, M., Lucas, K., Zimmermann, U. and Sukhorukov, V.L. (2003) Electrotransfection of anchorage-dependent mammalian cells. *Exp Cell Res*, **288**, 344-353.

- Muralikrishna Adibhatla, R. and Hatcher, J.F. (2006) Phospholipase A2, reactive oxygen species, and lipid peroxidation in cerebral ischemia. *Free Radic Biol Med*, **40**, 376-387.
- Murphy, R.C. and Messer, A. (2001) Gene transfer methods for CNS organotypic cultures: a comparison of three nonviral methods. *Mol Ther*, **3**, 113-121.
- Musil, L.S., Beyer, E.C. and Goodenough, D.A. (1990a) Expression of the gap junction protein connexin43 in embryonic chick lens: molecular cloning, ultrastructural localization, and post-translational phosphorylation. *J Membr Biol*, **116**, 163-175.
- Musil, L.S., Cunningham, B.A., Edelman, G.M. and Goodenough, D.A. (1990b) Differential phosphorylation of the gap junction protein connexin43 in junctional communication-competent and -deficient cell lines. *J Cell Biol*, **111**, 2077-2088.
- Musil, L.S. and Goodenough, D.A. (1991) Biochemical analysis of connexin43 intracellular transport, phosphorylation, and assembly into gap junctional plaques. *J Cell Biol*, **115**, 1357-1374.
- Musil, L.S. and Goodenough, D.A. (1993) Multisubunit assembly of an integral plasma membrane channel protein, gap junction connexin43, occurs after exit from the ER. *Cell*, **74**, 1065-1077.
- Musil, L.S., Le, A.C., VanSlyke, J.K. and Roberts, L.M. (2000) Regulation of connexin degradation as a mechanism to increase gap junction assembly and function. *J Biol Chem*, **275**, 25207-25215.
- Muthalif, M.M., Hefner, Y., Canaan, S., Harper, J., Zhou, H., Parmentier, J.H., Aebersold, R., Gelb, M.H. and Malik, K.U. (2001) Functional interaction of calcium/calmodulin-dependent protein kinase II and cytosolic phospholipase A(2). *J Biol Chem*, **276**, 39653-39660.
- Nadarajah, B., Jones, A.M., Evans, W.H. and Parnavelas, J.G. (1997) Differential expression of connexins during neocortical development and neuronal circuit formation. *J Neurosci*, **17**, 3096-3111.
- Naus, C.C., Hearn, S., Zhu, D., Nicholson, B.J. and Shivers, R.R. (1993) Ultrastructural analysis of gap junctions in C6 glioma cells transfected with connexin43 cDNA. *Exp Cell Res*, **206**, 72-84.
- Nefussi, J.R., Sautier, J.M., Nicolas, V. and Forest, N. (1991) How osteoblasts become osteocytes: a decreasing matrix forming process. *J Biol Buccale*, **19**, 75-82.
- Neyton, J. and Trautmann, A. (1985) Single-channel currents of an intercellular junction. *Nature*, **317**, 331-335.
- Niessen, H., Harz, H., Bedner, P., Kramer, K. and Willecke, K. (2000) Selective permeability of different connexin channels to the second messenger inositol 1,4,5-trisphosphate. *J Cell Sci*, **113** ( Pt 8), 1365-1372.
- North, R.A. (2002) Molecular physiology of P2X receptors. *Physiol Rev*, **82**, 1013-1067.
- Novak, I. (2003) ATP as a signaling molecule: the exocrine focus. *News Physiol Sci*, **18**, 12-17.
- Oh, S., Abrams, C.K., Verselis, V.K. and Bargiello, T.A. (2000) Stoichiometry of transjunctional voltage-gating polarity reversal by a negative charge substitution in the amino terminus of a connexin32 chimera. *J Gen Physiol*, **116**, 13-31.
- Oh, S., Rivkin, S., Tang, Q., Verselis, V.K. and Bargiello, T.A. (2004) Determinants of gating polarity of a connexin 32 hemichannel. *Biophys J*, **87**, 912-928.
- Oh, S., Rubin, J.B., Bennett, M.V., Verselis, V.K. and Bargiello, T.A. (1999) Molecular determinants of electrical rectification of single channel conductance in gap junctions formed by connexins 26 and 32. *J Gen Physiol*, **114**, 339-364.
- Oliveira-Castro, G.M. and Loewenstein, W.R. (1971) Junctional membrane permeability: effects of divalent cations. *J Membr Biol*, **5**, 51-77.

- Olofsson, J., Nolkrantz, K., Ryttsen, F., Lambie, B.A., Weber, S.G. and Orwar, O. (2003) Single-cell electroporation. *Curr Opin Biotechnol*, **14**, 29-34.
- Omori, Y. and Yamasaki, H. (1999) Gap junction proteins connexin32 and connexin43 partially acquire growth-suppressive function in HeLa cells by deletion of their C-terminal tails. *Carcinogenesis*, **20**, 1913-1918.
- Orwar, O., Li, X., Andine, P., Bergstrom, C.M., Hagberg, H., Folestad, S. and Sandberg, M. (1994) Increased intra- and extracellular concentrations of gamma-glutamylglutamate and related dipeptides in the ischemic rat striatum: involvement of glutamyl transpeptidase. *J Neurochem*, **63**, 1371-1376.
- Pahujaa, M., Anikin, M. and Goldberg, G.S. (2007) Phosphorylation of connexin43 induced by Src: Regulation of gap junctional communication between transformed cells. *Exp Cell Res*.
- Palumbo, C., Palazzini, S. and Marotti, G. (1990) Morphological study of intercellular junctions during osteocyte differentiation. *Bone*, **11**, 401-406.
- Panchin, Y., Kelmanson, I., Matz, M., Lukyanov, K., Usman, N. and Lukyanov, S. (2000) A ubiquitous family of putative gap junction molecules. *Curr Biol*, **10**, R473-474.
- Panchin, Y.V. (2005) Evolution of gap junction proteins--the pannexin alternative. *J Exp Biol*, **208**, 1415-1419.
- Parekh, A.B. and Putney, J.W., Jr. (2005) Store-operated calcium channels. *Physiol Rev*, **85**, 757-810.
- Parfitt, A.M. and Kleerekoper, M. (1980) The divalent ion homeostasis system: physiology and metabolism of calcium, phosphorus, magnesium and bone. In Hill, M. (ed.), *Clinical disorders of fluid and electrolyte metabolism*. Maxwell, M. H., Kleeman, C. R., New York, pp. 269-398.
- Parpura, V., Basarsky, T.A., Liu, F., Jęftinija, K., Jęftinija, S. and Haydon, P.G. (1994) Glutamate-mediated astrocyte-neuron signalling. *Nature*, **369**, 744-747.
- Parpura, V., Scemes, E. and Spray, D.C. (2004) Mechanisms of glutamate release from astrocytes: gap junction "hemichannels", purinergic receptors and exocytotic release. *Neurochem Int*, **45**, 259-264.
- Paul, D.L., Ebihara, L., Takemoto, L.J., Swenson, K.I. and Goodenough, D.A. (1991) Connexin46, a novel lens gap junction protein, induces voltage-gated currents in nonjunctional plasma membrane of *Xenopus* oocytes. *J Cell Biol*, **115**, 1077-1089.
- Paulson, A.F., Lampe, P.D., Meyer, R.A., TenBroek, E., Atkinson, M.M., Walseth, T.F. and Johnson, R.G. (2000) Cyclic AMP and LDL trigger a rapid enhancement in gap junction assembly through a stimulation of connexin trafficking. *J Cell Sci*, **113** ( Pt 17), 3037-3049.
- Pearson, R.A., Dale, N., Llaudet, E. and Mobbs, P. (2005) ATP released via gap junction hemichannels from the pigment epithelium regulates neural retinal progenitor proliferation. *Neuron*, **46**, 731-744.
- Pelegriin, P. and Surprenant, A. (2006) Pannexin-1 mediates large pore formation and interleukin-1beta release by the ATP-gated P2X7 receptor. *Embo J*, **25**, 5071-5082.
- Pelegriin, P. and Surprenant, A. (2007) Pannexin-1 couples to maitotoxin- and nigericin-induced interleukin-1beta release through a dye uptake-independent pathway. *J Biol Chem*, **282**, 2386-2394.
- Penuela, S., Bhalla, R., Gong, X.Q., Cowan, K.N., Celetti, S.J., Cowan, B.J., Bai, D., Shao, Q. and Laird, D.W. (2007) Pannexin 1 and pannexin 3 are glycoproteins that exhibit many distinct characteristics from the connexin family of gap junction proteins. *J Cell Sci*.

- Pepper, M.S. and Meda, P. (1992) Basic fibroblast growth factor increases junctional communication and connexin 43 expression in microvascular endothelial cells. *J Cell Physiol*, **153**, 196-205.
- Peracchia, C. (1988) The calmodulin hypothesis for gap junction regulation six years later. In Hertzberg, E.L. and Johnson, R.G. (eds.), *Gap Junctions*. Alan R. Liss, New York, pp. 267-282.
- Peracchia, C. (1990a) Effects of caffeine and ryanodine on low pHi-induced changes in gap junction conductance and calcium concentration in crayfish septate axons. *J Membr Biol*, **117**, 79-89.
- Peracchia, C. (1990b) Increase in gap junction resistance with acidification in crayfish septate axons is closely related to changes in intracellular calcium but not hydrogen ion concentration. *J Membr Biol*, **113**, 75-92.
- Peracchia, C. (2004) Chemical gating of gap junction channels; roles of calcium, pH and calmodulin. *Biochim Biophys Acta*, **1662**, 61-80.
- Peracchia, C., Bernardini, G. and Peracchia, L.L. (1983) Is calmodulin involved in the regulation of gap junction permeability? *Pflugers Arch*, **399**, 152-154.
- Peracchia, C., Sotkis, A., Wang, X.G., Peracchia, L.L. and Persechini, A. (2000a) Calmodulin directly gates gap junction channels. *J Biol Chem*, **275**, 26220-26224.
- Peracchia, C., Wang, X.G. and Peracchia, L.L. (2000b) Behavior of chemical- and slow voltage-sensitive gating of connexin channels: the "cork" gating hypothesis. In Peracchia, C. (ed.), *Gap Junctions. Molecular Basis of Communication in Health and Disease*. Academic Press, San Diego, CA, pp. 271-295.
- Perez-Pinzon, M.A., Tao, L. and Nicholson, C. (1995) Extracellular potassium, volume fraction, and tortuosity in rat hippocampal CA1, CA3, and cortical slices during ischemia. *J Neurophysiol*, **74**, 565-573.
- Perisic, O., Fong, S., Lynch, D.E., Bycroft, M. and Williams, R.L. (1998) Crystal structure of a calcium-phospholipid binding domain from cytosolic phospholipase A2. *J Biol Chem*, **273**, 1596-1604.
- Petersen, O.H., Burdakov, D. and Tepikin, A.V. (1999) Polarity in intracellular calcium signaling. *Bioessays*, **21**, 851-860.
- Pfahnl, A. and Dahl, G. (1999) Gating of cx46 gap junction hemichannels by calcium and voltage. *Pflugers Arch*, **437**, 345-353.
- Phelan, P. (2005) Innexins: members of an evolutionarily conserved family of gap-junction proteins. *Biochim Biophys Acta*, **1711**, 225-245.
- Phelan, P. and Starich, T.A. (2001) Innexins get into the gap. *Bioessays*, **23**, 388-396.
- Piehl, M., Lehmann, C., Gumpert, A., Denizot, J.P., Segretain, D. and Falk, M.M. (2007) Internalization of large double-membrane intercellular vesicles by a clathrin-dependent endocytic process. *Mol Biol Cell*, **18**, 337-347.
- Pliquett, U. (2003) Joule heating during solid tissue electroporation. *Med Biol Eng Comput*, **41**, 215-219.
- Plotkin, L.I. and Bellido, T. (2001) Bisphosphonate-induced, hemichannel-mediated, anti-apoptosis through the Src/ERK pathway: a gap junction-independent action of connexin43. *Cell Commun Adhes*, **8**, 377-382.
- Plotkin, L.I., Manolagas, S.C. and Bellido, T. (2002) Transduction of cell survival signals by connexin-43 hemichannels. *J Biol Chem*, **277**, 8648-8657.
- Plum, A., Hallas, G., Magin, T., Dombrowski, F., Hagendorff, A., Schumacher, B., Wolpert, C., Kim, J., Lamers, W.H., Evert, M., Meda, P., Traub, O. and Willecke, K. (2000) Unique and shared functions of different connexins in mice. *Curr Biol*, **10**, 1083-1091.

- Postma, F.R., Hengeveld, T., Alblas, J., Giepmans, B.N., Zondag, G.C., Jalink, K. and Moolenaar, W.H. (1998) Acute loss of cell-cell communication caused by G protein-coupled receptors: a critical role for c-Src. *J Cell Biol*, **140**, 1199-1209.
- Puc, M., Corovic, S., Flisar, K., Petkovsek, M., Nastran, J. and Miklavcic, D. (2004) Techniques of signal generation required for electroporation. Survey of electroporation devices. *Bioelectrochemistry*, **64**, 113-124.
- Pusch, M., Accardi, A., Liantonio, A., Guida, P., Traverso, S., Camerino, D.C. and Conti, F. (2002) Mechanisms of block of muscle type CLC chloride channels (Review). *Mol Membr Biol*, **19**, 285-292.
- Qiu, Z.H., Gijon, M.A., de Carvalho, M.S., Spencer, D.M. and Leslie, C.C. (1998) The role of calcium and phosphorylation of cytosolic phospholipase A2 in regulating arachidonic acid release in macrophages. *J Biol Chem*, **273**, 8203-8211.
- Quist, A.P., Rhee, S.K., Lin, H. and Lal, R. (2000) Physiological role of gap-junctional hemichannels. Extracellular calcium-dependent isosmotic volume regulation. *J Cell Biol*, **148**, 1063-1074.
- Ramachandran, S., Xie, L.H., John, S.A., Subramaniam, S. and Lal, R. (2007) A novel role for connexin hemichannel in oxidative stress and smoking-induced cell injury. *PLoS ONE*, **2**, e712.
- Rana, S. and Dringen, R. (2007) Gap junction hemichannel-mediated release of glutathione from cultured rat astrocytes. *Neurosci Lett*, **415**, 45-48.
- Ray, A., Zoidl, G., Weickert, S., Wahle, P. and Dermietzel, R. (2005) Site-specific and developmental expression of pannexin1 in the mouse nervous system. *Eur J Neurosci*, **21**, 3277-3290.
- Retamal, M.A., Cortes, C.J., Reuss, L., Bennett, M.V. and Saez, J.C. (2006) S-nitrosylation and permeation through connexin 43 hemichannels in astrocytes: induction by oxidant stress and reversal by reducing agents. *Proc Natl Acad Sci U S A*, **103**, 4475-4480.
- Retamal, M.A., Froger, N., Palacios-Prado, N., Ezan, P., Saez, P.J., Saez, J.C. and Giaume, C. (2007a) Cx43 hemichannels and gap junction channels in astrocytes are regulated oppositely by proinflammatory cytokines released from activated microglia. *J Neurosci*, **27**, 13781-13792.
- Retamal, M.A., Schalper, K.A., Shoji, K.F., Bennett, M.V. and Saez, J.C. (2007b) Opening of connexin 43 hemichannels is increased by lowering intracellular redox potential. *Proc Natl Acad Sci U S A*, **104**, 8322-8327.
- Reuss, B., Dermietzel, R. and Unsicker, K. (1998) Fibroblast growth factor 2 (FGF-2) differentially regulates connexin (cx) 43 expression and function in astroglial cells from distinct brain regions. *Glia*, **22**, 19-30.
- Revilla, A., Bennett, M.V. and Barrio, L.C. (2000) Molecular determinants of membrane potential dependence in vertebrate gap junction channels. *Proc Natl Acad Sci U S A*, **97**, 14760-14765.
- Revilla, A., Castro, C. and Barrio, L.C. (1999) Molecular dissection of transjunctional voltage dependence in the connexin-32 and connexin-43 junctions. *Biophys J*, **77**, 1374-1383.
- Rhee, S.K., Bevans, C.G. and Harris, A.L. (1996) Channel-forming activity of immunoaffinity-purified connexin32 in single phospholipid membranes. *Biochemistry*, **35**, 9212-9223.
- Rhoads, A.R. and Friedberg, F. (1997) Sequence motifs for calmodulin recognition. *Faseb J*, **11**, 331-340.
- Riendeau, D., Guay, J., Weech, P.K., Laliberte, F., Yergey, J., Li, C., Desmarais, S., Perrier, H., Liu, S., Nicoll-Griffith, D. and et al. (1994) Arachidonyl trifluoromethyl ketone, a potent inhibitor of 85-kDa phospholipase A2, blocks production of arachidonate and

- 12-hydroxyeicosatetraenoic acid by calcium ionophore-challenged platelets. *J Biol Chem*, **269**, 15619-15624.
- Riordan, J.R., Rommens, J.M., Kerem, B., Alon, N., Rozmahel, R., Grzelczak, Z., Zielenski, J., Lok, S., Plavsic, N., Chou, J.L. and et al. (1989) Identification of the cystic fibrosis gene: cloning and characterization of complementary DNA. *Science*, **245**, 1066-1073.
- Rivedal, E. and Opsahl, H. (2001) Role of PKC and MAP kinase in EGF- and TPA-induced connexin43 phosphorylation and inhibition of gap junction intercellular communication in rat liver epithelial cells. *Carcinogenesis*, **22**, 1543-1550.
- Rizo, J. and Sudhof, T.C. (1998) C2-domains, structure and function of a universal Ca<sup>2+</sup>-binding domain. *J Biol Chem*, **273**, 15879-15882.
- Romanov, R.A., Rogachevskaja, O.A., Bystrova, M.F., Jiang, P., Margolskee, R.F. and Kolesnikov, S.S. (2007) Afferent neurotransmission mediated by hemichannels in mammalian taste cells. *Embo J*, **26**, 657-667.
- Rose, B. and Loewenstein, W.R. (1975) Permeability of cell junction depends on local cytoplasmic calcium activity. *Nature*, **254**, 250-252.
- Rose, B. and Loewenstein, W.R. (1976) Permeability of a cell junction and the local cytoplasmic free ionized calcium concentration: a study with aequorin. *J Membr Biol*, **28**, 87-119.
- Roskoski, R., Jr. (2004) Src protein-tyrosine kinase structure and regulation. *Biochem Biophys Res Commun*, **324**, 1155-1164.
- Roskoski, R., Jr. (2005) Src kinase regulation by phosphorylation and dephosphorylation. *Biochem Biophys Res Commun*, **331**, 1-14.
- Rostovtseva, T.K., Antonsson, B., Suzuki, M., Youle, R.J., Colombini, M. and Bezrukov, S.M. (2004) Bid, but not Bax, regulates VDAC channels. *J Biol Chem*, **279**, 13575-13583.
- Rostovtseva, T.K., Komarov, A., Bezrukov, S.M. and Colombini, M. (2002a) Dynamics of nucleotides in VDAC channels: structure-specific noise generation. *Biophys J*, **82**, 193-205.
- Rostovtseva, T.K., Komarov, A., Bezrukov, S.M. and Colombini, M. (2002b) VDAC channels differentiate between natural metabolites and synthetic molecules. *J Membr Biol*, **187**, 147-156.
- Rouach, N., Pebay, A., Meme, W., Cordier, J., Ezan, P., Etienne, E., Giaume, C. and Tence, M. (2006) S1P inhibits gap junctions in astrocytes: involvement of G and Rho GTPase/ROCK. *Eur J Neurosci*, **23**, 1453-1464.
- Rubin, J.B., Verselis, V.K., Bennett, M.V. and Bargiello, T.A. (1992) Molecular analysis of voltage dependence of heterotypic gap junctions formed by connexins 26 and 32. *Biophys J*, **62**, 183-193; discussion 193-185.
- Ruch, R.J., Trosko, J.E. and Madhukar, B.V. (2001) Inhibition of connexin43 gap junctional intercellular communication by TPA requires ERK activation. *J Cell Biochem*, **83**, 163-169.
- Rustom, A., Saffrich, R., Markovic, I., Walther, P. and Gerdes, H.H. (2004) Nanotubular highways for intercellular organelle transport. *Science*, **303**, 1007-1010.
- Ryan, L.M., Rachow, J.W., McCarty, B.A. and McCarty, D.J. (1996) Adenosine triphosphate levels in human plasma. *J Rheumatol*, **23**, 214-219.
- Sabirov, R.Z. and Okada, Y. (2004) Wide nanoscopic pore of maxi-anion channel suits its function as an ATP-conductive pathway. *Biophys J*, **87**, 1672-1685.
- Saez, J.C., Berthoud, V.M., Branes, M.C., Martinez, A.D. and Beyer, E.C. (2003) Plasma membrane channels formed by connexins: their regulation and functions. *Physiol Rev*, **83**, 1359-1400.

- Saez, J.C., Berthoud, V.M., Moreno, A.P. and Spray, D.C. (1993a) Gap junctions. Multiplicity of controls in differentiated and undifferentiated cells and possible functional implications. *Adv Second Messenger Phosphoprotein Res*, **27**, 163-198.
- Saez, J.C., Martinez, A.D., Branes, M.C. and Gonzalez, H.E. (1998) Regulation of gap junctions by protein phosphorylation. *Braz J Med Biol Res*, **31**, 593-600.
- Saez, J.C., Nairn, A.C., Czernik, A.J., Fishman, G.I., Spray, D.C. and Hertzberg, E.L. (1997) Phosphorylation of connexin43 and the regulation of neonatal rat cardiac myocyte gap junctions. *J Mol Cell Cardiol*, **29**, 2131-2145.
- Saez, J.C., Nairn, A.C., Czernik, A.J., Spray, D.C. and Hertzberg, E.L. (1993b) Rat connexin 43: regulation by phosphorylation in heart. *Prog Cell Res*, **3**, 275-281.
- Saez, J.C., Nairn, A.C., Czernik, A.J., Spray, D.C., Hertzberg, E.L., Greengard, P. and Bennett, M.V. (1990) Phosphorylation of connexin 32, a hepatocyte gap-junction protein, by cAMP-dependent protein kinase, protein kinase C and Ca<sup>2+</sup>/calmodulin-dependent protein kinase II. *Eur J Biochem*, **192**, 263-273.
- Saez, J.C., Retamal, M.A., Basilio, D., Bukauskas, F.F. and Bennett, M.V. (2005) Connexin-based gap junction hemichannels: gating mechanisms. *Biochim Biophys Acta*, **1711**, 215-224.
- Saez, J.C., Spray, D.C., Nairn, A.C., Hertzberg, E., Greengard, P. and Bennett, M.V. (1986) cAMP increases junctional conductance and stimulates phosphorylation of the 27-kDa principal gap junction polypeptide. *Proc Natl Acad Sci U S A*, **83**, 2473-2477.
- Sagara, J.I., Miura, K. and Bannai, S. (1993) Maintenance of neuronal glutathione by glial cells. *J Neurochem*, **61**, 1672-1676.
- Sasakura, Y., Shoguchi, E., Takatori, N., Wada, S., Meinertzhagen, I.A., Satou, Y. and Satoh, N. (2003) A genomewide survey of developmentally relevant genes in *Ciona intestinalis*. X. Genes for cell junctions and extracellular matrix. *Dev Genes Evol*, **213**, 303-313.
- Satkauskas, S., Bureau, M.F., Puc, M., Mahfoudi, A., Scherman, D., Miklavcic, D. and Mir, L.M. (2002) Mechanisms of in vivo DNA electrotransfer: respective contributions of cell electropermeabilization and DNA electrophoresis. *Mol Ther*, **5**, 133-140.
- Schiavo, G., Benfenati, F., Poulain, B., Rossetto, O., Polverino de Laureto, P., DasGupta, B.R. and Montecucco, C. (1992) Tetanus and botulinum-B neurotoxins block neurotransmitter release by proteolytic cleavage of synaptobrevin. *Nature*, **359**, 832-835.
- Schilling, W.P., Wasylyna, T., Dubyak, G.R., Humphreys, B.D. and Sinkins, W.G. (1999) Maitotoxin and P2Z/P2X(7) purinergic receptor stimulation activate a common cytolytic pore. *Am J Physiol*, **277**, C766-776.
- Schirmmacher, K., Nonhoff, D., Wiemann, M., Peterson-Grine, E., Brink, P.R. and Bingmann, D. (1996) Effects of calcium on gap junctions between osteoblast-like cells in culture. *Calcif Tissue Int*, **59**, 259-264.
- Schlessinger, J. (2000) Cell signaling by receptor tyrosine kinases. *Cell*, **103**, 211-225.
- Schorey, J.S. and Cooper, A.M. (2003) Macrophage signalling upon mycobacterial infection: the MAP kinases lead the way. *Cell Microbiol*, **5**, 133-142.
- Schubert, A.L., Schubert, W., Spray, D.C. and Lisanti, M.P. (2002) Connexin family members target to lipid raft domains and interact with caveolin-1. *Biochemistry*, **41**, 5754-5764.
- Schuyler, S.C. and Pellman, D. (2001) Search, capture and signal: games microtubules and centrosomes play. *J Cell Sci*, **114**, 247-255.
- Schwarzmann, G., Wiegandt, H., Rose, B., Zimmerman, A., Ben-Haim, D. and Loewenstein, W.R. (1981) Diameter of the cell-to-cell junctional membrane channels as probed with neutral molecules. *Science*, **213**, 551-553.

- Schwiebert, E.M. and Zsembery, A. (2003) Extracellular ATP as a signaling molecule for epithelial cells. *Biochim Biophys Acta*, **1615**, 7-32.
- Segretain, D. and Falk, M.M. (2004) Regulation of connexin biosynthesis, assembly, gap junction formation, and removal. *Biochim Biophys Acta*, **1662**, 3-21.
- Seki, A., Coombs, W., Taffet, S.M. and Delmar, M. (2004a) Loss of electrical communication, but not plaque formation, after mutations in the cytoplasmic loop of connexin43. *Heart Rhythm*, **1**, 227-233.
- Seki, A., Duffy, H.S., Coombs, W., Spray, D.C., Taffet, S.M. and Delmar, M. (2004b) Modifications in the biophysical properties of connexin43 channels by a peptide of the cytoplasmic loop region. *Circ Res*, **95**, e22-28.
- Severs, N.J., Shovel, K.S., Slade, A.M., Powell, T., Twist, V.W. and Green, C.R. (1989) Fate of gap junctions in isolated adult mammalian cardiomyocytes. *Circ Res*, **65**, 22-42.
- Shah, M.M., Martinez, A.M. and Fletcher, W.H. (2002) The connexin43 gap junction protein is phosphorylated by protein kinase A and protein kinase C: in vivo and in vitro studies. *Mol Cell Biochem*, **238**, 57-68.
- Shaw, G., Morse, S., Ararat, M. and Graham, F.L. (2002) Preferential transformation of human neuronal cells by human adenoviruses and the origin of HEK 293 cells. *Faseb J*, **16**, 869-871.
- Shaw, R.M., Fay, A.J., Puthenveedu, M.A., von Zastrow, M., Jan, Y.N. and Jan, L.Y. (2007) Microtubule plus-end-tracking proteins target gap junctions directly from the cell interior to adherens junctions. *Cell*, **128**, 547-560.
- Shears, S.B. (1998) The versatility of inositol phosphates as cellular signals. *Biochim Biophys Acta*, **1436**, 49-67.
- Shimizu, S., Nomoto, M., Ishii, M., Naito, S., Yamamoto, T. and Momose, K. (1997) Changes in nitric oxide synthase activity during exposure to hydrogen peroxide in cultured endothelial cells. *Res Commun Mol Pathol Pharmacol*, **97**, 279-289.
- Shin, C.Y., Choi, J.W., Ryu, J.R., Ryu, J.H., Kim, W., Kim, H. and Ko, K.H. (2001) Immunostimulation of rat primary astrocytes decreases intracellular ATP level. *Brain Res*, **902**, 198-204.
- Shintani-Ishida, K., Uemura, K. and Yoshida, K.I. (2007) Hemichannels in cardiomyocytes open transiently during ischemia and contribute to reperfusion injury following brief ischemia. *Am J Physiol Heart Circ Physiol*.
- Shiokawa-Sawada, M., Mano, H., Hanada, K., Kakudo, S., Kameda, T., Miyazawa, K., Nakamaru, Y., Yuasa, T., Mori, Y., Kumegawa, M. and Hakeda, Y. (1997) Down-regulation of gap junctional intercellular communication between osteoblastic MC3T3-E1 cells by basic fibroblast growth factor and a phorbol ester (12-O-tetradecanoylphorbol-13-acetate). *J Bone Miner Res*, **12**, 1165-1173.
- Shoshan-Barmatz, V. and Gincel, D. (2003) The voltage-dependent anion channel: characterization, modulation, and role in mitochondrial function in cell life and death. *Cell Biochem Biophys*, **39**, 279-292.
- Simonian, N.A. and Coyle, J.T. (1996) Oxidative stress in neurodegenerative diseases. *Annu Rev Pharmacol Toxicol*, **36**, 83-106.
- Slivka, A., Spina, M.B. and Cohen, G. (1987) Reduced and oxidized glutathione in human and monkey brain. *Neurosci Lett*, **74**, 112-118.
- Soderling, T.R. (1999) The Ca-calmodulin-dependent protein kinase cascade. *Trends Biochem Sci*, **24**, 232-236.
- Sohl, G. and Willecke, K. (2003) An update on connexin genes and their nomenclature in mouse and man. *Cell Commun Adhes*, **10**, 173-180.
- Sohl, G. and Willecke, K. (2004) Gap junctions and the connexin protein family. *Cardiovasc Res*, **62**, 228-232.



- Solan, J.L., Fry, M.D., TenBroek, E.M. and Lampe, P.D. (2003) Connexin43 phosphorylation at S368 is acute during S and G2/M and in response to protein kinase C activation. *J Cell Sci*, **116**, 2203-2211.
- Solan, J.L. and Lampe, P.D. (2005) Connexin phosphorylation as a regulatory event linked to gap junction channel assembly. *Biochim Biophys Acta*, **1711**, 154-163.
- Solan, J.L. and Lampe, P.D. (2007) Key Connexin 43 Phosphorylation Events Regulate the Gap Junction Life Cycle. *J Membr Biol*.
- Sorgen, P.L., Duffy, H.S., Spray, D.C. and Delmar, M. (2004) pH-dependent dimerization of the carboxyl terminal domain of Cx43. *Biophys J*, **87**, 574-581.
- Sotkis, A., Wang, X.G., Yasumura, T., Peracchia, L.L., Persechini, A., Rash, J.E. and Peracchia, C. (2001) Calmodulin colocalizes with connexins and plays a direct role in gap junction channel gating. *Cell Commun Adhes*, **8**, 277-281.
- Spinella, F., Rosano, L., Di Castro, V., Nicotra, M.R., Natali, P.G. and Bagnato, A. (2003) Endothelin-1 decreases gap junctional intercellular communication by inducing phosphorylation of connexin 43 in human ovarian carcinoma cells. *J Biol Chem*, **278**, 41294-41301.
- Sprague, R.S., Ellsworth, M.L., Stephenson, A.H., Kleinhenz, M.E. and Lonigro, A.J. (1998) Deformation-induced ATP release from red blood cells requires CFTR activity. *Am J Physiol*, **275**, H1726-1732.
- Spray, D.C., Harris, A.L. and Bennett, M.V. (1981) Equilibrium properties of a voltage-dependent junctional conductance. *J Gen Physiol*, **77**, 77-93.
- Spray, D.C., Stern, J.H., Harris, A.L. and Bennett, M.V. (1982) Gap junctional conductance: comparison of sensitivities to H and Ca ions. *Proc Natl Acad Sci U S A*, **79**, 441-445.
- Spray, D.C., Ye, Z.C. and Ransom, B.R. (2006) Functional connexin "hemichannels": a critical appraisal. *Glia*, **54**, 758-773.
- Srinivas, M., Calderon, D.P., Kronengold, J. and Verselis, V.K. (2006) Regulation of connexin hemichannels by monovalent cations. *J Gen Physiol*, **127**, 67-75.
- Srinivas, M., Costa, M., Gao, Y., Fort, A., Fishman, G.I. and Spray, D.C. (1999) Voltage dependence of macroscopic and unitary currents of gap junction channels formed by mouse connexin50 expressed in rat neuroblastoma cells. *J Physiol*, **517** ( Pt 3), 673-689.
- Stagg, R.B. and Fletcher, W.H. (1990) The hormone-induced regulation of contact-dependent cell-cell communication by phosphorylation. *Endocr Rev*, **11**, 302-325.
- Starich, T.A., Miller, A., Nguyen, R.L., Hall, D.H. and Shaw, J.E. (2003) The Caenorhabditis elegans innexin INX-3 is localized to gap junctions and is essential for embryonic development. *Dev Biol*, **256**, 403-417.
- Stauffer, K.A. (1995) The gap junction proteins beta 1-connexin (connexin-32) and beta 2-connexin (connexin-26) can form heteromeric hemichannels. *J Biol Chem*, **270**, 6768-6772.
- Stebbing, L.A., Todman, M.G., Phillips, R., Greer, C.E., Tam, J., Phelan, P., Jacobs, K., Bacon, J.P. and Davies, J.A. (2002) Gap junctions in Drosophila: developmental expression of the entire innexin gene family. *Mech Dev*, **113**, 197-205.
- Stein, L.S., Boonstra, J. and Burghardt, R.C. (1992) Reduced cell-cell communication between mitotic and nonmitotic coupled cells. *Exp Cell Res*, **198**, 1-7.
- Sterck, J.G., Klein-Nulend, J., Lips, P. and Burger, E.H. (1998) Response of normal and osteoporotic human bone cells to mechanical stress in vitro. *Am J Physiol*, **274**, E1113-1120.
- Stergiopoulos, K., Alvarado, J.L., Mastroianni, M., Ek-Vitorin, J.F., Taffet, S.M. and Delmar, M. (1999) Hetero-domain interactions as a mechanism for the regulation of connexin channels. *Circ Res*, **84**, 1144-1155.

- Stewart, A.F. and Broadus, A.E. (1987) Mineral metabolism. In Hill, M. (ed.), *Endocrinology and metabolism*. Felig, P., Baxter, J. D., Broadus, A. E., Frohman, L. A., New York, pp. 1317-1453.
- Stone, T.W. (2002) Purines and neuroprotection. *Adv Exp Med Biol*, **513**, 249-280.
- Stong, B.C., Chang, Q., Ahmad, S. and Lin, X. (2006) A novel mechanism for connexin 26 mutation linked deafness: cell death caused by leaky gap junction hemichannels. *Laryngoscope*, **116**, 2205-2210.
- Stout, C. and Charles, A. (2003) Modulation of intercellular calcium signaling in astrocytes by extracellular calcium and magnesium. *Glia*, **43**, 265-273.
- Stout, C.E., Costantin, J.L., Naus, C.C. and Charles, A.C. (2002) Intercellular calcium signaling in astrocytes via ATP release through connexin hemichannels. *J Biol Chem*, **277**, 10482-10488.
- Strange, K., Emma, F. and Jackson, P.S. (1996) Cellular and molecular physiology of volume-sensitive anion channels. *Am J Physiol*, **270**, C711-730.
- Suadicani, S.O., Brosnan, C.F. and Scemes, E. (2006) P2X7 receptors mediate ATP release and amplification of astrocytic intercellular Ca<sup>2+</sup> signaling. *J Neurosci*, **26**, 1378-1385.
- Suarez, S. and Ballmer-Hofer, K. (2001) VEGF transiently disrupts gap junctional communication in endothelial cells. *J Cell Sci*, **114**, 1229-1235.
- Sun, W., Wei, X., Kesavan, K., Garrington, T.P., Fan, R., Mei, J., Anderson, S.M., Gelfand, E.W. and Johnson, G.L. (2003) MEK kinase 2 and the adaptor protein Lad regulate extracellular signal-regulated kinase 5 activation by epidermal growth factor via Src. *Mol Cell Biol*, **23**, 2298-2308.
- Surprenant, A., Rassendren, F., Kawashima, E., North, R.A. and Buell, G. (1996) The cytolytic P2Z receptor for extracellular ATP identified as a P2X receptor (P2X7). *Science*, **272**, 735-738.
- Swenson, K.I., Piwnica-Worms, H., McNamee, H. and Paul, D.L. (1990) Tyrosine phosphorylation of the gap junction protein connexin43 is required for the pp60v-src-induced inhibition of communication. *Cell Regul*, **1**, 989-1002.
- Swietach, P., Rossini, A., Spitzer, K.W. and Vaughan-Jones, R.D. (2007a) H<sup>+</sup> ion activation and inactivation of the ventricular gap junction: a basis for spatial regulation of intracellular pH. *Circ Res*, **100**, 1045-1054.
- Swietach, P., Spitzer, K.W. and Vaughan-Jones, R.D. (2007b) pH-Dependence of extrinsic and intrinsic H<sup>(+)</sup>-ion mobility in the rat ventricular myocyte, investigated using flash photolysis of a caged-H<sup>(+)</sup> compound. *Biophys J*, **92**, 641-653.
- Swietach, P. and Vaughan-Jones, R.D. (2005) Relationship between intracellular pH and proton mobility in rat and guinea-pig ventricular myocytes. *J Physiol*, **566**, 793-806.
- Takahashi, K., Sawasaki, Y., Hata, J., Mukai, K. and Goto, T. (1990) Spontaneous transformation and immortalization of human endothelial cells. *In Vitro Cell Dev Biol*, **26**, 265-274.
- Takeda, A., Saheki, S., Shimazu, T. and Takeuchi, N. (1989) Phosphorylation of the 27-kDa gap junction protein by protein kinase C in vitro and in rat hepatocytes. *J Biochem (Tokyo)*, **106**, 723-727.
- Takeda, H., Matozaki, T., Fujioka, Y., Takada, T., Noguchi, T., Yamao, T., Tsuda, M., Ochi, F., Fukunaga, K., Narumiya, S., Yamamoto, T. and Kasuga, M. (1998) Lysophosphatidic acid-induced association of SHP-2 with SHPS-1: roles of RHO, FAK, and a SRC family kinase. *Oncogene*, **16**, 3019-3027.
- Takeda, H., Matozaki, T., Takada, T., Noguchi, T., Yamao, T., Tsuda, M., Ochi, F., Fukunaga, K., Inagaki, K. and Kasuga, M. (1999) PI 3-kinase gamma and protein

- kinase C-zeta mediate RAS-independent activation of MAP kinase by a Gi protein-coupled receptor. *Embo J*, **18**, 386-395.
- Takens-Kwak, B.R., Jongsma, H.J., Rook, M.B. and Van Ginneken, A.C. (1992) Mechanism of heptanol-induced uncoupling of cardiac gap junctions: a perforated patch-clamp study. *Am J Physiol*, **262**, C1531-1538.
- Taylor, H.J., Chaytor, A.T., Evans, W.H. and Griffith, T.M. (1998) Inhibition of the gap junctional component of endothelium-dependent relaxations in rabbit iliac artery by 18-alpha glycyrrhetic acid. *Br J Pharmacol*, **125**, 1-3.
- Tekle, E., Astumian, R.D. and Chock, P.B. (1991) Electroporation by using bipolar oscillating electric field: an improved method for DNA transfection of NIH 3T3 cells. *Proc Natl Acad Sci U S A*, **88**, 4230-4234.
- Tekle, E., Astumian, R.D., Friauf, W.A. and Chock, P.B. (2001) Asymmetric pore distribution and loss of membrane lipid in electroporated DOPC vesicles. *Biophys J*, **81**, 960-968.
- TenBroek, E.M., Lampe, P.D., Solan, J.L., Reinhout, J.K. and Johnson, R.G. (2001) Ser364 of connexin43 and the upregulation of gap junction assembly by cAMP. *J Cell Biol*, **155**, 1307-1318.
- Ternovsky, V.I., Okada, Y. and Sabirov, R.Z. (2004) Sizing the pore of the volume-sensitive anion channel by differential polymer partitioning. *FEBS Lett*, **576**, 433-436.
- Teruel, M.N., Blanpied, T.A., Shen, K., Augustine, G.J. and Meyer, T. (1999) A versatile microporation technique for the transfection of cultured CNS neurons. *J Neurosci Methods*, **93**, 37-48.
- Thevananther, S., Sun, H., Li, D., Arjunan, V., Awad, S.S., Wyllie, S., Zimmerman, T.L., Goss, J.A. and Karpen, S.J. (2004) Extracellular ATP activates c-jun N-terminal kinase signaling and cell cycle progression in hepatocytes. *Hepatology*, **39**, 393-402.
- Thimm, J., Mechler, A., Lin, H., Rhee, S. and Lal, R. (2005) Calcium-dependent open/closed conformations and interfacial energy maps of reconstituted hemichannels. *J Biol Chem*, **280**, 10646-10654.
- Thomas, M.A., Zosso, N., Scerri, I., Demaurex, N., Chanson, M. and Staub, O. (2003) A tyrosine-based sorting signal is involved in connexin43 stability and gap junction turnover. *J Cell Sci*, **116**, 2213-2222.
- Thompson, R.J., Zhou, N. and MacVicar, B.A. (2006) Ischemia opens neuronal gap junction hemichannels. *Science*, **312**, 924-927.
- Thuringer, D. (2004) The vascular endothelial growth factor-induced disruption of gap junctions is relayed by an autocrine communication via ATP release in coronary capillary endothelium. *Ann N Y Acad Sci*, **1030**, 14-27.
- Tieleman, D.P. (2004) The molecular basis of electroporation. *BMC Biochem*, **5**, 10.
- Tordjmann, T., Berthon, B., Claret, M. and Combettes, L. (1997) Coordinated intercellular calcium waves induced by noradrenaline in rat hepatocytes: dual control by gap junction permeability and agonist. *Embo J*, **16**, 5398-5407.
- Torok, K., Stauffer, K. and Evans, W.H. (1997) Connexin 32 of gap junctions contains two cytoplasmic calmodulin-binding domains. *Biochem J*, **326 ( Pt 2)**, 479-483.
- Tour, O., Adams, S.R., Kerr, R.A., Meijer, R.M., Sejnowski, T.J., Tsien, R.W. and Tsien, R.Y. (2007) Calcium Green FAsH as a genetically targeted small-molecule calcium indicator. *Nat Chem Biol*, **3**, 423-431.
- Tran Van Nhieu, G., Clair, C., Bruzzone, R., Mesnil, M., Sansonetti, P. and Combettes, L. (2003) Connexin-dependent inter-cellular communication increases invasion and dissemination of *Shigella* in epithelial cells. *Nat Cell Biol*, **5**, 720-726.
- Traub, O., Druge, P.M. and Willecke, K. (1983) Degradation and resynthesis of gap junction protein in plasma membranes of regenerating liver after partial hepatectomy or cholestasis. *Proc Natl Acad Sci U S A*, **80**, 755-759.

- Traub, O., Look, J., Dermietzel, R., Brummer, F., Hulser, D. and Willecke, K. (1989) Comparative characterization of the 21-kD and 26-kD gap junction proteins in murine liver and cultured hepatocytes. *J Cell Biol*, **108**, 1039-1051.
- Traub, O., Look, J., Paul, D. and Willecke, K. (1987) Cyclic adenosine monophosphate stimulates biosynthesis and phosphorylation of the 26 kDa gap junction protein in cultured mouse hepatocytes. *Eur J Cell Biol*, **43**, 48-54.
- Trexler, E.B., Bennett, M.V., Bargiello, T.A. and Verselis, V.K. (1996) Voltage gating and permeation in a gap junction hemichannel. *Proc Natl Acad Sci U S A*, **93**, 5836-5841.
- Tsumura, T., Oiki, S., Ueda, S., Okuma, M. and Okada, Y. (1996) Sensitivity of volume-sensitive Cl<sup>-</sup> conductance in human epithelial cells to extracellular nucleotides. *Am J Physiol*, **271**, C1872-1878.
- Turin, L. and Warner, A. (1977) Carbon dioxide reversibly abolishes ionic communication between cells of early amphibian embryo. *Nature*, **270**, 56-57.
- Ulevitch, R.J. (1993) Recognition of bacterial endotoxins by receptor-dependent mechanisms. *Adv Immunol*, **53**, 267-289.
- Ullrich, A. and Schlessinger, J. (1990) Signal transduction by receptors with tyrosine kinase activity. *Cell*, **61**, 203-212.
- Unger, V.M., Kumar, N.M., Gilula, N.B. and Yeager, M. (1999) Three-dimensional structure of a recombinant gap junction membrane channel. *Science*, **283**, 1176-1180.
- Valiunas, V. (2002) Biophysical properties of connexin-45 gap junction hemichannels studied in vertebrate cells. *J Gen Physiol*, **119**, 147-164.
- Valiunas, V., Manthey, D., Vogel, R., Willecke, K. and Weingart, R. (1999) Biophysical properties of mouse connexin30 gap junction channels studied in transfected human HeLa cells. *J Physiol*, **519 Pt 3**, 631-644.
- Valiunas, V. and Weingart, R. (2000) Electrical properties of gap junction hemichannels identified in transfected HeLa cells. *Pflugers Arch*, **440**, 366-379.
- van der Wijk, T., Tomassen, S.F., Houtsmuller, A.B., de Jonge, H.R. and Tilly, B.C. (2003) Increased vesicle recycling in response to osmotic cell swelling. Cause and consequence of hypotonicity-provoked ATP release. *J Biol Chem*, **278**, 40020-40025.
- van Leeuwen, F.N., Giepmans, B.N., van Meeteren, L.A. and Moolenaar, W.H. (2003) Lysophosphatidic acid: mitogen and motility factor. *Biochem Soc Trans*, **31**, 1209-1212.
- van Rijen, H.V., van Veen, T.A., Hermans, M.M. and Jongsma, H.J. (2000) Human connexin40 gap junction channels are modulated by cAMP. *Cardiovasc Res*, **45**, 941-951.
- van Veen, T.A., van Rijen, H.V. and Jongsma, H.J. (2000) Electrical conductance of mouse connexin45 gap junction channels is modulated by phosphorylation. *Cardiovasc Res*, **46**, 496-510.
- van Zeijl, L., Ponsioen, B., Giepmans, B.N., Ariaens, A., Postma, F.R., Varnai, P., Balla, T., Divecha, N., Jalink, K. and Moolenaar, W.H. (2007) Regulation of connexin43 gap junctional communication by phosphatidylinositol 4,5-bisphosphate. *J Cell Biol*.
- Vandamme, W., Braet, K., Cabooter, L. and Leybaert, L. (2004) Tumour necrosis factor alpha inhibits purinergic calcium signalling in blood-brain barrier endothelial cells. *J Neurochem*, **88**, 411-421.
- Vaughan, D.K. and Lasater, E.M. (1990) Renewal of electrotonic synapses in teleost retinal horizontal cells. *J Comp Neurol*, **299**, 364-374.
- Vaughan-Jones, R.D., Peercy, B.E., Keener, J.P. and Spitzer, K.W. (2002) Intrinsic H(+) ion mobility in the rabbit ventricular myocyte. *J Physiol*, **541**, 139-158.
- Veenstra, R.D. (1996) Size and selectivity of gap junction channels formed from different connexins. *J Bioenerg Biomembr*, **28**, 327-337.

- Veenstra, R.D. and DeHaan, R.L. (1986) Measurement of single channel currents from cardiac gap junctions. *Science*, **233**, 972-974.
- Veenstra, R.D., Wang, H.Z., Beblo, D.A., Chilton, M.G., Harris, A.L., Beyer, E.C. and Brink, P.R. (1995) Selectivity of connexin-specific gap junctions does not correlate with channel conductance. *Circ Res*, **77**, 1156-1165.
- Veenstra, R.D., Wang, H.Z., Beyer, E.C. and Brink, P.R. (1994a) Selective dye and ionic permeability of gap junction channels formed by connexin45. *Circ Res*, **75**, 483-490.
- Veenstra, R.D., Wang, H.Z., Beyer, E.C., Ramanan, S.V. and Brink, P.R. (1994b) Connexin37 forms high conductance gap junction channels with subconductance state activity and selective dye and ionic permeabilities. *Biophys J*, **66**, 1915-1928.
- Velasco, A., Tabernero, A., Granda, B. and Medina, J.M. (2000) ATP-sensitive potassium channel regulates astrocytic gap junction permeability by a Ca<sup>2+</sup>-independent mechanism. *J Neurochem*, **74**, 1249-1256.
- Venance, L., Piomelli, D., Glowinski, J. and Giaume, C. (1995) Inhibition by anandamide of gap junctions and intercellular calcium signalling in striatal astrocytes. *Nature*, **376**, 590-594.
- Veracini, L., Franco, M., Boureux, A., Simon, V., Roche, S. and Benistant, C. (2005) Two functionally distinct pools of Src kinases for PDGF receptor signalling. *Biochem Soc Trans*, **33**, 1313-1315.
- Vergara, L., Bao, X., Bello-Reuss, E. and Reuss, L. (2003a) Do connexin 43 gap-junctional hemichannels activate and cause cell damage during ATP depletion of renal-tubule cells? *Acta Physiol Scand*, **179**, 33-38.
- Vergara, L., Bao, X., Cooper, M., Bello-Reuss, E. and Reuss, L. (2003b) Gap-junctional hemichannels are activated by ATP depletion in human renal proximal tubule cells. *J Membr Biol*, **196**, 173-184.
- Verselis, V.K., Ginter, C.S. and Bargiello, T.A. (1994) Opposite voltage gating polarities of two closely related connexins. *Nature*, **368**, 348-351.
- Vessey, J.P., Lalonde, M.R., Mizan, H.A., Welch, N.C., Kelly, M.E. and Barnes, S. (2004) Carbenoxolone inhibition of voltage-gated Ca channels and synaptic transmission in the retina. *J Neurophysiol*, **92**, 1252-1256.
- Vikhamar, G., Rivedal, E., Mollerup, S. and Sanner, T. (1998) Role of Cx43 phosphorylation and MAP kinase activation in EGF induced enhancement of cell communication in human kidney epithelial cells. *Cell Adhes Commun*, **5**, 451-460.
- Villain, M., Jackson, P.L., Manion, M.K., Dong, W.J., Su, Z., Fassina, G., Johnson, T.M., Sakai, T.T., Krishna, N.R. and Blalock, J.E. (2000) De novo design of peptides targeted to the EF hands of calmodulin. *J Biol Chem*, **275**, 2676-2685.
- Virginio, C., Church, D., North, R.A. and Surprenant, A. (1997) Effects of divalent cations, protons and calmidazolium at the rat P2X7 receptor. *Neuropharmacology*, **36**, 1285-1294.
- Vivancos, M. and Moreno, J.J. (2002) Role of Ca(2+)-independent phospholipase A(2) and cyclooxygenase/lipoxygenase pathways in the nitric oxide production by murine macrophages stimulated by lipopolysaccharides. *Nitric Oxide*, **6**, 255-262.
- Vogt, A., Hormuzdi, S.G. and Monyer, H. (2005) Pannexin1 and Pannexin2 expression in the developing and mature rat brain. *Brain Res Mol Brain Res*, **141**, 113-120.
- Wade, M.H., Trosko, J.E. and Schindler, M. (1986) A fluorescence photobleaching assay of gap junction-mediated communication between human cells. *Science*, **232**, 525-528.
- Wang, H.Z. and Veenstra, R.D. (1997) Monovalent ion selectivity sequences of the rat connexin43 gap junction channel. *J Gen Physiol*, **109**, 491-507.

- Wang, J., Ma, M., Locovei, S., Keane, R.W. and Dahl, G. (2007) Modulation of membrane channel currents by gap junction protein mimetic peptides: size matters. *Am J Physiol Cell Physiol*, **293**, C1112-1119.
- Warn-Cramer, B.J., Cottrell, G.T., Burt, J.M. and Lau, A.F. (1998) Regulation of connexin-43 gap junctional intercellular communication by mitogen-activated protein kinase. *J Biol Chem*, **273**, 9188-9196.
- Warn-Cramer, B.J., Lampe, P.D., Kurata, W.E., Kanemitsu, M.Y., Loo, L.W., Eckhart, W. and Lau, A.F. (1996) Characterization of the mitogen-activated protein kinase phosphorylation sites on the connexin-43 gap junction protein. *J Biol Chem*, **271**, 3779-3786.
- Warn-Cramer, B.J. and Lau, A.F. (2004) Regulation of gap junctions by tyrosine protein kinases. *Biochim Biophys Acta*, **1662**, 81-95.
- Warner, A., Clements, D.K., Parikh, S., Evans, W.H. and DeHaan, R.L. (1995) Specific motifs in the external loops of connexin proteins can determine gap junction formation between chick heart myocytes. *J Physiol*, **488** ( Pt 3), 721-728.
- Weaver, J.C. (1995a) Electroporation theory. Concepts and mechanisms. *Methods Mol Biol*, **55**, 3-28.
- Weaver, J.C. (1995b) Electroporation theory. Concepts and mechanisms. *Methods Mol Biol*, **48**, 3-28.
- Weaver, J.C. (1995c) Electroporation theory. Concepts and mechanisms. *Methods Mol Biol*, **47**, 1-26.
- Weber, P.A., Chang, H.C., Spaeth, K.E., Nitsche, J.M. and Nicholson, B.J. (2004) The permeability of gap junction channels to probes of different size is dependent on connexin composition and permeant-pore affinities. *Biophys J*, **87**, 958-973.
- Weerth, S.H., Holtzclaw, L.A. and Russell, J.T. (2007) Signaling proteins in raft-like microdomains are essential for Ca<sup>2+</sup> wave propagation in glial cells. *Cell Calcium*, **41**, 155-167.
- Weickert, S., Ray, A., Zoidl, G. and Dermietzel, R. (2005) Expression of neural connexins and pannexin1 in the hippocampus and inferior olive: a quantitative approach. *Brain Res Mol Brain Res*, **133**, 102-109.
- Weissman, A.M. (1997) Regulating protein degradation by ubiquitination. *Immunol Today*, **18**, 189-198.
- Wells, D.J. (2004) Gene therapy progress and prospects: electroporation and other physical methods. *Gene Ther*, **11**, 1363-1369.
- White, R.L., Doeller, J.E., Verselis, V.K. and Wittenberg, B.A. (1990) Gap junctional conductance between pairs of ventricular myocytes is modulated synergistically by H<sup>+</sup> and Ca<sup>++</sup>. *J Gen Physiol*, **95**, 1061-1075.
- White, T.W. (2002) Unique and redundant connexin contributions to lens development. *Science*, **295**, 319-320.
- White, T.W., Bruzzone, R., Wolfram, S., Paul, D.L. and Goodenough, D.A. (1994) Selective interactions among the multiple connexin proteins expressed in the vertebrate lens: the second extracellular domain is a determinant of compatibility between connexins. *J Cell Biol*, **125**, 879-892.
- White, T.W., Paul, D.L., Goodenough, D.A. and Bruzzone, R. (1995) Functional analysis of selective interactions among rodent connexins. *Mol Biol Cell*, **6**, 459-470.
- Willecke, K., Eiberger, J., Degen, J., Eckardt, D., Romualdi, A., Guldenagel, M., Deutsch, U. and Sohl, G. (2002) Structural and functional diversity of connexin genes in the mouse and human genome. *Biol Chem*, **383**, 725-737.

- Winston, B.W., Chan, E.D., Johnson, G.L. and Riches, D.W. (1997) Activation of p38mapk, MKK3, and MKK4 by TNF-alpha in mouse bone marrow-derived macrophages. *J Immunol*, **159**, 4491-4497.
- Won, S.J., Kim, D.Y. and Gwag, B.J. (2002) Cellular and molecular pathways of ischemic neuronal death. *J Biochem Mol Biol*, **35**, 67-86.
- Xie, H., Laird, D.W., Chang, T.H. and Hu, V.W. (1997) A mitosis-specific phosphorylation of the gap junction protein connexin43 in human vascular cells: biochemical characterization and localization. *J Cell Biol*, **137**, 203-210.
- Xiong, Z.G. and MacDonald, J.F. (1999) Sensing of extracellular calcium by neurones. *Can J Physiol Pharmacol*, **77**, 715-721.
- Xu, X., Berthoud, V.M., Beyer, E.C. and Ebihara, L. (2002) Functional role of the carboxyl terminal domain of human connexin 50 in gap junctional channels. *J Membr Biol*, **186**, 101-112.
- Yamamoto, T., Kardami, E. and Nagy, J.I. (1991) Basic fibroblast growth factor in rat brain: localization to glial gap junctions correlates with connexin43 distribution. *Brain Res*, **554**, 336-343.
- Ye, Z.C., Wyeth, M.S., Baltan-Tekkok, S. and Ransom, B.R. (2003) Functional hemichannels in astrocytes: a novel mechanism of glutamate release. *J Neurosci*, **23**, 3588-3596.
- Yegutkin, G.G. (2008) Nucleotide- and nucleoside-converting ectoenzymes: Important modulators of purinergic signalling cascade. *Biochim Biophys Acta* **E-pub**.
- Yen, M.R. and Saier, M.H., Jr. (2007) Gap junctional proteins of animals: the innexin/pannexin superfamily. *Prog Biophys Mol Biol*, **94**, 5-14.
- Yin, X., Gu, S. and Jiang, J.X. (2001) The development-associated cleavage of lens connexin 45.6 by caspase-3-like protease is regulated by casein kinase II-mediated phosphorylation. *J Biol Chem*, **276**, 34567-34572.
- Yoshioka, J., Prince, R.N., Huang, H., Perkins, S.B., Cruz, F.U., MacGillivray, C., Lauffenburger, D.A. and Lee, R.T. (2005) Cardiomyocyte hypertrophy and degradation of connexin43 through spatially restricted autocrine/paracrine heparin-binding EGF. *Proc Natl Acad Sci U S A*, **102**, 10622-10627.
- Yule, D.I., Stuenkel, E. and Williams, J.A. (1996) Intercellular calcium waves in rat pancreatic acini: mechanism of transmission. *Am J Physiol*, **271**, C1285-1294.
- Zajchowski, L.D. and Robbins, S.M. (2002) Lipid rafts and little caves. Compartmentalized signalling in membrane microdomains. *Eur J Biochem*, **269**, 737-752.
- Zaniboni, M., Rossini, A., Swietach, P., Banger, N., Spitzer, K.W. and Vaughan-Jones, R.D. (2003a) Proton permeation through the myocardial gap junction. *Circ Res*, **93**, 726-735.
- Zaniboni, M., Swietach, P., Rossini, A., Yamamoto, T., Spitzer, K.W. and Vaughan-Jones, R.D. (2003b) Intracellular proton mobility and buffering power in cardiac ventricular myocytes from rat, rabbit, and guinea pig. *Am J Physiol Heart Circ Physiol*, **285**, H1236-1246.
- Zhang, X. and Qi, Y. (2005) Role of intramolecular interaction in connexin50: mediating the Ca<sup>2+</sup>-dependent binding of calmodulin to gap junction. *Arch Biochem Biophys*, **440**, 111-117.
- Zhang, Y.W., Nakayama, K. and Morita, I. (2003) A novel route for connexin 43 to inhibit cell proliferation: negative regulation of S-phase kinase-associated protein (Skp 2). *Cancer Res*, **63**, 1623-1630.
- Zhou, L., Kaspersek, E.M. and Nicholson, B.J. (1999) Dissection of the molecular basis of pp60(v-src) induced gating of connexin 43 gap junction channels. *J Cell Biol*, **144**, 1033-1045.

- 
- Zhou, Y., Yang, W., Lurtz, M.M., Ye, Y., Huang, Y., Lee, H.W., Chen, Y., Louis, C.F. and Yang, J.J. (2007) Identification of the calmodulin binding domain of connexin43. *J Biol Chem*.
- Zhu, D., Caveney, S., Kidder, G.M. and Naus, C.C. (1991) Transfection of C6 glioma cells with connexin 43 cDNA: analysis of expression, intercellular coupling, and cell proliferation. *Proc Natl Acad Sci U S A*, **88**, 1883-1887.
- Zocchi, E., Usai, C., Guida, L., Franco, L., Bruzzone, S., Passalacqua, M. and De Flora, A. (1999) Ligand-induced internalization of CD38 results in intracellular Ca<sup>2+</sup> mobilization: role of NAD<sup>+</sup> transport across cell membranes. *Faseb J*, **13**, 273-283.
- Zorko, M. and Langel, U. (2005) Cell-penetrating peptides: mechanism and kinetics of cargo delivery. *Adv Drug Deliv Rev*, **57**, 529-545.



## Dankwoord

Ik heb er zolang naar uitgekeken en nu is het eindelijk zover, ik mag mijn dankwoord schrijven. Er zijn heel veel mensen die ik wil bedanken voor hun steun en begrip tijdens mijn doctoraat, waarbij voornamelijk de laatste maanden heel zwaar waren voor de mensen in mijn omgeving.

Eerst en vooral wil ik Prof. Dr. Ing. Luc Leybaert bedanken. Een aantal jaar geleden tekende ik voor een script waarvan ik het begin kende, maar niet het einde. Nu zoveel later, ben ik blij hoe alles gelopen is. U heeft mij ontzettend veel kansen gegeven. Hartelijk dank hiervoor Prof. Leybaert, Luc. Ik hoop dat we onze samenwerking nog vele jaren kunnen verder zetten. Verder wil ik ook nog Prof. Vandevoorde bedanken, in de gang was u steeds bereid om een praatje te slaan. Prof. Vanheel en Prof. De Ley, bedankt voor de leuke samenwerking voor de practica.

Eric (Tack), wat zou ik zonder jou gedaan hebben in de voorbije jaren. Jij was steeds bereid om mijn cellen te splitsen, zelfs al kwam ik juist voor je vertrok nog met iets extra langs, je deed het steeds met een glimlach. Onze band werd zo goed dat ik steeds meer uitkeek naar dinsdag en vrijdag, want dan was je bij ons, op het derde verdiep, en kon ik weer eens lekker gezellig kletsen met jou. Je was een collega, maar ondertussen ben je wel een goede vriend geworden. André, voor raad, telefoonnummers, hulp en zoveel meer kon ik steeds bij jou terecht. Ook voor een gewoon gesprek, als het even allemaal niet meer ging, stond jij steeds voor mij klaar, bedankt hiervoor. Julien, jij was het zonnetje in huis, en zorgde er steeds voor dat er voldoende eten (en water!!!) in het labo was. Voor buisjes, slangetjes en zoveel meer kon ik steeds bij jou terecht. Marc, op jou kon ik steeds rekenen om dingen in te scannen, om dingen voor het practicum te regelen, en zoveel meer. Dirk, jij bent ondertussen op pensioen, maar ik mis je nog steeds op het labo. Tom, Cyriel en Bart, geen enkel technisch probleem is jullie teveel, waar iedereen stopt, gaan jullie door, bedankt hiervoor.

Marijke (De Bock), ik vind het super om met jou samen in een bureau te zitten. Ik kan steeds bij jou terecht met een lach en een traan, ik kan mij geen beter bureaugenootje wensen. Ik vermoed dat de laatste maanden ook zwaar waren voor jou, jouw iwt moest af, en ik zat bijna constant te zagen over mijn doctoraat. Maar als je dit leest is het allemaal achter de rug, nog een paar jaartjes te gaan en het is aan jou, nog heel veel moed en ga ervoor hé!!!

Anja en Christophe, ik ben blij dat jullie in blok B zaten/zitten en niet in K12, jullie zijn superleuke collega's. Ik heb heel veel beroep kunnen doen op jullie, als ik iets kan terugdoen, doe ik het met heel veel plezier. Christophe, nog heel veel geluk bij het verdere onderzoek. Sofie, we zijn samen begonnen en stoppen samen met ons doctoraat, ik wens je nog veel geluk bij alles wat je doet. Nan, I would like to thank you for reading (together with Marijke

DB) my Ph.D.-thesis to find the last typing errors, thanks a lot. Maxime, a special thanks for you for “helping” me with my French summary. This would be terrible without you. Elke (Decrock), Marijke (Van Moorhem), Katleen, Kelly, Nele, Melissa en Bram, nog heel veel geluk met jullie verdere doctoraat.

Mama en papa, zonder jullie hulp, steun en vertrouwen zou ik dit nooit allemaal gedaan hebben. Jullie hebben mij geholpen op alle mogelijke manieren, als er iets was, moest ik maar bellen. Jullie speelden taxidienst, hotel, kuisploeg, wasserij, en keuken, alles wat maar nodig was. Maar nu ben ik eindelijk afgestudeerd. Mama, ik hoop dat alles terug goed komt met jou, blijf geloven, en het zal lukken. Moeke, dankzij jou ben ik nu wie ik ben, jammer genoeg heb jij dit niet meer kunnen meemaken. Ik hoop dat je van ergens boven kan meekijken en toch trots bent op wat ik gedaan heb en doe. Ik mis je na drie jaar nog altijd evenveel, *but nobody really dies, they all just end up in the sky so far away (Kriss Kross - Guillemots)*. Etienne en Henriette, ook jullie wil ik bedanken voor de vele hulp. Thibo, mijn metekindje, vanaf nu ga ik er meer zijn voor jou. Kevin, Simon en Nick, ik wens jullie heel veel geluk en moed in jullie verdere leven.

En dan last, but not least, Karl, mijn held, alles wat ik hier zeg is veel te weinig voor de dingen die je gedaan hebt. Ik weet dat het niet steeds van een leien dakje gelopen is, noch mijn doctoraat, noch de rest, maar nu is het zover, het is eindelijk gedaan. Ik ga eindelijk terug meer tijd hebben voor jou, voor ons, voor alles. *You got me off the sofa, just sprang out of the air, the best things come from nowhere, I can't believe you care, but you really do (Made-up lovesong #43 - Guillemots)*.

Bedankt aan iedereen voor de steun,  
Elke De Vuyst

---

## Curriculum vitae

### Personal details

Name: Elke De Vuyst  
Address: Pr. F. Rooseveltlaan 310  
9000 Ghent  
Date of birth: 28/05/1978 (Ninove)  
Civil state: Unmarried

### Training

Secondary education:  
IKSO Denderleeuw  
Middenstraat 10/ Nieuwstraat 1  
9470 Denderleeuw  
1990-1996: Latin-Sciences

### University Education:

Ghent University  
1996-1998: Bachelor in Chemistry  
1998-2000: Master in Biotechnology; Molecular Biology  
Graduated with distinction

### Master Thesis

Functional analysis of the human Armadillo protein p120ctn.  
Unit for Molecular Cell Biology  
Departement for Molecular Biomedical Research  
Faculty of Sciences; Ghent University

### Publications

De Vuyst E., Decrock E., Cabooter L., Dubyak GR, Naus CC, Evans WH and Leybaert L. (2006). Intracellular calcium changes trigger connexin 32 hemichannel opening. *EMBO J.* **25**, 34-44 (IF 10.53).

Evans WH, De Vuyst E. And Leybaert L. (2006). The cellular internet – connexin hemichannels enter the intercellular signaling limelight. *Biochem. J.* **397** (1): 1-14. Invited review (IF 4.101).

De Vuyst E., Decrock E., De Bock M., Yamasaki H., Naus C.C., Evans W.H. and Leybaert L. (2007). Connexin hemichannels and gap junction channels are

differentially influenced by lipopolysaccharide and basic fibroblast growth factor. *Mol. Biol. Cell.* **18** (1): 34-46 (IF 6.52).

Leybaert L., De Bock M., Van Moorhem M., Decrock E. and De Vuyst E. (2007). Neurobarrier coupling in the brain: adjusting glucose entry with demand. *J. Neurosci. Res.* **85** (15): 3213-20. Review (IF 3.476).

De Vuyst E., De Bock M., Naus C., Mabilde C. and Leybaert L. (2007). Bipolar pulsed high frequency electroporation: a technique to load a restricted zone of cells and to investigate dye spread via gap junctions. *Biophys. J.* **94** (2): 469-79 (IF 4.757).

De Vuyst E., Decrock E., De Bock M., Van Moorhem M., Vinken M., Rogiers V., Yamsaki H., Naus C.C., Evans W.H., and Leybaert L. (2008). Calcium activation of ATP release through Cx43 hemichannels via calmodulin, arachidonic acid and ROS/NO signaling. *Mol. Biol. Cell.* Submitted (IF 6.52).

Decrock E., De Vuyst E., Van Moorhem M., Van Laeken L., De Bock M., Vinken M., Rogiers V., D'Herde K., Evans W.H., Naus C.C, and Leybaert L. (2008). Connexin 43 hemichannels contribute to the propagation of apoptotic cell death in a rat C6 glioma cell model. *Cell Death Diff.* second revision (IF 7.463).

#### Abstracts and Posters

De Vuyst E., van Hengel J., Gilbert B., D'Hooge P., and Van Roy F. (2001): Murine p120 catenin: gene structure and high expression in developing somites. Belgian-Dutch Meeting on Cell Adhesion; Ghent, Belgium; November 9-10, 2001. Poster communication.

De Vuyst E., van Hengel J., Gilbert B., D'Hooge P., and Van Roy F. (2002): Murine p120 catenin: gene structure and high expression in developing somites. First Belgian PAI/UIAP meeting; Luik, Belgium; March 26, 2002. Poster communication.

van Hengel, J., Soubry, A., De Vuyst, E. and van Roy, F. (2002). Expression of p120 catenin and its interaction partner Kaiso in cell lines and tumors. Second ELSO meeting; Nice, France; June 29-July 3, 2002. Poster communication.

De Vuyst E., van Hengel J., Gilbert B., D'Hooge P., and Van Roy F. (2002): Murine p120 catenin: gene structure and high expression in developing somites. EMBO practical course; Zagreb, Croatia; September 15-22, 2002. Poster communication.

De Vuyst E. and Leybaert L. (2004): Regulation of connexins by kinases: gap junctions versus hemichannels. Belgian Society of Fundamental and Clinical Physiology and Pharmacology; Leuven, Belgium; November 20, 2004. Oral Presentation (Pflügers Archiv European Journal of Physiology, **449** (6): R7).

De Vuyst E., Yamasaki H., Naus C., Evans H. and Leybaert L. (2005): PKC, Src and LPA inhibit both gap junction channel and hemichannel function in C6-Cx43 cells, while LPS has divergent actions depending on the cell type and presence of the Cx43 C-terminal tail. International Gap Junction Conference; Vancouver, Canada; August 13-18, 2005. Poster Communication.

De Vuyst E., Cabooter L., Naus C., Evans H. and Leybaert L. (2005): Intracellular calcium changes trigger connexin 32 hemichannel opening. International Gap Junction Conference; Vancouver, Canada; August 13-18, 2005. Poster Communication.

De Vuyst E., Decrock E., Yamasaki H., Naus C., Evans H. and Leybaert, L. (2006): Lipopolysaccharide and bFGF differentially affect gap junction channels and hemichannels in connexin 43 expressing cells. 5<sup>th</sup> Forum of European Neuroscience; Vienna, Austria; July 8-12, 2006. Poster Communication.

De Vuyst E., Vanlander A., Nauss C., Evans H. and Leybaert L. (2006): Gliotransmitter release via cytoplasmic calcium-triggered opening of connexin-32 and -43 hemichannels in C6 glioma. Society for Neuroscience; Atlanta, USA; October 14-18, 2006. Poster Communication.

De Vuyst E., De Bock M., Van Moorhem M., Decrock E. and Leybaert L. (2006): Gliotransmitter release via cytoplasmic calcium-triggered opening of connexin-32 and -43 hemichannels in C6 glioma. Neurobelgium 2006; Genval, Belgium; November 10-11, 2006 (Acta Neurologica Belgica, supp 2006, **106**, 1-2: P56).

De Vuyst E. and Leybaert L. (2007) Gap junction hemichannel control by cytoplasmic calcium, arachidonic acid and kinases. "Une Journée exceptionnelle", INSERM, Paris, France; May 25, 2007. Oral presentation.

De Bock M., De Vuyst E., Van Moorhem M., Decrock E. and Leybaert L. (2006): A role for endothelial calcium changes in neurobarriere coupling. Neurobelgium 2006;

Genval, Belgium; November 10-11, 2006 (Acta Neurologica Belgica, supp 2006, **106**, 1-2: P57).

Leybaert L., De Bock M., Van Moorhem M., Decrock E. and De Vuyst E. (2006): Neurobarrier coupling in the brain: adjusting glucose entry with demand. Neurobelgium 2006; Genval, Belgium; November 10-11, 2006 (Acta Neurologica Belgica, supp 2006, **106**, 1-2: P58).

Van Moorhem M., Decrock E., De Bock M., De Vuyst E., Van Den Bosch L., Callewaert G., Lambein F. and Leybaert L. (2006): Neurolathyrism:  $\beta$ -ODAP and the excitotoxicity hypothesis. Neurobelgium 2006; Genval, Belgium; November 10-11, 2006 (Acta Neurologica Belgica, supp 2006, **106**, 1-2: P25).

Decrock E., Van Moorhem M., De Bock M., De Vuyst E., D'Herde K. and Leybaert L. (2006): Connexin channels, possible mediators in apoptosis spread in a glioma cell model. Neurobelgium 2006; Genval, Belgium; November 10-11, 2006 (Acta Neurologica Belgica, supp 2006, **106**, 1-2: P30).

De Vuyst E., De Bock M., Decrock E., Van Moorhem M. And Leybaert L. (2007): Connexin43 hemichannel regulation by intracellular calcium: involvement of different signalling pathways. Belgian Society of Fundamental and Clinical Physiology and Pharmacology; Leuven, Belgium; November 17, 2007. Oral Presentation

De Vuyst E., De Bock M., Decrock E., Van Moorhem M. And Leybaert L. (2007): Connexin43 hemichannel regulation by intracellular calcium: involvement of different signalling pathways. IUAP-meeting; Hasselt, Belgium; December 1, 2007. Oral Presentation

## Grants

*Support grant* for participation to the International Gap Junction Conference 2005 in Vancouver (Vancouver, Canada; August 13-18, 2005).

*FENS/IBRO WERC stipend* for participating the FENS Forum 2006 in Vienna (Vienna, Austria; July 8-12, 2006).



